UCLA
COMPUTATIONAL AND APPLIED MATHEMATICS

Approximate Solutions of Nonlinear Conservation Laws

Eitan Tadmor

November 1997

CAM Report 97-51

Department of Mathematics
University of California, Los Angeles
Los Angeles, CA. 90095-1555

Approximate Solutions of Nonlinear Conservation Laws

Eitan Tadmor

Lectures Notes from CIME Course on

Advanced Numerical Approximation of
Nonlinear Hyperbolic Equations

Cetraro (Cosenza), Italy, 22 - 28 June 1997

Approximate Solutions of Nonlinear Conservation Laws

Lectures Notes from CIME Course on

Advanced Numerical Approximation of Nonlinear Hyperbolic Equations

Cetraro (Cosenza), Italy, 22 - 28 June 1997

Eitan Tadmor[1]

[1]Department of Mathematics UCLA, Los-Angeles CA 90095; School of Mathematical Sciences Tel-Aviv University, Tel-Aviv. Email: tadmor@math.ucla.edu

PREFACE

This is a summary of five lectures delivered at the CIME course on "Advanced Numerical Approximation of Nonlinear Hyperbolic Equations" held in Cetraro, Italy, on June 1997.

Following the introductory lecture I — which provides a general overview of approximate solution to nonlinear conservation laws, the remaining lectures deal with the specifics of four complementing topics:

- Lecture II. Finite-difference methods – non-oscillatory central schemes;
- Lecture III. Spectral approximations – the Spectral Viscosity method;
- Lecture IV. Convergence rate estimates – a Lip' convergence theory;
- Lecture V. Kinetic approximations – regularity of kinetic formulations.

Acknowledgment. I thank Alfio Quarteroni for the invitation, B. Cockburn, C. Johnson & C.-W Shu for the team discussions, the Italian participants for their attention, and the hosting Grand Hotel at San Michelle for its remarkably unique atmosphere.
Research was supported in part by ONR grant #N00014-91-J-1076 and NSF grant #97-06827.

AMS Subject Classification. Primary 35L65, 35L60. Secondary 65M06, 65M12, 65M15, 65M60, 65M70

Contents

Chapter 1

A General Overview

Abstract. In this introductory lecture, we overview the development of modern, high-resolution approximations to hyperbolic conservation laws and related nonlinear equations. Since this overview also serves as an introduction for the other lectures in this volume, it is less of a comprehensive overview, and more of a bird's eye view of topics which play a pivotal role in the lectures ahead. It consists of a dual discussion on the various mathematical concepts and the related discrete algorithms which are the required ingredients for these lectures.

I start with a brief overview on the mathematical theory for nonlinear hyperbolic conservation laws. The theory of the continuum (– and in this case, the dis-continuum), is intimately related to the construction, analysis and implementation of the corresponding discrete approximations. Here, the basic the notions of viscosity regularization, entropy, monotonicity, total variation bounds and Riemann's problem are introduced. Then follow the the basic ingredients of the discrete theory: the Lax-Wendroff theorem, and the pivotal finite-difference schemes of Godunov, Lax-Friedrichs, and Glimm.

To proceed, our dual presentation of high-resolution approximations is classified according to the analytical tools which are used in the development of their convergence theories. These include classical compactness arguments based on Total Variation (TV) bounds, e.g., TVD finite-difference approximations. The use of compensated compactness arguments based on H^{-1}-compact entropy production is demonstrated in the context of streamline diffusion finite-element method and spectral viscosity approximations. Measure valued solutions – measured by their negative entropy production, are discussed in the context of multidimensional finite-volume schemes. Finally, we discuss the recent use of averaging lemmas which yield new compactness and regularity results for approximate solutions of nonlinear conservation laws (as well as some related equations), which admit an underlying kinetic formulation, e.g., finite-volume and relaxation schemes.

1.1 Introduction

The lectures in this volume deal with modern algorithms for the accurate computation of shock discontinuities, slip lines, and other similar phenomena which could be characterized by spontaneous evolution of change in scales. Such phenomena pose a considerable computational challenge, which is answered, at least partially, by these newly constructed algorithms. New modern algorithms were devised, that achieve one or more of the desirable properties of high-resolution, efficiency, stability — in particular, lack of spurious oscillations, etc. The impact of these new algorithms ranges from the original impetus in the field of Computational Fluid Dynamics (CFD), to the fields oil recovery, moving fronts, image processing,... [75], [138], [132], [1].

In this introduction we survey a variety of these algorithms for the approximate solution of nonlinear conservation laws. The presentation is neither comprehensive nor complete — the scope is too wide for the present framework Instead, we discuss the analytical tools which are used to study the stability and convergence of these modern algorithms. We use these analytical issues as our 'touring guide' to provide a readers' digest on the relevant approximate methods, while studying there convergence properties. They include

- *Finite-difference methods.* These are the most widely used methods for solving nonlinear conservation laws. Godunov-type difference schemes play a pivotal role. Two canonical examples include the upwind ENO schemes (discussed in C.-W. Shu's lectures) and a family of high-resolution non-oscillatory central schemes (discussed in Lecture II);

- *Finite element schemes.* Here, the streamline diffusion method and its extensions are canonical example, discussed in C. Johnson's lectures;

- *Spectral approximations.* The Spectral Viscosity (SV) methods is discussed in Lecture III.

- *Finite-volume schemes.* Finite-Volume (FV) schemes offer a particular advantage for integration over multidimensional general triangulation, beyond the Cartesian grids. More can be found in B. Cockburn's lectures.

- *Kinetic formulations.* Compactness and regularizing effects of approximate solutions is quantified in terms of their underlying kinetic formulations, Lecture V.

Some general references are in order. The theory of hyperbolic conservation laws is covered in [94], [178],[157], [149]. For the theory of their numerical approximation consult [102],[58],[59],[159]. We are concerned with analytical tools which are used in the convergence theories of such numerical approximations. The monograph [50] could be consulted on recent development regarding weak convergence. The reviews of [171], [123, 124] are recommended references for the theory of compensated compactness, and [40, 41],[17] deal with applications

to conservation laws and their numerical approximations. Measure-valued solutions in the context of nonlinear conservation laws were introduced in [42]. The articles [62], [53], [45] prove the averaging lemma, and [111],[112],[77] contain applications in the context of kinetic formulation for nonlinear conservation laws and related equations.

A final word about notations. Different authors use different notations. In this introduction, the conservative variable are denoted by the "density" ρ, the spatial flux is $A(\cdot)$, (η, F) are entropy pairs, etc. In later lectures, these are replaced by the more generic notations: conservative variables are $u, v, \ldots$, fluxes are denoted by $f, g, \ldots$, the entropy function is denoted U, etc.

1.2 Hyperbolic Conservation Laws

1.2.1 A very brief overview — m equations in d spatial dimensions

The general set-up consists of m equations in d spatial dimensions

$$\partial_t \rho + \nabla_x \cdot A(\rho) = 0, \quad (t,x) \in \mathbb{R}^+_t \times \mathbb{R}^d_x. \tag{1.2.1}$$

Here, $A(\rho) := (A_1(\rho), \ldots, A_d(\rho))$ is the d-dimensional flux, and $\rho := (\rho_1(t,x), \ldots, \rho_m(t,x))$ is the unknown m-vector subject to initial conditions $\rho(0,x) = \rho_0(x)$.

The basic facts concerning such nonlinear hyperbolic systems are, consult [94],[113], [35],[157],[58],[149],

- The evolution of *spontaneous* shock discontinuities which requires weak (distributional) solutions of (1.2.1);
- The existence of possibly infinitely *many* weak solutions of (1.2.1);
- To *single* out a unique 'physically relevant' weak solution of (1.2.1), we seek a solution, $\rho = \rho(t,x)$, which can be realized as a viscosity limit solution, $\rho = \lim \rho^\varepsilon$,

$$\partial_t \rho^\varepsilon + \nabla_x \cdot A(\rho^\varepsilon) = \varepsilon \nabla_x \cdot (Q \nabla_x \rho^\varepsilon), \quad \varepsilon Q > 0; \tag{1.2.2}$$

- *The entropy condition.* The notion of a viscosity limit solution is intimately related to the notion of an *entropy solution*, ρ, which requires that for all convex entropy functions, $\eta(\rho)$, there holds, [93], [88, §5]

$$\partial_t \eta(\rho) + \nabla_x \cdot F(\rho) \leq 0. \tag{1.2.3}$$

A scalar function, $\eta(\rho)$, is *an entropy function* associated with (1.2.1), if its Hessian, $\eta''(\rho)$, symmetrizes the spatial Jacobians, $A'_j(\rho)$,

$$\eta''(\rho) A'_j(\rho) = A'_j(\rho)^\top \eta''(\rho), \qquad j = 1, \ldots, d.$$

It follows that in this case there exists an entropy flux, $F(\rho) := (F_1(\rho), \ldots, F_d(\rho))$, which is determined by the compatibility relations,

$$\eta'(\rho)^\top A_j'(\rho) = F_j'(\rho)^\top, \ j = 1, \ldots, d. \tag{1.2.4}$$

What is the relation between the entropy condition (1.2.3) and the viscosity limit solution in (1.2.2)? multiply the latter, on the left, by $\eta'(\rho^\varepsilon)$; the compatibility relation (1.2.4) implies that the resulting two terms on the left of (1.2.2) amount to the sum of *perfect derivatives*, $\partial_t \eta(\rho)^\varepsilon + \nabla_x \cdot F(\rho^\varepsilon)$. Consider now the right hand side of (1.2.2) (for simplicity, we assume the viscosity matrix on the right to be the identity matrix, $Q = I$). Here we invoke the identity

$$\varepsilon \eta'(\rho^\varepsilon)\Delta_x \rho^\varepsilon \equiv \varepsilon \Delta_x \eta(\rho^\varepsilon) - \varepsilon(\nabla_x \rho^\varepsilon)^\top \eta''(\rho^\varepsilon)\nabla_x \rho^\varepsilon .$$

The first term tends to zero (in distribution sense); the second term is nonpositive thanks to the convexity of η, and hence tend to a nonpositive measure. Thus, a viscosity limit solution must satisfy the entropy inequality (1.2.3). The inverse implication: (1.2.3) $\Longrightarrow \rho = \lim \rho^\varepsilon$ of viscosity solutions ρ^ε satisfying (1.2.2), holds in the scalar case; the question requires a more intricate analysis for systems, consult [93],[157] and the references therein.

Indeed, the basic questions regarding the existence, uniqueness and stability of entropy solutions for general systems are open. Instead, the present trend seems to concentrate on special systems with additional properties which enable to answer the questions of existence, stability, large time behavior, etc. One-dimensional 2×2 systems is a notable example for such systems: their properties can be analyzed in view of the existence of Riemann invariants and a family of entropy functions, [56], [94, §6], [157], [40, 41]. The system of $m \geq 2$ chromatographic equations, [77], is another example for such systems.

The difficulty of analyzing general systems of conservation laws is demonstrated by the following negative result due to Temple, [174], which states that already for systems with $m \geq 2$ equations, there exists no metric, $\mathcal{D}(\cdot;\cdot)$, such that the problem (1.2.1), (1.2.3) is contractive, i.e.,

$$\not\exists \mathcal{D}: \quad \mathcal{D}(\rho^1(t,\cdot);\rho^2(t,\cdot)) \leq \mathcal{D}(\rho^1(0,\cdot);\rho^2(0,\cdot)), \quad 0 \leq t \leq T, \quad (m \geq 2). \tag{1.2.5}$$

In this context we quote from [168] the following

Theorem 1.2.1 *Assume the system (1.2.1) is endowed with a one-parameter family of entropy pairs, $(\eta(\rho;c),\ F(\rho;c))$, $c \in \mathbf{R}^m$, satisfying the symmetry property*

$$\eta(\rho;c) = \eta(c;\rho), \quad F(\rho;c) = F(c;\rho). \tag{1.2.6}$$

Let ρ^1, ρ^2 be two entropy solutions of (1.2.1). Then the following a priori estimate holds

$$\int_x \eta(\rho^1(t,x);\rho^2(t,x))dx \leq \int_x \eta(\rho_0^1(x);\rho_0^2(x))dx. \tag{1.2.7}$$

Theorem 1.2.1 is based on the observation that the symmetry property (1.2.6) is the key ingredient for Kružkov's penetrating ideas in [88], which extends his scalar arguments into the case of general systems. This extension seems to be part of the 'folklore' familiar to some, [36],[150]); a sketch of the proof can be found in [168].

Remark. Theorem 1.2.1 seems to circumvent the negative statement of (1.2.5). This is done by replacing the metric $\mathcal{D}(\cdot;\cdot)$, with the weaker topology induced by a *family* of convex entropies, $\eta(\cdot;\cdot)$. Many physically relevant systems are endowed with at least one convex entropy function (– which in turn, is linked to the hyperbolic character of these systems, [61],[52],[120]). Systems with "rich" families of entropies like those required in Theorem 1.2.1 are rare, however, consult [148]. The instructive (yet exceptional...) scalar case is dealt in §1.2.2. If we relax the contractivity requirement, then we find a uniqueness theory for one-dimensional systems which was recently developed by Bressan and his coworkers, [11]-[14]; Bressan's theory is based on the L^1-stability (rather than contractivity) of the entropy solution operator of one-dimensional systems.

1.2.2 Scalar conservation laws $(m = 1, d \geq 1)$

In the scalar case, the Jacobians $A'_j(\rho)$ are just scalars that can be always symmetrized, so that the compatibility relation (1.2.4) in fact *defines* the entropy fluxes, $F_j(\rho)$, for all convex η's. Consequently, the family of admissible entropies in the scalar case consists of *all* convex functions, and the envelope of this family leads to Kružkov's entropy pairs [88]

$$\eta(\rho;c) = |\rho - c|, \quad F(\rho;c) = sgn(\rho - c)(A(\rho) - A(c)), \qquad c \in R. \tag{1.2.8}$$

Theorem 1.2.1 applies in this case and (1.2.7) now reads

- *L^1-contraction.* If ρ^1, ρ^2 are two entropy solutions of the scalar conservation law (1.2.1), then

$$\|\rho^2(t,\cdot) - \rho^1(t,\cdot)\|_{L^1(x)} \leq \|\rho_0^2(\cdot) - \rho_0^1(\cdot)\|_{L^1(x)}. \tag{1.2.9}$$

Thus, the entropy solution operator associated with scalar conservation laws is L^1-contractive (– or non-expansive to be exact), and hence, by the Crandall-Tartar lemma (discussed below), it is also monotone

$$\rho_0^2(\cdot) \geq \rho_0^1(\cdot) \Longrightarrow \rho^2(t,\cdot) \geq \rho^1(t,\cdot). \tag{1.2.10}$$

The notions of conservation, L^1contraction and monotonicity play an important role in the theory of nonlinear conservation laws, at least in the scalar case. We discuss the necessary details of these notions, by proving the *inverse* implication: the monotonicity property (1.2.10) implies the all important Kružkov's entropy pairs (1.2.8) satisfying (1.2.3).

Monotonicity and Kružkov's entropy pairs

An operator T is called monotone (or order preserving) if the following implication holds for all ρ's (in some unspecified measure subspace of L^1_{loc})

$$\rho_2 \geq \rho_1 \quad \text{a.e.} \Longrightarrow \mathrm{T}(\rho_2) \geq \mathrm{T}(\rho_1) \quad \text{a.e.} \tag{1.2.11}$$

We use the terminology that if ρ_2 dominates (pointwise, a.e.) ρ_1, then $T(\rho_2)$ dominates $T(\rho_1)$.

The following lemma due to Crandall & Tartar, [32], provides a useful characterization for such monotone operators.

Lemma 1.2.1 (Crandall-Tartar [32]) *Consider an operator T, which is* conservative *in the sense that $\int T(\rho) = \int \rho, \quad \forall \rho$'s. Then T is monotone iff it is an* L^1-contraction,

$$\int |T(\rho_2) - T(\rho_1)| \leq \int |\rho_2 - \rho_1|. \tag{1.2.12}$$

Proof. The standard notations, $\rho_1 \vee \rho_2 := \max(\rho_1, \rho_2)$ and $\rho_1 \wedge \rho_2 := \min(\rho_1, \rho_2)$ will be used. Since $|\rho_1 - \rho_2| \equiv \rho_1 \vee \rho_2 - \rho_1 \wedge \rho_2$, we find by conservation that

$$\int |\rho_1 - \rho_2| = \int \rho_1 \vee \rho_2 - \int \rho_1 \wedge \rho_2 = \int T(\rho_1 \vee \rho_2) - \int T(\rho_1 \wedge \rho_2). \tag{1.2.13}$$

Now, $\rho_1 \vee \rho_2$ dominates (pointwise a.e.) both ρ_1 and ρ_2; hence, if T is order preserving, then $T(\rho_1 \vee \rho_2)$ dominates both $T(\rho_1)$ and $T(\rho_2)$, that is, $T(\rho_1 \vee \rho_2) \geq T(\rho_1) \vee T(\rho_2)$; similarly, $-T(\rho_1 \wedge \rho_2) \geq -T(\rho_1) \wedge T(\rho_2)$. We conclude that T is an L^1-contraction, for

$$\int |\rho_1 - \rho_2| \geq \int T(\rho_1) \vee T(\rho_2) - \int T(\rho_1) \wedge \int T(\rho_2) = \int |T(\rho_1) - T(\rho_2)|. \tag{1.2.14}$$

The inverse implication (attributed to Stampacchia, I believe) starts with the identity $2w_+ \equiv |w| + w$, where w_+ denotes, as usual, the 'positive part of', $w_+ := w \vee 0$. Setting $w = T(\rho_1) - T(\rho_2)$ the integrated version of this identity reads

$$2\int (T(\rho_1) - T(\rho_2)_+ = \int |T(\rho_1) - T(\rho_2)| + \int T(\rho_1) - T(\rho_2).$$

Given that T is L^1-contractive, then together with conservation it yields that the two integrals on the right do not exceed

$$2\int (T(\rho_1) - T(\rho_2) \vee 0 \leq \int |\rho_1 - \rho_2| + \int \rho_1 - \rho_2. \tag{1.2.15}$$

Now, if ρ_2 dominates ρ_1, i.e., $\rho_1 \leq \rho_2$ a.e., then the sum of the two integrals on the RHS vanishes, and consequently, the non-negative integrand on the LHS vanishes as well, i.e., $T(\rho_1) - T(\rho_2) \leq 0$.

Remark. For *linear* operators T, monotonicity coincides with positivity, $T(\rho) \geq 0, \quad \forall \rho \geq 0$. Positive operators play a classical role in various branches of analysis. They are encountered frequently, for example, in approximation theory, e.g., [37, §9.4]. A well known example is provided by Bernstein polynomials, $B_n(\rho)(x) := \sum_{k \leq n} \binom{n}{k} x^k (1-x)^{n-k} \rho(\frac{k}{n})$. They produce a positive linear map(s), $\rho \to B_n(\rho)$ of $C[0,1]$ into the space of n-degree polynomials. Linear monotone operators, like Bernstein projections, are at most first-order accurate.

We turn to discuss the relation between monotone operators and the entropy condition. Let $\{T_t,\ t \geq 0\}$ be a one-parameter family of operators which form a semi-group of constant-preserving, monotone operators. Thus we make

- **Semi-group** It is assumed that $\{T_t\}$ satisfies the basic semi-group 'closure' (causality) relations,

$$T_{t+s} = T_t T_s, \quad T_0 = \text{the identity mapping}, \tag{1.2.16}$$

and that it has an infinitesimal generator, $\nabla_x \cdot A(\rho) := \lim_{\Delta t \downarrow 0} (\Delta t)^{-1} (T_t(\rho) - \rho)$.

Remark. The existence of such a generator is outlined by the Hille-Yosida linear theory. Extensions within the context of *nonlinear* evolution equations are available: Kato's approach in semi-Hilbert spaces and Crandall-Liggett approach in Banach spaces, consult [179, §XIV.6&7]. A concise informative account of this theory, which was specifically 'tailored' within the L^1-setup for quasilinear evolution equations can be found in [28].

With this in mind we may identify, $T_t \rho_0 =: \rho(t)$, as the solution of the abstract Cauchy problem

$$\rho_t + \nabla_x \cdot A(\rho(t)) = 0, \tag{1.2.17}$$

subject to given initial conditions $\rho(0) = \rho_0$. We assume that the following two basic properties hold.

- **Constant-preserving** T_t preserves constants, namely

$$T_t[\rho \equiv Const.] = Const. \tag{1.2.18}$$

Finally, we bring in the key assumption of monotonicity.

- **Monotonicity** Our basic assumption is the monotonicity of the solution operators associated with (1.2.17),

$$\rho_0^2(\cdot) \geq \rho_0^1(\cdot) \Longrightarrow \rho^2(t,\cdot) \geq \rho^1(t,\cdot), \quad \forall t \geq 0. \tag{1.2.19}$$

The main result of this section, following the ingredients in [116] and in particular, [142], states that *monotone, constant-preserving* solution operators of the Cauchy problem (1.2.17), are uniquely identified by the following entropy condition.

Theorem 1.2.2 (Kružkov's Entropy Condition) *Assume* $\{\rho(t), t \geq 0\}$ *is a family of solutions for the Cauchy problem (1.2.17) which is constant-preserving, (1.2.18), and satisfies the monotonicity condition (1.2.19). Then the following* entropy inequality *holds:*

$$\partial_t|\rho(t) - c| + \nabla_x \cdot \{sgn(\rho - c)(A(\rho) - A(c))\} \leq 0, \quad \forall c's. \tag{1.2.20}$$

Thus, monotonicity (+constant preserving) recover Kružkov entropy pairs.

Proof. Starting with $\rho(t)$ at arbitrary $t \geq 0$, we compare $\rho(t + \Delta t) := T_{\Delta t}\rho(t)$ with $\zeta(t+\Delta t) := T_{\Delta t}\zeta(t)$, where $\zeta(t) := (\rho(t) \vee c)$ which is cut-off at an arbitrary constant level, c. Since $\rho(t) \vee c$ dominates both $\rho(t)$ and c, the monotonicity of $T_{\Delta t}$ implies that at later times, $\zeta(t + \Delta t)$ should dominate both, $T_{\Delta t}\rho(t)$ $(= \rho(t+\Delta t)$ by to our notations), and $T_{\Delta t}(c)$ $(= c$ since $T_{\Delta t}$ is assumed constant-preserving). Thus $\zeta(t + \Delta t) \geq \rho(t + \Delta t) \vee c$ and hence

$$\frac{\rho(t + \Delta t) \vee c - \rho(t) \vee c}{\Delta t} \leq \frac{\zeta(t + \Delta t) - \zeta(t)}{\Delta t}.$$

Let $\Delta t \downarrow 0$. By definition, the LHS gives $\partial_t(\rho(t) \vee c)$; the RHS is governed by its Cauchy problem, $\partial_t\zeta(t) = -\nabla_x \cdot A(\zeta(t)) = \nabla_x \cdot A(\rho(t) \vee c)$. We conclude that an arbitrary $t \geq 0$

$$\partial_t(\rho(t) \vee c) + \nabla_x \cdot A(\rho(t) \vee c) \leq 0. \tag{1.2.21}$$

Similar arguments yield

$$-\partial_t(\rho(t) \wedge c) + \nabla_x \cdot A(\rho(t) \wedge c) \leq 0. \tag{1.2.22}$$

Together, the last two inequalities add up to the entropy inequality (1.2.20). ■

Early constructions of approximate solutions for scalar conservation laws, most notably — finite-difference approximations, utilized this monotonicity property to construct convergent schemes, [30], [143]. Monotone approximations are limited, however, to first-order accuracy [72]. At this stage we note that the limitation of first-order accuracy for monotone approximations, can be avoided if L^1-contractive solutions are replaced with (the weaker) requirement of bounded variation solutions.

- *TV bound.* The solution operator associated with (1.2.1) is translation invariant. Comparing the scalar entropy solution, $\rho(t, \cdot)$, with its translate, $\rho(t, \cdot + \Delta x)$, the L^1-contraction statement in (1.2.9) yields the TV bound, [177],

$$\|\rho(t, \cdot)\|_{BV} \leq \|\rho_0(\cdot)\|_{BV}, \quad \|\rho(t, \cdot)\|_{BV} := \sup_{\Delta x \neq 0} \frac{\|\rho(t, \cdot + \Delta x) - \rho(t, \cdot)\|_{L^1}}{\Delta x}. \tag{1.2.23}$$

Construction of scalar entropy solutions by TV-bounded approximations were used in the pioneering works of Oleĭnik [129], Vol'pert [177], Kružkov [88] and Crandall [28]. In the one-dimensional case, the TVD property (1.2.23) enables to construct convergent difference schemes with high-order (> 1) resolution; Harten initiated the construction of high-resolution TVD schemes in [70], following the earlier works [6], [98]. A whole generation of TVD schemes was then developed during the beginning of the '80s; some aspects of these developments can be found in §1.3.2.

1.2.3 One dimensional systems ($m \geq 1, d = 1$)

We focus our attention on one-dimensional hyperbolic systems governed by

$$\partial_t \rho + \partial_x A(\rho) = 0, \quad (t, x) \in \mathbb{R}_t^+ \times \mathbb{R}_x, \tag{1.2.24}$$

and subject to initial condition, $\rho(0, x) = \rho_0(x)$. The hyperbolicity of the system (1.2.24) is understood in the sense that its Jacobian, $A'(\rho)$, has a complete *real* eigensystem, $(a_k(\rho), r_k(\rho)), k = 1, \ldots, m$. For example, the existence of a convex entropy function guarantees the symmetry of $A'(\rho)$ (— w.r.t. $\eta''(\rho)$), and hence the complete real eigensystem. For most of our discussion we shall assume the stronger *strict hyperbolicity*, i.e, distinct real eigenvalues, $a_k(\rho) \neq a_j(\rho)$.

A fundamental building block for the construction of approximate solutions in the one-dimensional case is the solution of *Riemann's problem*.

Riemann's problem

Here one seeks a weak solution of (1.2.24) subject to the piecewise constant initial data

$$\rho(x, 0) = \begin{cases} \rho_\ell, & x < 0 \\ \rho_r, & x > 0. \end{cases} \tag{1.2.25}$$

The solution is composed of m simple waves, each of which is associated with one (right-)eigenpair, $(a_k(\rho), r_k(\rho))$, $1 \leq k \leq m$. There are three types of such waves: if the k-th field is *genuinely nonlinear* in the sense that $r_k \cdot \nabla_\rho a_k \neq 0$, these are either k-shock or k-rarefaction waves; or, if the k-th field is *linearly degenerate* in the sense that $r_k \cdot \nabla_\rho a_k \equiv 0$, this is a k-th contact wave.

These three simple waves are *centered*, depending on $\xi = \frac{x}{t}$ (which is to be expected from the dilation invariance of (1.2.24),(1.2.25)). The structure of these three centered waves is as follows:

- A k-shock discontinuity of the form

$$\rho(\xi) = \begin{cases} \rho_\ell, & \xi < s \\ \rho_r, & \xi > s; \end{cases}$$

here s denotes the shock speed which is determined by a Rankine-Hugoniot relation so that $a_k(\rho_\ell) > s > a_k(\rho_r)$.

- A k-rarefaction wave, $\rho(\xi)$, which is directed along the corresponding k-th eigenvector, $\dot{\rho}(\xi) = r_k(\rho(\xi))$. Here r_k is the normalized k-eigenvector, $r_k \cdot \nabla a_k \equiv 1$ so that the gap between $a_k(\rho_\ell) < a_k(\rho_r)$ is filled with a fan of the form

$$a_k(\rho(\xi)) = \begin{cases} a_k(\rho_\ell), & \xi < a_k(\rho_\ell) \\ \xi, & a_k(\rho_\ell) < \xi < a_k(\rho_r) \\ a_k(\rho_r), & a_k(\rho_r) < \xi \end{cases}$$

- A k-contact discontinuity of the form

$$\rho(\xi) = \begin{cases} \rho_\ell, & \xi < s \\ \rho_r, & \xi > s \end{cases}$$

where s denotes the shock speed which is determined by a Rankine-Hugoniot relation so that $a_k(\rho_\ell) = s = a_k(\rho_r)$.

We are concerned with *admissible* systems — systems which consist of either genuinely nonlinear or linearly degenerate fields. We refer to [92] for the full story which is summarized in the celebrated

Theorem 1.2.3 (Lax solution of Riemann's problem) *The strictly hyperbolic admissible system (1.2.24), subject to Riemann initial data (1.2.25) with $\rho_\ell - \rho_r$ sufficiently small, admits a weak entropy solution, which consists of shock- rarefaction- and contact-waves.*

For a detailed account on the solution of Riemann problem consult [16]. An extension to a generalized Riemann problem subject to piecewise-linear initial data can be found in [5], [99]. In this context we also mention the *approximate* Riemann solvers, which became useful computational alternatives to Lax's construction. Roe introduced in [139] a linearized Riemann solver, which resolves jumps discontinuities solely in terms of shock waves. Roe's solver has the computational advantage of sharp resolution (at least when there is one dominant wave per computational cell); it may lead, however, to unstable shocks. Osher and Solomon in [131] used, instead, an approximate Riemann solver based solely on rarefaction fans; one then achieves stability at the expense of deteriorated resolution of shock discontinuities.

Godunov, Lax-Friedrichs and Glimm schemes

We let $\rho^{\Delta x}(t,x)$ be the entropy solution in the slab $t^n \le t < t + \Delta t$, subject to piecewise constant data $\rho^{\Delta x}(t = t^n, x) = \sum \rho_\nu^n \chi_\nu(x)$. Here χ denotes the usual indicator function, $\chi_\alpha(x) := 1_{\{|x-\alpha\Delta x| \le \Delta x/2\}}$. Observe that in each slab, $\rho^{\Delta x}(t,x)$ consists of successive *noninteracting* Riemann solutions, at least for a sufficiently small time interval Δt, for which the CFL condition, $\Delta t/\Delta x \max|a_k(\rho)| \le \frac{1}{2}$ is met. In order to realize the solution in the next time level, $t^{n+1} = t^n + \Delta t$, it is extended with a jump discontinuity across the line t^{n+1}, by projecting it back into the finite-dimensional space of piecewise constants. Different projections yield different schemes. We recall the basic three.

Godunov Scheme. Godunov scheme [60] sets

$$\rho^{\Delta x}(t^{n+1},x)=\sum_{\nu}\bar{\rho}_{\nu}^{n+1}\chi_{\nu}(x),$$

where $\bar{\rho}_{\nu}^{n+1}$ stands for the cell-average,

$$\bar{\rho}_{\nu}^{n+1}:=\frac{1}{\Delta x}\int_{x}\rho^{\Delta x}(t^{n+1}-0,x)\chi_{\nu}(x)dx,$$

which could be explicitly evaluated in terms of the flux of Riemann solution across the cell interfaces at $x_{\nu\pm\frac{1}{2}}$,

$$\bar{\rho}_{\nu}^{n+1}=\bar{\rho}_{\nu}^{n}-\frac{\Delta t}{\Delta x}\Big\{A(\rho^{\Delta x}(t^{n+\frac{1}{2}},x_{\nu+\frac{1}{2}})-A(\rho^{\Delta x}(t^{n+\frac{1}{2}},x_{\nu-\frac{1}{2}})\Big\}. \quad (1.2.26)$$

Godunov scheme had a profound impact on the field of Computational Fluid Dynamics. His scheme became the forerunner for a large class of upwind finite-volume methods which are evolved in terms of (exact or approximate) Riemann solvers. In my view, the most important aspect of what Richtmyer & Morton describe as Godunov's "ingenious method" ([141, p. 338]), lies in its *global* point of view: one does not simply evolve discrete pointvalues $\{\rho_{\nu}^{n}\}$, but instead, one evolves a globally defined solution, $\rho^{\Delta x}(t,x)$, which is realized in terms of its discrete averages, $\{\bar{\rho}_{\nu}^{n}\}$.

Lax-Friedrichs Scheme. If the piecewise constant projection is carried out over alternating staggered grids,$\bar{\rho}_{\nu+\frac{1}{2}}^{n+1}:=\frac{1}{\Delta x}\int_{x}\rho^{\Delta x}(t^{n+1}-0,x)\chi_{\nu+\frac{1}{2}}(x)dx$, then one effectively integrates 'over the Riemann fan' which is centered at $(x_{\nu+\frac{1}{2}},t^{n})$. This recovers the Lax-Friedrichs (LxF) scheme, [91], with an explicit recursion formula for the evolution of its cell-averages which reads

$$\bar{\rho}_{\nu+\frac{1}{2}}^{n+1}=\frac{\bar{\rho}_{\nu}^{n}+\bar{\rho}_{\nu+1}^{n}}{2}-\frac{\Delta t}{\Delta x}\Big\{A(\bar{\rho}_{\nu+1}^{n})-A(\bar{\rho}_{\nu}^{n})\Big\}. \quad (1.2.27)$$

The Lax-Friedrichs scheme had a profound impact on the construction and analysis of approximate methods for time-dependent problems, both linear problems [51] and nonlinear systems [91]. The Lax-Friedrichs scheme was and still is the stable, all purpose benchmark for approximate solution of nonlinear systems.

Both Godunov and Lax-Friedrichs schemes realize the exact solution operator in terms of its finite-dimensional cell-averaging projection. This explains the versatility of these schemes, and at the same time, it indicates their limited resolution due to the fact that waves of different families that are averaged together at each computational cell.

Glimm Scheme. Rather than averaging, Glimm's scheme, [55], keeps its sharp resolution by *randomly sampling* the evolving Riemann waves,

$$\rho^{\Delta x}(t^{n+1},x)=\sum_{\nu}\rho^{\Delta x}(t^{n+1}-0,x_{\nu+\frac{1}{2}}+r^{n}\Delta x)\chi_{\nu+\frac{1}{2}}(x).$$

This defines the Glimm's approximate solution, $\rho^{\Delta x}(t,x)$, depending on the mesh parameters $\Delta x \equiv \lambda \Delta t$, and on the set of random variable $\{r^n\}$, uniformly distributed in $[-\frac{1}{2}, \frac{1}{2}]$. In its deterministic version, Liu [114] employs equidistributed rather than a random sequence of numbers $\{r^n\}$.

Glimm solution, $\rho^{\Delta x}(t,x)$, was then used to construct a solution for one-dimensional admissible systems of conservation laws. Glimm's celebrated theorem, [55], is still serving today as the cornerstone for existence theorems which are concerned with general one-dimensional systems, e.g. [114],[20],[146].

Theorem 1.2.4 (Existence in the large) . *There exists a weak entropy solution, $\rho(t,\cdot) \in L^\infty[[0,T], BV \cap L^\infty(\mathbb{R}_x)]$, of the strictly hyperbolic system (1.2.24), subject to initial conditions with sufficiently small variation, $||\rho_0(\cdot)||_{BV\cap L^\infty(\mathbb{R}_x)} \leq \epsilon$.*

Glimm's scheme has the advantage of retaining sharp resolution, since in each computational cell, the local Riemann solution is realized by a randomly chosen 'physical' Riemann wave. Glimm's scheme was turned into a computational tool known as the Random Choice Method (RCM) in [22], and it serves as the building block inside the front tracking method of Glimm and his co-workers, [57], [21].

1.2.4 Multidimensional systems ($m > 1, d > 1$)

Very little rigor is known on m conservation laws in d spatial dimensions once $(m-1)(d-1)$ becomes positive, i.e., general multidimensional systems. We address few major achievements.

Short time existence. For H^s-initial data ρ_0, with $s > \frac{d}{2}$, an H^s-solution exists for a time interval $[0,T]$, with $T = T(||\rho_0||_{H^s})$, consult e.g, [83],[78, §5.3].

Short time existence – piecewise analytic data. An existence resultconjectured by Richtmyer was proved by Harabetian in terms of a Cauchy-Kowalewski type existence result [68].

Short time stability – piecewise smooth shock data. Existence for piecewise smooth initial data where smoothness regions are separated by shock discontinuities was studied in [118],[106].

Riemann invariants. The gradients of *Riemann invariants* enable us to 'diagonalize' one-dimensional systems. More is known about 2×2 systems in one space dimension thanks to the existence of Riemann invariants. Consult [56], [157], [148]. Beyond $m = 2$ equations, only special systems admits a full set of Riemann invariants (consult [148] and the references therein).

Riemann problem. Already in the $d = 2$-dimensional case, the collection of simple waves and their composed interaction in the construction of Riemann solution (– subject to piecewise constant initial data), is considerably more complicated than in the one-dimensional setup. We refer to the recent book [33] for a detailed discussion.

Compressible Euler equations. These system of $m = 5$ equations governing the evolution of density, 3-vector of momentum and Energy in $d = 3$-space variables was – and still is, the prime target for further developments in our understanding of general hyperbolic conservation laws. We refer to Majda, [118], for a definitive summary of this aspect.

1.3 Total Variation Bounds

1.3.1 Finite Difference Methods

We begin by covering the space and time variables with a discrete grid: it consists of time-steps of size Δt and rectangular spatial cells of size $\Delta x := (\Delta x_1, \ldots, \Delta x_d)$. Let $\mathcal{C}_\nu$ denotes the cell which is centered around the gridpoint $x_\nu = \nu \Delta x := (\nu_1 \Delta x_1, \ldots, \nu_d \Delta x_d)$, and let $\{\rho_\nu^n\}$ denote the gridfunction associated with this cell at time $t^n = n\Delta t$. The gridfunction $\{\rho_\nu^n\}$ may represent approximate gridvalues, $\rho(t^n, x_\nu)$, or approximate cell averages, $\bar{\rho}(t^n, x_\nu)$ (as in the Godunov and LxF schemes), or a combination of higher moments, e.g., [23].

To construct a finite difference approximation of the conservation law (1.2.1), one introduce a discrete *numerical flux*, $H(\rho^n) := (H_1(\rho^n), \ldots, H_d(\rho^n))$, where $H_j(\rho^n) = H_j(\rho_{\nu-p}^n, \ldots, \rho_{\nu+q}^n)$ is an approximation to the $A_j(\rho^n)$ flux across the interface separating the cell $\mathcal{C}_\nu$ and its neighboring cell on the x_j's direction, $\mathcal{C}_{\nu+e_j}$. Next, exact derivatives in (1.2.1) are replaced by divided differences: the time-derivative is replaced with forward time difference, and spatial derivatives are replaced by spatial divided differences expressed in terms of $D_{+x_j}\phi_\nu := (\phi_{\nu+e_j} - \phi_\nu)/\Delta x_j$. We arrive at the finite-difference scheme of the form

$$\rho_\nu^{n+1} = \rho_\nu^n - \Delta t \sum_{j=1}^{d} D_{+x_j} H_j(\rho_{\nu-p}^n, \ldots, \rho_{\nu+q}^n). \tag{1.3.1}$$

The essential feature of the difference schemes (1.3.1) is their *conservation form*: perfect derivatives in (1.2.1) are replaced here by 'perfect differences'. It implies that the change in mass over any spatial domain Ω, $\sum_{\{\nu|x_\nu \in \Omega\}} \rho_\nu^{n+1}|\mathcal{C}_\nu| - \sum_{\{\nu|x_\nu \in \Omega\}} \rho_\nu^n|\mathcal{C}_\nu|$, depends solely on the discrete flux across the boundaries of that domain. This is a discrete analogue for the notion of a weak solution of (1.2.1). In their seminal paper [96], Lax & Wendroff introduced the notion of conservative schemes, and prove that their *strong* limit solutions are indeed weak solutions of (1.2.1).

Theorem 1.3.1 (Lax & Wendroff [96]) *Consider the conservative difference scheme (1.3.1), with consistent numerical flux so that $H_j(\rho, \ldots, \rho) = A_j(\rho)$. Let*

$\Delta t \downarrow 0$ with fixed grid-ratios $\lambda_j := \frac{\Delta t}{\Delta x_j} \equiv Const_j$, and let $\rho^{\Delta t} = \{\rho_\nu^n\}$ denote the corresponding solution (parameterized w.r.t. the vanishing grid-size). Assume that $\rho^{\Delta t}$ converges strongly, $s\lim \rho^{\Delta t}(t^n, x_\nu) = \rho(t,x)$, then $\rho(x,t)$ is a weak solution of the conservation law (1.2.1).

The Lax-Wendroff theorem plays a fundamental role in the development of the so called 'shock capturing' methods. Instead of tracking jump discontinuities (– by evolving the smooth pieces of the approximate solution on both sides of such discontinuities), conservative schemes capture a discretized version of shock discontinuities. Equipped with the Lax-Wendroff theorem, it remains to prove strong convergence, which leads us to discuss the compactness of $\{\rho_\nu^n\}$.

1.3.2 TVD schemes ($m = d = 1$)

We deal with scalar gridfunctions, $\{\rho_\nu^n\}$, defined on the one-dimensional Cartesian grid $x_\nu := \nu\Delta x, t^n := n\Delta t$ with fixed mesh ratio $\lambda := \frac{\Delta t}{\Delta x}$. The total variation of such gridfunction at time-level t^n is given by $\sum_\nu |\Delta\rho_{\nu+\frac{1}{2}}^n|$, where $\Delta\rho_{\nu+\frac{1}{2}}^n := \rho_{\nu+1}^n - \rho_\nu^n$. It is said to be total-variation-diminishing (TVD) if

$$\sum_\nu |\Delta\rho_{\nu+\frac{1}{2}}^n| \leq \sum_\nu |\Delta\rho_{\nu+\frac{1}{2}}^0|. \tag{1.3.2}$$

Clearly, the TVD condition (1.3.2) is the discrete analogue of the scalar TV-bound (1.2.23). Approximate solutions of difference schemes which respect the TVD property (1.3.2), share the following desirable properties:

- *Convergence* – by Helly's compactness argument, the piecewise-constant approximate solution, $\rho^{\Delta x}(t^n, x) = \sum_\nu \rho_\nu^n \chi_\nu(x)$, converges strongly to a limit function, $\rho(t^n, x)$ as we refine the grid, $\Delta x \downarrow 0$. This together with equicontinuity in time and the Lax-Wendroff theorem, yield a weak solution, $\rho(t,x)$, of the conservation law (1.2.1).

- *Spurious oscillations* – are excluded by the TVD condition (1.2.23).

- *Accuracy* – is not restricted to the first-order limitation of monotone schemes. To be more precise, let us use $\rho^{\Delta t}(t,x)$ to denote a global realization (say – piecewise polynomial interpolant) of the approximate solution $\rho_\nu^n \sim \rho^{\Delta t}(t^n, x_\nu)$. The *truncation error* of the difference scheme is the amount by which the approximate solution, $\rho^{\Delta t}(t,x)$, fails to satisfy the conservation laws (1.2.1). The difference scheme is α-order accurate if its truncation error is, namely,

$$\|\partial_t \rho^{\Delta t} + \nabla_x \cdot A(\rho^{\Delta t})\| = \mathcal{O}((\Delta t)^\alpha). \tag{1.3.3}$$

(Typically, a strong norm $\|\cdot\|$ is used which is appropriate to the problem; in general, however, accuracy is indeed a norm-dependent quantity). Consider for example, monotone difference schemes. Monotone schemes are

characterized by the fact that ρ_ν^{n+1} is an increasing function of the preceding gridvalues which participate in its stencil (1.3.1), $\rho_{\nu-p}^n, \ldots, \rho_{\nu+q}^n$ (— so that the monotonicity property (1.2.10) holds) . A classical result of Harten, Hyman & Lax [72] states that monotone schemes are at most first-order accurate. TVD schemes, however, are not restricted to this first-order accuracy limitation, at least in the one-dimensional case[1]. We demonstrate this point in the context of second-order TVD difference schemes.

We distinguish between two types of TVD schemes, depending on the size of their stencils.

Three-point schemes

Three-point schemes ($p = q = 1$ in (1.3.1)) are the simplest ones – their stencil occupies the three neighboring gridvalues, $\rho_{\nu-1}^n, \rho_\nu^n, \rho_{\nu+1}^n$. Three-point conservative schemes take the form

$$\rho_\nu^{n+1} = \rho_\nu^n - \frac{\lambda}{2}\Big\{A(\rho_{\nu+1}^n) - A(\rho_{\nu-1}^n)\Big\} + \frac{1}{2}\Big\{Q_{\nu+\frac{1}{2}}^n \Delta\rho_{\nu+\frac{1}{2}}^n - Q_{\nu-\frac{1}{2}}^n \Delta\rho_{\nu-\frac{1}{2}}^n\Big\}. \quad (1.3.4)$$

Thus, three-point schemes are identified solely by their numerical viscosity coefficient, $Q_{\nu+\frac{1}{2}}^n = Q(\rho_\nu^n, \rho_{\nu+1}^n)$, which characterize the TVD condition

$$\lambda|a_{\nu+\frac{1}{2}}^n| \le Q_{\nu+\frac{1}{2}}^n \le 1, \qquad a_{\nu+\frac{1}{2}}^n := \frac{\Delta A_{\nu+\frac{1}{2}}^n}{\Delta\rho_{\nu+\frac{1}{2}}^n}. \quad (1.3.5)$$

The schemes of Roe [139], Godunov [60], and Engquist-Osher (EO) [47], are canonical examples of *upwind* schemes, associated with (increasing amounts of) numerical viscosity coefficients, which are given by,

$$Q_{\nu+\frac{1}{2}}^{\text{Roe}} = \lambda|a_{\nu+\frac{1}{2}}^n|, \quad (1.3.6)$$

$$Q_{\nu+\frac{1}{2}}^{\text{Godunov}} = \lambda \max_{\zeta\in\mathcal{C}_{\nu+\frac{1}{2}}}\Big[\frac{A(\rho_{\nu+1}^n) - 2A(\zeta) + A(\rho_\nu^n)}{\Delta\rho_{\nu+\frac{1}{2}}^n}\Big], \quad (1.3.7)$$

$$Q_{\nu+\frac{1}{2}}^{\text{EO}} = \lambda\frac{1}{\Delta\rho_{\nu+\frac{1}{2}}^n}\int_{\rho_\nu^n}^{\rho_{\nu+1}^n} |A'(\zeta)|d\zeta. \quad (1.3.8)$$

The viscosity coefficients of the three upwind schemes are the same, $Q_{\nu+\frac{1}{2}}^n = \lambda|a_{\nu+\frac{1}{2}}^n|$, except for their different treatment of sonic points (where $a(\rho_\nu^n) \cdot a(\rho_{\nu+1}^n) < 0$). The Lax-Friedrichs (LxF) scheme (1.2.27) is the canonical *central* scheme. It has a larger numerical viscosity coefficient,

$$Q_{\nu+\frac{1}{2}}^{LxF} \equiv 1. \quad (1.3.9)$$

[1]Consult [65], regarding the first-order accuracy limitation for multidimensional $d > 1$ TVD schemes.

All the three-point TVD schemes are limited to first-order accuracy. Indeed, condition (1.3.5) is *necessary* for the TVD property of three-point schemes, [162], and hence it excludes numerical viscosity associated with the second-order Lax-Wendroff scheme, [96], $Q^{LW}_{\nu+\frac{1}{2}} = \lambda^2(a^n_{\nu+\frac{1}{2}})^2$. Therefore, scalar TVD schemes with more than first-order accuracy require at least five-point stencils.

Five-point schemes

Following the influential works of Boris & Book [6], van Leer [98], Harten [70], Osher [130], Roe [139] and others, many authors have constructed second order TVD schemes, using five-point (– or wider) stencils. For a more complete account of these works we refer to the recent books by LeVeque, [102], and Godlewski & Raviart, [58]. A large number of these schemes were constructed as second-order upgraded versions of the basic three-point *upwind* schemes. The FCT scheme of Boris & Book, [6], van Leer's MUSCL scheme [98], and the ULTIMATE scheme of Harten, [70], are prototype for this trend. In particular, in [70], Harten provided a useful sufficient criterion for the scalar TVD property, which led to the development of many non-oscillatory high-resolution schemes in the mid-80's.

Higher order *central* schemes can be constructed by upgrading the staggered LxF scheme (1.2.27). This will be the subject of our next lecture II. Here we quote a five-point TVD scheme of Nessyahu-Tadmor (NT) [126] – a second-order predictor-corrector upgrade of the staggered LxF scheme,

$$\rho^{n+\frac{1}{2}}_\nu = \bar\rho^n_\nu - \frac{\lambda}{2}(A(\bar\rho^n_\nu))', \tag{1.3.10}$$

$$\bar\rho^{n+1}_{\nu+\frac{1}{2}} = \frac{\bar\rho^n_\nu + \bar\rho^n_{\nu+1}}{2} + \\ -\frac{(\rho^n_\nu)' - (\rho^n_{\nu+1})'}{8} - \frac{\Delta t}{\Delta x}\Big\{A(\rho^{n+\frac{1}{2}}_{\nu+1}) - A(\rho^{n+\frac{1}{2}}_\nu)\Big\}. \tag{1.3.11}$$

Here, $\{w'_\nu\}$ denotes the *discrete numerical derivative* of an arbitrary grid-function $\{w_\nu\}$. The choice $w'_\nu \equiv 0$ recovers the original first-order LxF scheme (1.2.27). Second-order accuracy requires $w'_\nu \sim \Delta x \partial_x w(x_\nu)$. To guarantee the non-oscillatory properties is a key issue in the construction of higher (– than first-order..) resolution schemes; this requires more than just the naive divided differences as discrete numerical derivatives. A prototype example is the so called min-mod limiter,

$$w'_\nu = \frac{1}{2}(s_{\nu-\frac{1}{2}} + s_{\nu+\frac{1}{2}}) \cdot \min\{|\Delta w_{\nu-\frac{1}{2}}|, |\Delta w_{\nu+\frac{1}{2}}|\}, \quad s_{\nu+\frac{1}{2}} := sgn(\Delta w_{\nu+\frac{1}{2}}). \tag{1.3.12}$$

(We shall say more on (nonlinear) limiters like the min-mod below.) With this choice of a limiter, the central NT scheme (1.3.10)-(1.3.11) satisfies the TVD property, and at the same time, it retains formal second order accuracy (at least away from extreme gridvalues, ρ_ν, where $\rho'_\nu = s_{\nu-\frac{1}{2}} + s_{\nu+\frac{1}{2}} = 0$).

We conclude we few additional remarks.

Limiters A variety of discrete TVD limiters like (1.3.12) was explored during the '80s, e.g, [161] and the references therein. For example, a generalization of (1.3.12) is provided by the family of min-mod limiters depending on tuning parameters, $0 < \theta_{\nu\pm\frac{1}{2}} < 1$,

$$\begin{aligned} w'_\nu(\theta) &= \frac{1}{2}(s_{\nu-\frac{1}{2}} + s_{\nu+\frac{1}{2}}) \times \\ &\min\{\theta_{\nu-\frac{1}{2}}|\Delta w_{\nu-\frac{1}{2}}|, \frac{1}{2}|w_{\nu+1} - w_{\nu-1}|, \theta_{\nu+\frac{1}{2}}|\Delta w_{\nu+\frac{1}{2}}|\} \end{aligned} \tag{1.3.13}$$

An essential feature of these limiters is *co-monotonicity*: they are 'tailored' to produce piecewise-linear reconstruction of the form $\sum[w_\nu + \frac{1}{\Delta x}w'_\nu(x - x_\nu)]\chi_\nu(x)$, which is co-monotone with (and hence, share the TVD property of –) the underlying piecewise-constant approximation $\sum w_\nu\chi_\nu(x)$. Another feature is the limiting property at extrema gridvalues (where $w'_\nu = 0$), which is necessary in order to satisfy the TVD property (1.3.2). In this context, limiters can viewed as extrema detectors: the detection is *global*, yet they are activated *locally* (at extrema gridvalues). The study of the TVD property along these lines can be found in [164]. In particular, limiters are necessarily *nonlinear* in the sense of their stencils' dependence on the discrete gridfunction.

Systems – one-dimensional Godunov-type schemes The question of convergence for approximate solution of hyperbolic systems is tied to the question of existence of an entropy solution – in both cases there are no general theories with $m > 1$ equations[2]. Nevertheless, the ingredients of scalar high-resolution schemes were successfully integrated in the approximate solution of system of conservation laws.

Many of these high-resolution methods for systems, employ the Godunov approach, where one evolves a globally defined approximate solution, $\rho^{\Delta x}(t, x)$, which is governed by iterating the evolution-projection cycle,

$$\rho^{\Delta x}(\cdot, t) = \begin{cases} T_{\{t-t^{n-1}\}}\rho(\cdot, t^{n-1}), & t^{n-1} < t < t^n = n\Delta t, \\ P^{\Delta x}\rho(\cdot, t^n - 0), & t = t^n, \end{cases} \tag{1.3.14}$$

Here, T_t denotes the evolution operator (see (1.2.16), and $P^{\Delta x}$ is an *arbitrary, possibly nonlinear* conservative projection, which which is realized as a piecewise polynomial,

$$\rho^{\Delta x}(x, t^n) = \sum_j p_j(x)\chi_j(x), \quad \bar{p}_\nu(x_\nu) = \bar{\rho}^n_\nu. \tag{1.3.15}$$

Typically, this piecewise polynomial approximate solution is reconstructed from the previously computed cell averages, $\{\bar{\rho}^n_\nu\}$, and in this context we

[2]There is a large literature concerning two equations – the 2×2 p-system and related equations are surveyed in [157].

may, again, distinguish between two main classes of methods: *upwind* and *central* methods.

Upwind schemes evaluate cell averages at the center of the piecewise polynomial elements; integration of (1.2.24) over $C_\nu \times [t^n, t^{n+1}]$ yields

$$\bar{\rho}_\nu^{n+1} = \bar{\rho}_\nu^n - \frac{1}{\Delta x}\left[\int_{\tau=t^n}^{t^{n+1}} f(\rho(\tau, x_{\nu+\frac{1}{2}},))d\tau - \int_{\tau=t^n}^{t^{n+1}} f(\rho(\tau, x_{\nu-\frac{1}{2}},))d\tau\right].$$

This in turn requires the evaluation of fluxes along the discontinuous cell interfaces, $(\tau \times x_{\nu+\frac{1}{2}})$. Consequently, upwind schemes must take into account the characteristic speeds along such interfaces. Special attention is required at those interfaces in which there is a combination of forward- and backward-going waves, where it is necessary to decompose the "Riemann fan" and determine the separate contribution of each component by tracing "the direction of the wind". The original first-order accurate Godunov scheme (1.2.26) is the forerunner for all other upwind Godunov-type schemes. A variety of second- and higher-order sequels to Godunov upwind scheme were constructed, analyzed and implemented with great success during the seventies and eighties, starting with van-Leer's MUSCL scheme [98], followed by [139, 70, 130, 26]. These methods were subsequently adapted for a variety of nonlinear related systems, ranging from incompressible Euler equations, [4], [46], to reacting flows, semiconductors modeling, ... We refer to [59, 102] and the references therein a for a more complete accounts on these developments.

In contrast to upwind schemes, *central* schemes evaluate staggered cell averages at the breakpoints between the piecewise polynomial elements,

$$\bar{\rho}_{\nu+\frac{1}{2}}^{n+1} = \bar{\rho}_{\nu+\frac{1}{2}}^n - \frac{1}{\Delta x}\left[\int_{\tau=t^n}^{t^{n+1}} f(\tau, \rho(x_{\nu+1}))d\tau - \int_{\tau=t^n}^{t^{n+1}} f(\rho(\tau, x_\nu))d\tau\right].$$

Thus, averages are integrated over the entire Riemann fan, so that the corresponding fluxes are now evaluated at the smooth centers of the cells, (τ, x_ν). Consequently, costly Riemann-solvers required in the upwind framework, can be now replaced by straightforward quadrature rules. The first-order Lax-Friedrichs (LxF) scheme (1.2.27) is the canonical example of such central difference schemes. The LxF scheme (like Godunov's scheme) is based on a piecewise constant approximate solution, $p_\nu(x) = \bar{\rho}_\nu$. Its Riemann-solver-free recipe, however, is considerably simpler. Unfortunately, the LxF scheme introduces excessive numerical viscosity (already in the scalar case outlined in §1.3.2 we have $Q^{LxF} \equiv 1 > Q^{\text{Godunov}}$), resulting in relatively poor resolution. The central scheme (1.3.10)-(1.3.11) is a second-order sequel to LxF scheme, with greatly improved resolution. An attractive feature of the central scheme (1.3.10)-(1.3.11) is that it avoids Riemann solvers: instead of characteristic variables, one may use a componentwise extension of the non-oscillatory limiters (1.3.13).

Multidimensional systems There are basically two approaches.

One approach is to reduce the problem into a series of one-dimensional problems. Alternating Direction (ADI) methods and the closely related dimensional splitting methods, e.g., [141, §8.8-9], are effective, widely used tools to solve multidimensional problems by piecing them from one-dimensional problems – one dimension at a time. Still, in the context of nonlinear conservation laws, dimensional splitting encounters several limitations, [31]. A particular instructive example for the effect of dimensional splitting errors can be found in the approximate solution of the weakly hyperbolic system studied in [49],[81, §4.3].

The other approach is 'genuinely multidimensional'. There is a vast literature in this context. The beginning is with the pioneering multidimensional second-order Lax-Wendroff scheme, [97]. To retain high-resolution of multidimensional schemes without spurious oscillations, requires one or more of several ingredients: a careful treatment of waves propagations ('unwinding'), or alternatively, a correctly tuned numerical dissipation which is free of Riemann-solvers ('central differencing'), or the use of adaptive grids (which are not-necessarily rectangular), ... Waves propagation in the context of multidimensional upwind algorithms were studied in [25, 103, 140, 156] .... Another 'genuinely multidimensional' approach can be found in the positive schemes of [95]. The pointwise formulation of ENO schemes due to Shu & Osher, [153, 154], is another approach which avoids dimensional splitting: here, the reconstruction of cell-averages is bypassed by the reconstruction *pointvalues* of the fluxes in each dimension; the semi-discrete fluxed are then integrated in time using non-oscillatory ODEs solvers (which are briefly mentioned in §1.3.4 below). Multidimensional non-oscillatory *central* scheme was presented in [81], generalizing the one-dimensional (1.3.10)-(1.3.11); consult [105],[89] for applications to the multidimensional incompressible Euler equations. Finite volume methods, [85, 86, 24, 29]... , and finite-element methods (the streamline-diffusion and discontinuous Galerkin schemes, [76, 79, 80, 148, 122]...) have the advantage of a 'built-in' recipe for discretization over general triangular grids (we shall say more on these methods in §1.5.1 below). Another 'genuinely multidimensional' approach is based on a relaxation approximation was introduced in [82]. It employs a central scheme of the type (1.3.10)-(1.3.11) to discretize the relaxation models models, [178], [19], [125],....

1.3.3 TVD filters

Every discretization method is associated with an appropriate finite-dimensional projection. It is well known that *linear* projections which are monotone (or equivalently, positive), are at most first-order accurate, [60]. The lack of monotonicity for higher order projections is reflected by spurious oscillations in the vicinity of jump discontinuities. These are evident with the second-order (and higher) centered differences, whose dispersive nature is responsible to the formation of binary oscillations [64],[104]. With highly-accurate spectral projections,

for example, these $\mathcal{O}(1)$ oscillations reflect the familiar Gibbs phenomena.

TVD schemes avoid spurious oscillations — to this end they use the necessarily *nonlinear* projections (expressed in terms of nonlinear limiters like those in (1.3.13)). TVD filters, instead, suppress spurious oscillations. At each time-level, one post-process the computed (possibly oscillatory) solution $\{\rho(t^n)\}$. In this context we highlight the following.

• **Linear filters**. Consider linear convection problems with discontinuous initial data. Approximate solutions of such problems suffer from loss of accuracy due to propagation of singularities and their interference over domain of dependence of the numerical scheme. Instead, one can show, by duality argument, that the numerical scheme retains its original order of accuracy when the truncation in (1.3.3) is measured w.r.t. sufficiently large negative norm, [121]. Linear filters then enable to accurately recover the exact solution in any smoothness region of the exact solution, bounded away from its singular support. These filters amount to finite-order mollifiers [121], or spectrally accurate mollifiers, [119], [67], which accurately recover pointvalues from high-order moments.

• **Artificial compression**. Artificial compression was introduced by Harten [69] as a method to sharpen the poor resolution of contact discontinuities. (Typically, the resolution of contacts by α-order schemes diffuses over a fan of width $(\Delta t)^{(\alpha)/(\alpha+1)}$). The idea is to enhance the focusing of characteristics by adding an anti-diffusion modification to the numerical fluxes: if we let $H_{\nu+\frac{1}{2}}$ denote the numerical flux of a three-point TVD scheme (1.3.4), then one replaces it with a modified flux, $H_{\nu+\frac{1}{2}} \longrightarrow H_{\nu+\frac{1}{2}} + \tilde{H}_{\nu+\frac{1}{2}}$, which is expressed in terms of the min-mod limiter (1.3.12)

$$\tilde{H}_{\nu+\frac{1}{2}} := \frac{1}{\lambda}\{\rho'_\nu + \rho'_{\nu+1} - sgn(\Delta\rho_{\nu+\frac{1}{2}})|\rho'_{\nu+1} - \rho'_\nu|\}. \tag{1.3.16}$$

Artificial compression can be used as a second-order TVD filter as well. Let $Q_{\nu+\frac{1}{2}}$ be the numerical viscosity of a three-point TVD scheme (1.3.4). Then, by adding an artificial compression modification (1.3.16) which is based on the θ-limiters (1.3.13), $\rho'_\nu = \rho'_\nu(\theta)$ with $\theta_{\nu+\frac{1}{2}} := Q_{\nu+\frac{1}{2}} - \lambda^2 a^2_{\nu+\frac{1}{2}}$, one obtains a second-order TVD scheme, [70], [133]. Thus, in this case the artificial compression (1.3.16) can be viewed as a second-order anti-diffusive TVD filter of first-order TVD schemes

$$\rho^{n+1}_\nu \longleftarrow \rho^{n+1}_\nu - \{\tilde{H}_{\nu+\frac{1}{2}}(\rho^n) - \tilde{H}_{\nu-\frac{1}{2}}(\rho^n)\}. \tag{1.3.17}$$

• **TVD filters**. A particularly useful and effective, general-purpose TVD filter was introduced by Engquist et. al. in [48]; it proceeds in three steps.
{i} (Isolate extrema). First, isolate extrema cells where $\Delta\rho^n_{\nu-\frac{1}{2}} \cdot \Delta\rho^n_{\nu+\frac{1}{2}} < 0$.
{ii} (Measure local oscillation). Second, measure local oscillation, osc_ν, by setting

$$osc_\nu := \min\{m_\nu, \frac{1}{2}M_\nu\}, \qquad \left\{ \begin{matrix} m_\nu \\ M_\nu \end{matrix} \right\} = \left\{ \begin{matrix} \min \\ \max \end{matrix} \right\}(\Delta\rho^n_{\nu-\frac{1}{2}}, \Delta\rho^n_{\nu+\frac{1}{2}})$$

{iii} (Filtering). Finally, oscillatory minima (respectively – oscillatory maxima) are increased (and respectively, increased) by updating $\rho_\nu^n \to \rho_\nu^n + sgn(\Delta\rho^n_{\nu+\frac{1}{2}})osc_\nu$, and the corresponding neighboring gridvalues is modified by subtracting the same amount to retain conservation. This post-processing can be repeated, if necessary, and one may use a local maximum principle, $\min_j \rho_j^n \le \rho_\nu^n \le \max_j \rho_j^n$ as a stopping criterion. In this case, the above filter becomes TVD once the binary oscillations are removed, [155].

1.3.4 TVB approximations ($m \ge 1, d = 1$)

One sided stability

As an example for Total variation Bounded (TVB) approximations, we begin with the example of approximate solutions satisfying the one-sided Lip^+ stability condition.

Let $\{\rho^\varepsilon(t,x)\}$ be a family of approximate solutions, tagged by their small-scale parameterization, ε. To upper-bound the convergence rate of such approximations, we shall need the usual two ingredients of stability and consistency.

- *Lip^+-stability.* The family $\{\rho^\varepsilon\}$ is Lip^+-stable if

$$\|\rho^\varepsilon(t,\cdot)\|_{Lip^+} := \sup_x \partial_x \rho^\varepsilon(t,x) \le Const. \tag{1.3.18}$$

This notion of Lip^+-stability is motivated by Oleĭnik's One-Sided Lipschitz Condition (OSLC), $\rho_x(t,\cdot) \le Const$, which uniquely identifies the entropy solution of *convex* conservation laws, (1.2.24), with scalar $A'' > 0$ (we refer to [100] for a recent contribution concerning the one-sided stability of one-dimensional systems). Since the Lip^+-(semi)-norm dominates the total-variation,

$$\|\rho^\varepsilon(t,\cdot)\|_{BV} \le Const.\|\rho^\varepsilon(t,\cdot)\|_{Lip^+} + \|\rho_0^\varepsilon(\cdot)\|_{L^1}, \quad Const = 2|\mathrm{supp}_x \rho^\varepsilon(t,\cdot)|,$$

$\{\rho^\varepsilon\}$ are TVB and by compactness, convergence follows. Equipped with Lip^+-stability, we are able to *quantify* this convergence statement. To this end, we measure the local truncation error in terms of

- *Lip'-consistency.* The family $\{\rho^\varepsilon\}$ is Lip'-consistent of order ε if

$$\|\partial_t \rho^\varepsilon + \partial_x A(\rho^\varepsilon)\|_{Lip'(t,x)} \sim \varepsilon. \tag{1.3.19}$$

It follows that the stability+consistency in the above sense, imply the convergence of $\{\rho^\varepsilon\}$ to the entropy solution, ρ, and that the following error estimates hold [166], [127],

$$\|\rho^\varepsilon(t,\cdot) - \rho(t,\cdot)\|_{W^s(L^p(x))} \sim \varepsilon^{\frac{1-sp}{2p}}, \quad -1 \le s \le 1/p. \tag{1.3.20}$$

The case $(s,p) = (-1,1)$ corresponds to a sharp Lip'-error estimate of order ε — the Lip'-size of the truncation in (1.3.19); the case $(s,p) = (0,1)$ yields an L^1-error estimate of order one-half, in agreement with Kuznetsov's general convergence theory, [90].

Multidimensional extensions to convex Hamilton-Jacobi equations are treated in [107]. We note in passing that the requirement of Lip^+ stability restricts our discussion to *convex* problems; at the same time, it yields more than just convergence. Indeed, the above error estimate, as well as additional *local* error estimates will discussed in lecture IV.

Higher resolution schemes (with three letters acronym)

We have already mentioned the essential role played by nonlinear limiters in TVD schemes. The mechanism in these nonlinear limiters is switched on in extrema cells, so that the zero discrete slope $\rho' = 0$ avoids new spurious extrema. This, in turn, leads to deteriorated first-order local accuracy at non-sonic extrema, and global accuracy is therefore limited to second-order[3].

To obtain an improved accuracy, one seeks a more accurate realization of the approximate solution, in terms of higher (than first-order) piecewise polynomials

$$\rho^{\Delta x}(t^n, x) = \sum_\nu p_\nu(x)\chi_\nu(x), \quad p_\nu(x) = \sum_j \rho_\nu^{(j)}(\frac{x - x_\nu}{\Delta x})^j/j!. \tag{1.3.21}$$

Here, the exact solution is represented in a cell $\mathcal{C}_\nu$ in terms of an r-order polynomial p_ν, which is reconstructed from the its neighboring cell averages, $\{\bar\rho_{\nu_\mu}\}$. If we let $\rho^{\Delta x}(t \geq t^n, \cdot)$ denote the entropy solution subject to the reconstructed data at $t = t^n$, $P^{\Delta x}\rho(t^n, \cdot)$, then the corresponding Godunov-type scheme governs the evolution of cell averages

$$\bar\rho_\nu^{n+1} := \frac{1}{\Delta x}\int_x \rho^{\Delta x}(t^{n+1} - 0, x)\chi_\nu(x)dx. \tag{1.3.22}$$

The properties of Godunov-type scheme are determined by the polynomial reconstruction should meet three contradicting requirements:

{i} *Conservation*: $p_\nu(x)$ should be cell conservative in the sense that $\fint_{\mathcal{C}_\nu} p_\nu(x) = \fint_{\mathcal{C}_\nu} \rho_\nu(x)$. This tells us that $P^{\Delta x}$ is a (possibly nonlinear) projection, which in turn makes (1.3.22) a conservative scheme in the sense of Lax-Wendroff, (1.3.1).

{ii} *Accuracy*: $\rho_\nu^{(j)} \sim (\Delta x\partial_x)^j\rho(t^n, x_\nu)$.

At this stage, we have to relax the TVD requirement. This brings us to the third requirement of

{iii} *TVB bound*: we seek a bound on the total variation on the computed solution. Of course, a bounded variation, $\|\rho^{\Delta x}(t^n, \cdot)\|_{BV} \leq$ Const. will suffice for convergence by L^1-compactness arguments (Helly's theorem).

The (re-)construction of non-oscillatory polynomials led to new high-resolution schemes. In this context we mention the following methods (which were popularized by their trade-mark of three-letters acronym ...): the Piecewise-Parabolic

[3]The implicit assumption is that we seek an approximation to *piecewise-smooth* solutions with finitely many oscillations, [169]. The convergence theories apply to general BV solutions. Yet, general BV solutions cannot be resolved in *actual* computations in terms of 'classical' macroscopic discretizations – finite-difference, finite-element, spectral methods, etc. Such methods can faithfully resolve piecewise smooth solutions.

Method (PPM) [26], the Uniformly Non-Oscillatory (UNO) scheme [74], and the Essentially Non-Oscillatory schemes (ENO) of Harten et. al. [71]. The particular topic of ENO schemes is covered in C.-W. Shu's lectures elsewhere in this volume.

There is large numerical evidence that these highly-accurate methods are TVB (and hence convergent), at least for a large class of piecewise-smooth solutions. We should note, however, that the convergence question of these schemes is open. (It is my opinion that new characterizations of the (piecewise) regularity of solutions to conservation laws, e.g., [38],[169] together with additional tools to analyze their compactness, are necessary in order to address the questions of convergence and stability of these highly-accurate schemes).

There are alternative approach to to construct high-resolution approximations which circumvent the TVD limitations. We conclude by mentioning the following two.

One approach is to evolve more than one-piece of information per cell. This is fundamentally different from standard Godunov-type schemes where only the cell average is evolved (and higher order projections are *reconstructed* from these averages – one per cell). In this context we mention the quasi-monotone TVB schemes introduced in [23]. Here, one use a TVD evolution of cell averages together with additional higher moments. Another instructive example for this approach is found in the third-order TVB scheme, [144]: in fact, Sanders constructed a third-order non-expansive scheme (circumventing the first-order limitation of [72]), by using a 2×2 system which governs the first two moments of the scalar solution. More recently, Bouchut et. al. [8], constructed a second-order MUSCL scheme which respects a discrete version of the entropy inequality (1.2.3) w.r.t *all* Kružkov's scalar entropy pairs in (1.2.8); this circumvents the second-order limitation of Osher & Tadmor [133, Theorem 7.3], by evolving *both* – the cell average and the discrete slope in each computational cell.

Another approach to enforce a TVB bound on higher(> 2)-resolution schemes, makes use of gridsize-dependent limiters, $\rho^{(j)} = \rho^{(j)}\{\bar{\rho}^n, \Delta x\}$, such that the following holds, e.g., [151],

$$\|\rho^{\Delta x}(t^{n+1}, \cdot)\|_{BV} \leq \|\rho^{\Delta x}(t^{n+1}, \cdot)\|_{BV} + \text{Const} \cdot \Delta x.$$

Such Δx-dependent limiters fail to satisfy, however, the basic dilation invariance of (1.2.24)-(1.2.25), $(t, x) \to (ct, cx)$.

Time discretizations

One may consider separately the discretization of time and spatial variables. Let P_N denote a (possibly nonlinear) finite-dimensional spatial discretization of (1.2.1); this yields an N-dimensional approximate solution, $\rho_N(t)$, which is governed by the system of N nonlinear ODEs

$$\frac{d}{dt}\rho_N(t) = P_N(\rho_N(t)). \tag{1.3.23}$$

System (1.3.23) is a *semi-discrete* approximation of (1.2.1). For example, if we let $P_N = P^{\Delta x}$, $N \sim (\Delta x)^{-d}$, to be one of the piecewise-polynomial reconstructions associated with Godunov-type methods in (1.3.21), then one ends up with a semi-discrete finite-difference method, the so called method of lines. In fact, our discussion on streamline-diffusion and spectral approximations in §1.4.2 and §1.4.3 below will be primarily concerned with such semi-discrete approximations.

An explicit time discretization of (1.3.23) proceeds by either a multi-level or a Runge-Kutta method. A CFL condition should be met, unless one accounts for wave interactions, consult [101]. For the construction of non-oscillatory schemes, one seeks time discretizations which retain the non-oscillatory properties of the spatial discretization, P_N. In this context we mention the TVB time-discretizations of Shu & Osher, [152],[153, 154]. Here, one obtains high-order multi-level and Runge-Kutta time discretizations as *convex combinations* of the standard forward time differencing, which amounts to the first-order accurate forward Euler method. Consequently, the time discretizations [153, 154] retain the nonoscillatory properties of the low-order forward Euler time differencing — in particular, TVD/TVB bounds, and at the same time, they enable to match the time accuracy with the high-order spatial accuracy.

Cell entropy inequality

Approximate solutions with bounded variation (obtained by TVD/TVB schemes) converge to *a weak* solution; the question of uniqueness is addressed by an entropy condition. In the context of finite-difference scheme, one seeks a cell entropy inequality – a conservative discrete analogue of the entropy inequality (1.2.3),

$$\eta(\rho_\nu^{n+1}) \le \eta(\rho_\nu^n) - \Delta t \sum_{j=1}^{d} D_{+x_j} G_j(\rho_{\nu-p}^n, \ldots, \rho_{\nu+q}^n). \tag{1.3.24}$$

By arguments à la Lax & Wendroff (Theorem 1.3.1), any approximate solution which satisfies (1.3.24) with a consistent numerical entropy flux, $G_j(\rho, \ldots, \rho) = F_j(\rho)$, its strong limit satisfies (1.2.3), which in turn yields uniqueness, at least in the scalar case. Crandall & Majda, [30], following Harten, Hyman & Lax in [72], were the first to implement this approach in the context of monotone difference schemes (in fact, the abstract setup of Theorem 1.2.2 directly applies in this case). Osher [130] introduced the so-called numerical E-fluxes to guarantee the cell entropy inequality. In [163] we prove the entropy inequality for general fully-discrete E-schemes: the proof is based on the key observation that the numerical viscosity (— quantified in terms of the numerical viscosity coefficient Q in (1.3.4)), associated with any E-flux, is a convex combination of the Godunov and Lax-Friedrichs viscosities, given in (1.3.7) and (1.3.9), respectively. Applications to the question of multidimensional convergence can be found in [85],[86],[24],[128].... E-fluxes are restricted to first-order accuracy, since they are consistent with *all* Kružkov's entropy pairs. A systematic study of the cell entropy inequality for second-order resolution scheme can be found in [133] (for

upwind schemes) and in [126] (for central schemes). The above discussion is restricted to scalar problems. Of course, general Godunov and LxF schemes ($m > 1, d = 1$), satisfy a cell entropy inequality because the Riemann solutions do. (For the LxF scheme, we refer to Lax, [93], who proved the cell entropy inequity *independently* of the Riemann solution.

1.4 Entropy Production Bounds

1.4.1 Compensated compactness ($m \leq 2, d = 1$)

We deal with a family of approximate solutions, $\{\rho^\varepsilon\}$, such that

(i) *It is uniformly bounded*, $\rho^\varepsilon \in L^\infty$, with a weak* limit, $\rho^\varepsilon \rightharpoonup \rho$;

(ii) *The entropy production*, for all convex entropies η, lies in a compact subset of $W^{-1}_{loc}(L^2(t,x))$,

$$\forall \eta'' > 0: \qquad \partial_t \eta(\rho^\varepsilon) + \partial_x F(\rho^\varepsilon) \hookrightarrow W^{-1}_{loc}(L^2(t,x)). \tag{1.4.1}$$

The conclusion is that $A(\rho^\varepsilon) \rightharpoonup A(\rho)$, and hence ρ is a weak solution; in fact, there is a strong convergence, $\rho^\varepsilon \to \rho$, on any nonaffine interval of $A(\cdot)$. For a complete account on the theory of compensated compactness we refer to the innovative works of Tartar [171] and Murat [124]. In the present context, compensated compactness argument is based on a clever application of the div-curl lemma. First scalar applications are due to Murat-Tartar, [123],[171], followed by extensions to certain $m = 2$ systems by DiPerna [40] and Chen [17].

The current framework has the advantage of dealing with L^2-type estimates rather than the more intricate BV framework. How does one verify the $W^{-1}_{loc}(L^2)$-condition (1.4.1)? we illustrate this point with canonical viscosity approximation (1.2.2). Multiplication by η' shows that its entropy production amounts to $\varepsilon(\eta' Q \rho^\varepsilon_x)_x - \varepsilon \eta'' Q (\rho^\varepsilon_x)^2$. By entropy convexity, $\varepsilon \eta'' Q > 0$[4], and space-time integration yields

- *An entropy production bound*

$$\sqrt{\varepsilon} \| \frac{\partial \rho^\varepsilon}{\partial x} \|_{L^2_{loc}(t,x)} \leq Const. \tag{1.4.2}$$

Though this bound is too weak for strong compactness, it is the key estimate behind the $W^{-1}_{loc}(L^2)$-compactness condition (1.4.1). We continue with the specific examples of streamline-diffusion in §1.4.2 and spectral viscosity methods in §1.4.3.

[4] Observe that the viscosity matrix is therefore required to be positive w.r.t. the Hessian η''.

1.4.2 The streamline diffusion finite-element method

The Streamline Diffusion (SD) finite element scheme, due to Hughes, Johnson, Szepessy and their co-workers [76], [79], [80], was one of the first methods whose convergence was analyzed by compensated compactness arguments. (Of course, finite-element methods fit into L^2-type Hilbert-space arguments). In the SD method, formulated here in several space dimensions, one seeks a piecewise polynomial, $\{\rho^{\Delta x}\}$, which is uniquely determined by requiring for all piecewise polynomial test functions $\psi^{\Delta x}$,

$$\left(\partial_t \rho^{\Delta x} + \nabla_x \cdot A(\rho^{\Delta x}),\ \psi^{\Delta x} + |\Delta x| \cdot \boxed{(\psi_t^{\Delta x} + A'(\rho^{\Delta x})\psi_x^{\Delta x})}\right) = 0. \qquad (1.4.3)$$

Here, Δx denotes the spatial grid size (for simplicity we ignore time discretization). The expression inside the framed box on the left represents a diffusion term along the streamlines, $\dot{x} = A'(\rho^{\Delta x})$. Setting the test function, $\psi^{\Delta x} = \rho^{\Delta x}$, (1.4.3) yields the desired entropy production bound

$$\sqrt{\Delta x}\|\partial_t \rho^{\Delta x} + \nabla_x \cdot A(\rho^{\Delta x})\|_{L^2_{loc}(t,x)} \leq Const. \qquad (1.4.4)$$

Thus, the spatial derivative in (1.4.2) is replaced here by a streamline-directional gradient. This together with an L^∞-bound imply $W^{-1}_{loc}(L^2)$-compact entropy production, (1.4.1), and convergence follows [79],[80],[160]. We note in passing that the extension of the SD method for systems of equations is carried out by projection into entropy variables, [120], which in turn provide the correct interpretation of (1.4.4) as an entropy production bound.
The lectures of C. Johnson in this volume will present a comprehensive discussion of the streamline diffusion method and its related extensions.

1.4.3 The spectral viscosity method

Since spectral projections are inherently oscillatory, they do not lend themselves to á priori TVB bound. Spectral methods provide another example for a family of approximate solutions whose convergence could be better dealt, therefore, by compensated compactness arguments. Spurious Gibbs oscillations violate the strict TVD condition in this case. Instead, an entropy production bound, analogous to (1.4.2) is sought. Indeed, such bound could be secured by spectrally accurate hyper-viscosity which is expressed in terms of the computed Fourier coefficients. This leads us to a discussion on the Spectral Viscosity (SV) method.

Let P_N denote an appropriate spatial projection into the space of N-degree polynomials,

$$P_N \rho(t,x) = \sum_{|k| \leq N} \hat{\rho}_k(t)\phi_k(x);$$

here $\{\phi_k\}$ stands for a given family of orthogonal polynomials, either trigonometric or algebraic ones, e.g., $\{e^{ikx}\}$, $\{L_k(x)\}$, $\{T_k(x)\}$, etc. The corresponding N-degree approximate solution, $\rho_N(t,x)$, is governed by the spectral viscosity

(SV) approximation

$$\partial_t \rho_N + \partial_x P_N A(\rho_N) = \frac{(-1)^{s+1}}{N^{2s-1}} \partial_x^s (Q * \partial_x^s \rho_N). \tag{1.4.5}$$

The left hand side of (1.4.5) is the standard spectral approximation of the conservation law (1.2.1). The expression on the right

$$\frac{(-1)^{s+1}}{N^{2s-1}} \partial_x^s (Q * \partial_x^s \rho_N) := \frac{(-1)^{s+1}}{N^{2s-1}} \sum_{|k|>N^\theta} \hat{Q}_k \hat{\rho}_k(t) \phi_k^{(2s)}(x), \tag{1.4.6}$$

represents the so called spectral viscosity introduced in [165]. It contains a minimal amount of high-modes regularization which retains the underlying spectral accuracy of the overall approximation. The case $s = 1$ corresponds to a truncated second-order viscosity

$$\frac{1}{N} \partial_x (Q * \partial_x \rho_N) := \frac{1}{N} \sum_{|k|>N^\theta} \hat{Q}_k \hat{\rho}_k(t) \phi_k''(x).$$

It involves a viscous-free zone for the first N^θ modes, $0 < \theta < \frac{1}{2}$. High modes diffusion is tuned by the viscosity coefficients $\hat{Q}_k$.

Larger s's corresponds to truncated hyper-diffusion of order $2s$. This allows for even a larger viscosity-free zone of size N^θ, with $0 < \theta < \frac{2s-1}{2s}$ (with possibly $s = s_N \leq \sqrt{N}$), consult [167]. The underlying hyper-viscosity approximation (for say $s = 2$) reads

$$\partial_t \rho^\varepsilon + \partial_x A(\rho^\varepsilon) + \varepsilon^3 \partial_x^4 \rho^\varepsilon = 0. \tag{1.4.7}$$

We note that already the solution operator associated with (1.4.7) is not monotone, hence L^1-contraction and the TVD condition fail in this case.

Instead, an L^2-type entropy production estimate analogous to (1.4.2)

$$\frac{1}{\sqrt{N}} \| \frac{\partial \rho_N}{\partial x} \|_{L^2_{loc}(t,x)} \leq Const.$$

together with an L^∞-bound, carry out the convergence analysis by compensated compactness arguments, [165], [117]. Extensions to certain $m = 2$ systems can be found in [145]. We shall return to a detailed discussion on the SV method in our lecture III.

1.5 Measure-valued solutions($m = 1, d \geq 1$)

We turn our attention to the multidimensional scalar case, dealing with a families of uniformly bounded approximate solutions, $\{\rho^\varepsilon\}$, with weak* limit, $\rho^\varepsilon \rightharpoonup \rho$. DiPerna's result [42] states that if the entropy production of such a family tends weakly to a negative measure, $m \leq 0$,

$$\forall \eta'' > 0 : \qquad \partial_t \eta(\rho^\varepsilon) + \nabla_x \cdot F(\rho^\varepsilon) \rightharpoonup m \leq 0, \tag{1.5.1}$$

then the measure-valued solution ρ coincides with the entropy solution, and convergence follows. This framework was used to prove the convergence of multi-dimensional finite-difference schemes [27], streamline diffusion method [79],[80], spectral-viscosity approximations [18] and finite-volume schemes [24], [86],[85]. We focus our attention on the latter.

1.5.1 Finite volume schemes ($d \geq 1$)

We are concerned with finite-volume schemes based on possibly *unstructured* triangulation grid $\{T_\nu\}$ (for simplicity we restrict attention to the $d = 2$ case). The spatial domain is covered by a triangulation, $\{T_\nu\}$, and we compute approximate averages over these triangles, $\bar{\rho}_\nu^n \sim \frac{1}{|T_\nu|}\int_{T_\nu} \rho(t^n, x)dx$, governed by the finite volume (FV) scheme

$$\bar{\rho}_\nu^{n+1} = \bar{\rho}_\nu^n - \frac{\Delta t}{|T_\nu|}\sum_\mu \tilde{A}_{\nu_\mu}(\rho_\nu^n, \rho_{\nu_\mu}^n). \tag{1.5.2}$$

Here $\tilde{A}_{\nu_\mu}$ stand for approximate fluxes across the interfaces of T_ν and its neighboring triangles (identified by a secondary index μ).

Typically, the approximate fluxes, $\tilde{A}_{\nu_\mu}$ are derived on the basis of approximate Riemann solvers across these interfaces, which yield a monotone scheme. That is, the right hand side of (1.5.2) is a monotone function of its arguments $(\rho_\nu^n, \rho_{\nu_\mu}^n)$, and hence the corresponding FV scheme is L^1-contractive. However, at this stage one cannot proceed with the previous compactness arguments which apply to TVD schemes over fixed Cartesian grid: since the grid is unstructured, the discrete solution operator is not translation invariant and L^1-contraction need not imply a TV bound. Instead, an entropy dissipation estimate yields

$$\sum_n \Delta t \sum_{\nu,\mu} |\rho_\nu^n - \rho_{\nu_\mu}^n|(\Delta x)^\theta \leq Const, \quad 0 < \theta < 1. \tag{1.5.3}$$

Observe that (1.5.3) is weaker than a TV bound (corresponding to $\theta = 0$), yet it suffices for convergence to a measure-valued solution, consult [24], [85].
These questions will be addressed in B. Cockburn's lectures, later in this volume.

1.6 Kinetic Approximations

By a *kinetic formulation* of (1.2.1) we mean a representation of the solution $\rho(t, x)$ as the average of a 'microscopic' density function, $f(t, x, v)$. The formulation is a kinetic one by its analogy with the classical kinetic models such as Boltzmann or Vlasov models - see for instance [15],[44]. In particular, we add a real-valued variable called velocity, v, and the unknown becomes a 'density-like' function, $f(t, x, v)$, which is governed by an appropriate transport equation.

A useful tool in this context is the *velocity averaging lemma*, dealing with the regularity of the moments for such transport solutions.

1.6.1 Velocity averaging lemmas ($m \geq 1, d \geq 1$)

We deal with solutions to transport equations

$$a(v) \cdot \nabla_x f(x,v) = \partial_v^s g(x,v). \tag{1.6.1}$$

The averaging lemmas, [62], [53], [45], state that in the generic non-degenerate case, averaging over the velocity space, $\bar{f}(x) := \int_v f(x,v)dv$, yields a gain of *spatial* regularity. The prototype statement reads

Lemma 1.6.1 ([62],[45],[111]) . *Let $f \in L^p(x,v)$ be a solution of the transport equation (1.6.1) with $g \in L^q(x,v), 1 \leq q < p \leq 2$. Assume the following non-degeneracy condition holds*

$$meas_v\{v|\ |a(v)\cdot\xi| < \delta\}_{|\xi|=1} \leq Const \cdot \delta^\alpha, \quad \alpha \in (0,1). \tag{1.6.2}$$

Then $\bar{f}(x) := \int_v f(x,v)dv$ belongs to Sobolev space $W^\theta(L^r(x))$,

$$\bar{f}(x) \in W^\theta(L^r(x)), \qquad \theta < \frac{\alpha}{\alpha(1-\frac{p'}{q'})+(s+1)p'}, \quad \frac{1}{r} = \frac{\theta}{q} + \frac{1-\theta}{p}. \tag{1.6.3}$$

Variants of the averaging lemmas were used by DiPerna and Lions to construct global weak (renormalized) solutions of Boltzmann, Vlasov-Maxwell and related kinetic systems, [43], [44]; in Bardos et. al., [2], averaging lemmas were used to construct solutions of the incompressible Navier-Stokes equations. We turn our attention to their use in the context of nonlinear conservation laws and related equations.

1.6.2 Nonlinear conservation laws

As a prototype example we begin with a Boltzmann-like – or more precisely, a BGK-like model proposed in [136]. Its 'hydrodynamical limit' describes both the scalar conservation law (1.2.1) together with its entropy inequalities, (1.2.20). It consists in solving the transport equation

$$\frac{\partial f^\varepsilon}{\partial t} + a(v)\cdot\nabla_x f^\varepsilon = \frac{1}{\varepsilon}\left(\chi_{\rho^\varepsilon}(v) - f^\varepsilon\right), \quad (t,x,v) \in \mathbb{R}_t^+ \times \mathbb{R}_x^d \times \mathbb{R}_v, \tag{1.6.4}$$

$$f^\varepsilon|_{t=0} = \chi_{\rho_0(x)}(v), \quad (x,v) \in \mathbb{R}_x^d \times \mathbb{R}_v. \tag{1.6.5}$$

Here, $\chi_{\rho^\varepsilon(t,x)}(v)$ denotes the 'pseudo-Maxwellian',

$$\chi_{\rho^\varepsilon}(v) := \begin{cases} +1 & 0 < v < \rho^\varepsilon \\ -1 & \rho^\varepsilon < v < 0 \\ 0 & |v| > \rho^\varepsilon \end{cases}, \tag{1.6.6}$$

which is associated with the average of f^ε,

$$\rho^\varepsilon(t,x) = \bar{f^\varepsilon} := \int_{\mathbb{R}} f^\varepsilon(t,x,v)dv, \quad (t,x) \in R_t^+ \times R_x^d. \tag{1.6.7}$$

Notice that the BGK-like model in (1.6.4)-(1.6.7) is a semilinear, nonlocal, hyperbolic (first-order) equation which is rather simple to solve for fixed $\varepsilon > 0$. This kinetic model was introduced in [136], following the earlier works [9],[54]. It follows that that if $\rho_0 \in L^1(\mathbb{R}^d) \cap L^\infty(\mathbb{R}^d)$, then ρ^ε converges in $L^1((0,T) \times \mathbb{R}^d)$ to the unique entropy solution (1.2.1), (1.2.20). In fact, there is a convergence on the underlying microscopic level, to a kinetic formulation of (1.2.1), (1.2.20). The latter is described by a limiting 'density-function', $f(t,x,v)$, which is governed by the transport equation

$$\frac{\partial f}{\partial t} + a(v) \cdot \nabla_x f = \frac{\partial m}{\partial v} \qquad (t,x,v) \in \mathcal{D}'(\mathbb{R}_t^+ \times \mathbb{R}_x^d \times \mathbb{R}_v) \tag{1.6.8}$$

subject to initial conditions

$$f = \chi_{\rho_0(t,x)}(v). \tag{1.6.9}$$

Here, m is a nonnegative bounded measure on $\mathbb{R}_t^+ \times \mathbb{R}_x^d \times \mathbb{R}_v$.

In what sense does the kinetic formulation (1.6.8-1.6.9) 'describe' the conservation law (1.2.1-1.2.20)? observe that by averaging of (1.6.8) one recovers the conservation law (1.2.1), and taking its higher moments by integration against $\eta'(v)$, one recovers Kružkov entropy inequalities (1.2.20)) for *all convex* entropies η.

Theorem 1.6.1 *Consider the BGK-like model (1.6.4)-(1.6.5).*

{i} There exists a nonnegative measure, $m^\varepsilon(t,x,v)$, which is bounded independently of ε, such that the relaxation term on the right of (1.6.4) admits

$$\frac{1}{\varepsilon}(\chi_{\rho^\varepsilon} - f^\varepsilon) = \frac{\partial m^\varepsilon}{\partial v}, \quad m^\varepsilon \geq 0. \tag{1.6.10}$$

{ii} The solution f^ε of the kinetic model (1.6.4)-(1.6.5) converges in $L^1((0,T) \times \mathbb{R}_x^d \times \mathbb{R}_v)$ $(\forall\, T < \infty)$ to the solution of (1.6.8)-(1.6.9). In addition, its associated measure, m^ε, converges weakly to the measure, m, uniquely determined by the kinetic formulation (1.6.8)-(1.6.9) with $f = \chi_\rho$.

Remark. One may deduce from the above result and from [136] that m vanishes on open sets of the form $\{(x,v,t) \,/\, (x,t) \in \mathcal{O}\, v \in \mathbb{R}\}$ where $\mathcal{O}$ is an open set on which ρ is locally Lipschitz. In other words, m is 'supported by the shocks".

Proof. Several proof are available, each highlights the related aspects of this issue.

One approach makes use of the simple H-functions, à la Boltzmann, constructed in [136], $H_c(f^\varepsilon) := |f^\varepsilon - \chi_c|$.

Lemma 1.6.2 *[136, Corollary 3.2] For any real c the following functions*

$$H_c(f^\varepsilon) := |f^\varepsilon - \chi_c|$$

are kinetic entropy functions, i.e., we have

$$\int_v [\partial_t + a(v) \cdot \nabla_x] |f^\varepsilon - \chi_c| dv \leq 0. \tag{1.6.11}$$

Let us remark that our kinetic entropy functions, $H_c(f^\varepsilon)$, are intimately related to Kružkov entropy functions, (1.2.8). Indeed, in [136] we prove that as $\varepsilon \downarrow 0$, f_ε approaches χ_ρ. With this in mind, the inequality (1.6.11) turns into Kružkov's entropy inequality (1.2.20). The entropy (or H-)inequality, (1.6.11), then yields macroscopic convergence by compensated compactness arguments in the one-dimensional case, and by BV+entropy production bounds in the multidimensional case. Earlier works on kinetic models related to (1.6.8) can be found in [9],[54],[84].

An alternative proof, presented in [111], makes use of the averaging lemma, 1.6.1. In view of the results recalled above, we just have to verify that (1.6.10) holds, $\frac{1}{\varepsilon}\left(\chi_{\rho^\varepsilon} - f^\varepsilon\right) = \frac{\partial m_\varepsilon}{\partial v}$. This fact can be shown in several ways.

One way is to observe that if $g(v)$ is an $L^1(\mathbb{R})$ function which satisfy (– as f^ε does),

$$0 \le \operatorname{sign}(v) g \le 1, \quad \int_{\mathbb{R}} g(v)\, dv = \alpha \tag{1.6.12}$$

then there exists a nonnegative, bounded, continuous q such that

$$\chi_\alpha(v) - g(v) \;=\; q'(v), \quad q \in \mathcal{C}_+. \tag{1.6.13}$$

Indeed, set $q(v) = \int_{-\infty}^{v} (\chi_\alpha(w) - g(w)) dw$: in the case $\alpha > 0$ (– the other case being treated similarly), we see that q is nondecreasing on $(-\infty, \alpha)$ and nonincreasing on $(\alpha, +\infty)$ and we conclude since $q(-\infty) = 0$ and $q(+\infty) = \alpha - \int_{\mathbb{R}} g\, dv = 0$.

The characterization in (1.6.13) of g's satisfying (1.6.12), is in fact equivalent with the following elementary lemma due to Brenier [9], which in turn yields still another possible proof for the desired representation of the relaxation term in (1.6.10).

Lemma 1.6.3 *[9] Let $\alpha \in \mathbb{R}$ and let φ be a C^1 convex function on $\mathbb{R}$ such that φ' is bounded. Then, $\chi_\alpha(v)$ is a minimizer of $\inf_{\mathcal{G}} \left\{ \int_{\mathbb{R}} \varphi'(v) g(v)\, dv \right\}$ where the infimum is taken over all $g \in \mathcal{G} := \left\{ g \in L^1(\mathbb{R}), \quad \int_{\mathbb{R}} g dv = \alpha, \quad 0 \le g \operatorname{sign}(v) \le 1 \right\}$. In addition, $\chi_\alpha(v)$ is the unique minimizer if φ' is strictly increasing on $\mathbb{R}$.*

Granted that (1.6.10) holds, i.e., the relaxation term on the right of (1.6.4) belongs to $W_v^{-1}(\mathcal{M}_{t,x})$, then the averaging lemma 1.6.1 applies with $s = q = 1$, $p = 2$ (here we identify, $t \leftrightarrow x_0$, $\tau \leftrightarrow \xi_0$, $a_0(v) \equiv 1$). It follows that if the conservation law is linearly non-degenerate in the sense that (1.6.2) holds, that is, if $\exists \alpha \in (0,1)$ such that

$$meas\{v|\ |\tau + A'(v) \cdot \xi| < \delta\} \le Const \cdot \delta^\alpha, \quad \forall\ \tau^2 + |\xi|^2 = 1, \tag{1.6.14}$$

then, $\{\rho^\varepsilon\}$ is compact – in fact $\{\rho^\varepsilon(t > 0, \cdot)\}$ gains Sobolev regularity of order $s = \frac{\alpha}{\alpha+4}$. ■

We conclude this section with several remarks.

Regularizing effect

We have shown above how the averaging lemma implies convergence under the non-degeneracy condition (1.6.14). Moreover, in this case we quantified the Sobolev W^s-regularity of the approximate solutions, $\{\rho^\varepsilon\}$. In fact, even more can be said if the solution operator associated with $\{\rho^\varepsilon\}$ is translation invariant: a bootstrap argument presented in [111] yields the improved regularity of order $s = \frac{\alpha}{\alpha+2}$,

$$\rho^\varepsilon(t > 0, \cdot) \in W^{\frac{\alpha}{\alpha+2}}(L^1(x)). \tag{1.6.15}$$

This shows that due to nonlinearity, (1.6.14), the corresponding solution operator, T_t, has a *regularization* effect, as it maps $L^\infty_c \longrightarrow W^s(L^1)$ with $s, t > 0$.

In particular, this framework provides an alternative route to analyze the convergence of general entropy stable multidimensional schemes, *independent* of the underlying kinetic formulations. Here we refer to finite-difference, finite-volume, streamline-diffusion and spectral approximations ..., which were studied in [29, 24, 85, 86, 79, 80, 18], for example. Indeed, the key feature in the convergence proof for all of these methods is the $W^{-1}_{loc}(L^2)$-compact entropy production,

$$\partial_t \eta(\rho^\varepsilon) + \nabla_x \cdot F(\rho^\varepsilon) \hookrightarrow W^{-1}_{loc}(L^2(t,x)), \quad \forall \eta'' > 0. \tag{1.6.16}$$

Hence, if the underlying conservation law satisfies the non-linear degeneracy condition (1.6.14), then the corresponding family of approximate solutions, $\{\rho^\varepsilon(t > 0, \cdot)\}$ becomes compact. Moreover, if the entropy production is in fact a bounded measure, (– and here positive measures are included compared with the *nonpositive* entropy production required from measure-valued solutions in (1.5.1)), then there is actually a *gain* of Sobolev regularity of order $\frac{\alpha}{\alpha+4}$, and of order $\frac{\alpha}{\alpha+2}$ for the translation invariant case. (The expected optimal order is α). We shall outline this general framework for studying the regularizing effect of approximate solutions to multidimensional scalar equations in Lecture V.

Kinetic schemes

There is more than one way to convert microscopic kinetic formulations of non-linear equations, into macroscopic algorithms for the approximate solution of such equations. We mention the following three examples (in the context of conservation laws).

- Brenier's transport collapse method, [9], is a macroscopic projection method which preceded the BGK-like model (1.6.4), see also [54]. Here one alternates between transporting microscopic 'pseudo-Maxwellians' which start with $f(t^n, \cdot, v) := \chi_{\rho(t^n,\cdot)}(v)$, and projecting their macroscopic averaging, $\rho(t^{n+1}, \cdot) = \bar{f}(t^{n+1}, \cdot, v)$. A convergence analysis of this method by the velocity averaging lemma was recently worked out in [176].

- Another approach is based on Chapman-Enskog asymptotic expansions, [15]. We refer to [147], for an example of macroscopic approximation other than the usual Navier-Stokes-like viscosity regularization (– the scalar version of this regularized Chapman-Enskog expansion is studied in Lecture IV).

- Still another approach is offered by Godunov-type schemes, (1.3.14), based on projections of the Maxwellians associated with the specific kinetic formulations. These amount to specific Riemann solvers which were studied in [39], [135], [137].

We conclude by noting that kinetic formulations like those mentioned above in the context of scalar conservation laws apply in more general situations. For extensions consult [111] for degenerate parabolic equations, [112],[110] for the system of 2×2 isentropic equations, [77] for the system of chromatographic equations, ... We shall say more on these issues in Lecture V.

Bibliography

[1] L. Alvarez and J.-M. Morel *Formulation and computational aspects of image analysis*, Acta Numerica (1994), 1–59.

[2] C. Bardos, F. Golse and D. Levermore, *Fluid dynamic limits of kinetic equations II: convergence proofs of the Boltzmann equations*, Comm. Pure Appl. Math. XLVI (1993), 667–754.

[3] G. Barles and P.E. Souganidis, *Convergence of approximation schemes for fully nonlinear second order equations*, Asympt. Anal. 4 (1991), 271–283.

[4] J.B. Bell, P. Colella, and H.M. Glaz, *A Second-Order Projection Method for the Incompressible Navier-Stokes Equations*, J. Comp. Phys. 85 (1989), 257–283.

[5] M. Ben-Artzi and J. Falcovitz, *Recent developments of the GRP method*, JSME (Ser.b) 38 (1995), 497–517.

[6] J.P. Boris and D. L. Book, *Flux corrected transport: I. SHASTA, a fluid transport algorithm that works*, J. Comput. Phys. 11 (1973), 38–69.

[7] F. Bouchut and B. Perthame *Kružkov's estimates for scalar conservation laws revisited*, Universite D'Orleans, preprint, 1996.

[8] F. Bouchot, CH. Bourdarias and B. Perthame, *A MUSCL method satisfying all the numerical entropy inequalities*, Math. Comp. 65 (1996) 1439–1461.

[9] Y. Brenier, *Résolution d'équations d'évolution quasilinéaires en dimension N d'espace à l'aide d'équations linéaires en dimension N + 1*, J. Diff. Eq. 50 (1983), 375–390.

[10] Y. Brenier and S.J. Osher, *The discrete one-sided Lipschitz condition for convex scalar conservation laws*, SIAM J. Numer. Anal. 25 (1988), 8–23.

[11] A. Bressan, *The semigroup approach to systems of conservation laws*, 4^{th} Workshop on PDEs, Part I (Rio de Janeiro, 1995). Mat. Contemp. 10 (1996), 21–74.

[12] A. Bressan, *Decay and structural stability for solutions of nonlinear systems of conservation laws*, 1^{st} Euro-Conference on Hyperbolic Conservation Laws, Lyon, Feb. 1997.

[13] A. Bressan and R. Colombo *The semigroup generated by* 2×2 *conservation laws*, Arch. Rational Mech. Anal. 133 (1995), no. 1, 1–75.

[14] A. Bressan and R. Colombo *Unique solutions of* 2×2 *conservation laws with large data*, Indiana Univ. Math. J. 44 (1995), no. 3, 677–725.

[15] C. Cercignani, The Boltzmann Equation and its Applications, Appl. Mathematical Sci. 67, Springer, New-York, 1988.

[16] T. Chang and L. Hsiao, *The Riemann Problem and Interaction of Waves in Gasdynamics*, Pitman monographs and surveys in pure appl. math, 41, John Wiley, 1989.

[17] G.-Q. Chen, *The theory of compensated compactness and the system of isentropic gas dynamics*, Preprint MCS-P154-0590, Univ. of Chicago, 1990.

[18] G.-Q. Chen, Q. Du and E. Tadmor, *Spectral viscosity approximation to multidimensional scalar conservation laws*, Math. of Comp. 57 (1993).

[19] G.-Q. CHEN, D. LEVERMORE AND T. P. LIU, *Hyperbolic conservation laws with stiff relaxation terms and entropy* Comm. Pure Appl. Math. 47 (1994) 787–830.

[20] I. L. CHERN, *Stability theorem and truncation error analysis for the Glimm scheme and for a front tracking method for flows with strong discontinuities*, Comm. Pure Appl. Math. XLII (1989), 815–844.

[21] I.L. CHERN, J. GLIMM, O. MCBRYAN, B. PLOHR AND S. YANIV, *Front Tracking for gas dynamics* J. Comput. Phys. 62 (1986) 83–110.

[22] A. J. CHORIN, *Random choice solution of hyperbolic systems*, J. Comp. Phys. 22 (1976), 517–533.

[23] B. COCKBURN, *Quasimonotone schemes for scalar conservation laws. I. II, III.* SIAM J. Numer. Anal. 26 (1989) 1325–1341, 27 (1990) 247–258, 259–276.

[24] B. COCKBURN, F. COQUEL AND P. LEFLOCH, *Convergence of finite volume methods for multidimensional conservation laws*, SIAM J. Numer. Anal. 32 (1995), 687–705.

[25] P. COLELLA, *Multidimensional upwind methods for hyperbolic conservation laws*, J. Comput. Phys. 87 (1990), 87–171.

[26] P. COLELLA AND P. WOODWARD, *The piecewise parabolic method (PPM) for gas-dynamical simulations*, JCP 54 (1984), 174–201.

[27] F. COQUEL AND P. LEFLOCH, *Convergence of finite difference schemes for conservation laws in several space dimensions: a general theory*, SIAM J. Numer. Anal. (1993).

[28] M. G. CRANDALL, *The semigroup approach to first order quasilinear equations in several space dimensions*, Israel J. Math. 12 (1972), 108–132.

[29] M. G. CRANDALL AND P. L. LIONS, *Viscosity solutions of Hamilton-Jacobi equations*, Trans. Amer. Math. Soc. 277 (1983), 1–42.

[30] M. G. CRANDALL AND A. MAJDA, *Monotone difference approximations for scalar conservation laws*, Math. of Comp. 34 (1980), 1–21.

[31] M. G. CRANDALL AND A. MAJDA, *The method of fractional steps for conservation laws*, Numer. Math. 34 (1980), 285–314.

[32] M. G. CRANDALL AND L. TARTAR, *Some relations between non expansive and order preserving mapping*, Proc. Amer. Math. Soc. 78 (1980), 385–390.

[33] T. CHANG AND S. YANG, Two-Dimensional Riemann Problems for Systems of Conservation Laws, Pitman Monographs and Surveys in Pure and Appl. Math., 1995.

[34] C. DAFERMOS, *Polygonal approximations of solutions of initial-value problem for a conservation law*, J. Math. Anal. Appl. 38 (1972) 33–41.

[35] C. DAFERMOS, *Hyperbolic systems of conservation laws*, in "Systems of Nonlinear PDEs", J. M. Ball, ed, NATO ASI Series C, No. 111, Dordrecht, D. Reidel (1983), 25–70.

[36] C. DAFERMOS, private communication.

[37] R. DEVORE & G. LORENTZ, Constructive Approximation, Springer-Verlag, 1993.

[38] R. DEVORE AND B. LUCIER, *High order regularity for conservation laws*, Indiana Univ. Math. J. 39 (1990), 413–430.

[39] S. M. DESHPANDE, *A second order accurate, kinetic-theory based, method for inviscid compressible flows*, NASA Langley Tech. paper No. 2613, 1986.

[40] R. DIPERNA, *Convergence of approximate solutions to conservation laws*, Arch. Rat. Mech. Anal. 82 (1983), 27–70.

[41] R. DIPERNA, *Convergence of the viscosity method for isentropic gas dynamics*, Comm. Math. Phys. 91 (1983), 1–30.

[42] R. DIPERNA, *Measure-valued solutions to conservation laws*, Arch. Rat. Mech. Anal. 88 (1985), 223-270.

[43] R. DiPERNA AND P. L. LIONS, *On the Cauchy problem for Boltzmann equations: Global existence and weak stability*, Ann. Math. 130 (1989), 321–366.

[44] R. DiPERNA AND P.L. LIONS, *Global weak solutions of Vlasov-Maxwell systems*, Comm. Pure Appl. Math. 42 (1989), 729–757.

[45] R. DiPERNA, P.L. LIONS AND Y. MEYER, *L^p regularity of velocity averages*, Ann. I.H.P. Anal. Non Lin. 8(3-4) (1991), 271–287.

[46] W. E. AND C.-W.SHU, *A numerical resolution study of high order essentially non-oscillatory schemes applied to incompressible flow* J. Comp. Phys. 110, (1993) 39-46.

[47] B. ENGQUIST AND S.J. OSHER *One-sided difference approximations for nonlinear conservation laws*, Math. Comp. 36 (1981) 321–351.

[48] B. ENGQUIST, P. LOTSTEDT AND B. SJOGREEN, *Nonlinear filters for efficient shock computation*, Math. Comp. 52 (1989), 509–537.

[49] B. ENGQUIST AND O. RUNBORG, *Multi-phase computations in geometrical optics*, J. Comp. Appl. Math. 74 (1996) 175–192.

[50] C. EVANS, Weak Convergence Methods for Nonlinear Partial Differential equations, AMS Regional Conference Series in Math. 74, Providence R.I. 1990.

[51] K. FRIEDRICHS *Symmetric hyperbolic linear differential equations*, CPAM 7 (1954) 345–.

[52] K. O. FRIEDRICHS AND P. D. LAX, *Systems of conservation laws with a convex extension*, Proc. Nat. Acad. Sci. USA 68 (1971), 1686–1688.

[53] P. GÉRARD, *Microlocal defect measures*, Comm. PDE 16 (1991), 1761–1794.

[54] Y. GIGA AND T. MIYAKAWA, *A kinetic construction of global solutions of first-order quasilinear equations*, Duke Math. J. 50 (1983), 505–515.

[55] J. GLIMM, *Solutions in the large for nonlinear hyperbolic systems of equations*, Comm. Pure Appl. Math. 18 (1965), 697–715.

[56] J. GLIMM AND P. D. LAX, Decay of solutions of systems of nonlinear hyperbolic conservation laws, Amer. Math. Soc. Memoir 101, AMS Providence, 1970.

[57] J. GLIMM, B. LINDQUIST AND Q. ZHANG, *Front tracking, oil reservoirs, engineering scale problems and mass conservation* in *Multidimensional Hyperbolic Problems and Computations*, Proc. IMA workshop (1989) IMA vol. Math Appl 29 (J. Glimm and A. Majda Eds.), Springer-Verlag, New-York (1991), 123-139.

[58] E. GODLEWSKI AND P.-A. RAVIART, Hyperbolic Systems of Conservation Laws, Ellipses, Paris, 1991.

[59] E. GODLEWSKI AND P.-A. RAVIART, Numerical Approximation of Hyperbolic Systems of Conservation Laws, Springer, 1996.

[60] S. K. GODUNOV, *A difference scheme for numerical computation of discontinuous solutions of fluid dynamics*, Mat. Sb. 47 (1959), 271–306.

[61] S. K. GODUNOV, *An interesting class of quasilinear systems*, Dokl. Akad. Nauk. SSSR 139(1961), 521–523.

[62] F. GOLSE, P. L. LIONS, B. PERTHAME AND R. SENTIS, *Regularity of the moments of the solution of a transport equation*, J. of Funct. Anal. 76 (1988), 110–125.

[63] J. GOODMAN, private communication.

[64] J. GOODMAN AND P. D. LAX, *On dispersive difference schemes. I*, Comm. Pure Appl. Math. 41 (1988), 591–613.

[65] J. GOODMAN AND R. LEVEQUE, *On the accuracy of stable schemes for 2D scalar conservation laws*, Math. of Comp. 45 (1985), 15–21.

[66] J. GOODMAN AND XIN, *Viscous limits for piecewise smooth solutions to systems of conservation laws*, Arch. Rat. Mech. Anal. 121 (1992), 235–265.

[67] D. GOTTLIEB AND E. TADMOR, *Recovering Pointwise Values of Discontinuous Data within Spectral Accuracy*, in "Progress and Supercomputing in Computational Fluid Dynamics", Progress in Scientific Computing, Vol. 6 (E. M. Murman and S. S. Abarbanel, eds.), Birkhauser, Boston, 1985, 357–375.

[68] E. HARABETIAN, *A convergent series expansion for hyperbolic systems of conservation laws*, Trans. Amer. Math. Soc. 294 (1986), no. 2, 383–424.

[69] A. HARTEN, *The artificial compression method for the computation of shocks and contact discontinuities:I. single conservation laws*, CPAM 39 (1977), 611–638.

[70] A. HARTEN, *High resolution schemes for hyperbolic conservation laws*, J. Comput. Phys. 49 (1983), 357–393.

[71] A. HARTEN, B. ENGQUIST, S. OSHER AND S.R. CHAKRAVARTHY, *Uniformly high order accurate essentially non-oscillatory schemes. III*, JCP 71, 1982, 231–303.

[72] A. HARTEN M. HYMAN AND P. LAX, *On finite-difference approximations and entropy conditions for shocks*, Comm. Pure Appl. Math. 29 (1976), 297–322.

[73] A. HARTEN P.D. LAX AND B. VAN LEER, *On upstream differencing and Godunov-type schemes for hyperbolic conservation laws*, SIAM Rev. 25 (1983), 35–61.

[74] A. HARTEN AND S. OSHER, *Uniformly high order accurate non-oscillatory scheme. I*, SIAM J. Numer. Anal. 24 (1982) 229–309.

[75] C. HIRSCH, Numerical Computation of Internal and External Flows, Wiley, 1988.

[76] T. J. R. HUGHES AND M. MALLET, *A new finite element formulation for the computational fluid dynamics: III. The general streamline operator for multidimensional advective-diffusive systems*, Comput. Methods Appl. Mech. Engrg. 58 (1986), 305–328.

[77] F. JAMES, Y.-J PENG AND B. PERTHAME, *Kinetic formulation for chromatography and some other hyperbolic systems*, J. Math. Pures Appl. 74 (1995), 367–385.

[78] F. JOHN, Partial Differential Equations, 4th ed. Springer, New-York, 1982.

[79] C. JOHNSON AND A. SZEPESSY, *Convergence of a finite element methods for a nonlinear hyperbolic conservation law*, Math. of Comp. 49 (1988), 427–444.

[80] C. JOHNSON, A. SZEPESSY AND P. HANSBO, *On the convergence of shock-capturing streamline diffusion finite element methods for hyperbolic conservation laws*, Math. of Comp. 54 (1990), 107–129.

[81] G.-S. JIANG AND E. TADMOR, *Nonoscillatory Central Schemes for Multidimensional Hyperbolic Conservation Laws*, SIAM J. Sci. Compt., in press.

[82] S. JIN AND Z. XIN, *The relaxing schemes for systems of conservation laws in arbitrary space dimensions*, Comm. Pure Appl. Math. 48 (1995) 235–277.

[83] T. KATO, *The Cauchy problem for quasi-linear symmetric hyperbolic systems*, Arch. Rat. Mech. Anal. 58 (1975), 181–205.

[84] Y. KOBAYASHI, *An operator theoretic method for solving* $u_t = \Delta\psi(u)$, Hiroshima Math. J. 17 (1987) 79–89.

[85] D. KRÖNER, S. NOELLE AND M. ROKYTA, *Convergence of higher order upwind finite volume schemes on unstructured grids for scalar conservation laws in several space dimensions*, Numer. Math. 71 (1995) 527–560.

[86] D. KRÖNER AND M. ROKYTA, *Convergence of Upwind Finite Volume Schemes for Scalar Conservation Laws in two space dimensions*, SINUM 31 (1994) 324–343.

[87] S.N. KRUŽKOV, *The method of finite difference for a first order non-linear equation with many independent variables*, USSR comput Math. and Math. Phys. 6 (1966), 136–151. (English Trans.)

[88] S.N. KRUŽKOV, *First order quasilinear equations in several independent variables*, Math. USSR Sbornik 10 (1970), 217–243.

[89] R. KUPFERMAN AND E. TADMOR, *A fast high-resolution second-order central scheme for incompressible flows*, Proc. Nat. Acad. Sci.

[90] N.N. KUZNETSOV, *Accuracy of some approximate methods for computing the weak solutions of a first-order quasi-linear equation*, USSR Comp. Math. and Math. Phys. 16 (1976), 105–119.

[91] P.D. LAX, *Weak solutions of non-linear hyperbolic equations and their numerical computations*, Comm. Pure Appl. Math. 7 (1954), 159–193.

[92] P. D. LAX, *Hyperbolic systems of conservation laws II*, Comm. Pure Appl. Math. 10 (1957), 537–566.

[93] P.D. LAX, *Shock waves and entropy*, in *Contributions to nonlinear functional analysis*, E.A. Zarantonello Ed., Academic Press, New-York (1971), 603–634.

[94] P.D. LAX, Hyperbolic Systems of Conservation Laws and the Mathematical Theory of Shock Waves (SIAM, Philadelphia, 1973).

[95] P.D. LAX AND X.-D. LIU, *Positive schemes for solving multi-dimensional hyperbolic systems of conservation laws*, Courant Mathematics and Computing Laboratory Report NYU, 95-003 (1995), Comm. Pure Appl. Math.

[96] P. LAX AND B. WENDROFF, *Systems of conservation laws*, Comm. Pure Appl. Math. 13 (1960), 217–237.

[97] P. LAX AND B. WENDROFF, *Difference schemes for hyperbolic equations with high order of accuracy*, Comm. Pure Appl. Math. 17 (1964), 381–.

[98] B. VAN LEER, *Towards the ultimate conservative difference scheme. V. A second-order sequel to Godunov's method*, J. Comput. Phys. 32 (1979), 101–136.

[99] F. LEFLOCH AND P.A. RAVIART, *An asymptotic expansion for the solution of the generalized Riemann problem, Part I: General theory*, Ann. Inst. H. Poincare, Nonlinear Analysis 5 (1988), 179–

[100] P. LEFLOCH AND Z. XIN, *Uniqueness via the adjoint problem for systems of conservation laws*, CIMS Preprint.

[101] R. LEVEQUE, *A large time step generalization of Godunov's method for systems of conservation laws*, SIAM J. Numer. Anal. 22(6) (1985), 1051–1073.

[102] R. LEVEQUE, Numerical Methods for Conservation Laws, Lectures in Mathematics, Birkhäuser, Basel 1992.

[103] R. LEVEQUE, *Wave propagation algorithms for multi-dimensional hyperbolic systems*, Preprint.

[104] D. LEVERMORE AND J.-G. LIU, *Oscillations arising in numerical experiments*, NATO ARW seies, Plenum, New-York (1993), To appear.

[105] D. LEVY AND E. TADMOR, *Non-oscillatory central schemes for the incompressible 2-D Euler equations*, Math. Res. Lett., 4 (1997) 1-20.

[106] D. LI, *Riemann problem for multi-dimensional hyperbolic conservation laws*, Free boundary problems in fluid flow with applications (Montreal, PQ, 1990), 64–69, Pitman Res. Notes Math. Ser., 282.

[107] C.-T. LIN AND E. TADMOR, *L^1-stability and error estimates for approximate Hamilton-Jacobi solutions*, in preparation.

[108] P. L. LIONS, Generalized Solutions of Hamilton-Jacobi Equations, Pittman, London 1982.

[109] P.L. LIONS, *On kinetic equations*, in Proc. Int'l Congress of Math., Kyoto, 1990, Vol. II, Math. Soc. Japan, Springer (1991), 1173-1185.

[110] P. L. LIONS, B. PERTHAME AND P. SOUGANIDIS, *Existence and stability of entropy solutions for the hyperbolic systems of isentropic gas dynamics in Eulerian and Lagrangian coordinates*, Comm. Pure and Appl. Math. 49 (1996), 599-638.

[111] P. L. LIONS, B. PERTHAME AND E. TADMOR, *Kinetic formulation of scalar conservation laws and related equations*, J. Amer. Math. Soc. 7(1) (1994), 169–191

[112] P. L. LIONS, B. PERTHAME AND E. TADMOR, *Kinetic formulation of the isentropic gas-dynamics equations and p-systems*, Comm. Math. Phys. 163(2) (1994), 415–431.

[113] T.-P. LIU, *The entropy condition and the admissibility of shocks*, J. Math. Anal. Appl. 53 (1976), 78–88.

[114] T. P. LIU, *The deterministic version of the Glimm scheme*, Comm. Math. Phys. 57 (1977), 135–148.

[115] B. LUCIER, *Error bounds for the methods of Glimm, Godunov and LeVeque*, SIAM J. Numer. Anal. 22 (1985), 1074–1081.

[116] *B. Lucier, Lecture Notes*, 1993.

[117] Y. MADAY, S. M. OULD-KABER AND E. TADMOR, *Legendre pseudospectral viscosity method for nonlinear conservation laws*, SIAM J. Numer. Anal. 30 (1993), 321–342.

[118] A. MAJDA, Compressible Fluid Flow and Systems of Conservation Laws in Several Space Variables, Springer-Verlag New-York, 1984.

[119] A. MAJDA, J. MCDONOUGH AND S. OSHER, *The Fourier method for nonsmooth initial data*, Math. Comp. 30 (1978), 1041–1081.

[120] M.S. MOCK, *Systems of conservation laws of mixed type*, J. Diff. Eq. 37 (1980), 70–88.

[121] M. S. MOCK AND P. D. LAX, The computation of discontinuous solutions of linear hyperbolic equations, Comm. Pure Appl. Math. 31 (1978), 423–430.

[122] K.W. MORTON, *Lagrange-Galerkin and characteristic-Galerkin methods and their applications*, 3^{rd} Int'l Conf. Hyperbolic Problems (B. Engquist & B. Gustafsson, eds.), Studentlitteratur, (1991), 742–755.

[123] F. MURAT, *Compacité par compensation*, Ann. Scuola Norm. Sup. Pisa 5 (1978), 489–507.

[124] F. MURAT, *A survey on compensated compactness*, in 'Contributions to Modern calculus of variations' (L. Cesari, ed), Pitman Research Notes in Mathematics Series, John Wiley New-York, 1987, 145–183.

[125] R. NATALINI, *Convergence to equilibrium for the relaxation approximations of conservation laws*, Comm. Pure Appl. Math. 49 (1996), 1–30.

[126] H. NESSYAHU AND E. TADMOR, Non-oscillatory central differencing for hyperbolic conservation laws. J. Comp. Phys. 87 (1990), 408–463.

[127] H. NESSYAHU AND E. TADMOR, *The convergence rate of approximate solutions for nonlinear scalar conservation laws*, SIAM J. Numer. Anal. 29 (1992), 1–15.

[128] S. NOELLE, *A note on entropy inequalities and error estimates for higher-order accurate finite volume schemes on irregular grids*, Math. Comp. to appear.

[129] O. A. OLĒINIK *Discontinuous solutions of nonlinear differential equations*, Amer. Math. Soc. Transl. (2), 26 (1963), 95–172.

[130] S. OSHER, *Riemann solvers, the entropy condition, and difference approximations*, SIAM J. Numer. Anal. 21 (1984), 217-235.

[131] S. OSHER AND F. SOLOMON, *Upwind difference schemes for hyperbolic systems of conservation laws*, Math. Comp. 38 (1982), 339–374.

[132] S. OSHER AND J. SETHIAN, *Fronts propagating with curvature dependent speed: Algorithms based on Hamilton-Jacobi formulations*, J. Comp. Phys. 79 (1988), 12–49.

[133] S. OSHER AND E. TADMOR, *On the convergence of difference approximations to scalar conservation laws*, Math. of Comp. 50 (1988), 19–51.

[134] B. PERTHAME, *Global existence of solutions to the BGK model of Boltzmann equations*, J. Diff. Eq. 81 (1989), 191-205.

[135] B. PERTHAME, *Second-order Boltzmann schemes for compressible Euler equations*, SIAM J. Num. Anal. 29, (1992), 1–29.

[136] B. PERTHAME AND E. TADMOR, *A kinetic equation with kinetic entropy functions for scalar conservation laws*, Comm. Math. Phys.136 (1991), 501–517.

[137] K. H. PRENDERGAST AND K. XU, *Numerical hydrodynamics from gas-kinetic theory*, J. Comput. Phys. 109(1) (1993), 53–66.

[138] A. RIZZI AND B. ENGQUIST, Selected topics in the theory and practice of computational fluid dynamics, J. Comp. Phys. 72 (1987), 1–69.

[139] P. ROE, *Approximate Riemann solvers,parameter vectors, and difference schemes*, J. Comput. Phys. 43 (1981), 357–372.

[140] P. ROE, *Discrete models for the numerical analysis of time-dependent multidimensional gas dynamics*, J. Comput. Phys. 63 (1986), 458–476.

[141] R. RICHTMYER AND K.W. MORTON, Difference Methods for Initial-Value Problems, Interscience, 2nd ed., 1967.

[142] F. SABAC, PhD Thesis, Univ. S. Carolina, 1994.

[143] R. SANDERS, *On Convergence of monotone finite difference schemes with variable spatial differencing*, Math. of Comp. 40 (1983), 91–106.

[144] R. SANDERS, *A third-order accurate variation nonexpansive difference scheme for single conservation laws*, Math. Comp. 51 (1988), 535–558.

[145] S. SCHOCHET, *The rate of convergence of spectral viscosity methods for periodic scalar conservation laws*, SIAM J. Numer. Anal. 27 (1990), 1142–1159.

[146] S. SCHOCHET, *Glimm's scheme for systems with almost-planar interactions*, Comm. Partial Differential Equations 16(8-9) (1991), 1423–1440.

[147] S. SCHOCHET AND E. TADMOR, *Regularized Chapman-Enskog expansion for scalar conservation laws*, Archive Rat. Mech. Anal. 119 (1992), 95–107.

[148] D. SERRE, *Richness and the classification of quasilinear hyperbolic systems*, in "Multidimensional Hyperbolic Problems and Computations", Minneapolis MN 1989, IMA Vol. Math. Appl. 29, Springer NY (1991), 315–333.

[149] D. SERRE, Systemés de Lois de Conservation, Diderot, Paris 1996.

[150] D. SERRE, private communication.

[151] C.W. SHU, *TVB uniformly high-order schemes for conservation laws*, Math. Comp. 49 (1987) 105–121.

[152] C. W. SHU, *Total-variation-diminishing time discretizations*, SIAM J. Sci. Comput. 6 (1988), 1073–1084.

[153] C. W. SHU AND S. OSHER, *Efficient implementation of essentially non-oscillatory shock-capturing schemes*, J. Comp. Phys. 77 (1988), 439–471.

[154] C. W. SHU AND S. OSHER, *Efficient implementation of essentially non-oscillatory shock-capturing schemes. II*, J. Comp. Phys. 83 (1989), 32–78.

[155] W. SHYY, M.-H CHEN, R. MITTAL AND H.S. UDAYKUMAR, *On the suppression on numerical oscillations using a non-linear filter*, J. Comput. Phys. 102 (1992), 49–62.

[156] D. SIDILKOVER, *Multidimensional upwinding: unfolding the mystery*, Barriers and Challenges in CFD, ICASE workshop, ICASE, Aug, 1996.

[157] J. SMOLLER, Shock Waves and Reaction-Diffusion Equations, Springer-Verlag, New York, 1983.

[158] G. SOD, *A survey of several finite difference methods for systems of nonlinear hyperbolic conservation laws*, JCP 22 (1978) 1–31.

[159] G. SOD, Numerical Methods for Fluid Dynamics, Cambridge University Press, 1985.

[160] A. SZEPESSY, *Convergence of a shock-capturing streamline diffusion finite element method for scalar conservation laws in two space dimensions*, Math. of Comp. (1989), 527–545.

[161] P. R. SWEBY, *High resolution schemes using flux limiters for hyperbolic conservation laws*, SIAM J. Num. Anal. 21 (1984), 995–1011.

[162] E. TADMOR, *The large-time behavior of the scalar, genuinely nonlinear Lax-Friedrichs scheme* Math. Comp. 43 (1984), no. 168, 353–368.

[163] E. TADMOR, *Numerical viscosity and the entropy condition for conservative difference schemes* Math. Comp. 43 (1984), no. 168, 369–381.

[164] E. TADMOR, *Convenient total variation diminishing conditions for nonlinear difference schemes*, SIAM J. on Numer. Anal. 25 (1988), 1002-1014.

[165] E. TADMOR, *Convergence of Spectral Methods for Nonlinear Conservation Laws*, SIAM J. Numer. Anal. 26 (1989), 30–44.

[166] E. TADMOR, *Local error estimates for discontinuous solutions of nonlinear hyperbolic equations*, SIAM J. Numer. Anal. 28 (1991), 891–906.

[167] E. TADMOR, *Super viscosity and spectral approximations of nonlinear conservation laws*, in "Numerical Methods for Fluid Dynamics", Proceedings of the 1992 Conference on Numerical Methods for Fluid Dynamics (M. J. Baines and K. W. Morton, eds.), Clarendon Press, Oxford, 1993, 69–82.

[168] E. TADMOR, *Approximate Solution of Nonlinear Conservation Laws and Related Equations*, in "Recent Advances in Partial Differential Equations and Applications" Proceedings of the 1996 Venice Conference in honor of Peter D. Lax and Louis Nirenberg on their 70th Birthday (S. Venakides Ed.), AMS Proceedings, Providence

[169] E. TADMOR AND T. TASSA, *On the piecewise regularity of entropy solutions to scalar conservation laws*, Com. PDEs 18 91993), 1631-1652.

[170] T. TANG & Z. H. TENG, *Viscosity methods for piecewise smooth solutions to scalar conservation laws*, Math. Comp., 66 (1997), pp. 495–526.

[171] L. TARTAR, *Compensated compactness and applications to partial differential equations*, in *Research Notes in Mathematics 39*, Nonlinear Analysis and Mechanics, Heriott-Watt Symposium, Vol. 4 (R.J. Knopps, ed.) Pittman Press, (1975), 136–211.

[172] L. TARTAR, *Discontinuities and oscillations*, in Directions in PDEs, Math Res. Ctr Symposium (M.G. Crandall, P.H. Rabinowitz and R.E. Turner eds.) Academic Press (1987), 211-233.

[173] T. TASSA, *Applications of compensated compactness to scalar conservation laws*, M.Sc. thesis (1987), Tel-Aviv University (in Hebrew).

[174] B. TEMPLE, *No L^1 contractive metrics for systems of conservation laws*, Trans. AMS 288(2) (1985), 471–480.

[175] Z.-H. TENG *Particle method and its convergence for scalar conservation laws*, SIAM J. Num. Anal. 29 (1992) 1020–1042.

[176] VASSEUR, *Kinetic semi-discretization of scalar conservation laws and convergence using averaging lemmas*, SIAM J. Numer. Anal.

[177] A. I. VOL'PERT, *The spaces BV and quasilinear equations*, Math. USSR-Sb. 2 (1967), 225–267.

[178] G.B. WHITHAM, Linear and Nonlinear Waves, Wiley-Interscience, 1974.

[179] K. YOSIDA, Functional Analysis, Springer-Verlag, 1980.

Chapter 2

Non-oscillatory central schemes

Abstract. We discuss a new class of high-resolution approximations for hyperbolic systems of conservation laws, which are based on *central* differencing. Its two main ingredients include:

#1. A non-oscillatory reconstruction of pointvalues from their given cell averages; and

#2. A central differencing based on *staggered* evolution of the reconstructed averages.

Many of the modern high-resolution schemes for such systems, are based on Godunov-type *upwind* differencing; their intricate and time consuming part involves the field-by-field characteristic decomposition, which is required in order to identify the "direction of the wind". Instead, our proposed central (staggered) stencils enjoy the main advantage is simplicity: no Riemann problems are solved, and hence field-by-field decompositions are avoided. This could be viewed as the high-order sequel to the celebrated Lax-Friedrichs (staggered) scheme. Typically, staggering suffers from excessive numerical dissipation. Here, excessive dissipation is compensated by using modern, high-resolution, non-oscillatory reconstructions.

We highlight several features of this new class of central schemes.

`Scalar equations`. For both the second- and third-order schemes we prove variation bounds (– which in turn yield convergence with precise error estimates), as well as entropy and multidimensional L^∞-stability estimates.

`Systems of equations`. Extension to systems is carried out by *componentwise* application of the scalar framework. It is in this context that our central schemes offer a remarkable advantage over the corresponding upwind framework.

`Multidimensional problems`. Since we bypass the need for (approximate) Riemann solvers, multidimensional problems are solved *without* dimensional splitting. In fact, the proposed class of central schemes is utilized for a variety of nonlinear transport equations.

A variety of numerical experiments confirm the high-resolution content of the proposed central schemes. They include second- and third-order approximations for one- and two-dimensional Euler, MHD, as well as other compressible and incompressible equations. These numerical experiments demonstrate that the proposed central schemes offer *simple, robust, Riemann-solver-free* approximations, while at the same time, they retain the high-resolution content of the

more expensive upwind schemes.

2.1 Introduction

In recent years, central schemes for approximating solutions of hyperbolic conservation laws, received a considerable amount of renewed attention. A family of high-resolution, non-oscillatory, *central* schemes, was developed to handle such problems. Compared with the 'classical' *upwind* schemes, these *central* schemes were shown to be both simple and stable for a large variety of problems ranging from one-dimensional scalar problems to multi-dimensional systems of conservation laws. They were successfully implemented for a variety of other related problems, such as, e.g., the incompressible Euler equations [25],[22],[20], [21], the magneto-hydrodynamics equations [42], viscoelastic flows—[20] hyperbolic systems with relaxation source terms [4],[34],[35] non-linear optics [33],[7], and slow moving shocks [17].

The family of high-order *central* schemes we deal with, can be viewed as a direct extension to the first-order, Lax-Friedrichs (LxF) scheme [9], which on one hand is robust and stable, but on the other hand suffers from excessive dissipation. To address this problematic property of the LxF scheme, a Godunov-like second-order central scheme was developed by Nessyahu and Tadmor (NT) in [29] (see also [38]). It was extended to higher-order of accuracy as well as for more space dimensions (consult [1], [16], [2], [3] and [21], for the two-dimensional case, and [37], [14], [28] and [24] for the third-order schemes).

The NT scheme is based on reconstructing, in each time step, a piecewise-polynomial interpolant from the cell-averages computed in the previous time step. This interpolant is then (exactly) evolved in time, and finally, it is projected on its staggered averages, resulting with the staggered cell-averages at the next time-step. The one- and two-dimensional second-order schemes, are based on a piecewise-linear MUSCL-type reconstruction, whereas the third-order schemes are based on the non-oscillatory piecewise-parabolic reconstruction [27],[28]. Higher orders are treated in [36].

Like *upwind* schemes, the reconstructed piecewise-polynomials used by the central schemes, also make use of non-linear limiters which guarantee the overall non-oscillatory nature of the approximate solution. But unlike the upwind schemes, central schemes avoid the intricate and time consuming Riemann solvers; this advantage is particularly important in the multi-dimensional setup, where no such Riemann solvers exist.

2.2 A Short Guide to Godunov-Type schemes

We want to solve the hyperbolic system of conservation laws

$$u_t + f(u)_x = 0 \tag{2.2.1}$$

by Godunov-type schemes. To this end we proceed in two steps. First, we introduce a small spatial scale, Δx, and we consider the corresponding (Steklov) sliding average of $u(\cdot,t)$,

$$\bar{u}(x,t) := \frac{1}{|I_x|}\int_{I_x} u(\xi,t)d\xi, \qquad I_x = \left\{\xi \;\middle|\; |\xi - x| \le \frac{\Delta x}{2}\right\}.$$

The sliding average of (2.2.1) then yields

$$\bar{u}_t(x,t) + \frac{1}{\Delta x}\left[f(u(x+\frac{\Delta x}{2},t)) - f(u(x-\frac{\Delta x}{2},t))\right] = 0. \tag{2.2.2}$$

Next, we introduce a small time-step, Δt, and integrate over the slab $t \le \tau \le t+\Delta t$,

$$\begin{aligned} \bar{u}(x,t+\Delta t) &= \bar{u}(x,t) \\ &\quad -\frac{1}{\Delta x}\left[\int_{\tau=t}^{t+\Delta t} f(u(x+\frac{\Delta x}{2},\tau))d\tau - \int_{\tau=t}^{t+\Delta t} f(u(x-\frac{\Delta x}{2},\tau))d\tau\right]. \end{aligned} \tag{2.2.3}$$

We end up with an equivalent reformulation of the conservation law (2.2.1): it expresses the precise relation between the sliding averages, $\bar{u}(\cdot,t)$, and their underlying pointvalues, $u(\cdot,t)$. We shall use this reformulation, (2.2.3), as the starting point for the construction of Godunov-type schemes.

We construct an approximate solution, $w(\cdot,t^n)$, at the discrete time-levels, $t^n = n\Delta t$. Here, $w(x,t^n)$ is a piecewise polynomial written in the form

$$w(x,t^n) = \sum p_j(x)\chi_j(x), \quad \chi_j(x) := 1_{I_j},$$

where $p_j(x)$ are algebraic polynomials supported at the discrete cells, $I_j = I_{x_j}$, centered around the midpoints, $x_j := j\Delta x$. An *exact* evolution of $w(\cdot,t^n)$ based on (2.2.3), reads

$$\begin{aligned} \bar{w}(x,t^{n+1}) &= \bar{w}(x,t^n) \\ &\quad -\frac{1}{\Delta x}\left[\int_{t^n}^{t^{n+1}} f(w(x+\frac{\Delta x}{2},\tau))d\tau - \int_{t^n}^{t^{n+1}} f(w(x-\frac{\Delta x}{2},\tau))d\tau\right]. \end{aligned} \tag{2.2.4}$$

To construct a Godunov-type scheme, we *realize* (2.2.4) — or at least an accurate approximation of it, at discrete gridpoints. Here, we distinguish between the main methods, according to their way of *sampling* (2.2.4): these two main sampling methods correspond to upwind schemes and central schemes.

2.2.1 Upwind schemes

Let $\bar{w}_j^n$ abbreviates the cell averages, $\bar{w}_j^n := \frac{1}{\Delta x}\int_{I_j} w(\xi,t^n)d\xi$. By sampling (2.2.4) at the *mid-cells*, $x = x_j$, we obtain an evolution scheme for these averages, which reads

$$\bar{w}_j^{n+1} = \bar{w}_j^n - \frac{1}{\Delta x}\left[\int_{\tau=t^n}^{t^{n+1}} f(w(x_{j+\frac{1}{2}},\tau))d\tau - \int_{\tau=t^n}^{t^{n+1}} f(w(x_{j-\frac{1}{2}},\tau))d\tau\right]. \tag{2.2.5}$$

Here, it remains to recover the *pointvalues*, $\{w(x_{j+\frac{1}{2}},\tau)\}_j$, $t^n \le \tau \le t^{n+1}$, in terms of their known cell averages, $\{\bar{w}_j^n\}_j$, and to this end we proceed in two steps:

- First, the *reconstruction* – we recover the pointwise values of $w(\cdot,\tau)$ at $\tau = t^n$, by a reconstruction of a piecewise polynomial approximation

$$w(x,t^n) = \sum_j p_j(x)\chi_j(x), \quad \bar{p}_j(x_j) = \bar{w}_j^n. \tag{2.2.6}$$

- Second, the *evolution* — $w(x_{j+\frac{1}{2}},\ \tau \geq t^n)$ are determined as the solutions of the generalized Riemann problems

$$w_t + f(w)_x = 0, \quad t \geq t^n; \quad w(x,t^n) = \begin{cases} p_j(x) & x < x_{j+\frac{1}{2}}, \\ p_{j+1}(x) & x > x_{j+\frac{1}{2}}. \end{cases} \tag{2.2.7}$$

The solution of (2.2.7) is composed of a family of nonlinear waves – left-going and right-going waves. An exact Riemann solver, or at least an approximate one is used to distribute these nonlinear waves between the two neighboring cells, I_j and I_{j+1}. It is this distribution of waves according to their direction which is responsible for *upwind differencing*, consult Figure 2.2.1. We briefly recall few canonical examples for this category of upwind Godunov-type schemes.

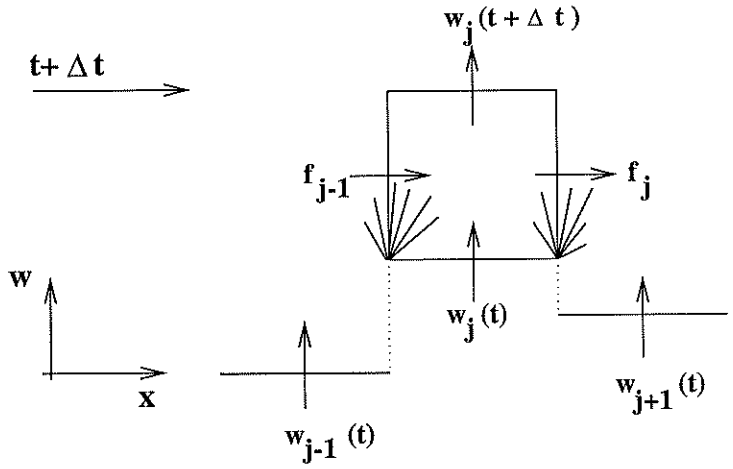

Figure 2.2.1: Upwind differencing by Godunov-type scheme.

The original Godunov scheme is based on piecewise-constant reconstruction, $w(x,t^n) = \Sigma\bar{w}_j^n\chi_j$, followed by an exact Riemann solver. This results in a first-order accurate upwind method [11], which is the forerunner for all other Godunov-type schemes. A second-order extension was introduced by van Leer [19]: his MUSCL scheme reconstructs a piecewise linear approximation, $w(x,t^n) = \Sigma p_j(x)\chi_j(x)$, with linear pieces of the form $p_j(x) = \bar{w}_j^n + w_j'\left(\frac{x-x_j}{\Delta x}\right)$ so that $\bar{p}_j(x_j) = \bar{w}_j^n$. Here the w_j'-s are possibly limited slopes which are reconstructed from the known cell-averages, $w_j' = \{(w_j^n)'\} = \{w'(\bar{w}_k^n)_{k=j-1}^{j+1}\}$. (Throughout this lecture we use primes, $w_j', w_j'', \ldots$, to denote *discrete* derivatives, which approximate the corresponding differential ones). A whole library

of limiters is available in this context, so that the co-monotonicity of $w(x,t^n)$ with $\Sigma\bar{w}_j\chi_j$ is guaranteed, e.g., [39]. The Piecewise-Parabolic Method (PPM) of Colella-Woodward [6] and respectively, ENO schemes of Harten et.al. [13], offer, respectively, third- and higher-order Godunov-type upwind schemes. (A detailed account of ENO schemes can be found in lectures of C.W. Shu in this volume). Finally, we should not give the impression that limiters are used exclusively in conjunction with Godunov-type schemes. The *positive schemes* of Liu and Lax, [26], offer simple and fast upwind schemes for multidimensional systems, based on an alternative positivity principle.

2.2.2 Central schemes

As before, we seek a piecewise-polynomial, $w(x,t^n)=\Sigma p_j(x)\chi_j(x)$, which serves as an approximate solution to the *exact* evolution of sliding averages in (2.2.4),

$$\bar{w}(x,t^{n+1})=\bar{w}(x,t^n)-\frac{1}{\Delta x}\left[\int_{t^n}^{t^{n+1}} f(w(x+\frac{\Delta x}{2},\tau))d\tau-\int_{t^n}^{t^{n+1}} f(w(x-\frac{\Delta x}{2},\tau))d\tau\right]. \tag{2.2.8}$$

Note that the polynomial pieces of $w(x,t^n)$ are supported in the cells, $I_j=\left\{\xi \;\middle|\; |\xi-x_j|\le\frac{\Delta x}{2}\right\}$, with interfacing breakpoints at the half-integers gridpoints, $x_{j+\frac{1}{2}}=\left(j+\frac{1}{2}\right)\Delta x$.

We recall that upwind schemes (2.2.5) were based on sampling (2.2.4) in the *midcells*, $x=x_j$. In contrast, central schemes are based on sampling (2.2.8) at the *interfacing breakpoints*, $x=x_{j+\frac{1}{2}}$, which yields

$$\bar{w}^{n+1}_{j+\frac{1}{2}}=\bar{w}^n_{j+\frac{1}{2}}-\frac{1}{\Delta x}\left[\int_{\tau=t^n}^{t^{n+1}} f(w(x_{j+1},\tau))d\tau-\int_{\tau=t^n}^{t^{n+1}} f(w(x_j,\tau))d\tau\right]. \tag{2.2.9}$$

We want to utilize (2.2.9) in terms of the known cell averages at time level $\tau=t^n$, $\{\bar{w}^n_j\}_j$. The remaining task is therefore to recover the *pointvalues* $\{w(\cdot,\tau)|\,t^n\le\tau\le t^{n+1}\}$, and in particular, the *staggered averages*, $\{\bar{w}^n_{j+\frac{1}{2}}\}$. As before, this task is accomplished in two main steps:

- First, we use the given cell averages $\{\bar{w}^n_j\}_j$, to *reconstruct* the pointvalues of $w(\cdot,\tau=t^n)$ as piecewise polynomial approximation

$$w(x,t^n)=\sum_j p_j(x)\chi_j(x),\quad \bar{p}_j(x_j)=\bar{w}^n_j. \tag{2.2.10}$$

  In particular, the staggered averages on the right of (2.2.9) are given by

$$\bar{w}^n_{j+\frac{1}{2}}=\frac{1}{\Delta x}\left[\int_{x_j}^{x_{j+\frac{1}{2}}} p_j(x)dx+\int_{x_{j+\frac{1}{2}}}^{x_{j+1}} p_{j+1}(x)dx\right]. \tag{2.2.11}$$

  The resulting central scheme (2.2.9) then reads

$$\bar{w}^{n+1}_{j+\frac{1}{2}} \;=\; \frac{1}{\Delta x}\left[\int_{x_j}^{x_{j+\frac{1}{2}}} p_j(x)dx+\int_{x_{j+\frac{1}{2}}}^{x_{j+1}} p_{j+1}(x)dx\right]+ \tag{2.2.12}$$

$$- \frac{1}{\Delta x}\left[\int_{\tau=t^n}^{t^{n+1}} f(w(x_{j+1},\tau))d\tau - \int_{\tau=t^n}^{t^{n+1}} f(w(x_j,\tau))d\tau\right].$$

- Second, we follow the *evolution* of the pointvalues along the mid-cells, $x = x_j$, $\{w(x_j, \tau \geq t^n)\}_j$, which are governed by

$$w_t + f(w)_x = 0, \quad \tau \geq t^n; \quad w(x,t^n) = p_j(x) \quad x \in I_j. \tag{2.2.13}$$

Let $\{a_k(u)\}_k$ denote the eigenvalues of the Jacobian $A(u) := \frac{\partial f}{\partial u}$. By hyperbolicity, information regarding the interfacing discontinuities at $(x_{j\pm\frac{1}{2}}, t^n)$ propagates no faster than $\max_k|a_k(u)|$. Hence, the mid-cells values governed by (2.2.13), $\{w(x_j, \tau \geq t^n)\}_j$, remain free of discontinuities, at least for sufficiently small time step dictated by the CFL condition $\Delta t \leq \frac{1}{2}\Delta x \cdot \max_k|a_k(u)|$. Consequently, since the numerical fluxes on the right of (2.2.12), $\int_{\tau=t^n}^{t^{n+1}} f(w(x_j,\tau))d\tau$, involve only smooth integrands, they can be computed within any degree of desired accuracy by an appropriate quadrature rule.

It is the *staggered* averaging over the fan of left-going and right-going waves centered at the half-integered interfaces, $(x_{j+\frac{1}{2}}, t^n)$, which characterizes the *central* differencing, consult Figure 2.2.2. A main feature of these central schemes – in contrast to upwind ones, is the computation of *smooth* numerical fluxes along the mid-cells, $(x = x_j, \tau \geq t^n)$, which avoids the costly (approximate) Riemann solvers. A couple of examples of central Godunov-type schemes is in order.

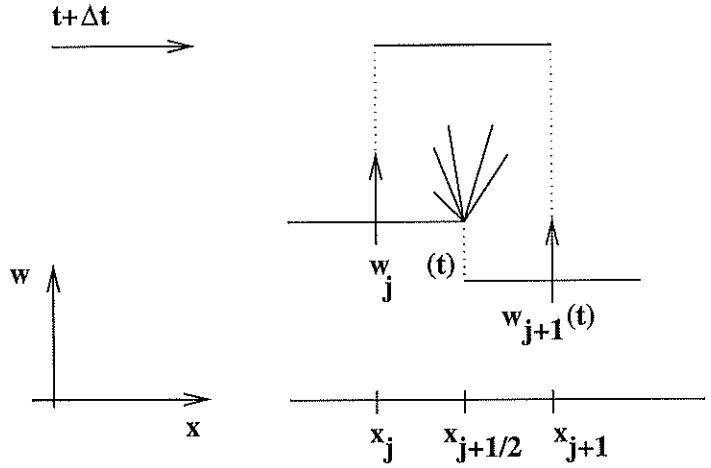

Figure 2.2.2: Central differencing by Godunov-type scheme.

The first-order Lax-Friedrichs (LxF) approximation is the forerunner for such central schemes — it is based on piecewise constant reconstruction, $w(x,t^n) = \Sigma p_j(x)\chi_j(x)$ with $p_j(x) = \bar{w}_j^n$. The resulting central scheme, (2.2.12), then reads (with the usual fixed mesh ratio $\lambda := \frac{\Delta t}{\Delta x}$)

$$\bar{w}_{j+\frac{1}{2}}^{n+1} = \frac{1}{2}(\bar{w}_j + \bar{w}_{j+1}) - \lambda\Big[f(\bar{w}_{j+1}) - f(\bar{w}_j)\Big]. \tag{2.2.14}$$

Our main focus in the rest of this chapter is on non-oscillatory higher-order extensions of the LxF schemes.

2.3 Central schemes in one-space dimension

2.3.1 The second-order Nessyahu-Tadmor scheme

In this section we overview the construction of high-resolution central schemes in one-space dimension. We begin with the reconstruction of the second-order, non-oscillatory Nessyahu and Tadmor (NT) scheme, [29]. To approximate solutions of (2.2.1), we introduce a piecewise-linear approximate solution at the discrete time levels, $t^n = n\Delta t$, based on linear functions $p_j(x,t^n)$ which are supported at the cells I_j (see Figure 2.3.1),

$$w(x,t)|_{t=t^n} = \sum_j p_j(x,t^n)\chi_j(x) := \sum_j \left[\bar{w}_j^n + w_j'\left(\frac{x-x_j}{\Delta x}\right)\right]\chi_j(x), \qquad \chi_j(x) := 1_{I_j}. \tag{2.3.1}$$

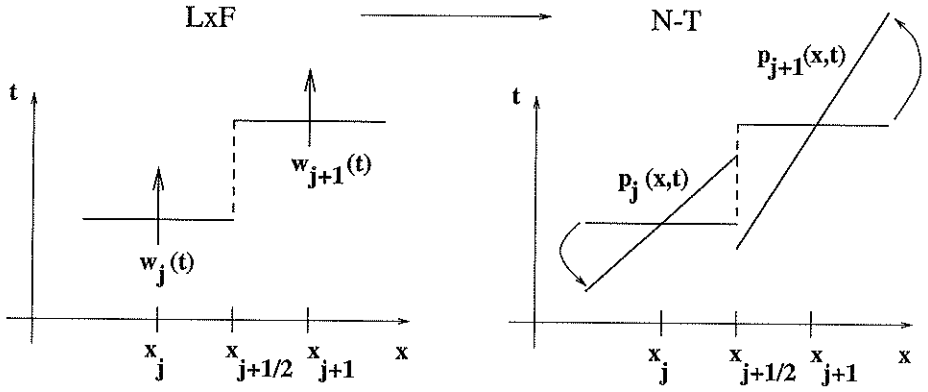

Figure 2.3.1: The second-order reconstruction

Second-order of accuracy is guaranteed if the discrete slopes approximate the corresponding derivatives, $w_j' \sim \Delta x \cdot \partial_x w(x_j,t^n) + O(\Delta x)^2$. Such a non-oscillatory approximation of the derivatives is possible, e.g., by using built-in non-linear limiters of the form

$$w_j' = MM\{\theta(\bar{w}_{j+1}^n - \bar{w}_j^n), \frac{1}{2}(\bar{w}_{j+1}^n - \bar{w}_{j-1}^n), \theta(\bar{w}_j^n - \bar{w}_{j-1}^n)\}. \tag{2.3.2}$$

Here and below, $\theta \in (0,2)$ is a non-oscillatory limiter and MM denotes the Min-Mod function

$$MM\{x_1,x_2,...\} = \begin{cases} \min_i\{x_i\} & \text{if } x_i > 0, \forall i \\ \max_i\{x_i\} & \text{if } x_i < 0, \forall i \\ 0 & \text{otherwise.} \end{cases}$$

An *exact* evolution of w, based on integration of the conservation law over the staggered cell, $I_{j+\frac{1}{2}}$, then reads, (2.2.9)

$$\bar{w}_{j+\frac{1}{2}}^{n+1} = \frac{1}{\Delta x}\int_{I_{j+\frac{1}{2}}} w(x,t^n)dx - \frac{1}{\Delta x}\int_{\tau=t^n}^{t^{n+1}} \left[f(w(x_{j+1},\tau)) - f(w(x_j,\tau))\right] d\tau.$$

The first integral is the staggered cell-average at time t^n, $\bar{w}_{j+\frac{1}{2}}^n$, which can be computed directly from the above reconstruction,

$$\bar{w}_{j+\frac{1}{2}}^n := \frac{1}{\Delta x}\int_{x_j}^{x_{n+1}} w(x,t^n)dx = \frac{1}{2}(\bar{w}_j^n + \bar{w}_{j+1}^n) + \frac{1}{8}(w_j' - w_{j+1}'). \qquad (2.3.3)$$

The time integrals of the flux are computed by the second-order accurate mid-point quadrature rule

$$\int_{\tau=t^n}^{t^{n+1}} f(w(x_j,\tau))d\tau \sim \Delta t \cdot f(w(x_j,t^{n+\frac{1}{2}})).$$

Here, the Taylor expansion is being used to predict the required mid-values of w

$$\begin{aligned} w(x_j,t^{n+\frac{1}{2}}) &\sim w(x_j,t) + \frac{\Delta t}{2}w_t(x_j,t^n) \\ &= \bar{w}_j^n - \frac{\Delta t}{2}A(\bar{w}_j^n)(p_j(x_j,t^n))_x = \bar{w}_j^n - \frac{\lambda}{2}A_j^n w_j'. \end{aligned}$$

In summary, we end up with the central scheme, [29], which consists of a first-order *predictor step*,

$$w_j^{n+\frac{1}{2}} = \bar{w}_j^n - \frac{\lambda}{2}A_j^n w_j', \quad A_j^n := A(\bar{w}_j^n), \qquad (2.3.4)$$

followed by the second-order *corrector step*, (2.2.12),

$$\bar{w}_{j+\frac{1}{2}}^{n+1} = \frac{1}{2}(\bar{w}_j^n + \bar{w}_{j+1}^n) + \frac{1}{8}(w_j' - w_{j+1}') - \lambda\left[f(w_{j+1}^{n+\frac{1}{2}}) - f(w_j^{n+\frac{1}{2}})\right]. \qquad (2.3.5)$$

The *scalar* non-oscillatory properties of (2.3.4)-(2.3.5) were proved in [29], [26], including the TVD property, cell entropy inequality, $L^1_{loc}-$ error estimates, etc. Moreover, the numerical experiments, reported in [27], [29], [2], [3], [42], [34], [35], [36], with one-dimensional *systems* of conservation laws, show that such second-order central schemes enjoy the same high-resolution as the corresponding second-order upwind schemes do. Thus, the excessive smearing typical to the first-order LxF central scheme is compensated here by the second-order accurate MUSCL reconstruction.

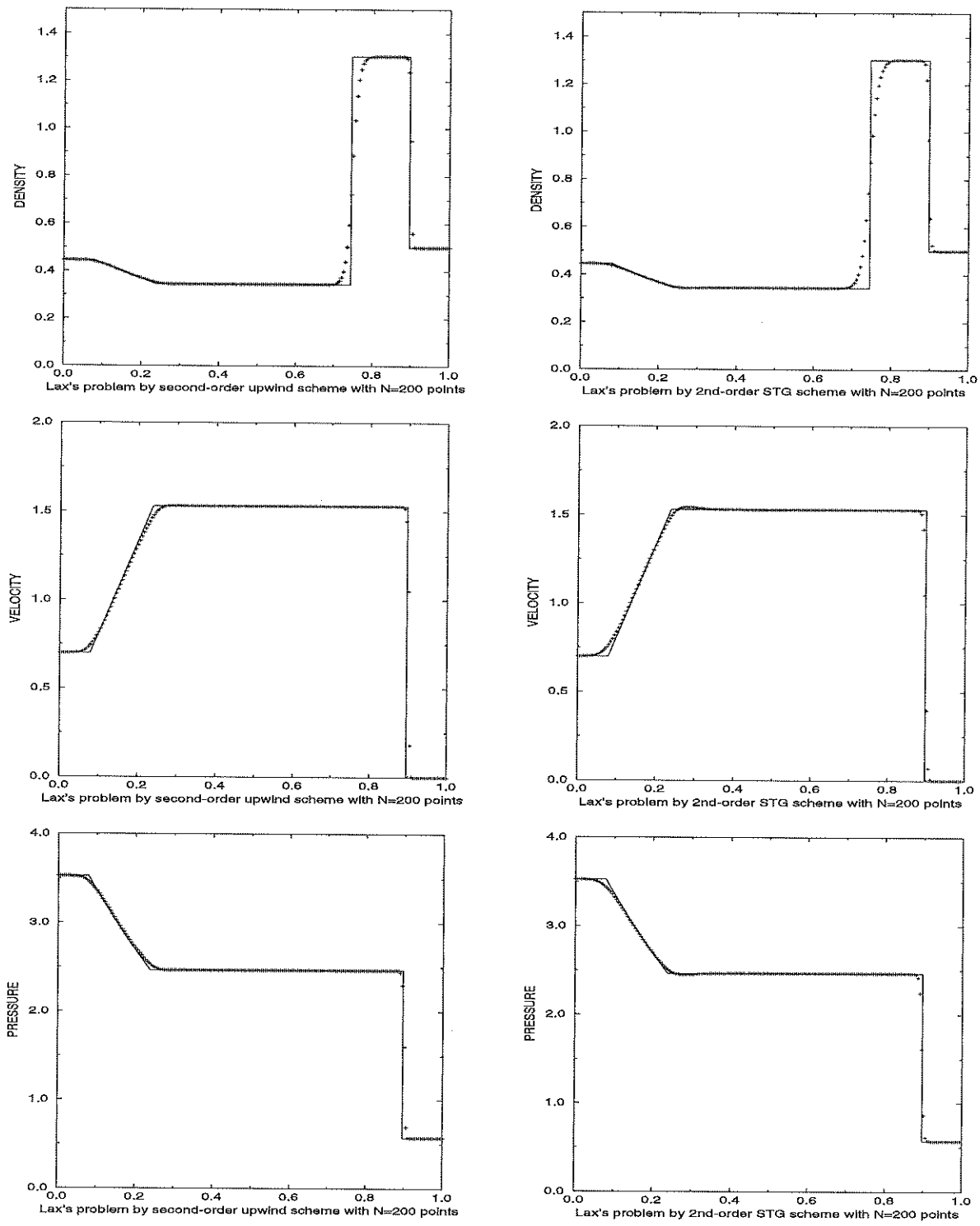

Figure 2.3.2: 2nd order: central (STG) vs. upwind (ULT) — Lax's Riemann problem

In figure 2.3.2 we compare, side by side, the upwind ULT scheme of Harten, [12], with our central scheme (2.3.4)-(2.3.5). The comparable high-resolution of this so called Lax's Riemann problem is evident.

At the same time, the central scheme (2.3.4)-(2.3.5) has the advantage over the corresponding upwind schemes, in that no (approximate) Riemann solvers, as in (2.2.7), are required. Hence, these Riemann-free central schemes provide an efficient high-resolution alternative in the one-dimensional case, and a particularly advantageous framework for multidimensional computations, e.g., [3], [2], [16]. This advantage in the multidimensional case will be explored in the next section. Also, *staggered* central differencing, along the lines of the Riemann-free Nessyahu-Tadmor scheme (2.3.4)-(2.3.5), admits simple efficient extensions in the presence of general source terms, [8], and in particular, stiff source terms, [3]. Indeed, it is a key ingredient behind the relaxation schemes studied in [18].

It should be noted, however, that the component-wise version of these central schemes might result in deterioration of resolution at the computed extrema. The second-order computation presented in figure 2.3.2 below demonstrates this point. (this will be corrected by higher order central methods). Of course, this – so called extrema clipping, is typical to high-resolution upwind schemes as well; but it is more pronounced with our central schemes due to the built-in extrema-switching to the dissipative LxF scheme. Indeed, once an extrema cell, I_j, is detected (by the limiter), it sets a zero slope, $w'_j = 0$, in which case the second-order scheme (2.3.4)-(2.3.5) is reduced back to the first-order LxF, (2.2.14).

2.3.2 The third-order central scheme

Following the framework outlined in §2.3.1, the upgrade to third-order central scheme consists of two main ingredients:

(i) A third-order accurate, piecewise-quadratic polynomial reconstruction which enjoys desirable non-oscillatory properties;

(ii) An appropriate quadrature rule to approximate the numerical fluxes along cells' interfaces.

Following [28], we proceed as follows. The piecewise-parabolic reconstruction takes the form

$$p_j(x) = w_j^n + w'_j\left(\frac{x-x_j}{\Delta x}\right) + \frac{1}{2}w''_j\left(\frac{x-x_j}{\Delta x}\right)^2. \tag{2.3.6}$$

Here, w''_j are the (pointvalues of) the *reconstructed second derivatives*

$$w''_j := \theta_j \Delta_+\Delta_-\bar{w}_j^n; \tag{2.3.7}$$

w'_j are the (pointvalues of) the *reconstructed slopes*,

$$w'_j := \theta_j \Delta_0\bar{w}_j^n; \tag{2.3.8}$$

and w_j^n are the *reconstructed pointvalues*

$$w_j^n := \bar{w}_j^n - \frac{w''_j}{24}. \tag{2.3.9}$$

Observe that, starting with third- (and higher-) order accurate methods, pointwise values *cannot* be interchanged with cell averages, $w_j^n \neq \bar{w}_j^n$.

Here, θ_j are appropriate nonlinear limiters which guarantee the non-oscillatory behavior of the third-order reconstruction; its precise form can be found in [27], [28]. They guarantee that the reconstruction (2.3.6) is non-oscillatory in the sense that $N(w(\cdot,t^n))$ — the number of extrema of $w(x,t^n)$, does not exceed that of its piecewise-constant projection, $N(\Sigma\bar{w}_j^n\chi_j(\cdot))$,

$$N(w(\cdot,t^n)) \leq N(\Sigma\bar{w}_j^n\chi_j(\cdot)). \tag{2.3.10}$$

Next we turn to the evolution of the piecewise-parabolic reconstructed solution. To this end we need to evaluate the staggered averages, $\{\bar{w}_{j+\frac{1}{2}}^n\}$, and to approximate the interface fluxes, $\left\{\int_{\tau=t^n}^{t^{n+1}} f(w(x_j,\tau))d\tau\right\}$.

With $p_j(x) = w_j^n + w_j'\left(\frac{x-x_j}{\Delta x}\right) + \frac{1}{2}w_j''\left(\frac{x-x_j}{\Delta x}\right)^2$ specified in (2.3.6)-(2.3.9), one evaluates the staggered averages of the third order reconstruction $w(x,t^n) = \Sigma p_j(x)\ \chi_j(x)$

$$\bar{w}_{j+\frac{1}{2}}^n = \frac{1}{\Delta x}\int_{x_j}^{x_{j+1}} w(x,t^n)dx = \frac{1}{2}(\bar{w}_j + \bar{w}_{j+1}) + \frac{1}{8}(w_j' - w_{j+1}'). \tag{2.3.11}$$

Remarkably, we obtain here the same formula for the staggered averages as in the second-order cases, consult (2.3.3); the only difference is the use of the new limited slopes in (2.3.8), $w_j' = \theta_j\Delta_0\bar{w}_j^n$.

Next, we approximate the (exact) numerical fluxes by Simpson's quadrature rule, which is (more than) sufficient for retaining the overall third-order accuracy,

$$\frac{1}{\Delta x}\int_{\tau=t^n}^{t^{n+1}} f(w(x_j,\tau))d\tau \sim \frac{\lambda}{6}\left[f(w_j^n) + 4f(w_j^{n+\frac{1}{2}}) + f(w_j^{n+1})\right]. \tag{2.3.12}$$

This in turn, requires the three approximate *pointvalues* on the right, $w_j^{n+\beta} \sim w(x_j,t^{n+\beta})$ for $\beta = 0, \frac{1}{2}, 1$. Following our approach in the second-order case, [29], we use Taylor expansion to *predict*

$$w_j^n = \bar{w}_j^n - \frac{w_j''}{24}; \tag{2.3.13}$$

$$\dot{w}_j^n \equiv (\Delta x\cdot\partial_t)w(x_j,t^n) = -\Delta x\cdot\partial_x f(w(x_j,t^n)) = \\ = -a(w_j^n)\cdot w_j',; \tag{2.3.14}$$

$$\ddot{w}_j^n \equiv (\Delta x\cdot\partial_t)^2 w(x_j,t^n) = \\ = \Delta x\cdot\partial_x\left[a(w_j^n)\Delta x\cdot\partial_x f(w(x_j,t^n))\right] = \\ = a^2(w_j^n)w_j'' + 2a(w_j^n)a'(w_j^n)(w_j')^2. \tag{2.3.15}$$

In summary of the scalar setup, we end up with a two step scheme where, starting with the reconstructed pointvalues

$$w_j^n = \bar{w}_j^n - \frac{w_j''}{24}, \tag{2.3.16}$$

we *predict* the pointvalues $w_j^{n+\beta}$ by, e.g. Taylor expansions,

$$w_j^{n+\beta} = w_j^n + \lambda\beta\dot{w}_j^n + \frac{(\lambda\beta)^2}{2}\ddot{w}_j^n, \qquad \beta = \frac{1}{2}, 1; \tag{2.3.17}$$

this is followed by the *corrector* step

$$\begin{aligned} \bar{w}_{j+\frac{1}{2}}^n = \frac{1}{2}(\bar{w}_j^n + \bar{w}_{j+1}^n) \quad &+ \quad \frac{1}{8}(w_j' - w_{j+1}') + \\ &- \quad \frac{\lambda}{6}\left\{\left[f(w_{j+1}^n) + 4f(w_{j+1}^{n+\frac{1}{2}}) + f(w_{j+1}^{n+1})\right]\right. \\ &\qquad - \quad \left.\left[f(w_j^n) + 4f(w_j^{n+\frac{1}{2}}) + f(w_j^{n+1})\right]\right\}. \end{aligned} \tag{2.3.18}$$

In figure 2.3.2 we revisit the so called Woodward-Colella problem, [43], where we compare the second vs. the third-order results. The improvement in resolving the density field is evident.

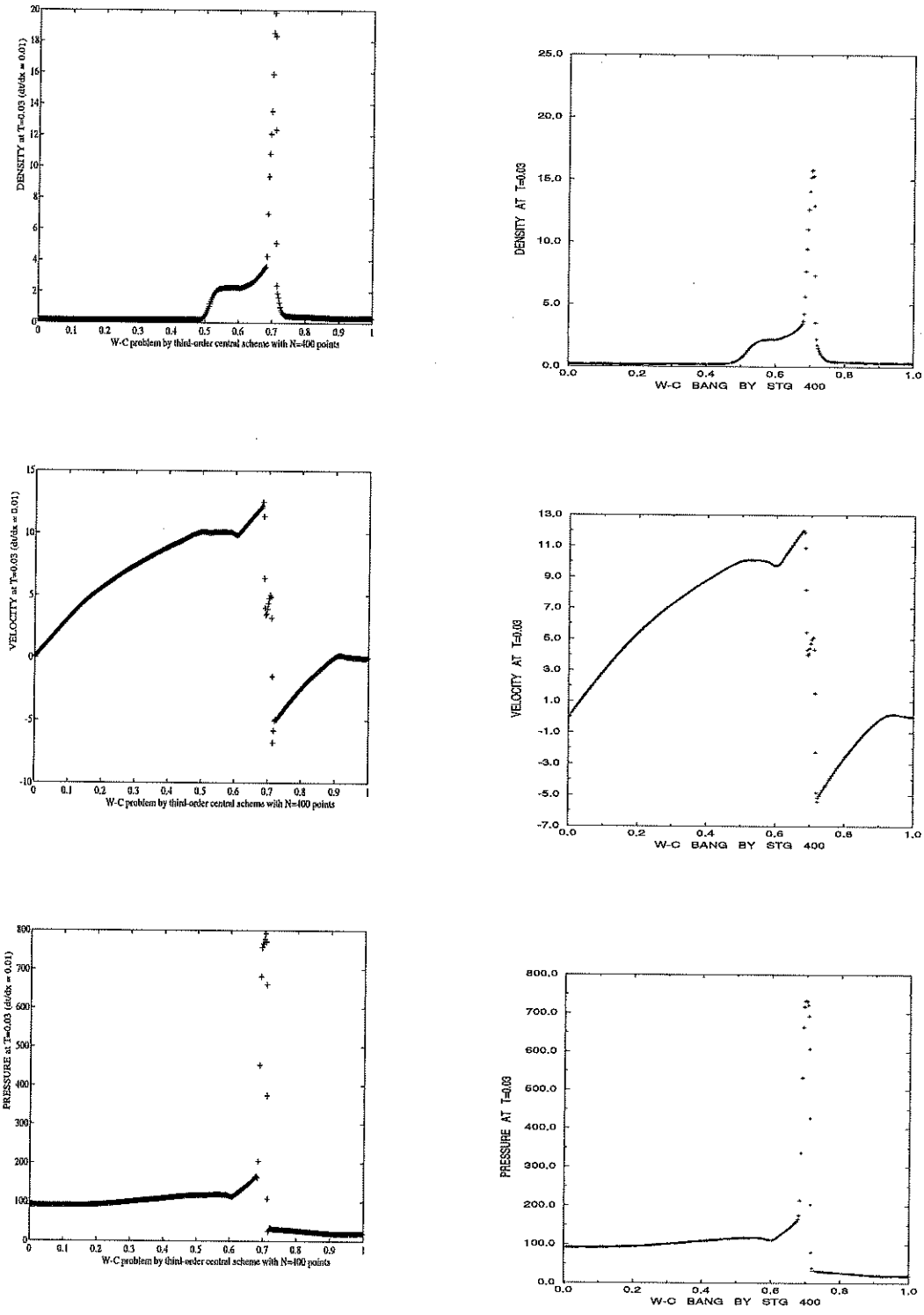

Figure 2.3.3: 3^{rd} vs. 2^{nd} order central schemes — Woodward-Colella problem at $t = 0.03$

We conclude this section with several remarks.

Remarks.

1. Stability.

   We briefly mention the stability results for the scalar central schemes. In the second order case, the NT scheme was shown to be both TVD and entropy stable in the sense of satisfying a cell entropy inequality – consult [29]. The third-order scalar central scheme is stable in the sense of satisfying the NED property, (2.3.10), namely

   Theorem 2.3.1 ([28]) *Consider the central scheme (2.3.16),(2.3.17),(2.3.18), based on the third-order accurate quadratic reconstruction, (2.3.6)-(2.3.9). Then it satisfies the so-called Number of Extrema Diminishing (NED) property, in the sense that*

$$N\left(\sum_{\nu}\bar{w}^{n+1}_{\nu+\frac{1}{2}}\chi_{\nu+\frac{1}{2}}(x)\right)\leq N\left(\sum_{\nu}\bar{w}^{n}_{\nu}\chi_{\nu}(x)\right). \tag{2.3.19}$$

2. Source terms, radial coordinates, ...

   Extensions of the central framework which deal with both, stiff and non-stiff source terms can be found in [34],[35], [8], [4]. In particular, Kupferman in [20],[21] developed the central framework within the radial coordinates which require to handle both – variable coefficients + source terms.

3. Higher order central schemes.

   We refer to [36], where a high-order ENO reconstruction is realized by a staggered cell averaging. Here, intricate Riemann solvers are replaced by high order quadrature rules. and for this purpose, one can effectively use the RK method (rather than the Taylor expansion outlined above):

4. Taylor vs. Runge-Kutta.

   The evaluations of Taylor expansions could be substituted by the more economical Runge-Kutta integrations; the simplicity becomes more pronounced with *systems*. A particular useful approach in this context was proposed in [36], using the natural continuous extensions of RK schemes.

5. Systems.

   One of the main advantages of our central-staggered framework over that of the upwind schemes, is that expensive and time-consuming characteristic decompositions can be avoided. Specifically, all the non-oscillatory computations can be carried out with diagonal limiters, based on a *componentwise* extension of the scalar limiters outlined above.

2.4 Central schemes in two space dimensions

Following the one dimensional setup, one can derive a non-oscillatory, two-dimensional central scheme. Here we sketch the construction of the second-order two-dimensional scheme following [16] (see also [2],[1]). For the two-dimensional third-order accurate scheme, we refer to [24].

We consider the two-dimensional hyperbolic system of conservation laws

$$u_t + f(u)_x + g(u)_y = 0. \tag{2.4.1}$$

To approximate a solution to (2.4.1), we start with a two-dimensional linear reconstruction

$$w(x,y,t^n) = \sum_{j,k} p_{j,k}(x,y)\chi_{j,k}(x,y), \quad p_{j,k}(x,y) = \bar{w}^n_{j,k} + w'_{j,k}\left(\frac{x-x_j}{\Delta x}\right) + w\backslash_{j,k}\left(\frac{y-y_k}{\Delta y}\right). \tag{2.4.2}$$

Here, the discrete slopes in the x and in the y direction approximate the corresponding derivatives, $w'_{j,k} \sim \Delta x \cdot w_x(x_j,y_k,t^n) + O(\Delta x)^2$, $w\backslash_{j,k} \sim \Delta y \cdot w_y(x_j,y_k,t^n) + O(\Delta y)^2$, and $\chi_{j,k}(x,y)$ is the characteristic function of the cell $\mathcal{C}_{j,k} := \left\{(\xi,\eta)\middle| |\xi - x_j| \le \frac{\Delta x}{2}, |\eta - y_k| \le \frac{\Delta y}{2}\right\} = I_j \otimes J_k$. Of course, it is essential to reconstruct the discrete slopes, u' and $u\backslash$, with built in *limiters*, which guarantee the non-oscillatory character of the reconstruction; the family of min-mod limiters is a prototype example

$$u'_{jk} = MM\{\theta(\bar{w}^n_{j+1,k} - \bar{w}^n_{j,k}), \frac{1}{2}(\bar{w}^n_{j+1,k} - \bar{w}^n_{j-1,k}), \theta(\bar{w}^n_{j,k} - \bar{w}^n_{j-1,k})\} \tag{2.4.3'}$$

$$u\backslash_{jk} = MM\{\theta(\bar{w}^n_{j,k+1} - \bar{w}^n_{j,k}), \frac{1}{2}(\bar{w}^n_{j,k+1} - \bar{w}^n_{j,k-1}), \theta(\bar{w}^n_{j,k} - \bar{w}^n_{j,k-1})\}. \tag{2.4.3\backslash}$$

An exact evolution of this reconstruction, which is based on integration of the conservation law over the staggered volume yields

$$\begin{aligned}
\bar{w}^{n+1}_{j+\frac{1}{2},k+\frac{1}{2}} &= \fint_{C_{j+\frac{1}{2},k+\frac{1}{2}}} w(x,y,t^n)dxdy + \\
&- \lambda\left\{\fint_{\tau=t^n}^{t^{n+1}} \fint_{y\in J_{k+\frac{1}{2}}} [f(w(x_{j+1},y,\tau)) - f(w(x_j,y,\tau))]\,dyd\tau\right\} + \\
&- \mu\left\{\fint_{\tau=t^n}^{t^{n+1}} \fint_{x\in I_{j+\frac{1}{2}}} [g(w(x,y_{k+1},\tau)) - g(w(x,y_k,\tau))]\,dxd\tau\right\}
\end{aligned} \tag{2.4.4}$$

The exact averages at t^n – consult the floor plan in Figure 2.4.1 yields

$$\begin{aligned}
\bar{w}^n_{j+\frac{1}{2},k+\frac{1}{2}} &:= \fint_{C_{j+\frac{1}{2},k+\frac{1}{2}}} w(x,y,t^n)dxdy = \\
&= \frac{1}{4}(\bar{w}^n_{jk} + \bar{w}^n_{j+1,k} + \bar{w}^n_{j,k+1} + \bar{w}^n_{j+1,k+1}) + \\
&+ \frac{1}{16}\Big\{(u'_{jk} - u'_{j+1,k}) + (u'_{j,k+1} - u'_{j+1,k+1}) + \\
&+ (u\backslash_{jk} - u\backslash_{j,k+1}) + (u\backslash_{j+1,k} - u\backslash_{j+1,k+1})\Big\}.
\end{aligned} \tag{2.4.5}$$

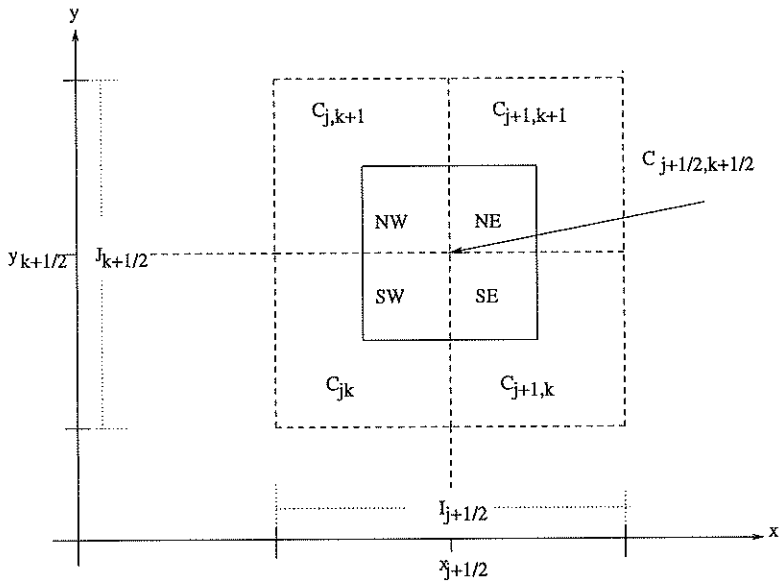

Figure 2.4.1: Floor plan of the staggered grid.

So far everything is *exact*. We now turn to *approximate* the four fluxes on the right of (2.4.4), starting with the one along the East face, consult figure 2.4.2, $\fint_{t^n}^{t^{n+1}} \fint_{J_{k+\frac{1}{2}}} f(w(x_{j+1},y,\tau))dyd\tau$. We use the midpoint quadrature rule for second-order approximation of the temporal integral, $\fint_{y\in J_{k+\frac{1}{2}}} f(w(x_{j+1},y,t^{n+\frac{1}{2}}))dy$; and, for reasons to be clarified below, we use the second-order rectangular quadrature rule for the spatial integration across the y-axis, yielding

$$\fint_{t^n}^{t^{n+1}} \fint_{y\in J_{k+\frac{1}{2}}} f(w(x_{j+1},y,\tau))dyd\tau \sim \frac{1}{2}\left[f(w_{j+1,k}^{n+\frac{1}{2}}) + f(w_{j+1,k+1}^{n+\frac{1}{2}})\right]. \quad (2.4.6)$$

In a similar manner we approximate the remaining fluxes.

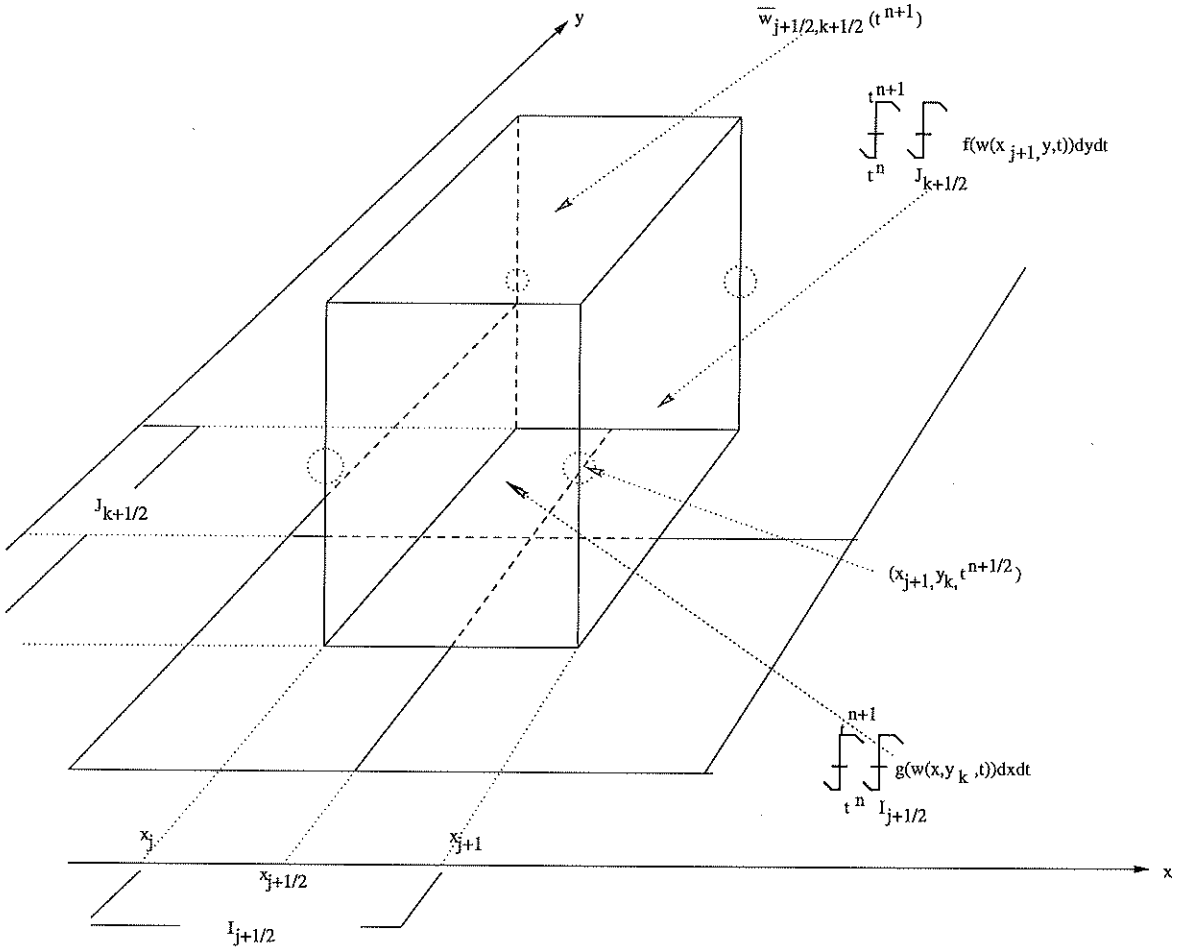

Figure 2.4.2: The central, staggered stencil.

These approximate fluxes make use of the midpoint values, $w_{jk}^{n+\frac{1}{2}} \equiv w(x_j, y_k, t^{n+\frac{1}{2}})$, and it is here that we take advantage of utilizing these midvalues for the spatial integration by the rectangular rule. Namely, since these midvalues are secured at the smooth center of their cells, C_{jk}, bounded away from the jump discontinuities along the edges, we may use Taylor expansion, $w(x_j, y_k, t^{n+\frac{1}{2}}) = \bar{w}_{jk}^n + \frac{\Delta t}{2} w_t(x_j, y_k, t^n) + \mathcal{O}(\Delta t)^2$. Finally, we use the conservation law (2.4.1) to

express the time derivative, w_t, in terms of the spatial derivatives, $f(w)'$ and $g(w)\backslash$,

$$w_{jk}^{n+\frac{1}{2}} = \bar{w}_{jk}^{n} - \frac{\lambda}{2} f(w)'_{jk} - \frac{\mu}{2} g(w)\backslash_{jk}. \tag{2.4.7}$$

Here, $f(w)'_{jk} \sim \Delta x \cdot f(w(x_j, y_k, t^n))_x$ and $g(w)\backslash_{jk} \sim \Delta y \cdot g(w(x_j, y_k, t^n))_y$, are one-dimensional discrete slopes in the x- and y-directions, of the type reconstructed in (2.4.3′)-(2.4.3\): for example, multiplication by the corresponding Jacobians A and B yields

$$f(w)'_{jk} = A(\bar{w}_{jk}^{n}) u'_{jk}, \qquad g(w)\backslash_{jk} = B(\bar{w}_{jk}^{n}) u\backslash_{jk}.$$

Equipped with the midvalues (2.4.7), we can now evaluate the approximate fluxes, e,g., (2.4.6). Inserting these values, together with the staggered average computed in (2.4.6), into (2.4.4), we conclude with new staggered averages at $t = t^{n+1}$, given by

$$\begin{aligned}
\bar{w}_{j+\frac{1}{2},k+\frac{1}{2}}^{n+1} &= \frac{1}{4}(\bar{w}_{jk}^{n} + \bar{w}_{j+1,k}^{n} + \bar{w}_{j,k+1}^{n} + \bar{w}_{j+1,k+1}^{n}) + \\
&+ \frac{1}{16}(u'_{jk} - u'_{j+1,k}) - \frac{\lambda}{2}\left[f(w_{j+1,k}^{n+\frac{1}{2}}) - f(w_{j,k}^{n+\frac{1}{2}})\right] \\
&+ \frac{1}{16}(u'_{j,k+1} - u'_{j+1,k+1}) - \frac{\lambda}{2}\left[f(w_{j+1,k+1}^{n+\frac{1}{2}}) - f(w_{j,k+1}^{n+\frac{1}{2}})\right] \\
&+ \frac{1}{16}(u\backslash_{jk} - u\backslash_{j,k+1}) - \frac{\mu}{2}\left[g(w_{j,k+1}^{n+\frac{1}{2}}) - g(w_{j,k}^{n+\frac{1}{2}})\right] \\
&+ \frac{1}{16}(u\backslash_{j+1,k} - u\backslash_{j+1,k+1}) - \frac{\mu}{2}\left[g(w_{j+1,k+1}^{n+\frac{1}{2}}) - g(w_{j+1,k}^{n+\frac{1}{2}})\right].
\end{aligned} \tag{2.4.8}$$

In summary, we end up with a simple two-step predictor-corrector scheme which could be conveniently expressed in terms on the one-dimensional staggered averaging notations

$$< w_{j,\cdot} >_{k+\frac{1}{2}} := \frac{1}{2}(w_{j,k} + w_{j,k+1}), \quad < w_{\cdot,k} >_{j+\frac{1}{2}} := \frac{1}{2}(w_{j,k} + w_{j+1,k}).$$

Our scheme consists of a *predictor step*

$$w_{j,k}^{n+\frac{1}{2}} = w_{j,k}^{n} - \frac{\lambda}{2} f'_{j,k} - \frac{\mu}{2} g\backslash_{j,k}, \tag{2.4.9}$$

followed by the *corrector step*

$$\begin{aligned}
\bar{w}_{j+\frac{1}{2},k+\frac{1}{2}}^{n+1} &= < \frac{1}{4}(\bar{w}_{j,\cdot}^{n} + \bar{w}_{j+1,\cdot}^{n}) + \frac{1}{8}(w'_{j,\cdot} - w'_{j+1,\cdot}) - \lambda(f_{j+1,\cdot}^{n+\frac{1}{2}} - f_{j,\cdot}^{n+\frac{1}{2}}) >_{k+\frac{1}{2}} + \\
&+ < \frac{1}{4}(\bar{w}_{\cdot,k}^{n} + \bar{w}_{\cdot,k+1}^{n}) + \frac{1}{8}(w\backslash_{\cdot,k} - w\backslash_{\cdot,k+1}) - \mu(g_{\cdot,k+1}^{n+\frac{1}{2}} - g_{\cdot,k}^{n+\frac{1}{2}}) >_{j+\frac{1}{2}}.
\end{aligned}$$

In figures 2.4.3 taken from [16], we present the two-dimensional computation of a double-Mach reflection problem; in figure 2.4.4 we quote from [42] the two-dimensional computation of MHD solution of Kelvin-Helmholtz instability due to shear flow. The computations are based on our second-order central scheme. It is remarkable that such a simple 'two-lines' algorithm, with no characteristic decompositions and no dimensional splitting, approximates the rather complicated double Mach reflection problem with such high resolution. Couple of remarks are in order.

- The two-dimensional computation is more sensitive to the type of limiter than in the one-dimensional framework [29]. In the context of the double Mach reflection problem, the MM_2 (consult (2.3.2) with $\theta = 2$) seems to yield the sharper results.
- No effort was made to optimize the boundary treatment. The staggered stencils require a different treatment for even-odd cells intersecting with the boundaries. A more careful treatment following [105] is presented in §2.4.1. The lack of boundary resolution could be observed at the bottom of the two Mach stems.

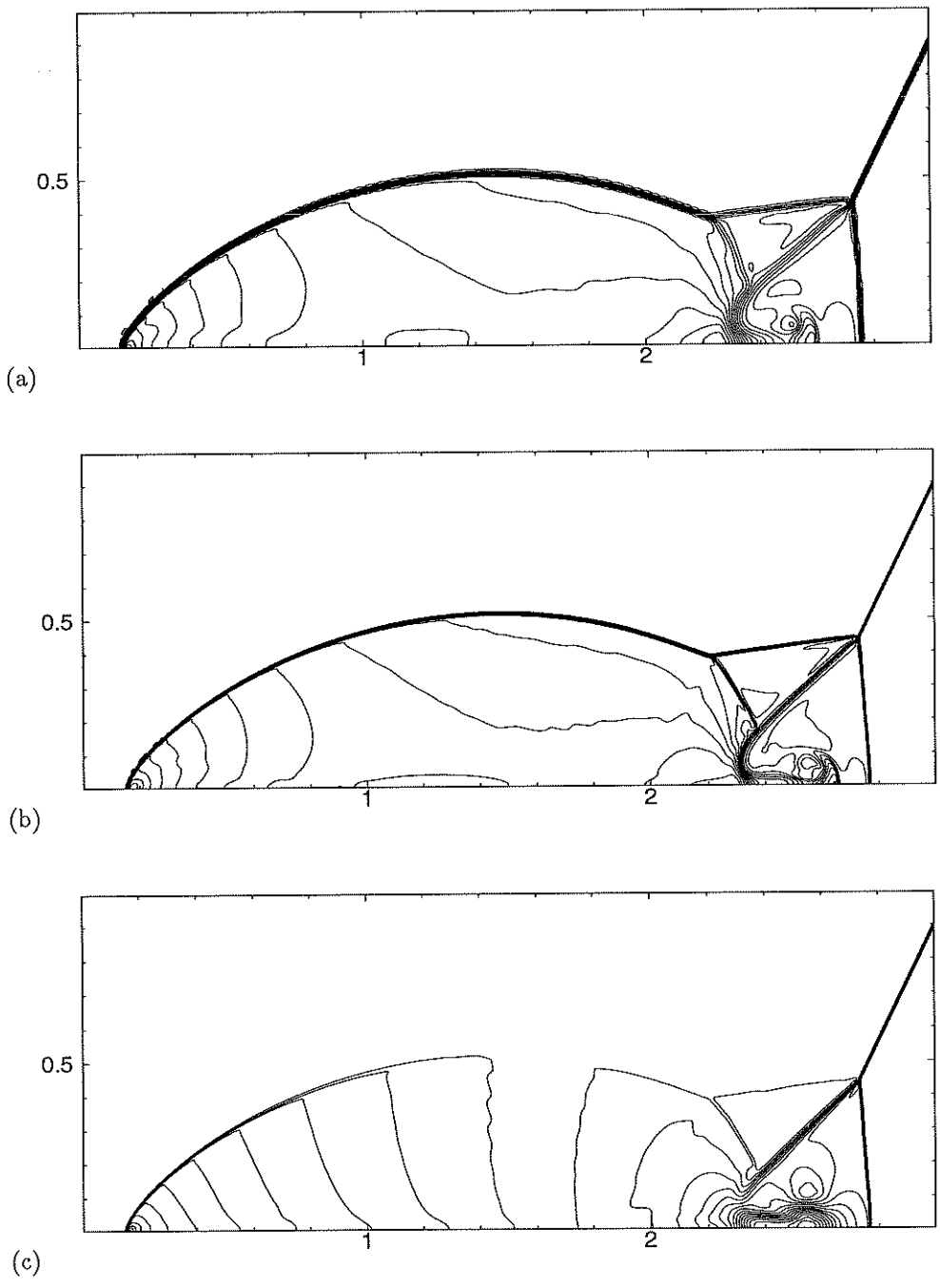

Figure 2.4.3: Double Mach reflection problem computed with the central scheme using MM_2 limiter with CFL=0.475 at $t = 0.2$ (a) density computed with 480×120 cells (b) density computed with 960×240 cells (c) x-velocity computed with 960×240 cells

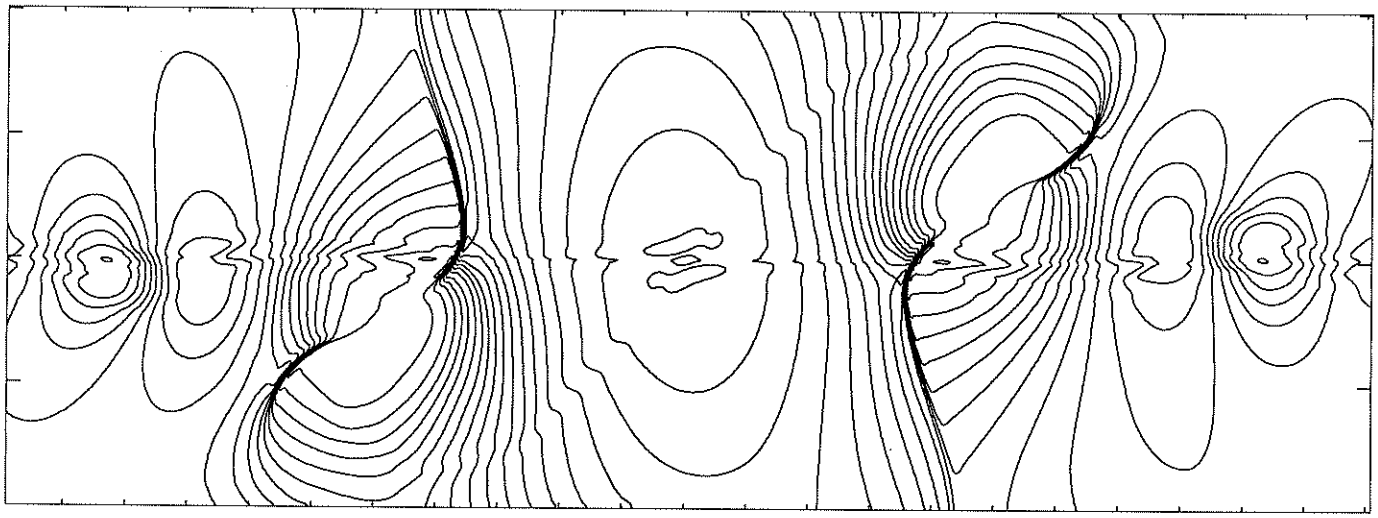

Figure 2.4.4: Kelvin-Helmholtz instability due to shear flow. Transverse configuration (B perpendicular to v). Pressure contours at $t = 140$

We conclude this section with brief remarks on further results related to central schemes.

Remarks.

1. Simplicity.

   Again, we would like to highlight the simplicity of the central schemes, which is particularly evident in the multidimensional setup: no characteristic information is required – in fact, even the exact Jacobians of the fluxes are not required; also, since no (approximate) Riemann solvers are involved, the central schemes require no dimensional splitting; as an example we refer to the approximation of the incompressible equations by central schemes, §2.5; the results in [7] provide another example of a *weakly* hyperbolic multidimensional system which could be efficiently solved in term of central schemes, by avoiding dimensional splitting.

2. Non-staggering. We refer to [15] for a non-staggered version of the central schemes.

3. Stability.

   The following maximum principle holds for the nonoscillatory scalar central schemes:

   Theorem 2.4.1 ([16]) *Consider the two-dimensional scalar scheme (2.4.7-2.4.8), with minmod slopes, u' and $u\backslash$, in (2.4.3'-2.4.3$\hat{}$)). Then for any $\theta < 2$ there exists a sufficiently small CFL number, C_θ (– e.g. $C_1 = (\sqrt{7}-2)/6 \sim 0.1$), such that if the CFL condition is fulfilled,*

$$\max(\lambda \cdot \max_u |f_u(u)|, \mu \cdot \max_u |g_u(u)|) \leq C_\theta,$$

then the following local maximum principle holds

$$\min_{\substack{|p-(j+\frac{1}{2})|=\frac{1}{2}\\ |q-(k+\frac{1}{2})|=\frac{1}{2}}}\{\bar{w}^n_{p,q}\} \le \bar{w}^{n+1}_{j+\frac{1}{2},k+\frac{1}{2}} \le \max_{\substack{|p-(j+\frac{1}{2})|=\frac{1}{2}\\ |q-(k+\frac{1}{2})|=\frac{1}{2}}}\{\bar{w}^n_{p,q}\}. \tag{2.4.10}$$

4. Third-order accuracy. Extensions to third-order accuracy in two space dimensions can be found in [24].

2.4.1 Boundary conditions

Following [25], we demonstrate our boundary treatment in the case of the left-boundary (see Figure 2.4.5).

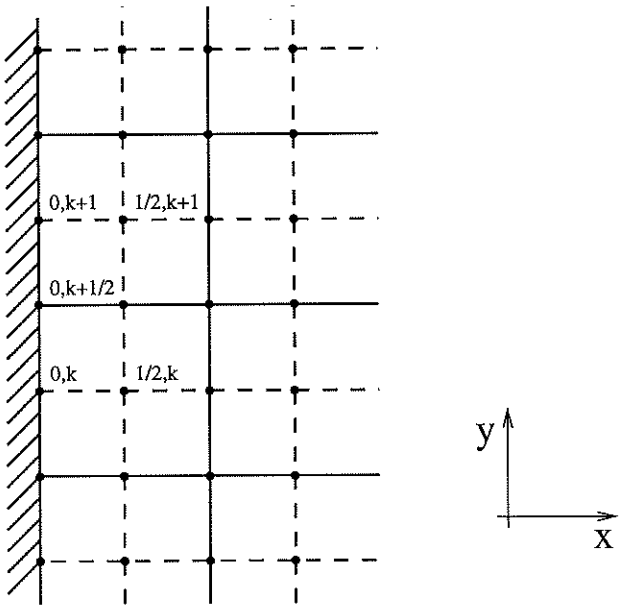

Figure 2.4.5: Two dimensions - left boundary

We distinguish between *inflow* ($f'(w^n_{1/2,k}) > 0$), and *outflow* ($f'(w^n_{1/2,k}) < 0$), boundary cells.

In *inflow* boundary cells, we reconstruct a constant interpolant from the prescribed point-values at these boundaries,

$$p_{1/2,k}(x,y,t^n) \equiv w^n_{0,k}, \qquad w'_{1/2,k} = 0. \tag{2.4.11}$$

This reconstruction is then used to build the approximate solution at time t^{n+1} in the interior cells. At the next-time step, t^{n+1}, the cell-averages at these boundary cells are defined according to the prescribed point-values as

$$\bar{w}^{n+1}_{1/4,k+1/2} := w^{n+1}_{0,k+1/2}.$$

We now turn to the *outflow* boundary cells. Here, we extrapolate the data from the interior of the domain, up to the boundary. First, we determine the discrete slope in the x-direction, $w'_{1/2,k}$. This slope is then used to extrapolate the cell-average up to the boundary,

$$w^n_{0,k} = w^n_{1/2,k} - \frac{\Delta x}{2} w'_{1/2,k},$$

which is then used to predict the mid-value, $w^{n+1/2}_{0,k} = w^n_{0,k} - \frac{\lambda}{2} f'_{0,k} - \frac{\mu}{2} g\backslash_{0,k}$. Here

$$f'_{0,k} = a(w^n_{0,k}) w'_{1/2,k}, \qquad g\backslash_{0,k} = b(w^n_{0,k}) w\backslash_{1/2,k}.$$

The discrete slope in the y-direction, $w\backslash_{0,k}$, is computed in that boundary cell in an analogous way to the interior computation. In summary, the staggered average at time t^{n+1} is given by

$$\begin{aligned} \bar{w}^{n+1}_{1/4,k+1/2} &= \frac{\bar{w}^n_{1/2,k} + \bar{w}^n_{1/2,k+1}}{2} + \\ &+ \frac{1}{8}(-w'_{1/2,k} - w'_{1/2,k+1} + w\backslash_{1/2,k} - w\backslash_{1/2,k+1}) - \\ &- \frac{\lambda}{2}(f(w^n_{1/2,k+1}) + f(w^n_{1/2,k}) - f(w^n_{0,k+1}) - f(w^n_{0,k})) - \\ &- \mu(g(w^n_{1/2,k+1}) + g(w^n_{0,k+1}) - g(w^n_{1/2,k}) - g(w^n_{0,k+1})) \end{aligned} \quad (2.4.12)$$

This concludes the boundary treatment of the left boundary. Similar expressions hold for the other three boundaries.

We now turn to the corners and as a prototype, consider the upper-left corner (see Figure 2.4.6). In the corner we repeat the previous boundary treatment with one simple modification. The main difference regarding the boundary scheme in the corner is based on the number of different possible inflow/outflow configurations in that corner.

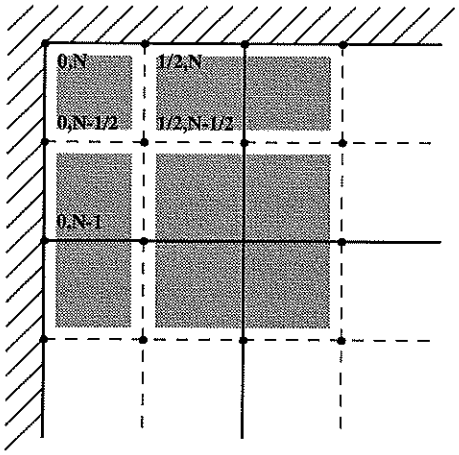

Figure 2.4.6: Upper-left corner

Computationally, the most complicated case is when the flow in that upper-left corner is outflow in both directions. In this case, the staggered average at time t^{n+1}, $\bar{w}^{n+1}_{1/4,N-1/4}$, is computed according to

$$\begin{cases} w'_{1/2,N-1/2} = \cdots & \text{Limited slopes} \\ w\backslash_{1/2,N-1/2} = \cdots \end{cases}$$

$$\begin{cases} w^n_{0,N-1/2} = w^n_{1/2,N-1/2} - \frac{\Delta x}{2} w'_{1/2,N-1/2} & \text{Predictor (west)} \\ w^{n+1/2}_{0,N-1/2} = w^n_{0,N-1/2} - \frac{\lambda}{2} f'_{0,N-1/2} - \frac{\mu}{2} g\backslash_{0,N-1/2} \end{cases}$$

$$\begin{cases} w^n_{1/2,N} = w^n_{1/2,N-1/2} + \frac{\Delta y}{2} w\backslash_{1/2,N-1/2} & \text{Predictor (north)} \\ w^{n+1/2}_{1/2,N} = w^n_{1/2,N} - \frac{\lambda}{2} f'_{1/2,N} - \frac{\mu}{2} g\backslash_{1/2,N} \end{cases}$$

$$\begin{cases} w^n_{0,N} = w^n_{1/2,N-1/2} - \frac{\Delta x}{2} w'_{1/2,N-1/2} + \frac{\Delta y}{2} w\backslash_{1/2,N-1/2} & \text{Predictor (north-west)} \\ w^{n+1/2}_{0,N} = w^n_{0,N} - \frac{\lambda}{2} f'_{0,N} - \frac{\mu}{2} g\backslash_{0,N} \end{cases}$$

The cell-average in the north-west edge of Figure 2.4.6 in time t^{n+1}, is given in this outflow-outflow case by the *corrector step*

$$\begin{aligned} \bar{w}^{n+1}_{1/4,N-1/4} \;=\; & \bar{w}^n_{1/2,N-1/2} + \frac{-w'_{1/2,N-1/2} + w\backslash_{1/2,N-1/2}}{4} - \\ & -\lambda(f(w^n_{1/2,N}) + f(w^n_{1/2,N-1/2}) - f(w^n_{0,N}) - f(w^n_{0,N-1/2})) - \\ & -\mu(g(w^n_{1/2,N}) + g(w^n_{0,N}) - g(w^n_{1/2,N-1/2}) - g(w_{0,N-1/2})) \end{aligned} \tag{2.4.13}$$

When one of the boundaries is inflow, we have $w'_{1/2,N-1/2} = w\backslash_{1/2,N-1/2} = 0$, and $\bar{w}^{n+1}_{1/4,N-1/4} = w^{n+1}_{0,N}$ (– the prescribed pointvalues at the corner).

As an example, we we approximate a solution to the two-dimensional Burgers equation

$$u_t + uu_x + uu_y = 0, \tag{2.4.14}$$

subject to the initial conditions,

$$u_0(x,y) = \begin{cases} 0.5 & -1 \le x < 0, -1 \le y < 0 \\ 0 & 0 \le x \le 1, -1 \le y < 0 \\ -1 & 0 \le x \le 1, 0 \le y \le 1 \\ -0.2 & -1 \le x < 0, 0 \le y \le 1. \end{cases}$$

and augmented with boundary conditions at the inflow boundaries which are equal to the initial values at these same boundaries. Figures 2.4.7 show the evolution of the solution in time for mesh sizes $41 * 41$ and $81 * 81$. Again, we

note that there are no spurious oscillations at the boundaries, oscillations that are inherent with a naive treatment of inflow boundaries.

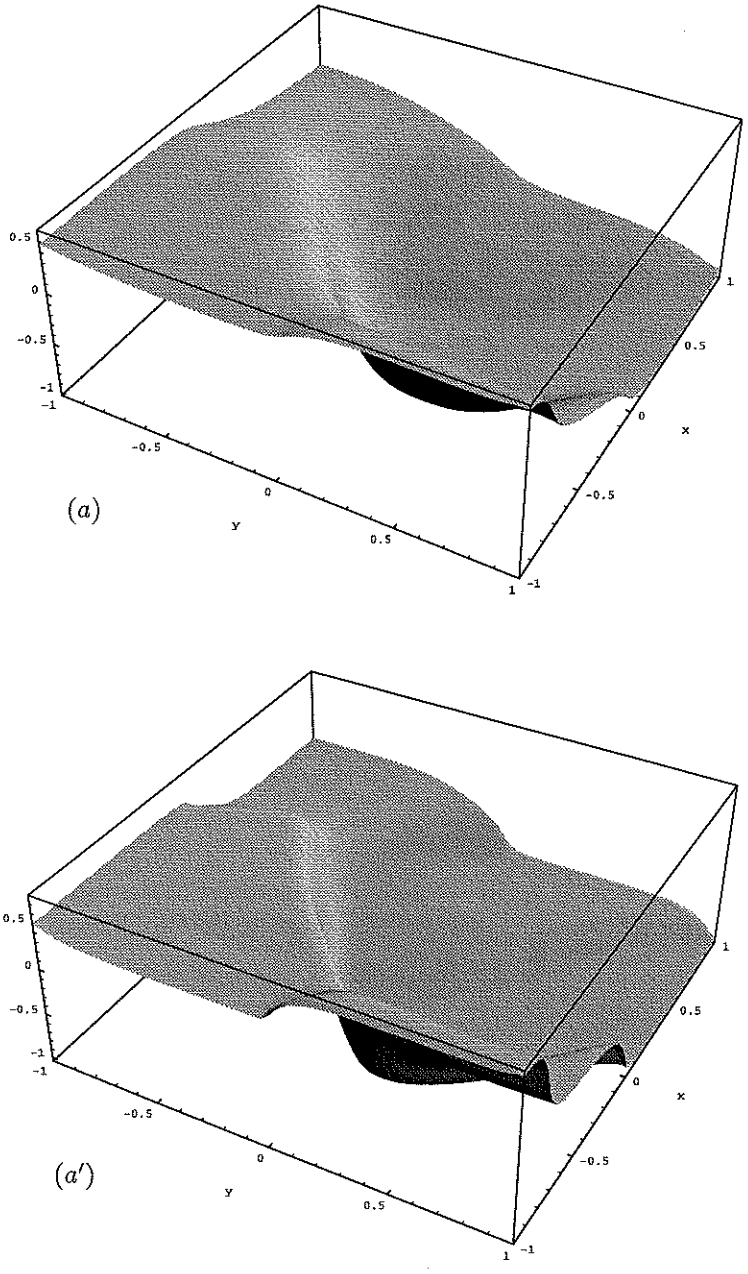

Figure 2.4.7: The 2D IBVP Burgers equation: T=1. (a) N=41, (a') N=81

2.5 Incompressible Euler equations

2.5.1 The vorticity formulation

We are concerned with the approximate solution of the 2D Euler (– and respectively – NS) equations, expressed in terms of the vorticity, $\omega := \nabla \times \vec{u}$,

$$\omega_t + (u\omega)_x + (v\omega)_y = 0 \ (\ +\nu\Delta\omega). \tag{2.5.1}$$

Here, $\vec{u} = (u, v)$, is the two-component divergence-free velocity field,

$$u_x + v_y = 0. \tag{2.5.2}$$

Equation (2.5.1) can be viewed as a nonlinear (viscous) conservation law,

$$\omega_t + f(\omega)_x + g(\omega)_y = 0 \ (\ +\nu\Delta\omega), \tag{2.5.3}$$

with a global flux, $(f, g) := (u\omega, v\omega)$. At the same time, the incompressibility (2.5.2) enables us to rewrite (2.5.1) in the equivalent convective form

$$\omega_t + u\omega_x + v\omega_y = 0. \tag{2.5.4}$$

Equation (2.5.4) guarantees that the vorticity, ω, propagates with finite speed, at least for uniformly bounded velocity field, $\vec{u} \in L^\infty$. This duality between the conservative and convective forms of the equations plays an essential role in our discussion.

To approximate (2.5.1) by a second-order central scheme (following [16, 29]) we introduce a piecewise-linear polynomial MUSCL approximate solution, $\omega(\cdot, \cdot, t)$, at the discrete time levels, $t^n = n\Delta t$,

$$\omega(x, y, t^n) = \sum_{j,k} \Big\{ \bar{\omega}^n_{j,k} + \omega'_{j,k} \left(\frac{x - x_j}{\Delta x} \right) + \omega\backslash_{j,k} \left(\frac{y - y_k}{\Delta y} \right) \Big\} 1_{C_{j,k}}. \tag{2.5.5}$$

with pieces supported in the cells, $C_{j,k} := \left\{ (\xi, \zeta) \,\middle|\, |\xi - x_j| \le \frac{\Delta x}{2}, |\zeta - y_k| \le \frac{\Delta y}{2} \right\}$.

As before, we use the *exact* staggered averages at t^n, followed by the midpoint rule to approximate the corresponding flux. For example, the averaged flux, $f = u\omega$ is approximated by Analogous expressions hold for the remaining fluxes. Note that finite speed of propagation (of ω – which is due to the discrete incompressibility relation (2.5.9) below), guarantees that these values are 'secured' inside a region of local smoothness of the flow. The missing midvalues, $\omega^{n+\frac{1}{2}}_{j,k}$, are predicted using a first-order Taylor expansion (where $\lambda := \frac{\Delta t}{\Delta x}$ and $\mu := \frac{\Delta t}{\Delta y}$, are the usual fixed mesh-ratios),

$$\omega^{n+\frac{1}{2}}_{j,k} = \bar{\omega}^n_{j,k} - \frac{\lambda}{2} f'_{j,k} - \frac{\mu}{2} g\backslash_{j,k} \ (\ +\Delta t\nu\nabla^2\bar{\omega}^n_{j,k}). \tag{2.5.6}$$

Equipped with these midvalues, we are now able to use the approximate fluxes which yield a second-order corrector step outlined in (2.5.11) below. Finally, we have to recover the velocity field from the computed values of vorticity. We end up with the following algorithm.

1. **Reconstruct**

(a) An exact discrete divergence-free reconstruction of the velocity field. We define the discrete vorticity at the mid-cells as the average of the four corners of each cell, i.e.

$$\omega_{j+\frac{1}{2},k+\frac{1}{2}} := \frac{1}{4}(\omega_{j+1,k+1} + \omega_{j,k+1} + \omega_{j,k} + \omega_{j+1,k}). \tag{2.5.7}$$

We then use a streamfunction, ψ, such that $\Delta\psi = -\omega$, which is obtained in the min-cells, e.g., by solving the five-points Laplacian, $\Delta\psi_{j+\frac{1}{2},k+\frac{1}{2}} = -\omega_{j+\frac{1}{2},k+\frac{1}{2}}$. Then, its gradient, $\nabla\psi$ recovers the velocity field

$$u_{j,k} = \mu_x \nabla_y \psi, \qquad v_{j,k} = -\mu_y \nabla_x \psi. \tag{2.5.8}$$

Here, μ_x and μ_y denote averaging in the x-direction and in the y-direction, respectively, such that, e.g.,

$$u_{j,k} = \frac{1}{2}\left(\psi_{j+\frac{1}{2},k+\frac{1}{2}} - \psi_{j+\frac{1}{2},k-\frac{1}{2}} + \psi_{j-\frac{1}{2},k+\frac{1}{2}} - \psi_{j-\frac{1}{2},k-\frac{1}{2}}\right).$$

Observe that with this integer indexed velocity field, we retain a discrete incompressibility relation, centered around $(j+\frac{1}{2}, k+\frac{1}{2})$,

$$\frac{< u_{j+1,\cdot} - u_{j,\cdot} >_{k+\frac{1}{2}}}{\Delta x} + \frac{< v_{\cdot,k+1} - v_{\cdot,k} >_{j+\frac{1}{2}}}{\Delta y} = 0, \tag{2.5.9}$$

which is essential for the maximum principle in (2.5.1).

2. **Predict**

(a) Prepare the pointvalues of the divergence-free velocity field , $\vec{u}(\cdot,\cdot,t^n)$, from the reconstructed vorticity pointvalues, $w^n_{j,k}$. To this end, use the Biot-Savart solver (2.5.8);

(b) Predict the midvalues of the vorticity, $\omega^{n+\frac{1}{2}}_{j,k}$,

$$\omega^{n+\frac{1}{2}}_{j,k} = \bar{\omega}^n_{j,k} - \frac{\lambda}{2} u^n_{j,k}\omega'_{j,k} - \frac{\mu}{2} v^n_{j,k}\omega^{\backslash}_{j,k}. \tag{2.5.10}$$

Note: Observe that here we use the predictor step (2.5.6) in its convective formulation (2.5.4), that is, $(f', g^{\backslash}) = (u\omega', v\omega^{\backslash})$.

3. **Correct**

(a) As in step (2a), use the previously calculated values of the vorticity to compute the divergence-free pointvalues of the velocity, at time $t^{n+\frac{1}{2}}$, $\vec{u}(\cdot,\cdot,t^{n+\frac{1}{2}})$.

(b) Finally, the previously calculated pointvalues of the velocities and vorticity are plugged into the second-order corrector step in order to compute the staggered cell-averages of the vorticity at time t^{n+1},

$$\begin{aligned}
\bar{\omega}^{n+1}_{j+\frac{1}{2},k+\frac{1}{2}} &= <\frac{1}{4}(\bar{\omega}^n_{j,\cdot}+\bar{\omega}^n_{j+1,\cdot})+\frac{1}{8}(\omega'_{j,\cdot}-\omega'_{j+1,\cdot})>_{k+\frac{1}{2}}+\\
&- <\lambda((u\omega)^{n+\frac{1}{2}}_{j+1,\cdot}-(u\omega)^{n+\frac{1}{2}}_{j,\cdot})>_{k+\frac{1}{2}}+\\
&+ <\frac{1}{4}(\bar{\omega}^n_{\cdot,k}+\bar{\omega}^n_{\cdot,k+1})+\frac{1}{8}(\omega'_{\cdot,k}-\omega'_{\cdot,k+1})>_{j+\frac{1}{2}}+\\
&- <\mu((v\omega)^{n+\frac{1}{2}}_{\cdot,k+1}-(v\omega)^{n+\frac{1}{2}}_{\cdot,k})>_{j+\frac{1}{2}}. \qquad (2.5.11)
\end{aligned}$$

The specific recovery of the velocity field outlined above, retains the dual convective-conservative form of the vorticity variable, which in turn leads to the maximum principle [25].

$$\min_{\substack{|p-(j+\frac{1}{2})|=\frac{1}{2}\\|q-(k+\frac{1}{2})|=\frac{1}{2}}}\{\bar{w}^n_{p,q}\}\le \bar{w}^{n+1}_{j+\frac{1}{2},k+\frac{1}{2}}\le \max_{\substack{|p-(j+\frac{1}{2})|=\frac{1}{2}\\|q-(k+\frac{1}{2})|=\frac{1}{2}}}\{\bar{w}^n_{p,q}\}. \qquad (2.5.12)$$

As in the compressible case – compare (2.4.10), the main idea in [25] is to rewrite $\bar{\omega}^{n+1}_{j+\frac{1}{2},k+\frac{1}{2}}$ as a *convex* combination of the cell averages at t^n, $\bar{\omega}^n_{j,k}, \bar{\omega}^n_{j+1,k}, \bar{\omega}^n_{j,k+1}, \bar{\omega}^n_{j+1,k+1}$.

In figure 2.5.2 we show the central computation of a 'thin' shear-layer problem, [5]. For details, consult [25].

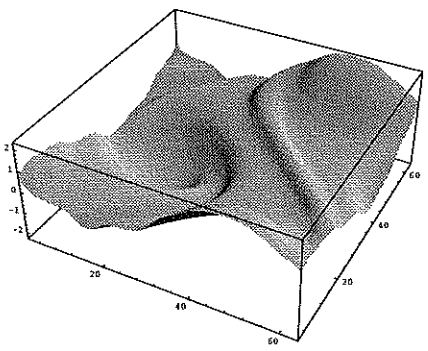

Figure 2.5.1: t = 8 , 64*64

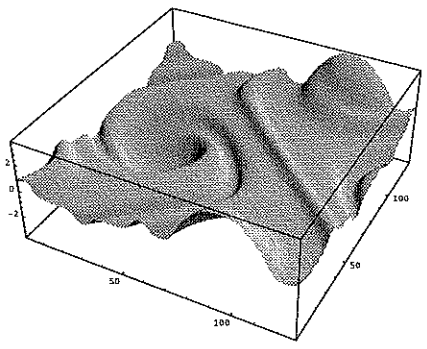

Figure 2.5.2: t = 8 , 128*128

The "thin" shear-layer problem, solved by the second-order central scheme (2.5.6),(2.5.11) with spectral reconstruction of the velocity field.

2.5.2 The velocity formulation

Following [22] our goal is introduce a second-order central difference scheme for incompressible flows, based on *velocity variables*. The use of the velocity

formulation yields a more versatile algorithm. The advantage of our proposed central scheme in its velocity formulation is two-fold: generalization to the three dimensional case is straightforward, and the treatment of boundary conditions associated with general geometries becomes simpler. The result is a simple fast high-resolution method, whose accuracy is comparable to that of an upwind scheme. In addition, numerical experiments show the new scheme to be immune to some of the well-known deleterious consequences of under-resolution.

We consider a two-dimensional incompressible flow field, $\mathbf{u} = (u, v)$, so that $\nabla \cdot \mathbf{u} = 0$. The equations of motion for a Newtonian fluid in conservation form are

$$\begin{aligned} u_t &= \left[-u^2 + \nu u_x - p\right]_x + \left[-uv + \nu u_y\right]_y \equiv f^u(u, v, u_x, \ldots)_x + g^u(u, v, u_x, \ldots)_y \\ v_t &= \left[-uv + \nu v_x\right]_x + \left[-v^2 + \nu v_y - p\right]_y \equiv f^v(u, v, u_x, \ldots)_x + g^v(u, v, u_x, \ldots)_y \end{aligned}, \tag{2.5.13}$$

where p is the pressure, ν is the kinematic viscosity, and subscripts denote partial derivatives. The functions $f^{u,v}(\cdot)$ and $g^{u,v}(\cdot)$ are components of the fluxes of the conserved quantities u and v.

The computational grid consists of rectangular cells of sizes Δx and Δy; at time level $t^n = n\Delta t$, these cells, $\mathcal{C}_{i,j}$, are centered at $(x_i = i\Delta x, y_j = j\Delta y)$. Starting with the corresponding cell averages, $\mathbf{u}^n = (u^n_{i,j}, v^n_{i,j})$, we first reconstruct a piecewise linear polynomial approximation which recovers the point values of the velocity field, $\mathbf{u}^n(x, y) = (u^n(x, y), v^n(x, y))$. For second-order accuracy, the piecewise linear reconstructed velocities take the form,

$$\mathbf{u}^n(x, y) = \mathbf{u}^n_{i,j} + \frac{\mathbf{u}'_{i,j}}{\Delta x}(x - x_i) + \frac{\mathbf{u}'_{i,j}}{\Delta y}(y - y_j), \qquad x, y \in \mathcal{C}_{i,j}. \tag{2.5.14}$$

As before, exact averaging over a staggered control volume yields

$$\begin{aligned} \tilde{u}_{i+\frac{1}{2},j+\frac{1}{2}}(t^{n+1}) &= \fint_{C_{i+\frac{1}{2},j+\frac{1}{2}}} u(x, y, t^n)dxdy + \\ &+ \Delta t \left\{ D^+_x \fint_{\tau=t^n}^{t^{n+1}} \fint_{y \in J_{j+\frac{1}{2}}} f^u(x_i, y, \tau)dyd\tau \right\} + \\ &+ \Delta t \left\{ D^+_y \fint_{\tau=t^n}^{t^{n+1}} \fint_{x \in I_{i+\frac{1}{2}}} g^u(x, y_j, \tau)dxd\tau \right\}, \end{aligned} \tag{2.5.15}$$

and a similar averaging applies for $\tilde{v}^{n+1}_{i+\frac{1}{2},j+\frac{1}{2}}$.

An exact computation yields

$$\fint_{C_{i+\frac{1}{2},j+\frac{1}{2}}} u(x, y, t^n)dxdy = \mu^+_x \mu^+_y u^n_{i,j} - \frac{\Delta x}{8} D^+_x \mu^+_y u'_{i,j} - \frac{\Delta y}{8} D^+_y \mu^+_x u'_{i,j}. \tag{2.5.16}$$

The incompressible fluxes, e.g., $f^u = -u^2 + \nu u_x - p_x$, are approximated in terms of the midpoint rule , which in turn employs predicted midvalues which are obtained from half-step Taylor expansion. Thus our scheme starts with a

predictor step of the form

$$u_{i,j}^{n+\frac{1}{2}} = u_{i,j}^n - \frac{\Delta t}{2}\left[2u_{i,j}^n \frac{u'_{i,j}}{\Delta x} + u_{i,j}^n \frac{v\backslash_{i,j}}{\Delta y} + v_{i,j}^n \frac{u\backslash_{i,j}}{\Delta y} + G_x p_{i,j}^n - \nu\nabla_h^2 u_{i,j}\right] \tag{2.5.17}$$

$$v_{i,j}^{n+\frac{1}{2}} = v_{i,j}^n - \frac{\Delta t}{2}\left[v_{i,j}^n \frac{u'_{i,j}}{\Delta x} + u_{i,j}^n \frac{v'_{i,j}}{\Delta x} + 2v_{i,j}^n \frac{v\backslash_{i,j}}{\Delta y} + G_y p_{i,j}^n - \nu\nabla_h^2 v_{i,j}\right].$$

Note that the predictor step is nothing but a forward Euler scheme; conservation form is not essential for the spatial discretization at this stage.

This is followed by a *corrector step*

$$\left(1 - \frac{\nu\Delta t}{2}\nabla_h^2\right)\tilde{\mathbf{u}}_{i+\frac{1}{2},j+\frac{1}{2}}^{n+1} = \mu_x^+\mu_y^+\mathbf{u}_{i,j}^n - \frac{\Delta x}{8}D_x^+\mu_y^+\mathbf{u}'_{i,j} - \frac{\Delta y}{8}D_y^+\mu_x^+\mathbf{u}\backslash_{i,j} + \tag{2.5.18}$$

$$- \Delta t D_x^+\mu_y^+\left[u_{i,j}^{n+\frac{1}{2}}\mathbf{u}_{i,j}^{n+\frac{1}{2}} - \frac{\nu\mathbf{u}'_{i,j}}{2\Delta x}\right] +$$

$$- \Delta t D_y^+\mu_x^+\left[v_{i,j}^{n+\frac{1}{2}}\mathbf{u}_{i,j}^{n+\frac{1}{2}} - \frac{\nu\mathbf{u}\backslash_{i,j}}{2\Delta y}\right].$$

Note that the viscous terms are handled here by the implicit Crank-Nicholson discretization which is favored due to its preferable stability properties. Here, we ignore the pressure terms; instead, the contribution of the pressure will be integrated by enforcing zero-divergence fluxes at the last *projection step*.

Compute the potential $\phi_{i,j}$ solving the Poisson equation

$$\left[D_x^+D_x^-\mu_y^+\mu_y^- + D_y^+D_y^-\mu_x^+\mu_x^-\right]\phi_{i,j} = \frac{1}{\Delta t}\left[D_x^-\mu_y^-\tilde{u}_{i+\frac{1}{2},j+\frac{1}{2}}^{n+1} + D_y^-\mu_x^-\tilde{v}_{i+\frac{1}{2},j+\frac{1}{2}}^{n+1}\right]. \tag{2.5.19}$$

Then, the pressure gradient at t^{n+1} is being updated,

$$G_x p_{i+\frac{1}{2},j+\frac{1}{2}}^{n+1} := D_x^+\mu_y^+\phi_{i,j}, \qquad G_y p_{i+\frac{1}{2},j+\frac{1}{2}}^{n+1} := D_y^+\mu_x^+\phi_{i,j}, \tag{2.5.20}$$

and finally, it is used to evaluate the divergence-free velocity field, $\mathbf{u}^{n+1}$

$$\mathbf{u}_{i+\frac{1}{2},j+\frac{1}{2}}^{n+1} = \tilde{\mathbf{u}}_{i+\frac{1}{2},j+\frac{1}{2}}^{n+1} - \Delta t\mathbf{G_x}p_{i+\frac{1}{2},j+\frac{1}{2}}^{n+1}. \tag{2.5.21}$$

In Figure 2.5.3, we plot vorticity contours for two shear layer problems studied in [5]: the inviscid "thick" shear layer problem corresponding to (u_0^ρ, v_0^δ) with $\rho = 30$, and a viscous "thin" shear layer problem (with $\nu = 5 \cdot 10^{-5}$), corresponding to (u_0^ρ, v_0^δ) with $\rho = 100$. As in [5], both plots in Figures 2.5.3a and 2.5.3b are recorded at time $t = 1.2$, and are subject to an initial perturbation v_0^δ, with $\delta = 0.05$.

Further applications of the central schemes for more complex incompressible flows (with 'variable' axisymmetric coefficients, forcing source/viscous terms, ...), can be found in [20],[21].

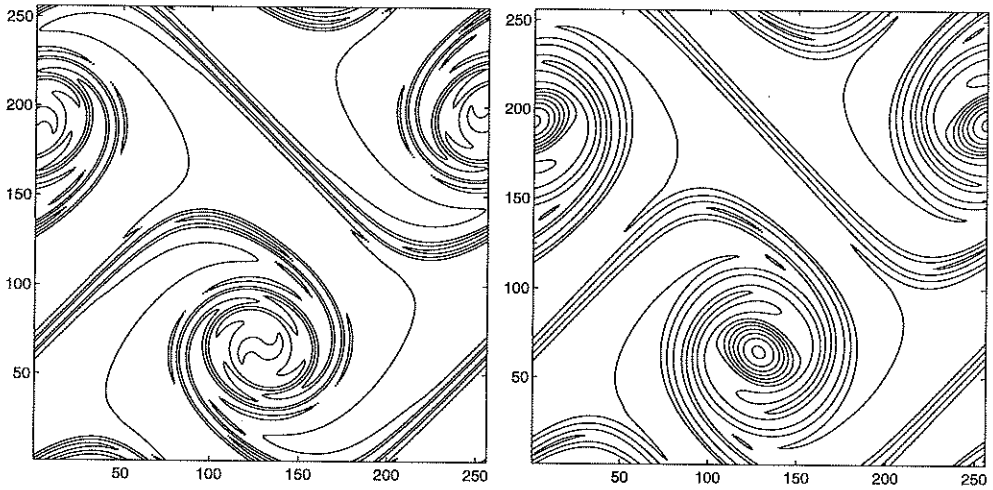

Figure 2.5.3: Contour lines of the vorticity, $\omega = v_x - u_y$, at $t = 1.2$ with initial $(u^\rho, v^\delta), \delta = 0.05$, using a 256×256 grid. (a) A "thick" shear layer with $\rho = 30$, and $\nu = 0$. The contour levels range from -36 to 36 (cf. Figure 3c in Ref. [5]). (b) A "thin" shear layer with $\rho = 100$, and $\nu = 5 \cdot 10^{-5}$. The contour levels range from -70 to 70 (cf. Figure 9b in Ref. [5]).

Bibliography

[1] P. ARMINJON, D. STANESCU & M.-C. VIALLON, *A Two-Dimensional Finite Volume Extension of the Lax-Friedrichs and Nessyahu-Tadmor Schemes for Compressible Flow*, (1995), preprint.

[2] P. ARMINJON, D. STANESCU & M.-C. VIALLON, *A two-dimensional finite volume extension of the Lax-Friedrichs and Nessyahu-Tadmor schemes for compressible flows*, Preprint.

[3] P. ARMINJON & M.-C. VIALLON, *Généralisation du Schéma de Nessyahu-Tadmor pour Une Équation Hyperbolique à Deux Dimensions D'espace*, C.R. Acad. Sci. Paris, **t. 320** , série I. (1995), pp. 85-88.

[4] F. BEREUX & L. SAINSAULIEU, *A Roe-type Riemann Solver for Hyperbolic Systems with Relaxation Based on Time-Dependent Wave Decomposition*, Numer. Math,. **77**, (1997), pp. 143-185.

[5] D. L. BROWN & M. L. MINION *Performance of under-resolved two-dimensional incompressible flow simulations*, J. Comp. Phys. **122**, (1985) 165–183.

[6] P. COLELLA & P. WOODWARD, *The piecewise parabolic method (PPM) for gas-dynamical simulations*, JCP **54**, 1984, pp. 174-201.

[7] B. ENGQUIST & O. RUNBORG, *Multi-phase computations in geometrical optics*, J. Comp. Appl. Math., 1996, in press.

[8] ERBES, *A high-resolution Lax-Friedrichs scheme for Hyperbolic conservation laws with source term. Application to the Shallow Water equations.* Preprint.

[9] K.O. FRIEDRICHS & P.D. LAX, *Systems of Conservation Equations with a Convex Extension*, Proc. Nat. Acad. Sci., **68**, (1971), pp.1686-1688.

[10] E. GODLEWSKI & P.-A. RAVIART, *Hyperbolic Systems of Conservation Laws*, Mathematics & Applications, Ellipses, Paris, 1991.

[11] S.K. GODUNOV, *A finite difference method for the numerical computation of discontinuous solutions of the equations of fluid dynamics*, Mat. Sb. **47**, 1959, pp. 271-290.

[12] A. HARTEN, *High Resolution Schemes for Hyperbolic Conservation Laws*, JCP, **49**, (1983), pp.357-393.

[13] A. HARTEN, B. ENGQUIST, S. OSHER & S.R. CHAKRAVARTHY, *Uniformly high order accurate essentially non-oscillatory schemes. III*, JCP **71**, 1982, pp. 231-303.

[14] HUYNH, *A piecewise-parabolic dual-mesh method for the Euler equations*, AIAA-95-1739-CP, The 12th AIAA CFD Conf., 1995.

[15] G.-S. JIANG, D. LEVY, C.-T. LIN, S. OSHER & E. TADMOR, *High-resolution Non-Oscillatory Central Schemes with Non-Staggered Grids for Hyperbolic Conservation Laws*, SIAM Journal on Num. Anal., to appear.

[16] G.-S JIANG & E. TADMOR, *Nonoscillatory Central Schemes for Multidimensional Hyperbolic Conservation Laws*, SIAM J. Scie. Comp., to appear.

[17] S. JIN, private communication.

[18] S. JIN AND Z. XIN, *The relaxing schemes for systems of conservation laws in arbitrary space dimensions*, Comm. Pure Appl. Math. 48 (1995) 235–277.

[19] B. VAN LEER, *Towards the Ultimate Conservative Difference Scheme, V. A Second-Order Sequel to Godunov's Method*, JCP, **32**, (1979), pp.101-136.

[20] R. KUPFERMAN, *Simulation of viscoelastic fluids: Couette-Taylor flow*, J. Comp. Phys., to appear.

[21] R. KUPFERMAN, *A numerical study of the axisymmetric Couette-Taylor problem using a fast high-resolution second-order central scheme*, SIAM. J. Sci. Comp., to appear.

[22] R. KUPFERMAN & E. TADMOR, *A Fast High-Resolution Second-Order Central Scheme for Incompressible Flow s*, Proc. Nat. Acad. Sci.,

[23] R.J. LEVEQUE, *Numerical Methods for Conservation Laws*, Lectures in Mathematics, Birkhauser Verlag, Basel, 1992.

[24] D. LEVY, *Third-order 2D Central Schemes for Hyperbolic Conservation Laws*, in preparation.

[25] D. LEVY & E. TADMOR, *Non-oscillatory Central Schemes for the Incompressible 2-D Euler Equations*, Math. Res. Let., **4**, (1997), pp.321-340.

[26] X.-D. LIU & P. D. LAX, *Positive Schemes for Solving Multi-dimensional Hyperbolic Systems of Conservation Laws, Courant Mathematics and Computing Laboratory Report,* Comm. Pure Appl. Math.

[27] X.-D. LIU & S. OSHER, *Nonoscillatory High Order Accurate Self-Similar Maximum Principle Satisfying Shock Capturing Schemes I*, SINUM, **33**, no. 2 (1996), pp.760-779.

[28] X.-D. LIU & E. TADMOR, *Third Order Nonoscillatory Central Scheme for Hyperbolic Conservation Laws*, Numer. Math., to appear.

[29] H. NESSYAHU & E. TADMOR, *Non-oscillatory Central Differencing for Hyperbolic Conservation Laws*, JCP, **87**, no. 2 (1990), pp.408-463.

[30] S. OSHER & E. TADMOR, *On the Convergence of Difference Approximations to Scalar Conservation Laws*, Math. Comp., **50**, no. 181 (1988), pp.19-51.

[31] P. L. ROE, *Approximate Riemann Solvers, Parameter Vectors, and Difference Schemes*, JCP, **43**, (1981), pp.357-372.

[32] A. ROGERSON & E. MEIBURG, *A numerical study of the convergence properties of ENO schemes*, J. Sci. Comput., **5**, 1990, pp. 127-149.

[33] O. RUNBORG, *Multiphase Computations in Geometrical Optics*, UCLA CAM report no. 96-52 (1996).

[34] V. ROMANO & G. RUSSO, *Numerical solution for hydrodynamical models of semiconductors*, IEEE, to appear.

[35] A.M. ANILE, V. ROMANO & G. RUSSO, *Extended hydrodymnamical model of carrier transport in semiconductors*, Phys. Rev. B., to appear.

[36] F. BIANCO, G. PUPPO & G. RUSSO, *High order central schemes for hyperbolic systems of conservation laws*, SIAM J. Sci. Comp., to appear.

[37] R. SANDERS, *A Third-order Accurate Variation Nonexpansive Difference Scheme for Single Conservation Laws*, Math. Comp., **41** (1988), pp.535-558.

[38] R. SANDERS R. & A. WEISER, *A High Resolution Staggered Mesh Approach for Nonlinear Hyperbolic Systems of Conservation Laws*, JCP, **1010** (1992), pp.314-329.

[39] P. K. SWEBY, *High Resolution Schemes Using Flux Limiters for Hyperbolic Conservation Laws*, SINUM, **21**, no. 5 (1984), pp.995-1011.

[40] C.-W. SHU, *Numerical experiments on the accuracy of ENO and modified ENO schemes*, JCP **5**, 1990, pp. 127-149.

[41] G. SOD, *A survey of several finite difference methods for systems of nonlinear hyperbolic conservation laws*, JCP **22**, 1978, pp. 1-31.

[42] E. TADMOR & C.C. WU, *Central Scheme for the Multidimensional MHD Equations*, in preparation.

[43] P. WOODWARD & P. COLELLA, *The numerical simulation of two-dimensional fluid flow with strong shocks*, JCP **54**, 1988, pp. 115-173.

Chapter 3

The Spectral Viscosity Method

3.1 Introduction

Let P_N stands for one of the standard spectral projections — Fourier, Chebyshev, Legendre .... It is well known that such spectral projections, $P_N u$, provide highly accurate approximations for sufficiently smooth u's. This superior accuracy is destroyed if u contains discontinuities. Indeed, $P_N u$ produces $\mathcal{O}(1)$ Gibbs' oscillations in the *local* neighborhoods of the discontinuities, and moreover, their *global* accuracy deteriorates to first-order.

We are interested in spectral approximations of nonlinear conservation laws

$$\frac{\partial u}{\partial t} + \frac{\partial}{\partial x} f(u) = 0, \tag{3.1.1}$$

subject to initial conditions, $u(x,0) = u_0$, and augmented with appropriate boundary conditions. The purpose of a spectral method is to compute an approximation to the *projection* of $u(\cdot,t)$ rather than $u(\cdot,t)$ itself. Consequently, since nonlinear conservation laws exhibit spontaneous shock discontinuities, the spectral approximation faces two difficulties:

Stability. Numerical tests indicate that the convergence of spectral approximations to nonlinear conservation laws fails. In [26]–[28] we prove[1] that this failure is related to the fact that spurious Gibbs oscillations pollute the entire computational domain, and that the lack of entropy dissipation then renders these spectral approximations unstable.

Accuracy. The accuracy of the spectral computation is limited by the first order convergence rate of $P_N u(\cdot,t)$.

With this in mind we turn to discuss the Spectral Viscosity (SV) method introduced in [26]. Our discussion focuses on three aspects: the periodic Fourier SV method in both – one and several space dimensions and the nonperiodic Legendre SV method.

[1] Consult the counterexamples in the introductory section of Lecture IV below.

In §3.2 we begin with the one-dimensional periodic problems. The purpose of the SV method is to stabilize the nonlinear spectral approximation without sacrificing its underlying spectral accuracy. This is achieved by augmenting the standard spectral approximation with high frequency regularization. In §3.2.1 we briefly review the convergence results of the periodic Fourier SV method, [26]–[29], [17], [5], [21]. These convergence results employ high frequency regularization based on *second order* viscosity. In §3.2.2 we discuss spectral approximations based on "super-viscosity", i.e., high-frequency parabolic regularizations of order > 2. These 'super' spectral viscosities were introduced and analyzed in [30]. Extensions of the spectral super viscosity to non-periodic problems was presented in [13]. We prove the H^{-1}-stability of these spectral 'super-viscosity' approximations, and together with L^∞-stability, convergence follows by compensated compactness arguments [31],[16].

In §3.3 we turn to the nonperiodic case and discuss the Legendre SV method, [18]. Extensions to and applications with Chebyshev SV method can be found in [12],[2],[15]. Finally, the multidimensional problem is treated in §3.5, along the lines of [5].

We close this introduction by referring to the numerical experiments in §3.4 quoted from [18]; see also [28]. These numerical tests show that by *post-processing* the spectral (super)-viscosity approximation, the exact entropy solution is recovered within spectral accuracy. This post-processing is carried out as a highly accurate mollification and operated either in the physical space as in [10],[1],[18], or in the dual Fourier space as in [11],[19],[32]. It should be emphasized that the role of post-processing is essential in order to realize the highly accurate content of the SV solution.
For further applications in two- and three-dimensional atmospheric simulations we refer to [2],[15],[7] and the references therein.

3.2 The Fourier Spectral Viscosity (SV) method

To solve the periodic conservation law (3.1.1) by a spectral method, one employs an N-degree trigonometric polynomial

$$u_N(x,t) = \sum_{|k|\le N} \widehat{u}_k(t) e^{ikx} \ , \tag{3.2.1}$$

in order to approximate the Fourier projection of the exact entropy solution, $P_N u$.[2] Starting with $u_N(x,0) = P_N u_0(x)$, the classical spectral method lets $u_N(x,t)$ evolve according to the approximate model

$$\frac{\partial u_N}{\partial t} + \frac{\partial}{\partial x}\big[P_N\big(f(u_N)\big)\big] = 0 \ . \tag{3.2.2}$$

As we have already noted, the convergence of u_N towards the entropy solution of (3.1.1), $u_N \underset{N\to\infty}{\longrightarrow} u$, may fail, [26]. Instead, we modify (3.2.2) by augmenting

[2]The spectral Fourier projection of $u(x)$ is given by $\sum_{|k|\le N}(u, e^{ikx})e^{ikx}$; the pseudospectral Fourier projection of $u(x)$ is given by $\sum_{|k|\le N} < u, e^{ikx} > e^{ikx}$, where $< u, e^{ikx} > := \Delta x \sum_\nu u(x_\nu)e^{-ikx_\nu}$ is collocated at the $2N+1$ equidistant gridvalues $x_\nu = 2\pi\nu\Delta x$. $P_N u$ denotes either one of these two projections.

it with high frequency viscosity regularization which amounts to

$$\frac{\partial u_N}{\partial t} + \frac{\partial}{\partial x}\left[P_N f(u_N(x,t))\right] = \varepsilon_N (-1)^{s+1} \frac{\partial^s}{\partial x^s}\left[Q_m(x,t) * \frac{\partial^s u_N}{\partial x^s}\right], \quad s \geq 1. \tag{3.2.3$_s$}$$

This kind of *spectral viscosity* can be efficiently implemented in Fourier space as

$$\varepsilon_N \frac{\partial^s}{\partial x^s}\left[Q_m(x,t) * \frac{\partial^s u_N}{\partial x^s}\right] := \varepsilon \sum_{m<|k|\leq N} (ik)^{2s} \widehat{Q}_k(t) \widehat{u}_k(t) e^{ikx}. \tag{3.2.4}$$

It involves the following three ingredients:

- the viscosity amplitude, $\varepsilon = \varepsilon_N$,

$$\varepsilon \equiv \varepsilon_N \sim \frac{2\mathcal{C}_s}{N^{2s-1}}; \tag{3.2.5}$$

  Here, $\mathcal{C}_s$ is a constant which may depend on the fixed order of super-viscosity, s. (A pessimistic upper bound of this constant will be specified below — consult [5, Theorem 2.1]).

- the effective size of the *inviscid* spectrum, $m = m_N$,

$$m \equiv m_N \sim N^\theta, \qquad \theta < \frac{2s-1}{2s}; \tag{3.2.6}$$

- the SV smoothing factors, $\widehat{Q}_k(t)$, which are activated only on high wavenumbers, $|k| > m_N$, satisfying

$$1 - \left(\frac{m}{|k|}\right)^{\frac{2s-1}{\theta}} \leq \widehat{Q}_k(t) \leq 1, \quad |k| > m_N. \tag{3.2.7}$$

The SV method can be viewed as a compromise between the total-variation stable viscosity approximation – see (3.2.9) and (3.2.15$_s$) below – which is restricted to first order accuracy (corresponding to $\theta = 0$), and the spectrally accurate yet unstable spectral method (3.2.2) (corresponding to $\theta = 1$). The additional SV on the right of (3.2.3$_s$) is small enough to retain the *formal* spectral accuracy of the underlying spectral approximation, i.e., the following estimate holds

$$\|\varepsilon_N \frac{\partial^{s+p}}{\partial x^{s+p}}\left[Q_m(x,t) * \frac{\partial^s u_N}{\partial x^s}\right]\|_{L^2(x)} \leq \text{Const} \cdot N^{-\theta(q-p-1)} \|\frac{\partial^q u_N}{\partial x^q}\|_{L^2(x)}, \quad \forall q \geq p+1 > -\infty. \tag{3.2.8}$$

At the same time this SV is shown in §3 & 4 to be large enough so that it enforces a sufficient amount of entropy dissipation, and hence — by compensated compactness arguments — [31],[16], to prevent the unstable spurious Gibbs' oscillations.

3.2.1 The Fourier SV method – 2nd order viscosity

The unique entropy solution of the scalar conservation law (3.1.1) is the one which is realized as the vanishing viscosity solution, $u = \lim_{\varepsilon \downarrow 0} u^\varepsilon$, where u^ε satisfies the standard viscosity equation

$$\frac{\partial u^\varepsilon}{\partial t} + \frac{\partial}{\partial x} f(u^\varepsilon(x,t)) = \varepsilon \frac{\partial^2}{\partial x^2} u^\varepsilon(x,t). \tag{3.2.9}$$

This section provides a brief review of the convergence results for the Fourier SV method ($3.2.3_s$) with $s = 1$. The convergence analysis is based on the close resemblance of the Fourier SV method ($3.2.3_s$) with $s = 1$ to the usual viscosity regularization (3.2.9). To quantify this similarity we rewrite ($3.2.3_s$) with $s = 1$ in the equivalent form

$$\begin{aligned} \frac{\partial u_N}{\partial t} \quad + \quad & \frac{\partial}{\partial x} f(u_N(x,t)) = \\ = \quad & \varepsilon_N \frac{\partial^2 u_N}{\partial x^2} - \varepsilon_N \frac{\partial}{\partial x} \left[R_N(x,t) * \frac{\partial u_N}{\partial x} \right] + \frac{\partial}{\partial x} (I - P_N) f(u_N), \end{aligned} \tag{3.2.10}$$

where

$$R_N(x,t) := \sum_{k=-N}^{N} \hat{R}_k(t) e^{ikx}, \quad \hat{R}_k(t) \equiv \begin{cases} 1 & |k| < m_N, \\ 1 - \hat{Q}_k(t) & |k| \geq m_N. \end{cases} \tag{3.2.11}$$

Observe that the SV approximation in (3.2.10) contains two additional modifications to the standard viscosity approximation in (3.2.9).

{i} The second term on the right of (3.2.10) measures the difference between the spectral viscosity, $\varepsilon_N \frac{\partial}{\partial x} \left[Q_m(x,t) * \frac{\partial u_N}{\partial x} \right]$, and the standard vanishing viscosity, $\varepsilon_N \frac{\partial^2 u_N}{\partial x^2}$. The following straightforward estimate shows this difference to be L^2-bounded, $\forall \theta < \frac{1}{2}$.

$$\begin{aligned} \| \varepsilon_N \frac{\partial}{\partial x} \left[R_N(\cdot,t) * \frac{\partial u_N}{\partial x} \right] \|_{L^2} \quad & \leq \quad \text{Const} \cdot \varepsilon_N \left[m_N^{1/\theta} \max_{|k| > m_N} |k|^{2-1/\theta} + m_N^2 \right] \|u_N(\cdot,t)\|_{L^2} \\ & \leq \quad \text{Const} \cdot N^{2\theta - 1} \|u_N(\cdot,t)\|_{L^2} \\ & \leq \quad \text{Const} \cdot \|u_N(\cdot,t)\|_{L^2}, \quad \theta \leq \tfrac{1}{2}. \end{aligned} \tag{3.2.12}$$

{ii} The spectral projection error contained in the third term on the right of (3.2.10) does not exceed

$$\|(I - P_N) f(u_N(\cdot,t))\|_{L^2} \leq \text{Const} \frac{1}{N} \| \frac{\partial}{\partial x} u_N(\cdot,t) \|_{L^2}. \tag{3.2.13}$$

Equipped with the last two estimates one concludes the standard entropy dissipation bound, [26], [17], [28], [5],

$$\|u_N(\cdot,t)\|_{L^2} + \sqrt{\varepsilon_N} \| \frac{\partial u_N}{\partial x} \|_{L^2_{\text{loc}}(x,t)} \leq \text{Const}, \qquad \varepsilon_N \sim \frac{1}{N}. \tag{3.2.14}$$

The inequality (3.2.14) is the usual statement of entropy stability familiar from the standard viscosity setup (3.2.9). For the L^∞-stability of the Fourier SV approximation consult e.g. [17],[27, §5] and [5, §4] for the one- and respectively, multi-dimensional problems. The convergence of the SV method then follows by compensated compactness arguments, [31],[16].

We note in passing that the the Fourier SV approximation (3.2.3$_s$), (3.2.5-(3.2.6) shares other familiar properties of the standard viscosity approximation (3.2.9), e.g., total variation boundedness, Oleinik's one-sided Lipschitz regularity (for $\theta < \frac{1}{3}$), L^1-convergence rate of order one-half, [21],[28].

3.2.2 Fourier SV method revisited – super viscosity

In this section we remove the restriction $\theta < \frac{1}{2}$ in (3.2.6), which limits the portion of the inviscid spectrum. The key is to replace the standard second-order viscosity regularization (3.2.9) with the "super-viscosity" regularization

$$\frac{\partial u^\varepsilon}{\partial t} + \frac{\partial}{\partial x} f(u^\varepsilon(x,t)) = \varepsilon(-1)^{s+1}\frac{\partial^{2s}}{\partial x^{2s}} u^\varepsilon(x,t). \qquad (3.2.15_s)$$

The convergence analysis of the spectral "super-viscosity" method (3.2.3$_s$) is linked to the behavior of the "super-viscosity" regularization (3.2.15$_s$). To this end we rewrite (3.2.3$_s$) in the equivalent form

$$\begin{aligned} \frac{\partial u_N}{\partial t} \quad + \quad & \frac{\partial}{\partial x} f(u_N(x,t)) = \varepsilon_N(-1)^{s+1}\frac{\partial^{2s} u_N}{\partial x^{2s}} + \\ & + \varepsilon_N \frac{(-\partial)^s}{\partial x^s}\left[R_N(x,t) * \frac{\partial^s u_N}{\partial x^s}\right] + \frac{\partial}{\partial x}(I - P_N) f(u_N) = \qquad (3.2.16) \\ := \quad & \mathcal{I}_1(u_N) + \mathcal{I}_2(u_N) + \mathcal{I}_3(u_N). \end{aligned}$$

As before, we observe that the second and third terms on the right of (3.2.16), $\mathcal{I}_2(u_N)$ and $\mathcal{I}_3(u_N)$, are the two additional terms which distinguish the spectral "super-viscosity" approximation (3.2.16) from the super-viscosity regularization (3.2.15$_s$). In the sequel we shall use the following upper-bounds on these two terms.

{i} The second term, $\mathcal{I}_2(u_N)$, measures the difference between the SV regularization in (3.2.16) and the "super-viscosity" in (3.2.15$_s$). Using the SV parameterization in (3.2.7), (3.2.6) and (3.2.5) (in this order), we find that this difference does not exceed

$$\begin{aligned} \|\varepsilon_N \frac{(-\partial)^s}{\partial x^s}\left[R_N(\cdot,t) * \frac{\partial^s u_N}{\partial x^s}\right]\|_{L^2} \quad & \leq \quad \varepsilon_N \left[m_N^{2s} + m_N^{\frac{2s-1}{\theta}} \max_{|k|>m_N} |k|^{2s-\frac{2s-1}{\theta}}\right] \|u_N(\cdot,t)\|_{L^2} \\ & \leq \quad \text{Const} \cdot N^{2s\theta-2s+1}\|u_N(\cdot,t)\|_{L^2} \leq \\ & \leq \quad \text{Const} \cdot \|u_N(\cdot,t)\|_{L^2}, \quad \forall \theta \leq \tfrac{2s-1}{2s}. \end{aligned} \qquad (3.2.17)$$

Thus, the second term on the right of (3.2.16), $\mathcal{I}_2(u_N)$, is L^2-bounded :

$$\|\mathcal{I}_2(u_N)\|_{L^2(x)} \leq \text{Const}\|u_N(\cdot,t)\|_{L^2(x)}. \tag{3.2.18}$$

{ii} Regarding the third term, $\mathcal{I}_3(u_N)$, we shall make a frequent use of the spectral estimate which we quote from [5, §2.3][3],

$$\|\frac{\partial^p}{\partial x^p}(I-P_N)f(u_N(\cdot,t))\|_{L^2} \leq C_q \frac{1}{N^{q-p}}\|\frac{\partial^q}{\partial x^q}u_N(\cdot,t)\|_{L^2}, \quad \forall q \geq p > -\infty,\ q > \frac{1}{2}. \tag{3.2.19}$$

(The restriction $q > \frac{1}{2}$ is required only for the *pseudospectral* Fourier projection, P_N, whose truncation estimate in provided in e.g., [25, Lemma 2.2]). An upper bound on the constants C_s appearing on the right of (3.2.19) is given by [5, Theorem 7.1]

$$C_s \sim \sum_{k=1}^{s} \|f(\cdot)\|_{C^k}\|u_N\|_{L^\infty}^{k-1}; \tag{3.2.20}$$

this estimate may serve as a (pessimistic) bound for the same constant used in conjunction with the viscosity amplitude, ε_N, in (3.2.5).

Next we turn to the behavior of the quadratic entropy of the SV solution, $U(u_N) = \frac{1}{2}u_N^2$. (A similar treatment applies to general convex entropy functions $U(u_N)$.) Multiplication of (3.2.16) by u_N implies

$$\begin{aligned} \frac{1}{2}\frac{\partial}{\partial t}u_N^2 \quad + \quad & \frac{\partial}{\partial x}\int^{u_N} \xi f'(\xi)d\xi = \\ = \quad & u_N\mathcal{I}_1(u_N) + u_N\mathcal{I}_2(u_N) + u_N\mathcal{I}_3(u_N) = \\ := \quad & \mathcal{II}_1(u_N) + \mathcal{II}_2(u_N) + \mathcal{II}_3(u_N). \end{aligned} \tag{3.2.21}$$

The three expressions on the right (3.2.21) represent the quadratic entropy dissipation + production of the SV method. Successive "differentiation by parts" enable us to rewrite the first expression as

$$\begin{aligned} \mathcal{II}_1(u_N) \quad \equiv \quad & \varepsilon_N \sum_{\substack{p+q=2s-1 \\ 0\leq p<s}} (-1)^{s+p+1}\frac{\partial}{\partial x}\left[\frac{\partial^p u_N}{\partial x^p}\frac{\partial^q u_N}{\partial x^q}\right] - \varepsilon_N\left(\frac{\partial^s u_N}{\partial x^s}\right)^2 \\ := \quad & \mathcal{II}_{11}(u_N) + \mathcal{II}_{12}(u_N). \end{aligned} \tag{3.2.22}$$

[3] As usual we let $\partial_x^p w(x) := \sum_{k\neq 0}(ik)^p\hat{w}(k)e^{ikx}$. Note that if $\int w(x)dx = 0$ then $\partial_x^p w(x)$ with $p < 0$ coincides with the $|p|$-th order primitive of $w(x)$.

Similarly, the second expression can be rewritten as

$$\begin{aligned}\mathcal{II}_2(u_N) &\equiv \varepsilon_N \sum_{p+q=s-1} (-1)^{s+p} \frac{\partial}{\partial x}\left(\frac{\partial^p u_N}{\partial x^p}\left[\frac{\partial^q R_N(x,t)}{\partial x^q} * \frac{\partial^s u_N}{\partial x^s}\right]\right)+ \\ &\quad +\varepsilon_N \frac{\partial^s u_N}{\partial x^s} R_N(x,t) * \frac{\partial^s u_N}{\partial x^s} \\ &:= \mathcal{II}_{21}(u_N) + \mathcal{II}_{22}(u_N).\end{aligned} \tag{3.2.23}$$

Finally, we have for the third expression

$$\begin{aligned}\mathcal{II}_3(u_N) &\equiv \sum_{p=0}^{s-1}(-1)^p \frac{\partial}{\partial x}\left[\frac{\partial^p u_N}{\partial x^p}\frac{\partial^{-p}}{\partial x^{-p}}(I-P_N)f(u_N)\right]+ \\ &\quad +(-1)^s \frac{\partial^s u_N}{\partial x^s}\frac{\partial^{-s+1}}{\partial x^{-s+1}}(I-P_N)f(u_N) \\ &:= \mathcal{II}_{31}(u_N) + \mathcal{II}_{32}(u_N).\end{aligned} \tag{3.2.24}$$

We arrive at the following entropy estimate which plays an essential role in the convergence analysis of the SV method.

Lemma 3.2.1 (Entropy dissipation estimate) *.There exists a constant,* Const $\sim \|u_N(\cdot,0)\|_{L^2}$*, (but otherwise is independent of N), such that the following estimate holds*

$$\|u_N(\cdot,t)\|_{L^2} + \sqrt{\varepsilon_N}\|\frac{\partial^s u_N}{\partial x^s}\|_{L^2_{loc}(x,t)} \le \text{Const}, \qquad \varepsilon_N = \frac{2\mathcal{C}_s}{N^{2s-1}}. \tag{3.2.25}$$

Remark. Observe that the entropy dissipation estimate in (3.2.25) is considerably *weaker* in the "super-viscosity" case where $s > 1$, than in the standard viscosity regularization, $s = 1$ quoted in (3.2.14).

Proof. Spatial integration of (3.2.21) yields

$$\frac{1}{2}\frac{d}{dt}\|u_N(\cdot,t)\|^2_{L^2} + \varepsilon_N\|\frac{\partial^s}{\partial x^s}u_N(\cdot,t)\|^2_{L^2} = (u_N, \mathcal{I}_2(u_N))_{L^2(x)} + (u_N, \mathcal{I}_3(u_N))_{L^2(x)}. \tag{3.2.26}$$

According to (3.2.18), the first expression on the right of the last inequality does not exceed

$$|(u_N, \mathcal{I}_2(u_N))_{L^2}| \le \text{Const} \cdot \|u_N(\cdot,t)\|^2_{L^2}. \tag{3.2.27}$$

According to (4.6c), the second expression on the right$= (-1)^s \frac{\partial^s u_N}{\partial x^s}\frac{\partial^{-s+1}}{\partial x^{-s+1}}(I - P_N)f(u_N)$, and by (3.2.19) it does not exceed

$$|(u_N, \mathcal{I}_3(u_N))_{L^2}| \le \|\frac{\partial^s u_N}{\partial x^s}\|_{L^2} \cdot \frac{\mathcal{C}_s}{N^{2s-1}}\|\frac{\partial^s u_N}{\partial x^s}\|_{L^2} \le \frac{1}{2}\varepsilon_N\|\frac{\partial^s}{\partial x^s}u_N(\cdot,t)\|^2_{L^2}. \tag{3.2.28}$$

(In fact, in the spectral case, the second expression vanishes by orthogonality). The result follows from Gronwall's inequality. ■

Equipped with Lemma 3.2.1 we now turn to the main result of this section, stating

Theorem 3.2.1 (Convergence.) *Consider the Fourier "super-viscosity" approximation (3.2.3$_s$)-(3.2.7), subject to L^∞-initial data, $u_N(\cdot,0)$. Then uniformly bounded u_N converges to the unique entropy solution of the convex conservation law (3.1.1).*

Proof. We proceed in three steps.

Step 1. (L^∞-stability). The L^∞-stability for spectral viscosity of 2nd order, $s=1$, follows by L^p-iterations along the lines of [17] and [5], (we omit the details). The issue of an L^∞ bound for spectral viscosity of 'super' order $s>1$ remains an open question. The intricate part of this question could be traced to the fact that already the underlying super-viscosity regularization (3.2.15$_s$), *lacks* monotonicity for $s>1$: instead, it exhibits additional oscillations which are added to the spectral Gibbs' oscillations (Both types of oscillations are post-processed without sacrificing neither stability nor spectral accuracy).

Step 2. (H^{-1}-stability). We want to show that both — the local error on the right hand-side of (3.2.16), $\sum_{1\le j\le 3}\mathcal{I}_j(u_N)$, and the *quadratic* entropy dissipation + production on the right of (3.2.21), $\sum_{1\le j\le 3}\mathcal{II}_j(u_N)$, belong to a compact subset of $H^{-1}_{loc}(x,t)$.

To this end we first prepare the following. Bernstein's inequality gives us $\forall p < s \le q$

$$\begin{aligned}
\|\varepsilon_N\left[\frac{\partial^p u_N}{\partial x^p}\frac{\partial^q u_N}{\partial x^q}\right]\|_{L^2_{loc}(x,t)} &\le \text{Const}\cdot\varepsilon_N\|\frac{\partial^p u_N}{\partial x^p}\|_{L^\infty}\cdot\|\frac{\partial^q u_N}{\partial x^q}\|_{L^2_{loc}(x,t)}\le\\
\dots\text{by Bernstein inequality}\dots &\le \text{Const}\cdot\varepsilon_N\cdot N^p\|u_N\|_{L^\infty}\cdot N^{q-s}\|\frac{\partial^s u_N}{\partial x^s}\|_{L^2_{loc}(x,t)}\le\\
\dots\text{by Lemma 3.2.1}\dots &\le \text{Const}\cdot\sqrt{\varepsilon_N}\cdot N^{p+q-s}\|u_N\|_{L^\infty}\sim\\
&\sim \sqrt{2\mathcal{C}_s}\cdot N^{p+q-2s+\frac{1}{2}}\cdot\|u_N\|_{L^\infty}.
\end{aligned}\tag{3.2.29}$$

Consider now the first two expressions, $\mathcal{I}_1(u_N)$ and $\mathcal{II}_1(u_N)$. The inequality (3.2.29) with $(p,q)=(0,2s-1)$ implies that $\mathcal{I}_1(u_N)$ tends to zero in $H^{-1}_{loc}(x,t)$, for

$$\|\mathcal{I}_1(u_N)\|_{H^{-1}_{loc}(x,t)}\le\text{Const}\cdot\sqrt{2\mathcal{C}_s/N}\cdot\|u_N\|_{L^\infty}\to 0.\tag{3.2.30}$$

We turn now to the expression $\mathcal{II}_1(u_N)$ in (3.2.22): its first half tends to zero in $H^{-1}_{loc}(x,t)$, for by (3.2.29) we have $\forall p+q=2s-1$,

$$\begin{aligned}\|\mathcal{II}_{11}(u_N) &\equiv \varepsilon_N \cdot \sum_{\substack{p+q=2s-1\\ 0\le p<s}} (-1)^{s+p}\frac{\partial}{\partial x}\left[\frac{\partial^p u_N}{\partial x^p}\frac{\partial^q u_N}{\partial x^q}\right]\|_{H^{-1}_{loc}(x,t)} \le \\ &\le \text{Const}\cdot\sqrt{2\mathcal{C}_s/N}\cdot\sum_{\substack{p+q=2s-1\\ 0\le p<s}}\|u_N\|_{L^\infty} \le \\ &\le \text{Const}\cdot s\sqrt{2\mathcal{C}_s/N}\cdot\|u_N\|_{L^\infty}\to 0;\end{aligned} \tag{3.2.31}$$

the second half of $\mathcal{II}_1$ in (3.2.22), $-\varepsilon_N\left(\frac{\partial^s u_N}{\partial x^s}\right)^2$, is bounded in $L^1_{loc}(x,t)$, consult Lemma 3.2.1, and hence by Murat's Lemma [16], belongs to a compact subset of $H^{-1}_{loc}(x,t)$. We conclude

$$\mathcal{II}_{12}(u_N)\underset{H^{-1}_{loc}(x,t)}{\longrightarrow}\le 0. \tag{3.2.32}$$

We continue with the next pair of expressions, $\mathcal{I}_2(u_N)$ and $\mathcal{II}_2(u_N)$. According to (3.2.18), $\mathcal{I}_2(u_N)$ — and therefore also $\mathcal{II}_2(u_N)=u_N\mathcal{I}_2(u_N)$ — are L^2-bounded, and hence belong to a compact subset of $H^{-1}_{loc}(x,t)$; in fact, by repeating our previous arguments which led to (3.2.18) one finds that

$$\|\mathcal{I}_2(u_N)\|_{H^{-1}(x,t)}\le\text{Const}\cdot\varepsilon_N m_N^{s-1}\|\frac{\partial^s u_N}{\partial x^s}\|_{L^2(x,t)}\le\text{Const}\cdot\sqrt{\varepsilon_N}m_N^{s-1}\sim\sqrt{2\mathcal{C}_s}\cdot N^{-\frac{2s-1}{2s}}\to 0. \tag{3.2.33}$$

A similar treatment shows that the first half of $\mathcal{II}_2(u_N)$ in (3.2.23) tends to zero in $H^{-1}_{loc}(x,t)$, for

$$\begin{aligned}\|\mathcal{II}_{21}(u_N) &\equiv \varepsilon_N\sum_{p+q=s-1}(-1)^{s+p}\frac{\partial}{\partial x}\left(\frac{\partial^p u_N}{\partial x^p}\left[\frac{\partial^q R_N(x,t)}{\partial x^q}*\frac{\partial^s u_N}{\partial x^s}\right]\right)\|_{H^{-1}_{loc}(x,t)}\le \\ &\le \varepsilon_N\cdot\sum_{p+q=s-1}N^p\|u_N\|_{L^\infty}\cdot m_N^q\|\frac{\partial^s u_N}{\partial x^s}\|_{L^2_{loc}(x,t)}\le \\ &\le \text{Const}\cdot\sqrt{\varepsilon_N}\sum_{p+q=s-1}N^{p+q}\|u_N\|_{L^\infty}\le s\sqrt{2\mathcal{C}_s/N}\cdot\|u_N\|_{L^\infty}\to 0.\end{aligned} \tag{3.2.34}$$

The second half of $\mathcal{II}_2(u_N)$ is L^1-bounded, for

$$\|\mathcal{II}_{22}(u_N)\equiv\varepsilon_N\frac{\partial^s u_N}{\partial x^s}R_N(x,t)*\frac{\partial^s u_N}{\partial x^s}\|_{L^1}\le\text{Const}\cdot\varepsilon_N\|\frac{\partial^s u_N}{\partial x^s}\|^2_{L^2_{loc}(x,t)}\le\text{Const}. \tag{3.2.35}$$

Finally we treat the third pair of expressions, $\mathcal{I}_3(u_N)$ and $\mathcal{II}_3(u_N)$. The spectral decay estimate (3.2.19) with $(p,q)=(0,s)$, together with Lemma 3.2.1

imply that $\mathcal{I}_3(u_N)$ tends to zero in $H^{-1}_{loc}(x,t)$; indeed

$$\|\mathcal{I}_3(u_N) \equiv \frac{\partial}{\partial x}(I-P_N)f(u_N)\|_{H^{-1}_{loc}(x,t)} \leq \frac{\mathcal{C}_s}{N^s}\|\frac{\partial^s u_N}{\partial x^s}\|_{L^2} \sim \sqrt{2\mathcal{C}_s/N} \to 0. \tag{3.2.36}$$

A similar argument applies to the expression $\mathcal{II}_3(u_N)$ given in (4.6c). Sobolev inequality – consult (3.2.29), followed by the spectral decay estimate (3.2.19) imply that the first half of $\mathcal{II}_3(u_N)$ does not exceed

$$\begin{aligned}
\|\mathcal{II}_{31}(u_N) &\equiv \sum_{p=0}^{s-1}(-1)^p\frac{\partial}{\partial x}\left[\frac{\partial^p u_N}{\partial x^p}\frac{\partial^{-p}}{\partial x^{-p}}(I-P_N)f(u_N)\right]\|_{H^{-1}_{loc}(x,t)} \leq \\
&\leq \sum_{p=0}^{s-1}\|\frac{\partial^p u_N}{\partial x^p}\|_{L^\infty}\cdot\|\frac{\partial^{-p}}{\partial x^{-p}}(I-P_N)f(u_N)\|_{L^2_{loc}(x,t)} \leq \\
&\leq \text{Const}\cdot\sum_{p=0}^{s-1}N^p\|u_N\|_{L^\infty}\frac{\mathcal{C}_s}{N^{s+p}}\|\frac{\partial^s u_N}{\partial x^s}\|_{L^2_{loc}(x,t)} \leq \\
&\sim \text{Const}\cdot s\sqrt{2\mathcal{C}_s/N}\|u_N\|_{L^\infty} \to 0.
\end{aligned} \tag{3.2.37}$$

According to Lemma 3.2.1, the second half of $\mathcal{II}_3(u_N)$ is L^1-bounded, for

$$\|\mathcal{II}_{32}(u_N) \equiv \frac{\partial^s u_N}{\partial x^s}\frac{\partial^{-s+1}}{\partial x^{-s+1}}(I-P_N)f(u_N)\|_{L^1} \leq \|\frac{\partial^s u_N}{\partial x^s}\|_{L^2}\frac{\mathcal{C}_s}{N^{2s-1}}\|\frac{\partial^s u_N}{\partial x^s}\|_{L^2} \leq \text{Const}, \tag{3.2.38}$$

and hence by Murat's Lemma [16], belongs to a compact subset of $H^{-1}_{loc}(x,t)$. We conclude that the entropy dissipation of the Fourier spectral 'super-viscosity' method, for both linear and quadratic entropies, belongs to a compact subset of $H^{-1}_{loc}(x,t)$.

Step 3. (Convergence). It follows that the SV solution u_N converges strongly (in $L^p_{loc}, \forall p < \infty$) to a weak solution of (3.1.1). In fact, except for the L^1-bounded terms $\mathcal{II}_{22}(u_N)$ and $\mathcal{II}_{32}(u_N)$, we have shown that all the other expressions which contribute to the entropy dissipation tend either to zero or to a negative measure. Using the strong convergence of u_N it follows that $\mathcal{II}_{22}(u_N)$ and $\mathcal{II}_{32}(u_N)$ also tend to zero, consult [17]. Hence the convergence to the unique entropy solution. ■

Remarks.

1. *Low pass filter* [8]. We note that the spectral "super-viscosity" in $(3.2.3_s)$ allows for an increasing order of parabolicity, $s \sim N^\mu$, $\mu < 1/2$ (at least for bounded $\mathcal{C}_s$'s). This enables us to rewrite the spectral "super-viscosity" method in the form

$$\frac{\partial u_N}{\partial t} + \frac{\partial}{\partial x}[P_N f(u_N)] = -N\sum_{|k|\leq N}\sigma(\frac{k}{N})\hat{u}_k(t)e^{ikx}, \tag{3.2.39}$$

where $\sigma(\xi)$ is a symmetric low pass filter satisfying

$$\sigma(\xi) \begin{cases} \leq |\xi|^{2s}, & |\xi| \leq 1, \\ \geq |\xi|^{2s} - \frac{1}{N}, & |\xi| > 0. \end{cases} \tag{3.2.40}$$

In particular, for $s \sim N^{\mu}$, one is led to a low pass filter which is C^{∞}-tailored at the origin, consult [32].

2. *Super viscosity regularization.* The estimates outlined in Theorem 3.2.1 imply the convergence of the regularized 'super-viscosity' approximation u^{ε} in $(3.2.15_s)$, to the entropy solution of the convex conservation law (3.1.1).

Assertion 3.2.1 *Consider the 'super-viscosity' regularization (3.2.15$_s$),*

$$\frac{\partial u^{\varepsilon}}{\partial t} + \frac{\partial}{\partial x} f(u^{\varepsilon}(x,t)) = \varepsilon(-1)^{s+1} \frac{\partial^{2s}}{\partial x^{2s}} u^{\varepsilon}(x,t), \tag{3.2.41}$$

subject to given $L^1 \bigcap L^{\infty}$-initial data, $u(\cdot,0)$. Assume that u^{ε} is uniformly bounded. Then u^{ε} converges to the unique entropy solution of the convex conservation law (3.1.1).

The question of L^{∞} bound for the superviscosity case – (3.2.41) with $s > 1$, is open. Unlike the regular viscosity case, the solution operator associated with (3.2.41) with $s > 1$ is *not* monotone — here there are "spurious" oscillations, on top of the Gibbs' oscillations due to the Fourier projection. What we have shown is that the oscillations of either type do not cause instability. Moreover, these oscillations contain, in some weak sense, highly accurate information on the exact entropy solution; this could be revealed by post-processing the spectral (super)-viscosity approximation, e.g. [18].

3.3 Non-periodic boundaries

In this section we discuss the Legendre SV method, [18]. Extensions to Chebyshev SV method can be found in [12], [15]. Applications to atmospheric simulations can be found in [2].

3.3.1 The Legendre SV approximation

In the spectral viscosity approximation of (3.1.1) we seek a $\mathbb{P}_N$-polynomial of the form $u_N(x,t) = \sum_{k=0}^{N} \hat{u}_k(t) L_k(x)$, such that $\forall \phi \in \mathbb{P}_N[-1,1]$, we have

$$(\frac{\partial}{\partial t} u_N + \frac{\partial}{\partial x} \mathcal{I}_N f(u_N), \phi)_N = -\varepsilon_N (Q \frac{\partial}{\partial x} u_N, \frac{\partial}{\partial x} \phi)_N + (B(u_N), \phi)_N. \tag{3.3.1}$$

The approximation (3.3.1) involves the boundary operator, $B(u_N)$, and the Spectral Viscosity operator, Q. Here, $B(u_N)$ is a forcing polynomial in $\mathbb{P}_N[-1,1]$ of the form

$$B(u_N) = [\lambda(t)(1-x) + \mu(t)(1+x)]L'_N(x), \tag{3.3.2}$$

involving (at most) two nonzero free parameters, $\lambda(t)$ and $\mu(t)$, which should enable $u_N(x,t)$ to match *inflow* boundary data prescribed at $x = \pm 1$ whenever $\pm f'(u_N(\pm 1,t)) < 0$. And, Q denotes the spectral viscosity operator,

$$Q\phi \equiv \sum_{k=0}^{N} \hat{Q}_k \hat{\phi}_k L_k, \quad \forall \phi = \sum_{k=0}^{\infty} \hat{\phi}_k L_k, \tag{3.3.3}$$

which is associated with bounded viscosity coefficients,

$$\begin{cases} \hat{Q}_k \equiv 0 & k \le m_N, \\ 1 \ge \hat{Q}_k \ge 1 - \left(\dfrac{m_N}{k}\right)^4 & k > m_N. \end{cases} \tag{3.3.4}$$

The free pair of spectral viscosity parameters (ε_N, m_N) will be chosen later, such that $\varepsilon_N \downarrow 0$ and $m_N \uparrow \infty$, in order to retain the formal spectral accuracy of (3.3.1) with (3.1.1). We close this section by explaining how the SV method (3.3.1) can be implemented as a collocation method. Let us 'test' (3.3.1) against $\phi = \phi_i$, where ϕ_i is the standard characteristic polynomial of $\mathbb{P}_N[-1,1]$ satisfying $\phi_i(\xi_j) = \delta_{ij}, 0 \le i,j \le N$. At the interior points we obtain

$$\frac{d}{dt}u_N(\xi_i,t) + \frac{\partial}{\partial x}\mathcal{I}_N f(u_N)(\xi_i,t) = \varepsilon_N \frac{\partial}{\partial x} Q(\frac{\partial}{\partial x}u_N)(\xi_i,t), \quad 1 \le i \le N-1. \tag{3.3.5}$$

These equations are augmented, at the outflow boundaries, (say at $x = +1$), with

$$\frac{d}{dt}u_N(+1,t) + \frac{\partial}{\partial x}\mathcal{I}_N f(u_N)(+1,t) = \varepsilon_N \frac{\partial}{\partial x} Q(\frac{\partial}{\partial x}u_N)(+1,t) - \frac{\varepsilon_N}{\omega_N} Q(\frac{\partial}{\partial x}u_N)(+1,t). \tag{3.3.6}$$

We note that the last term on the right of (3.3.6) prevents the creation of a boundary layer. Equations (3.3.5), (3.3.6) together with the prescribed inflow data (say at $x = -1$), furnish a complete equivalent statement of the pseudospectral (collocation) viscosity approximation (3.3.1).

The SV approximation (3.3.5),(3.3.6) enjoys *formal* spectral accuracy, i.e., its truncation error decays as fast as the global smoothness of the underlying solution permits. However, it is essential to keep in mind that this superior accuracy cannot be realized in the presence of shock discontinuities, unless the final SV solution is post-processed. The rest of this section is devoted to clarify this point.

Epilogue – on spectral post-processing

It is well-known that spectral projections like $\pi_N u$, $\mathcal{I}_N u$, etc., provide highly accurate approximations of u, provided u itself is sufficiently smooth. Indeed, these projections enjoy spectral convergence rate. This superior accuracy is destroyed if u contains discontinuities: both $\pi_N u$ and $\mathcal{I}_N u$ produce spurious $\mathcal{O}(1)$

Gibbs' oscillations which are *localized* in the neighborhoods of the discontinuities, and moreover, their *global* accuracy is deteriorated to first-order.

To accelerate the convergence rate in such cases, we follow a similar treatment in [10] for the Fourier projections of discontinuous data. We introduce a mollifier of the form

$$\Psi^{\alpha,p}(x;y) = \rho(\frac{x-y}{\alpha})K_p(x;y), \tag{3.3.7}$$

which consists of the following two ingredients:

- $\rho(x)$ is a $C_0^\infty(-1,1)$-localizer satisfying $\rho(0)=1$;
- $K_p(x;y)$ is the Christoffel-Darboux kernel

$$K_p(x;y) \equiv \sum_{j=0}^{p} \frac{L_j(x)L_j(y)}{\|L_j\|^2} = \frac{(p+1)}{2}\frac{L_{p+1}(x)L_p(y) - L_{p+1}(y)L_p(x)}{x-y}. \tag{3.3.8}$$

We let $F^{\alpha,\beta}$ denote the smoothing filter

$$F^{\alpha,\beta}w(x) \equiv \int_{x=-1}^{1} \Psi^{\alpha,p=[N^\beta]}(x;y)w(y)dy, \tag{3.3.9}$$

depending on the two fixed parameters, $\alpha,\beta \in (0,1)$. Then, the following spectral error estimate was derived in [20]: $\forall s \geq 1$ there exists a constant $C_{s,\alpha}$ such that

$$|u(x) - F^{\alpha,\beta}(\pi_N u)(x)| \leq C_{s,\alpha}\left[N^{2\beta-(1-2\beta)s}\|u\|_{L^2[-1,1]} + N^{-(\frac{3}{4}-s)\beta}\max_{\substack{|x-y|<\alpha \\ 0\leq j\leq s}}|D^j u(y)|\right]. \tag{3.3.10}$$

Similar estimate holds for $\mathcal{I}_N$. These estimates show (at least for $\beta < \frac{1}{2}$) that except for a small neighborhood of the discontinuities (measured by the free parameter α), one can filter the Legendre projections, $\pi_N u$ and $\mathcal{I}_N u$, in order to recover *pointwise* values of u within spectral accuracy.

Next, let u be the desired exact solution of a given problem. The purpose of a spectral method is to compute an approximation to the *projection* of u rather than u itself. Consequently, if the underlying solution of our problem is discontinuous, then the approximation computed by a spectral method, u_N, exhibits the two difficulties of local Gibbs' oscillations, and global, low(=first)-order accuracy.

With this in mind, we now turn to discuss the present context of nonlinear conservation laws. The standard, viscous-free spectral method supports the spurious Gibbs' oscillations which render the overall approximation unstable (consult the introductory counterexamples in Lecture IV below). The task of the Spectral Viscosity is therefore two fold: to stabilize the standard spectral method (— which is otherwise unstable), and to retain the overall spectral accuracy of the underlying spectral method.

The question of stability is addressed in the following sections: we prove that Spectral Viscosity guarantees the H^{-1}-stability (and hence the convergence) of the Legendre SV approximation,

$$L^p_{loc} - \lim u_N(x,t) = u(x,t), \quad \forall p < \infty. \tag{3.3.11}$$

The question of spectral accuracy requires further clarification. As noted above, the Legendre SV solution, $u_N(\cdot,t)$, should be considered as an accurate approximation of $\mathcal{I}_N u(\cdot,t)$, rather than $u(\cdot,t)$ itself. Therefore, the convergence *rate* of the SV method is limited by the first order convergence rate of $\mathcal{I}_N u(\cdot,t)$. (Of course, this limitation arises once shock-discontinuities are formed). We recall that according to (3.3.10), this first-order limitation can be avoided by filtering $\mathcal{I}_N u$: the *filtered* interpolant, $F^{\alpha,\beta}(\mathcal{I}_N u)$, retains a spectral convergence rate, at least in smooth regions of the discontinuous entropy solution $u(\cdot,t)$. This suggests to apply the same filtering procedure (3.3.9) to $u_N(\cdot,t)$, in order to accelerate the convergence rate of the SV method.

Let $\{\hat{u}_k(t)\}_{k=0}^N$ denote the computed coefficients of the Legendre SV method. The computation of the SV solution is based on adding spectral viscosity only to the "high" modes – those with wavenumbers $k > m_N$. Therefore, one *expects* the computation of the viscous-free coefficients, at least, $\hat{u}_k(t) \equiv \dfrac{(u_N, L_k)_N}{\|L_k\|_N^2}$, $k = 1,\ldots,m_N$, to be spectrally accurate approximation of the exact pseudospectral Legendre coefficients, $\dfrac{(u, L_k)_N}{\|L_k\|_N^2}$. Assuming that indeed this is the case, then according to (3.3.10) one can post-process the SV solution, $u_N(\cdot,t)$, in order to recover spectral convergence rate in smooth regions of the entropy solutions. Thus, at the final stage of the SV method, (3.3.5),(3.3.6) should be augmented with the post-processing procedure

$$F^{\alpha,\beta}u_N(x,t) = \int_{x=-1}^{1} \Psi^{\alpha,p=N^\beta}(x;y)u_N(y)dy. \tag{3.3.12}$$

The numerical experiments in [23] confirm that the SV method contains a spectrally accurate information about the discontinuous solution – by post-processing one recovers this information despite the presence of shock discontinuities.

We conclude by noting that the post-processing of the SV solution plays a necessary key role in realizing the spectral accuracy of the SV method *within* smooth regions of the underlying solution. The treatment of Gibbs' oscillations in the neighborhood of discontinuities requires an alternative 'one-sided' filtering procedure, which is studies in e.g., [9].

3.3.2 Convergence of the Legendre SV method

We want to prove the convergence of (3.3.1) by compensated compactness arguments. To this end we want to show that $\frac{\partial}{\partial t}U(u_N) + \frac{\partial}{\partial x}F(u_N)$ belongs to a compact subset of $H^{-1}_{loc}(x,t)$ for all convex entropy pairs $(U(u_N), F(u_N))$. Our main tool in this direction reads [18, §5]

Lemma 3.3.1 *A weak representation of the truncation error of the Legendre viscosity approximation (3.3.1) is given by*

$$(\frac{\partial}{\partial t}u_N + \frac{\partial}{\partial x}f(u_N), \phi) = \sum_{j=1}^{6} I_j(\phi), \qquad \phi(x,t) \in \mathcal{D}([-1,1]), \tag{3.3.13}$$

where the following estimates hold:

$$\sum_{j=1}^{3} |I_j(\phi)| \leq \mathcal{O}(\frac{1}{\sqrt{\varepsilon_N}}) \left[\|\phi - \phi_N\| + \frac{1}{N} \|\frac{\partial}{\partial x}\phi_N\| \right], \tag{3.3.14}$$

$$|I_4(\phi)| \leq \mathcal{O}(\varepsilon_N m_N^2 \sqrt{\ln N}) \|\frac{\partial}{\partial x}\phi_N\|, \tag{3.3.15}$$

$$|I_5(\phi) \equiv -\varepsilon_N (\frac{\partial}{\partial x}u_N, \frac{\partial}{\partial x}\phi_N)| \leq \mathcal{O}(\sqrt{\varepsilon_N}) \|\frac{\partial}{\partial x}\phi_N\|, \tag{3.3.16}$$

$$I_6(\phi) \equiv 2(-1)^{N+1} \int_{t=0}^{T} \lambda(t)\phi_N(-1,t)dt. \tag{3.3.17}$$

Here, $\phi_N(\cdot,t)$ *is an arbitrary* $\mathbb{P}_N$*-polynomial at our disposal.*

Appropriate choices of test functions, ϕ_N yield the desired convergence result.

Theorem 3.3.1 *Let $u_N(x,t)$ be the Legendre viscosity approximation of (3.3.1), (3.3.4), with spectral viscosity parameters (ε_N, m_N) which satisfy*

$$0 \downarrow \varepsilon_N \sim \frac{1}{N^\theta}, \quad m_N < \text{Const} \cdot N^{\frac{q}{4}} \qquad \textit{with} \quad 0 < q < \theta \leq 1. \tag{3.3.18}$$

Then, (a subsequence of) $u_N(x,t)$ converges strongly (in L^p_{loc}, $p < \infty$) to a weak solution of the conservation law (3.1.1). Moreover, if $\theta < 1$, then (the whole sequence of) $u_N(x,t)$ converges strongly to the unique entropy solution of (3.1.1).

3.4 Numerical results

In this section we will present numerical experiments which demonstrate the performance of the Legendre SV method for systems of conservation laws. We consider the approximate solution of the Euler equations of gas dynamics,

$$\frac{\partial}{\partial t}u(x,t) + \frac{\partial}{\partial x}f(u(x,t)) = 0, \qquad u = \begin{bmatrix} \rho \\ \rho v \\ E \end{bmatrix} \quad f(u) = \begin{bmatrix} \rho v \\ \rho v^2 + p \\ v(E+p) \end{bmatrix}, \tag{3.4.1}$$

where ρ denotes the density of the gas, v its velocity, $m \equiv \rho v$ its momentum, E its energy per unit volume and $p = (\gamma - 1) \cdot (E - \frac{1}{2}\rho v^2)$ its (polytropic) pressure, $\gamma = 1.4$.

The Legendre SV approximation of this system reads

$$\frac{d}{dt}u_N(\xi_i,t) + \frac{\partial}{\partial x}\mathcal{I}_N f(u_N)(\xi_i,t) = \varepsilon_N \frac{\partial}{\partial x} Q(\frac{\partial}{\partial x}u_N)(\xi_i,t), \quad 1 \leq i \leq N-1. \tag{3.4.2}$$

Here, $u_N \equiv {}^t(\rho_N, \rho_N v_N, E_N) \in \mathbb{P}_N^3[-1,1]$ denotes the polynomial approximation of the 3-vector of (density, momentum, energy), and Q abbreviates a general 3×3 spectral viscosity matrix, $\{\hat{Q}_k^{\ell,j}\}_{k=m_N}^N$, $1 \leq \ell, j \leq 3$ which is activated only

on 'high' Legendre modes, i.e., $\hat{Q}_k^{\ell,j} = 0$, $\forall k > m_N(\ell, j)$. The numerical results reported in this section were obtained using a simple scalar viscosity matrix,

$$Q(\frac{\partial}{\partial x}u_N) = {}^t(Q\frac{\partial}{\partial x}\rho_N, Q\frac{\partial}{\partial x}\rho_N v_N, Q\frac{\partial}{\partial x}E_N), \tag{3.4.3}$$

with the viscosity coefficients, $\hat{Q}_k$,given by

$$\hat{Q}_k = exp\{-\frac{(k-N)^2}{(k-m_N)^2}\}, \quad k > m_N, \tag{3.4.4}$$

The Legendre SV method (3.4.2,(3.4.3) amounts to a nonlinear system of $(N+1)^3$ ODEs which was integrated in time using the second order Adams-Bashforth ODE solver.

We implemented the SV method for two test problems.

• *The Riemann shock tube problem* [22]. Our first example is the Riemann problem (3.4.1), subject to initial conditions

$$u(x,0) = \begin{cases} u_\ell = {}^t(1.,\ 0,\ 2.5), & x < 0, \\ u_r = {}^t(0.125,\ 0,\ 0.25), & x > 0. \end{cases} \tag{3.4.5}$$

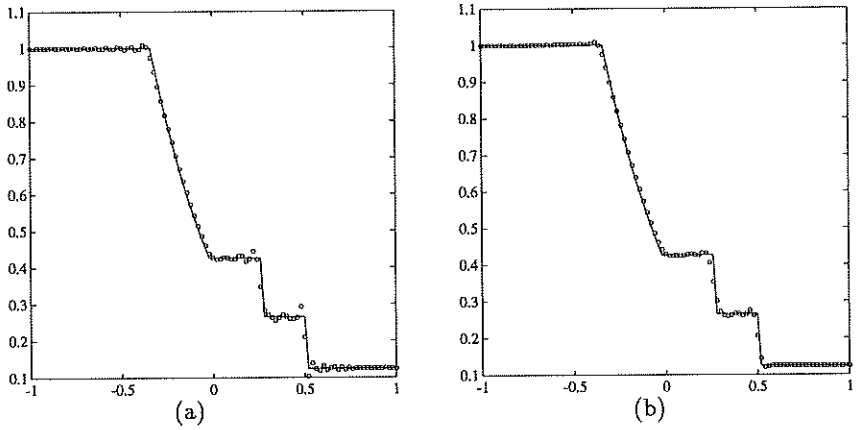

Figure 3.4.1: Density ρ_N with N=128 Legendre modes. (a) before and (b) after post-processing.

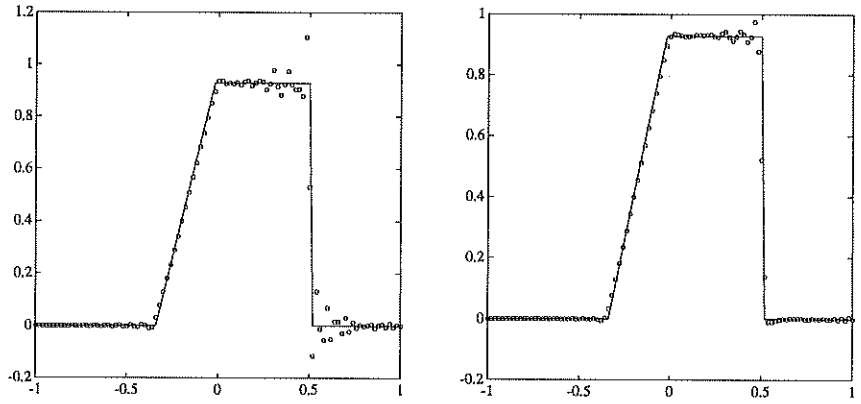

Figure 3.4.2: Velocity v_N with N=128 Legendre modes. (a) before and (b) after post-processing.

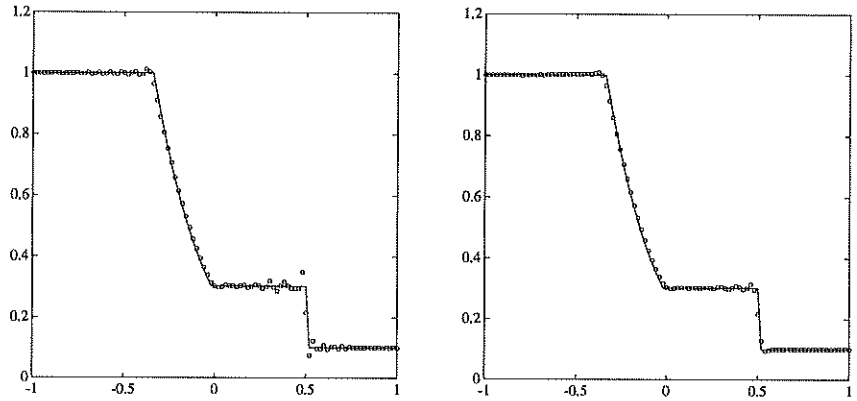

Figure 3.4.3: Pressure v_N with N=128 Legendre modes. (a) before and (b) after post-processing.

Figures 3.4.1a, 3.4.2a and 3.4.3a display the computed density ρ_N, velocity v_N, and pressure p_N, with $N = 128$ Legendre modes. The numerical results in these figures show that the presence of Spectral Viscosity guarantees the convergence of the pseudospectral Legendre method that is otherwise unstable. However, Gibbs' oscillations which are inherited from the *projected* solution, $\mathcal{I}_N u(\cdot, t)$, are still present.

To remove these oscillations without sacrificing spectral accuracy, the SV solution on the left side of figures (3.4.1)-(3.4.5) was post-processed using the filtering procedure (3.3.9), $F^{\alpha,\beta}$ with $(\alpha, \beta) = (0.2, 0.85)$. Again, as in the scalar case, the post-processing leads to a dramatic improvement in the quality of the computed results, revealing the high-resolution content of the SV computation. In particular, comparing the results obtained by the post-processed SV method in figures 3.4.1b-3.4.3b, we find the representation of the rarefaction wave and the capturing of the contact discontinuity to be better than the results obtained

by the finite-difference methods in [22] or the high-resolution schemes in [22]. (It is worthwhile noting that these high resolutions results of the SV computations were obtained *without* the costly characteristic decompositions which are employed in the modern high resolution finite difference approximations.)

The resolution of the shock discontinuity, however, still suffers from a smearing of spurious Gibbs' oscillations. As told by the error estimate (3.3.10), the oscillations in the neighborhood of the discontinuities cannot be removed by the filtering procedure (3.3.9). Instead, these oscillations can be avoided by using an alternative 'one-sided' filter which is currently under investigation [9].

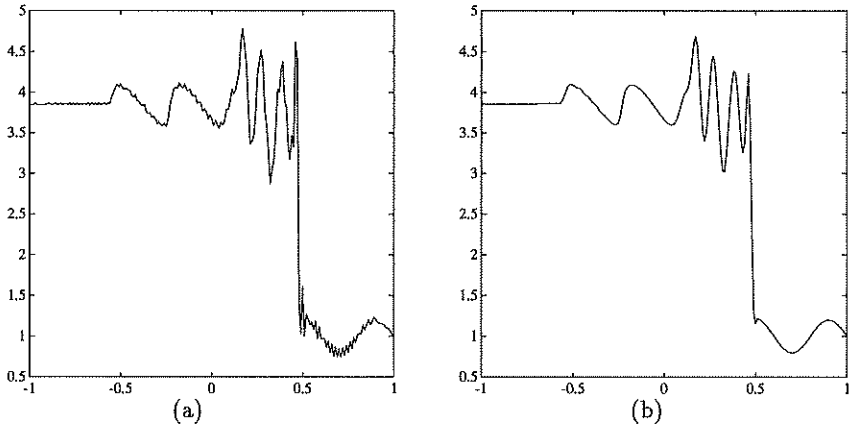

Figure 3.4.4: Density ρ_N with N=220 Legendre modes. (a) before and (b) after post-processing.

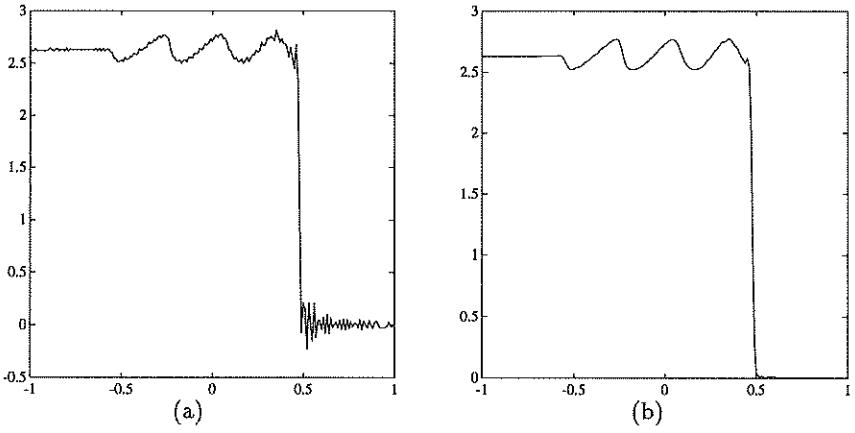

Figure 3.4.5: Velocity v_N with N=220 Legendre modes. (a) before and (b) after post-processing.

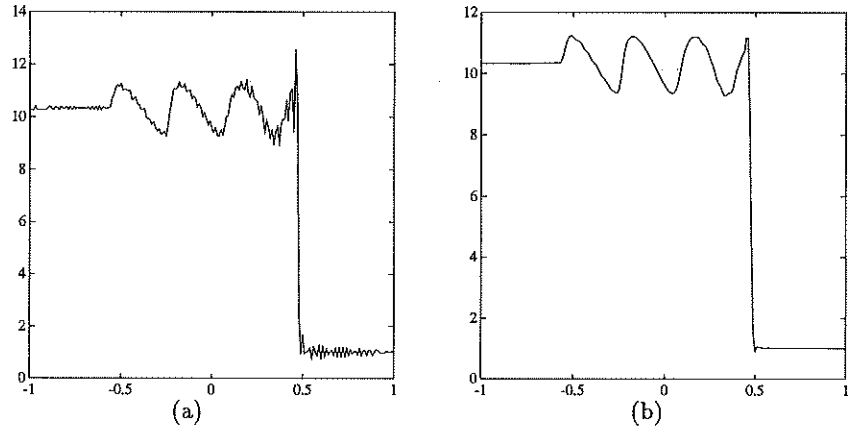

Figure 3.4.6: Pressure p_N with N=220 Legendre modes. (a) before and (b) after post-processing.

• *The shock-disturbance interaction* e.g., [SO]. Our second example models the interaction of a sinusoidal disturbance and a shock wave due to initial conditions

$$(\rho(x,0), v(x,0), p(x,0)) = \begin{cases} (3.857143,\ 10.333333,\ 2.629369), & x < -0.8, \\ (1. + 0.2\sin(5\pi x),\ 0.,\ 1.), & x > -0.8. \end{cases} \tag{3.4.6}$$

The exact solution of this problem, (3.4.1),(3.4.6), consists of a density wave that will emerge behind the shock discontinuity, and the fine structure of this density wave makes the current problem a suitable test case for high order methods. For example, second order MUSCL type schemes, [14], are unable to resolve the fine structure of the density wave unless the number of grid points is substantially increased.

The Legendre SV method was implemented in this case with SV parameters $(\varepsilon_N, m_N) = (\frac{1}{N}, 8\sqrt{N})$. Figures 3.4.4-3.4.6 display the numerical results of the SV approximation which was integrated in time by the second-order Adams-Bashforth method with time step $\Delta t = 2.5 \cdot 10^{-6}$.

Figures 3.4.4a, 3.4.5a, and 3.4.6a show the approximated density ρ_N, velocity v_N, and pressure p_N at $t = 0.36$, computed with $N = 220$ Legendre modes. These results were post-processed by the filtering procedure (3.3.9), $F^{\alpha,\beta}$, with $(\alpha, \beta) = (0.1, 0.89)$. Figures 3.4.4b, 3.4.5b and 3.4.6b present the post-processed results, which show that the velocity and pressure waves are well resolved. The density wave still contains Gibbs' oscillations in the neighborhood of the shock discontinuity, and its first extremum behind the shock is smeared by our smoothing filter. Here, a 'one-sided' filter would be recommended instead. A better resolution of the density profile near the shock was obtained by a different spectral method presented in [3]. However, the latter is a shock fitting like method which might not be easy to extend to higher dimensions.

3.5 Multidimensional Fourier SV method

We want to solve the *multidimensional* 2π-periodic initial-value problem, (3.1.1) by a spectral method. To this end we approximate the spectral/pseudo-spectral projection of the exact entropy solution, $P_N u(\cdot,t)$, using an N-trigonometric polynomial, $u_N(x,t) = \sum_{|\xi|\le N} \hat{u}_\xi(t) e^{i\xi\cdot x}$, which is governed by the semi-discrete approximation

$$\frac{\partial}{\partial t} u_N(x,t) + \partial_x \cdot P_N f(u_N(x,t)) = \varepsilon_N \sum_{j,k=1}^{d} \partial_{jk}^2 Q_N^{j,k}(x,t) * u_N(x,t). \quad (3.5.1)$$

Together with one's favorite ODE solver, (3.5.1) gives a fully discrete method for the approximate solution of (3.1.1).

To suppress these oscillations, without sacrificing the overall spectral accuracy, we augment the standard Fourier approximation on the right-hand side of (3.5.1) by *spectral viscosity*, which consists of the following three ingredients:

- A vanishing viscosity amplitude, ε_N, of size
$$\varepsilon_N \sim N^{-\theta}, \quad \theta < 1. \quad (3.5.2)$$
- A viscosity-free spectrum of size $m_N >> 1$,
$$m_N \sim \frac{N^{\frac{\theta}{2}}}{(\log N)^{\frac{d}{2}}}, \quad \theta < 1. \quad (3.5.3)$$
- A family of viscosity kernels, $Q_N^{j,k}(x,t) = \sum_{|\xi|=m_N}^{N} \hat{Q}_\xi^{j,k}(t) e^{i\xi\cdot x}$, $1 \le j,k \le d$, activated only on high wavenumbers $|\xi| \ge m_N$, which can be conveniently implemented in the Fourier space as

$$\varepsilon_N \sum_{j,k=1}^{d} \partial_{jk}^2 Q_N^{j,k} * u_N(x,t) \equiv -\varepsilon_N \sum_{|\xi|=m_N}^{N} < \hat{Q}_\xi \xi, \xi > \hat{u}_\xi(t) e^{i\xi\cdot x}, \quad < \hat{Q}_\xi \xi, \xi > \equiv \sum_{j,k=1}^{d} \hat{Q}_\xi^{j,k}(t) \xi_j \xi_k. \quad (3.5.4)$$

The viscosity kernels we deal with, $Q_N^{j,k}(x,t)$, are assumed to be spherically symmetric, that is, $\hat{Q}_\xi^{j,k} = \hat{Q}_p^{j,k}, \forall |\xi| = p$, with monotonically increasing Fourier coefficients, $\hat{Q}_p^{j,k}$, that satisfy

$$|\hat{Q}_p^{j,k} - \delta_{jk}| \le \text{Const.} \frac{\mathrm{m_N^2}}{\mathrm{p^2}}, \quad \forall \mathrm{p} \ge \mathrm{m_N}. \quad (3.5.5)$$

The main convergence result, quoted from [5], are based on the following two lemmas.

Lemma 3.5.1 (L^∞ stability) *There exists a constant such that*

$$||u_N(\cdot,t)||_{L^\infty(x)} \le \text{Const} \cdot ||u_N(\cdot,0)||_{L^\infty(x)}, \quad \forall \mathrm{t} \le \mathrm{T}. \quad (3.5.6)$$

Lemma 3.5.2 (Entropy Consistency) . *There exists a vanishing sequence, e_N, such that*

$$\frac{\partial}{\partial t}U(u_N) + \partial_x \cdot F(u_N) \leq e_N \to 0, \quad \text{in } \mathcal{D}'. \tag{3.5.7}$$

Proofs of Lemma 3.5.1 and Lemma 3.5.2can be found in [5]. Granted the L^∞-stability and the entropy consistency, we can combine DiPerna's uniqueness result for measure-valued solutions [6] with the finiteness of propagation speed (see also [24] for the case of bounded domains) to conclude the following.

Theorem 3.5.1 *Let u_N be the solution of the SV approximation (3.5.1)-(3.5.5), subject to bounded initial conditions satisfying*

$$\|u_N(\cdot,0)\|_{L^\infty(x)} + \varepsilon^s \|\partial_x^s u_N(\cdot,0)\|_{L^2(x)} \leq \text{Const.} \tag{3.5.8}$$

Then u_N converges strongly to the unique entropy solution of (3.1.1).

Bibliography

[1] S. ABARBANEL, D. GOTTLIEB & E. TADMOR, *Spectral methods for discontinuous problems*, in "Numerical Analysis for Fluid Dynamics II" (K.W. Morton and M.J. Baines, eds.), Oxford University Press, 1986, pp. 129–153.

[2] Ø. ANDREASSEN, I. LIE & C.-E. WASSBERG, *The spectral viscosity method applied to simulation of waves in a stratified atmosphere*, J. Comp. Phys. 110 (1994) pp. 257-273.

[3] W. CAI, D. GOTTLIEB & A. HARTEN, *Cell averaging Chebyshev method for hyperbolic problems*, Compu. and Math. with Appl., 24 (1992).

[4] C. CANUTO, M.Y. HUSSAINI, A. QUARTERONI & T. ZANG, Spectral Methods with Applications to Fluid Dynamics, Springer-Verlag, 1987.

[5] G.-Q. CHEN, Q. DU & E. TADMOR, *Spectral viscosity approximations to multidimensional scalar conservation laws*, Math. of Comp. 61 (1993), 629-643.

[6] R. DIPERNA, *Convergence of approximate solutions to systems of conservation laws*, Arch. Rat. Mech. Anal., Vol. 82, pp. 27-70 (1983).

[7] D.C. FRITTS, T. L. PALMER, Ø. ANDREASSEN, AND I. LIE, *Evolution and breakdown of Kelvin-Helmholtz billows in stratified compressible flows .1. Comparison of two- and three-dimensional flows*, J. Atmos. Sci. 53 (1996) pp. 3173-3191.

[8] D. GOTTLIEB, Private communication.

[9] D. GOTTLIEB, C.-W. SHU & H. VANDEVEN, *Spectral reconstruction of a discontinuous periodic function*, submitted to C. R. Acad. Sci. Paris.

[10] D. GOTTLIEB & E. TADMOR, *Recovering pointwise values of discontinuous data with spectral accuracy*, in "Progress and Supercomputing in Computational Fluid Dynamics" (E. M Murman and S.S. Abarbanel eds.), Progress in Scientific Computing, Vol. 6, Birkhauser, Boston,1985, pp. 357-375.

[11] H. -O. KREISS & J. OLIGER, *Stability of the Fourier method*, SINUM 16 1979, pp. 421-433.

[12] H. MA, *Chebyshev-Legendre spectral viscosity method for nonlinear conservation laws*, SINUM, to appear.

[13] H. MA, *Chebyshev-Legendre spectral super viscosity method for nonlinear conservation laws*, SINUM, to appear.

[14] B. VAN LEER, *Toward the ultimate conservative difference schemes. V. A second order sequel to Godunov method*, J. Compt. Phys. 32, (1979), pp. 101-136.

[15] I. LIE, *On the spectral viscosity method in multidomain Chebyshev discretizations*, preprint.

[16] F. MURAT, *Compacité per compensation*, *Ann. Scuola Norm. Sup. Disa Sci. Math. 5* (1978), pp. 489-507 and 8 (1981), pp. 69-102.

[17] Y. MADAY & E. TADMOR, *Analysis of the spectral viscosity method for periodic conservation laws*, SINUM 26, 1989, pp. 854-870.

[18] Y. MADAY, S.M. OULD KABER & E. TADMOR, *Legendre pseudospectral viscosity method for nonlinear conservation laws*, SINUM 30, 1993, pp. 321-342.

[19] A. MAJDA, J. MCDONOUGH & S. OSHER, *The Fourier method for nonsmooth initial data*, Math. Comp. 30, 1978, pp. 1041-1081.

[20] S.M. OULD KABER, *Filtrage d'ordre infini en non périodique*, in Thèse de Doctorat, Université Pierre et Marie Curie, Paris, 1991.

[21] S. SCHOCHET, *The rate of convergence of spectral viscosity methods for periodic scalar conservation laws*, SINUM 27, 1990, pp. 1142-1159.

[22] C.-W. SHU & S. OSHER, *Efficient Implementation of Essentially Nonoscillatory Shock-Capturing schemes, II*, J. Comp. Phys., 83 (1989), pp. 32–78.

[23] C.-W. SHU & P. WONG, *A note on the accuracy of spectral method applied to nonlinear conservation laws*, J. Sci. Comput., v10 (1995), pp. 357-369.

[24] A. SZEPESSY, *Measure valued solutions to scalar conservation laws with boundary conditions*, Arch. Rat. Mech. 107, 181–193 (1989).

[25] E. TADMOR, *The exponential accuracy of Fourier and Chebyshev differencing methods*, SINUM 23, 1986, pp. 1-10.

[26] E. TADMOR, *Convergence of spectral methods for nonlinear conservation laws*, SINUM 26, 1989, pp. 30-44.

[27] E. TADMOR, *Semi-discrete approximations to nonlinear systems of conservation laws; consistency and stability imply convergence*, ICASE Report no. 88-41.

[28] E. TADMOR, *Shock capturing by the spectral viscosity method*, Computer Methods in Appl. Mech. Engineer. 80 1990, pp. 197-208.

[29] E. TADMOR, *Total-variation and error estimates for spectral viscosity approximations*, Math. Comp. 60, 1993, pp. 245–256.

[30] E. TADMOR, *Super viscosity and spectral approximations of nonlinear conservation laws*, in "Numerical Methods for Fluid Dynamics IV", Proceedings of the 1992 Conference on Numerical Methods for Fluid Dynamics, (M. J. Baines and K. W. Morton, eds.), Clarendon Press, Oxford, 1993, pp. 69-82.

[31] L. TARTAR, *Compensated compactness and applications to partial differential equations*, in *Research Notes in Mathematics 39*, Nonlinear Analysis and Mechanics, Heriott-Watt Symposium, Vol. 4 (R.J. Knopps, ed.) Pittman Press, pp. 136-211 (1975).

[32] H. VANDEVEN, *A family of spectral filters for discontinuous problems*, J. Scientific Comput. 8, 1991, pp. 159–192.

Chapter 4

Convergence Rate Estimates

Abstract. Let $\{v^\varepsilon(x,t)\}_{\varepsilon>0}$ be a family of approximate solutions for the convex conservation law $u_t + f(u)_x = 0$ subject to C_0^1-initial data, $u_0(x)$. The notion of *approximate solutions* is quantified in terms of *Lip'*-consistency: we assume that $\{v^\varepsilon(x,t)\}$ are *Lip'-consistent* in the sense its initial+truncation errors are of order $\mathcal{O}(\varepsilon)$, $\|v^\varepsilon(\cdot,0) - u_0(\cdot)\|_{Lip'(x)} + \|v_t^\varepsilon + f(v^\varepsilon)_x\|_{Lip'(x,t)} = \mathcal{O}(\varepsilon)$. Here, ε is the 'small scale' of the approximate solution, e.g., the vanishing amplitude of size ε, a gridsize of order $\varepsilon \sim \Delta x$, etc. We then prove that stability implies convergence; namely, if $\{v^\varepsilon(x,t)\}$ are *Lip$^+$-stable* ($-$ in the sense that they satisfy Oleinik's E-entropy condition), then they converge to the entropy solution, and the convergence rate estimate $\|v^\varepsilon(\cdot,t) - u(\cdot,t)\|_{Lip'(x)} = \mathcal{O}(\varepsilon)$ holds. Consequently, the familiar L^p-type and new pointwise error estimates are derived. In particular, we recover classical L^1-estimates (à al Kuznetsov) of order $\mathcal{O}(\sqrt{\varepsilon})$. And we improve it to an $\mathcal{O}(\varepsilon)$ *pointwise* error estimate for all but finitely many $\mathcal{O}(\varepsilon)$-neighborhoods of shock discontinuities.

These convergence rate results are then demonstrated in the context of various approximate solutions, including Chapman-Enskog regularization, finite-difference schemes, Godunov-type methods, spectral viscosity methods, ...

4.1 Introduction

We are concerned here with the convergence *rate* of approximate solutions to the nonlinear scalar conservation law,

$$u_t + f(u)_x = 0, \tag{4.1.1}$$

subject to C_0^1-initial conditions,

$$u(x,0) = u_0(x). \tag{4.1.2}$$

In this context we first recall Strang's theorem which shows that the classical Lax-Richtmyer (LR) linear convergence theory applies for such nonlinear problem, as long as the underlying solution is sufficiently smooth e.g., [29, §5]. The

generic convergence error estimate in this context reads

$$\|v^\varepsilon(\cdot,t) - u(\cdot,t)\| \leq C_T \left[\|v^\varepsilon(\cdot,0) - u_0(\cdot)\| + \|v_t^\varepsilon + f(v^\varepsilon)_x\|\right],\ 0 \leq t \leq T. \quad (4.1.3)$$

Here, $\{v^\varepsilon\}$, is a family of approximate solutions which is tagged by its 'small scale', ε, e.g., a viscosity amplitude of size ε, a gridcells of size $\varepsilon \sim \Delta x$, the number of Fourier modes, $N \sim \varepsilon^{-1}$, etc. The linear Lax-Richtmyer theory tells us that if the approximate solution is *stable*, $\|v^\varepsilon(\cdot,t)\| \leq Const$, then the error, $\|v^\varepsilon(\cdot,t) - u(\cdot,t)\|$ is upper bounded by the initial+truncation errors, given respectively on the right of (4.1.3). In particular, if the approximation is *consistent* (— in the sense that that its initial+truncation errors tend to zero as $\varepsilon \downarrow 0$), then stability implies convergence.
What norm, $\|\cdot\|$, should be used in (4.1.3)? The *linear* Lax-Richtmyer theory is often implemented in term of the L^2 norm; likewise, Strang's extension to nonlinear smooth problems is usually expressed in terms of higher Sobolev H^s norms. There are two main reasons for the use of the L^2 framework:

1. It is the appropriate topology to measure stability and well-posedness of hyperbolic systems;

2. The Fourier space serves as a 'mirror site' for the real space L^2-stability and error analysis. The von-Neumann stability analysis for finite-difference schemes is a classical example.

Since the solutions of the nonlinear conservation laws develop spontaneous shock-discontinuities at a finite time, however, Strang's result does not apply beyond this critical time. Indeed, the Fourier method as well as other L^2-*conservative* schemes provide simple counterexamples of consistent approximations which fail to converge (to the discontinuous entropy solution), despite their linearized L^2-stability. Here are two counterexamples in this directions (more can be found in [38, 37, 13].)

Counterexample 1 [38]. The Fourier approximation of the 2π-periodic equation (4.1.1), expressed in term of the Fourier partial sum projection S_N, reads

$$\frac{\partial}{\partial t}[v_N(x,t)] + \frac{\partial}{\partial x}[S_N f(v_N(x,t))] = 0.$$

Multiplying this by $v_N(x,t)$ and integrating over the 2π-period, we obtain that v_N–being orthogonal to $\frac{\partial}{\partial x}[(I - S_N)f(v_N(x,t))]$, satisfies

$$\frac{1}{2}\frac{d}{dt}\int_0^{2\pi} v_N^2(x,t)dx = -\int_0^{2\pi} v_N(x,t)\frac{\partial}{\partial x}[f(v_N(x,t))]dx = -\int^{v_N(x,t)} uf'(u)du|_{x=0}^{x=2\pi} = 0.$$

Thus, the total quadratic entropy, $\eta(u) = \frac{1}{2}u^2$, is globally conserved in time

$$\frac{1}{2}\int_0^{2\pi} v_N^2(x,t)dx = \frac{1}{2}\int_0^{2\pi} v_N^2(x,0)dx, \quad (4.1.4)$$

which in turn yields the existence of a weak $L^2(x)$-limit, $\overline{u}(x,t) = w\lim_{N\to\infty} v_N(x,t)$. Yet, $\overline{u}(x,t)$ *cannot* be the entropy solution of a nonlinear equation (4.1.1) where $f''(\cdot) \neq 0$. Otherwise, $S_N f(v_N(x,t))$ and therefore $f(v_N(x,t))$ should tend, in the weak distributional sense, to $f(\overline{u}(x,t))$; consequently, since $f(u)$ is nonlinear,

$\overline{u}(x,t) = s\lim_{N\to\infty} v_N(x,t)$, which by (4.1.4) should satisfy $\frac{1}{2}\int_0^{2\pi} \overline{u}^2(x,t)dx = \frac{1}{2}\int_0^{2\pi} \overline{u}^2(x,0)dx$. But this is incompatible with the (quadratic) entropy inequality if $\overline{u}(x,t)$ contains shock discontinuities.

Our second example is a discrete one.

Counterexample 2. We consider the 2π-periodic conservation law

$$\frac{\partial u}{\partial t} + \frac{\partial(e^u)}{\partial x} = 0,$$

Expressed in terms of the trigonometric interpolant at the equidistant gridpoints $x_\nu = \frac{2\nu\pi}{2N+1}$, the corresponding ψdospectral approximation reads

$$\frac{\partial}{\partial t}[v_N(x,t)] + \frac{\partial}{\partial x}[\psi_N e^{v_N(x,t)}] = 0.$$

Multiply this by $\psi_N e^{v_N(x,t)}$ and integrate over the 2π-period: since the trapezoidal rule is exact with integration of the $2N$-trigonometric polynomial obtained from the second brackets, we have

$$\frac{d}{dt}\sum_{\nu=0}^{2N} e^{v_N(x_\nu,t)}\Delta x = -\int_0^{2\pi} \frac{\partial}{\partial x}[\frac{1}{2}(\psi_N e^{v_N(x,t)})^2]dx = 0.$$

Thus, the total exponential entropy, $\eta(u) = e^u$, is globally conserved in time

$$\sum_{\nu=0}^{2N} \eta(v_N(x_\nu,t))\Delta x = \sum_{\nu=0}^{2N} \eta(v_N(x_\nu,0))\Delta x, \qquad \eta(u) = e^u. \tag{4.1.5}$$

Hence, if $v_N(x,t)$ converges (even weakly) to a discontinuous weak solution, $\overline{u}(x,t)$, then $\psi_N e^{v_N(x,t)}$ tends (at least weakly) to $e^{\overline{u}(x,t)}$. Consequently, (4.1.5) would imply the global entropy conservation of $\int_0^{2\pi} e^{\overline{u}(x,t)}dx$ in time, which rules out the possibility of $\overline{u}(x,t)$ being the unique entropy solution.

In this chapter we extend the linear convergence theory into the weak regime. The extension is based on the usual two ingredients of stability and consistency. On the one hand, the counterexamples mentioned above show that one must *strengthen* the linearized L^2-stability requirement. We assume that the approximate solutions are Lip^+-stable in the sense that they satisfy a one-sided Lipschitz condition, in agreement with Oleinik's E-condition for the entropy solution. On the other hand, the lack of smoothness requires to *weaken* the consistency requirement, which is measured here in the Lip'-(semi)norm. As a guiding example, let us consider the usual viscosity approximation, v^ε, with 'truncation error' $\varepsilon v^\varepsilon_{xx}$. Localized to the neighborhood of shock discontinuities we find that $\|\varepsilon v^\varepsilon_{xx}\|_{L^p_{loc}} = \mathcal{O}(\varepsilon^{\frac{1-p}{p}})$ which rules out the L^p norms as possible measures for the à priori error estimate (4.1.3); instead, the *weak* Lip'-(semi)norm yields a truncation error of size $\|\varepsilon v^\varepsilon_{xx}\|_{Lip'} = \mathcal{O}(\varepsilon)$ which agrees with the fact that ε is the smallest scale present in a viscosity approximation in this case.

In §4.3.1 we prove for Lip^+-stable approximate solutions, that their Lip'-convergence rate to the entropy solution is of the same order as their Lip'-consistency. Thus, we show that under the assumption of Lip^+-stability, the basic Lax-Richtmyer à priori error bound (4.1.3) still holds when we replace the L^2 with the weaker Lip' norm.

Our Lip'-convergence rate estimates could be converted into stronger L^p convergence rate estimates. In particular, we recover the usual L^1-convergence rate of order one half, and we obtain new pointwise error estimates which depend on the *local* smoothness of the entropy solution. In fact, though the L^1-convergence rate of order $\mathcal{O}(\sqrt{\varepsilon})$ is optimal, *in practice* one obtains an L^1-rate of order $\mathcal{O}(\varepsilon)$, when there are finitely many shock discontinuities, [42],[43] (and these are the only solutions that can be computed!). In this case, we can use our Lip' theory to derive local error estimates which improve the L^1-result: using a bootstrap argument we show in [41], that the Lip^+-stable approximate solutions satisfy an $\mathcal{O}(\varepsilon)$ *pointwise* error estimate for all but finitely many $\mathcal{O}(\varepsilon)$-neighborhoods of shock discontinuities.

We now turn to the multidimensional setup. Kuznetsov [15] was the first to provide error estimates for scalar approximate solutions, $\{v^\varepsilon\}$, for both – the one- and multi-dimensional setups. Subsequently, many authors have used Kuznetsov's approach to prove convergence + L^1-error estimates; we refer for the detailed treatments of [31], [22], [42],... . A more recent treatment of [7] employs the entropy dissipation estimate (1.5.3), which in turn, by Kuznetsov arguments, yields an L^1-convergence rate estimate of order $(\Delta x)^{\frac{1-\delta}{2}}$ (independently of the BV bound).

Kuznetsov's approach employs a *regularized* version of Kružkov's entropy pairs in (1.2.8), $\eta^\delta(v^\varepsilon;c) \sim |v^\varepsilon - c|$, $F^\delta(v^\varepsilon;c) \sim sgn(v^\varepsilon - c)(A(v^\varepsilon) - A(c))$. Here, one measures by how much the entropy dissipation rate of $\{v^\varepsilon\}$ fails to satisfy the entropy inequality (1.2.3), with Kružkov's regularized entropies. Following the general recent convergence result of [2], we consider a family of approximate solutions, $\{v^\varepsilon\}$, which satisfies

$$\partial_t|v^\varepsilon - c| + \nabla_x \cdot \{sgn(v^\varepsilon - c)(A(v^\varepsilon) - A(c))\} \le \partial_t R_0(t,x) + \nabla_x \cdot R(t,x), \quad (4.1.6)$$

with

$$\|R_0(t,x)\|_{\mathcal{M}_{x,t}} + \|R(x,t)\|_{\mathcal{M}_{t,x}} \le \text{Const} \cdot \varepsilon. \quad (4.1.7)$$

Then, the convergence rate proof proceeds along the lines of Theorem 1.2.1: Using the key property of symmetry of the regularized entropy pairs, ($\eta^\delta := \phi_\delta \eta, F^\delta := \phi_\delta F$), one finds $\int_x \eta^\delta(v^\varepsilon;u)dx \le \text{Const.}\varepsilon/\delta$. In addition, there is a regularization error, $\|\eta^\delta - \eta\|_{L^1(x)}$, of size $\mathcal{O}(\delta)$, and an L^1 error estimate of order $\mathcal{O}(\sqrt{\varepsilon})$ follows (under reasonable assumptions on the L^1-initial error w.r.t. BV data), consult [2]

$$\|v^\varepsilon(\cdot,t) - u(\cdot,t)\|_{L^1_{\text{loc}}(x)} \le \text{Const.}\sqrt{\varepsilon}.$$

Observe that this error estimate, based on (4.1.6)-(4.1.7) is the multidimensional analogue of our Lip'-consistency requirement. In general, Kuznetsov approach makes a stronger requirement of approximate entropy inequalities (– i.e., in terms of *all* of Kružkov's pairs), and in return, ones obtains convergence results which apply to general, non-convex equations. The lectures by B. Cockburn provide a detailed account of Kuznetsov's L^1-convergence theory. In this

chapter we therefore focus our attention on the Lip'-convergence theory mentioned above. Its multidimensional extension deals with convex Hamilton-Jacobi equations (rather than conservation laws), consult §4.3.2.

In §4.4 we implement these error estimates for a variety of approximate solutions. The examples we discuss include

- Regularized Chapman-Enskog approximations [33];
- Finite-difference E-schemes [24];
- Godunov-type schemes [26];
- Glimm's scheme [24];
- Spectral viscosity approximations, [40]

Other examples dealing with 2×2 systems with and without stiff relaxation coupling terms could be found in [27],[18].

4.2 Approximate solutions

We study approximate solutions of the scalar convex conservation law

$$\frac{\partial}{\partial t}u(x,t) + \frac{\partial}{\partial x}f(u(x,t)) = 0, \quad f'' \geq \alpha > 0, \tag{4.2.1}$$

with compactly supported initial conditions prescribed at $t = 0$,

$$u(x, t = 0) = u_0(x). \tag{4.2.2}$$

Let $\{v^\varepsilon(x,t)\}_{\varepsilon>0}$ be a family of approximate solutions of the conservation law (4.2.1), (4.2.2) in the following sense.

Definition 4.2.1 *A. We say that* $\{v^\varepsilon(x,t)\}_{\varepsilon>0}$ *are* conservative *solutions if*

$$\int_x v^\varepsilon(x,t)dx = \int_x u_0(x)dx, \quad t \geq 0. \tag{4.2.3}$$

B. We say that $\{v^\varepsilon(x,t)\}_{\varepsilon>0}$ *are* Lip'-consistent *with the conservation law (4.2.1), (4.2.2) if the following estimates are fulfilled*[1]*:*

(i) consistency with the initial conditions (4.2.2),

$$\|v^\varepsilon(x,0) - u_0(x)\|_{Lip'} \leq K_0 \cdot \varepsilon \tag{4.2.4}$$

(ii) consistency with the conservation law (4.2.1),

$$\|v^\varepsilon_t(x,t) + f(v^\varepsilon(x,t))_x\|_{Lip'(x,[0,T])} \leq K_T \cdot \varepsilon. \tag{4.2.5}$$

[1] We let $\|\phi\|_{Lip}$, $\|\phi\|_{Lip^+}$ and $\|\phi\|_{Lip'}$ denote respectively, $\operatorname{esssup}_{x\neq y}\left|\frac{\phi(x)-\phi(y)}{x-y}\right|$, $\operatorname{esssup}_{x\neq y}\left[\frac{\phi(x)-\phi(y)}{x-y}\right]_+$ and $\sup_\psi \frac{(\phi-\hat{\phi}_0,\psi)}{\|\psi\|_{Lip}}$, where $\hat{\phi}_0 = \int_{\operatorname{supp}\phi}\phi$.

We are interested in the *convergence rate* of the approximate solutions, $v^\varepsilon(x,t)$, as their small parameter $\varepsilon \downarrow 0$. This requires an appropriate stability definition for such approximate solutions. Recall that the entropy solution of the nonlinear conservation law (4.2.1), (4.2.2) satisfies the a priori estimate [4, 39]

$$\|u(\cdot,t)\|_{Lip^+} \leq \frac{1}{\|u_0\|^{-1}_{Lip^+} + \alpha t}, \quad t \geq 0. \tag{4.2.6}$$

The case $\|u_0\|_{Lip^+} = \infty$ is included in (4.2.6), and it corresponds to the exact $\sim t^{-1}$ decay rate of an initial rarefaction.

Definition 4.2.2 *We say that $\{v^\varepsilon(x,t)\}_{\varepsilon>0}$ are Lip^+-*stable *if there exists a constant $\beta \geq 0$ (independent of t and ε) such that the following estimate, analogous to (4.2.6), is fulfilled:*

$$\|v^\varepsilon(\cdot,t)\|_{Lip^+} \leq \frac{1}{\|v^\varepsilon(\cdot,0)\|^{-1}_{Lip^+} + \beta t}, \quad t \geq 0. \tag{4.2.7}$$

Remarks.

1. The case of an initial rarefaction subject to the quadratic flux $f(u) = \frac{\alpha}{2}u^2$ demonstrates that the a priori decay estimate of the exact entropy solution in (4.2.6) is sharp. A comparison of (4.2.7) with (4.2.6) shows that a *necessary* condition for the convergence of $\{v^\varepsilon\}_{\varepsilon>0}$ is

   $$0 \leq \beta \leq \alpha, \tag{4.2.8}$$

   for otherwise, the decay rate of $\{v^\varepsilon(\cdot,t)\}$ (and hence of its $\varepsilon \to 0$ limit) would be *faster* than that of the exact entropy solution.

2. The case $\beta > 0$ in (4.2.7) corresponds to a *strict* Lip^+-stability in the sense that $\|v^\varepsilon(\cdot,t)\|_{Lip^+}$ decays in time, in agreement with the decay of rarefactions indicated in (4.2.6).

3. In general, any a priori bound

   $$\|v^\varepsilon(\cdot,t)\|_{Lip^+} \leq \text{Const}_T < \infty, \quad 0 \leq t \leq T, \tag{4.2.9}$$

   is a sufficient stability condition for the convergence results discussed below. In particular, we allow for $\beta = 0$ in (4.2.7), as long as the approximate initial conditions are Lip^+-bounded. We remark that the restriction of Lip^+-bounded initial data is indeed necessary for convergence, in view of the counterexample of Roe's scheme discussed in remark 4.4.2 in §4.4.2. Unless stated otherwise, we therefore restrict our attention to the class of Lip^+-bounded (i.e., rarefaction-free) initial conditions, where

   $$L_0^+ := \max(\|u_0\|_{Lip^+}, \|v^\varepsilon(\cdot,0)\|_{Lip^+}) < \infty. \tag{4.2.10}$$

4. Finally, we remark that in case of strict Lip^+-stability, i.e., in case (4.2.7) holds with $\beta > 0$, then one can remove this restriction of Lip^+-bounded initial data and our convergence results can be extended to include general L^∞_{loc}-initial conditions, initial rarefaction are included. The discussion of this case could be found in [25], and it leads to similar error estimates discussed in this chapter, with ε being replaced by $\varepsilon \log(\varepsilon)$.

4.3 Convergence rate estimates

4.3.1 Convex conservation laws

We begin with the following theorem which is at the heart of matter.

Theorem 4.3.1 *A. Let $\{v^\varepsilon(x,t)\}_{\varepsilon>0}$ be a family of conservative, Lip^+-stable approximate solutions of the convex conservation law (4.2.1),(4.2.2), subject to the Lip^+- bounded initial conditions (4.2.10). Then the following error estimate holds*

$$\|v^\varepsilon(\cdot,T)-u(\cdot,T)\|_{Lip'} \leq C_T\left[\|v^\varepsilon(\cdot,0)-u_0(\cdot)\|_{Lip'}+\|v_t^\varepsilon+f(v^\varepsilon)_x\|_{Lip'(x,[0,T])}\right], \tag{4.3.1}$$

where

$$C_T \sim (1+\beta L_0^+ T)^\eta, \quad \eta := \frac{\max f''}{\beta} \geq 1.$$

B. In particular, if the family $\{v^\varepsilon(x,t)\}_{\varepsilon>0}$ is also Lip'-consistent of order $\mathcal{O}(\varepsilon)$, i.e., (4.2.4),(4.2.5) hold, then $v^\varepsilon(x,t)$ converges to the entropy solution $u(x,t)$ and the following convergence rate estimate holds

$$\|v^\varepsilon(\cdot,T)-u(\cdot,T)\|_{Lip'} \leq M_T\cdot\varepsilon, \quad M_T := (K_0+K_T)(1+\beta L_0^+ T)^\eta. \tag{4.3.2}$$

Proof. We proceed along the lines of [39, 24]. The difference, $e^\varepsilon(x,t) := v^\varepsilon(x,t)-u(x,t)$, satisfies the error equation

$$\frac{\partial}{\partial t}e^\varepsilon(x,t)+\frac{\partial}{\partial x}[\overline{a}_\varepsilon(x,t)e^\varepsilon(x,t)] = F^\varepsilon(x,t), \tag{4.3.3}$$

where $\overline{a}_\varepsilon(x,t)$ stands for the mean-value

$$\overline{a}_\varepsilon(x,t) = \int_{\xi=0}^1 a[\xi v^\varepsilon(x,t)+(1-\xi)u(x,t)]d\xi, \quad a(\cdot)\equiv f'(\cdot),$$

and $F^\varepsilon(x,t)$ is the truncation error,

$$F^\varepsilon(x,t) := v_t^\varepsilon(x,t)+f(v^\varepsilon(x,t))_x.$$

Given an arbitrary $\phi(x)\epsilon W_0^{1,\infty}$, we let $\{\phi^\varepsilon(x,t)\}_{0\leq t\leq T}$ denote the solution of the backward transport equation

$$\phi_t^\varepsilon(x,t)+\overline{a}_\varepsilon(x,t)\phi_x^\varepsilon(x,t)=0, \quad t\leq T, \tag{4.3.4}$$

corresponding to the endvalues, $\phi(x)$, prescribed at $t=T$,

$$\phi^\varepsilon(x,T)=\phi(x).$$

Here, the following a priori estimate holds [39, Theorem 2.2]

$$\|\phi^\varepsilon(\cdot,t)\|_{Lip} \leq \exp\Big(\int_t^T \|\overline{a}_\varepsilon(\cdot,\tau)\|_{Lip^+}d\tau\Big)\cdot\|\phi(x)\|_{Lip}, \quad 0\leq t\leq T. \tag{4.3.5}$$

The Lip^+-stability of the entropy solution (4.2.6) and its approximate solutions in (4.2.7), provide us with the one-sided Lipschitz upper-bound required on the right-hand side of (4.3.5):

$$\|\overline{a}_\varepsilon(\cdot,\tau)\|_{Lip^+} \le \frac{\max f''}{2}[\|v^\varepsilon(\cdot,\tau)\|_{Lip^+} + \|u(\cdot,\tau)\|_{Lip^+}] \le \frac{\max f''}{[L_0^+]^{-1}+\beta\tau}. \quad (4.3.6)$$

Equipped with (4.3.5), (4.3.6) we conclude

$$\begin{aligned} \|\phi^\varepsilon(\cdot,t)\|_{Lip} &\le \frac{(1+\beta L_0^+ T)^\eta}{(1+\beta L_0^+ t)^\eta}\|\phi(x)\|_{Lip} \le \\ &\le C_T\|\phi(x)\|_{Lip}, \quad 0\le t\le T, \quad C_T := (1+\beta L_0^+ T)^\eta, \end{aligned} \quad (4.3.7)$$

and employing (4.3.4) we also have

$$\begin{aligned} \|\phi^\varepsilon(x,\cdot)\|_{Lip[0,T]} &\le |a|_\infty \max_{0\le t\le T}\|\phi^\varepsilon(\cdot,t)\|_{Lip(x)} \le \\ &\le |a|_\infty C_T\|\phi(x)\|_{Lip}, \quad |a|_\infty := \max|f'|. \end{aligned} \quad (4.3.8)$$

Of course, (4.3.4) is just the adjoint problem of the error equation (4.3.3) which gives us

$$(e^\varepsilon(\cdot,T),\phi(\cdot)) = (e^\varepsilon(\cdot,0),\phi^\varepsilon(\cdot,0)) + (F^\varepsilon(x,t),\phi^\varepsilon(x,t))_{L^2(x,[0,T])}. \quad (4.3.9)$$

Conservation implies that $\hat{e}_0^\varepsilon \equiv \int e^\varepsilon(x,0)dx = 0$ and by (4.3.7) we find

$$\begin{aligned} |(e^\varepsilon(\cdot,0),\phi^\varepsilon(\cdot,0))| &\le \|e^\varepsilon(\cdot,0)\|_{Lip'}\|\phi^\varepsilon(\cdot,0)\|_{Lip} \le \\ &\le (1+\beta L_0^+ T)^\eta\|e^\varepsilon(\cdot,0)\|_{Lip'}\cdot\|\phi(x)\|_{Lip}; \end{aligned}$$

similarly, conservation implies that $\hat{F}_0^\varepsilon \equiv \int_{x,[0,T]} F^\varepsilon(x,t)dxdt = 0$ and by (4.3.7),(4.3.8) we find

$$\begin{aligned} |(F^\varepsilon(x,t),\phi^\varepsilon(x,t))_{L^2(x,[0,T])}| &\le \|F^\varepsilon(x,t)\|_{Lip'(x,[0,T])}\|\phi^\varepsilon(x,t)\|_{Lip(x,[0,T])} \le \\ &\le (1+|a|_\infty)C_T\|F^\varepsilon(x,t)\|_{Lip'(x,[0,T])}\|\phi(x)\|_{Lip}. \end{aligned} \quad (4.3.10)$$

The error estimate (4.3.1) follows from the last two estimates together with (4.3.9). ■

The Lip'-convergence rate estimate (4.3.2) can be extended to more familiar $W^{s,p}_{loc}$-convergence rate estimates. The rest of this section is devoted to three corollaries which summarize these extensions.

We begin by noting that the conservation and Lip^+-stability of $v^\varepsilon(\cdot,t)$ imply that $v^\varepsilon(\cdot,T)$ – and consequently that the error, $v^\varepsilon(\cdot,T)-u(\cdot,T)$, have bounded variation,

$$\|v^\varepsilon(\cdot,T)-u(\cdot,T)\|_{BV} \le Const\frac{1}{[L_0^+]^{-1}+\beta T}. \quad (4.3.11)$$

We note in passing that the constant on the right of (4.3.11) depends on the *finite* size of the support of the error.

We can now interpolate between the BV-bound (4.3.11) and the Lip'-error estimate (4.3.2), to conclude the following.

Corollary 4.3.1 *Let $\{v^\varepsilon(x,t)\}_{\varepsilon>0}$ be a family of conservative, Lip'-consistent and Lip$^+$-stable approximate solutions of the conservation law (4.2.1), (4.2.2), with Lip$^+$-bounded initial conditions (4.2.10). Then the following convergence rate estimates hold $\forall p \le \infty$*

$$\|v^\varepsilon(\cdot,T) - u(\cdot,T)\|_{W^{s,p}} \le \mathrm{Const}_T \cdot \varepsilon^{\frac{1-sp}{2p}}, \quad -1 \le s \le \frac{1}{p}. \tag{4.3.12}$$

The error estimate (4.3.12) with $(s,p) = (0,1)$ yields L^1 convergence rate of order $\mathcal{O}(\sqrt{\varepsilon})$, which is familiar from the setup of monotone difference approximations [15, 22, 31]. Of course, uniform convergence (which corresponds to $(s,p) = (0,\infty)$) fails in this case, due to the possible presence of shock discontinuities in the entropy solution $u(\cdot,t)$. Instead, one seeks pointwise convergence away from the singular support of $u(\cdot,t)$. To this end, we employ a $C_0^1(-1,1)$-unit mass mollifier of the form $\zeta_\delta(x) = \frac{1}{\delta}\zeta(\frac{x}{\delta})$. The error estimate (4.3.1) asserts that

$$|(v^\varepsilon(\cdot,T) * \zeta_\delta)(x) - (u(\cdot,T) * \zeta_\delta)(x)| \le M_T \frac{\varepsilon}{\delta^2} \|\frac{d\zeta}{dx}\|_{L^\infty}.$$

Moreover, if $\zeta(x)$ is chosen so that

$$\int x^k \zeta(x) dx = 0 \quad \text{for } k = 1, 2, \ldots, r-1, \tag{4.3.13}$$

then a straightforward error estimate based on Taylor's expansion yields

$$|(u(\cdot,T) * \zeta_\delta)(x) - u(x,T)| \le \frac{\delta^r}{r!} \|\zeta\|_{L^1} \cdot |u^{(r)}|_{loc},$$

where $|u^{(r)}|_{loc}$ measures the degree of *local* smoothness of $u(\cdot,t)$,

$$|u^{(r)}|_{loc} := \|\frac{\partial^r}{\partial x^r} u(\cdot,T)\|_{L^\infty_{loc}(x+\delta\cdot\mathrm{supp}\zeta)}.$$

The last two inequalities (with $\delta \sim \varepsilon^{\frac{1}{r+2}}$) imply

Corollary 4.3.2 *Let $\{v^\varepsilon(x,t)\}_{\varepsilon>0}$ be a family of conservative, Lip'-consistent and Lip$^+$-stable approximate solutions of the conservation law (4.2.1), (4.2.2), with Lip$^+$-bounded initial conditions (4.2.10). Then, for any r-order mollifier $\zeta_\delta(x) \equiv \frac{1}{\delta}\zeta(\frac{x}{\delta})$ satisfying (4.3.13), the following convergence rate estimate holds*

$$|(v^\varepsilon(\cdot,T) * \zeta_\delta)(x) - u(x,T)| \le \mathrm{Const}(1 + \frac{|u^{(r)}|_{loc}}{r!}) \cdot \varepsilon^{\frac{r}{r+2}}. \tag{4.3.14}$$

Corollary 4.3.2 shows that by *post-processing* the approximate solutions $v^\varepsilon(\cdot,t)$, we are able to recover the pointwise values of $u(x,t)$ with an error as close to ε as the local smoothness of $u(\cdot,t)$ permits. A similar treatment enables the recovery of the derivatives of $u(x,t)$ as well, consult [39, §4].

The particular case $r = 1$ in (4.3.14), deserves special attention. In this case, post-processing of the approximate solution with *arbitrary* C_0^1-unit mass mollifier $\zeta(x)$, gives us

$$|(v^\varepsilon(\cdot,T) * \zeta_\delta)(x) - u(x,T)| \le \text{Const} \cdot (1 + |u_x(\cdot,T)|_{loc}) \cdot \sqrt[3]{\varepsilon}. \tag{4.3.15}$$

We claim that the pointwise convergence rate of order $\mathcal{O}(\sqrt[3]{\varepsilon})$ indicated in (4.3.15) holds even *without* post-processing of the approximate solution. Indeed, let us consider the difference

$$\begin{aligned} v^\varepsilon(x,T) - (v^\varepsilon(\cdot,T) * \zeta_\delta)(x) &= \int_y [v^\varepsilon(x,T) - v^\varepsilon(x-y,T)]\zeta_\delta(y)dy = \\ &= \int_y \left[\frac{v^\varepsilon(x,T) - v^\varepsilon(x-y,T)}{-y}\right] \cdot -\frac{y}{\delta}\zeta(\frac{y}{\delta})dy. \end{aligned}$$

By choosing a positive C_0^1-unit mass mollifier $\zeta(x)$ supported on $(-1,0)$ then, thanks to the Lip^+-stability condition (4.2.7), the integrand on the right does not exceed $\text{Const} \cdot \delta$, and hence

$$v^\varepsilon(x,T) - (v^\varepsilon(\cdot,T) * \zeta_\delta)(x) \le \text{Const} \cdot \delta\ . \tag{4.3.16}$$

Similarly, a different choice of a positive C_0^1-unit mass mollifier $\zeta(x)$ supported on $(0,1)$ leads to

$$v^\varepsilon(x,T) - (v^\varepsilon(\cdot,T) * \zeta_\delta)(x) \ge \text{Const} \cdot \delta. \tag{4.3.17}$$

Each of the last two inequalities (with $\delta \sim \sqrt[3]{\varepsilon}$) together with (4.3.15) show that the approximate solution itself converges with an $\mathcal{O}(\sqrt[3]{\varepsilon})$-rate, as asserted. We summarize what we have shown by stating the following.

Corollary 4.3.3 *Let $\{v^\varepsilon(x,t)\}_{\varepsilon>0}$ be a family of conservative, Lip'-consistent and Lip^+-stable approximate solutions of the conservation law (4.2.1), (4.2.2), with Lip^+-bounded initial conditions (4.2.10). Then the following convergence rate estimate holds:*

$$|v^\varepsilon(x,T) - u(x,T)| \le \mathrm{C}_x \cdot \sqrt[3]{\varepsilon}, \quad \mathrm{C}_x \sim |u_x(\cdot,T)|_{L^\infty(x-\sqrt[3]{\varepsilon},x+\sqrt[3]{\varepsilon})}. \tag{4.3.18}$$

The above derivation of pointwise error estimates applies in more general situations. Consider, for example, a family of approximate solutions, $\{v^\varepsilon(x,t)\}_{\varepsilon>0}$ which satisfies the stronger L^1 error estimate of order, say, $\mathcal{O}(\mu)$,

$$|(v^\varepsilon(\cdot,T) - u(\cdot,T), \phi(\cdot))| \le \mathrm{C}_x \cdot \mu ||\phi||_{L^\infty}. \tag{4.3.19}$$

Then our previous arguments show how to post-process $v^\varepsilon(\cdot,T)$ in order to recover the pointwise values of the entropy solution, $u(x,T)$ with an error as close to μ as the local smoothness of $u(\cdot,T)$ permits. In particular, using (4.3.19) with a positive C_0^1-unit mass mollifier, $\zeta_\delta(x) = \frac{1}{\delta}\zeta(\frac{x}{\delta})$ we obtain

$$|(v^\varepsilon(\cdot,T) * \zeta_\delta)(x) - (u(\cdot,T) * \zeta_\delta)(x)| \le \mathrm{C}_x \cdot \frac{\mu}{\delta}||\zeta||_{L^\infty}. \tag{4.3.20}$$

Using this together with

$$|(u(\cdot,T)*\zeta_\delta)(x)-u(x,T)|\le\delta\|\zeta\|_{L^1}\cdot\|u_x(\cdot,T)\|_{L^\infty_{loc}(x+\delta\cdot\mathrm{supp}\zeta)}, \tag{4.3.21}$$

we find (with $\delta\sim\sqrt{\mu}$)

$$|(v^\varepsilon(\cdot,T)*\zeta_\delta)(x)-u(x,T)|\le \mathrm{Const}_T(1+|u_x(\cdot,T)|_{loc})\sqrt{\mu}. \tag{4.3.22}$$

If the approximate solutions $\{v^\varepsilon(x,t)\}_{\varepsilon>0}$ are also Lip^+-stable, then we may augment (4.3.22) with (4.3.16)-(4.3.17) to conclude

Corollary 4.3.4 *Assume that $\{v^\varepsilon(x,t)\}$ is a family of Lip^+ stable approximate solutions with global L^1-convergence rate of order $\mathcal{O}(\mu)$, (4.3.19). Then the following local pointwise error estimate holds*

$$|v^\varepsilon(x,T)-u(x,T)|\le \mathrm{C}_x\cdot\sqrt{\mu},\quad \mathrm{C}_x\sim|u_x(\cdot,T)|_{L^\infty(x-\sqrt{\mu},x+\sqrt{\mu})}.$$

Remarks.

1. The usual L^1-rate of order $\mu\sim\sqrt{\varepsilon}$ leads to [24]

$$|v^\varepsilon(x,T)-u(x,T)|\le \mathrm{C}_x\cdot\sqrt[4]{\varepsilon},\quad \mathrm{C}_x\sim|u_x(\cdot,T)|_{L^\infty(x-\sqrt[4]{\varepsilon},x+\sqrt[4]{\varepsilon})}. \tag{4.3.23}$$

2. In case $u(\cdot,t)$ has finitely many shocks, [41], one obtain an L^1-rate of order $\mu\sim\varepsilon$, [42], and hence we find a *local* error of order $\sqrt{\varepsilon}$

$$|v^\varepsilon(x,T)-u(x,T)|\le \mathrm{C}_x\cdot\sqrt{\varepsilon},\quad \mathrm{C}_x\sim|u_x(\cdot,T)|_{L^\infty(x-\sqrt{\varepsilon},x+\sqrt{\varepsilon})}. \tag{4.3.24}$$

3. Finally, in [41] we improved the estimate (4.3.24) replacing $\sqrt{\varepsilon}$ by ε. Thus, we obtain an optimal pointwise error estimate of order $\mathcal{O}(\varepsilon)$ in all but finitely many neighborhoods of shock discontinuities of width $\mathcal{O}(\varepsilon)$.

4.3.2 Convex Hamilton-Jacobi equations

In this section we briefly comment on the *multidimensioal* generalization of the Lip'-convergence theory outlined above, to convex Hamilton-Jacobi (HJ) equations. We consider the multidimensional Hamilton-Jacobi (HJ) equation

$$\partial_t u+H(\nabla_x u)=0,\quad (t,x)\in R^+\times R^d, \tag{4.3.25}$$

with convex Hamiltonian, $H''>0$. Its unique viscosity solution is identified by the one-sided concavity condition, $D_x^2u\le$ Const., consult [16], [20]. Given a family of approximate HJ solutions, $\{v^\varepsilon\}$, we make the analogous one-sided stability requirement of

- *Demi-concave stability.* The family $\{v^\varepsilon\}$ is demi-concave stable if

$$D_x^2v^\varepsilon\le Const. \tag{4.3.26}$$

We then have the following.

Theorem 4.3.2 ([19]) *Assume $\{v_1^\varepsilon\}$ and $\{v_2^\varepsilon\}$ are two demi-concave stable families of approximate solutions. Then*

$$\begin{aligned}\|v_1^\varepsilon(t,\cdot)-v_2^\varepsilon(t,\cdot)\|_{L^1(x)} \;\le\; & Const.\|v_1^\varepsilon(0,\cdot)-v_2^\varepsilon(0,\cdot)\|_{L^1(x)}+\\ & + Const.\sum_{j=1}^{2}\|\partial_t v_j^\varepsilon + H(\nabla_x v_j^\varepsilon)\|_{L^1(t,x)}\end{aligned} \tag{4.3.27}$$

If we let $v_1^\varepsilon \equiv v^1$, $v_2^\varepsilon \equiv v^2$ denote two demi-concave viscosity solutions, then (4.3.27) is an L^1-stability statement (compared with the usual L^∞-stability statements of viscosity solutions, [8]). If we let $\{v_1^\varepsilon\} = \{v^\varepsilon\}$ denote a given family of demi-concave approximate HJ solutions, and let v_2^ε equals the exact viscosity solution u, then (4.3.27) yields the L^1-error estimate

$$\|v^\varepsilon(\cdot,t)-u(\cdot,t)\|_{L^1(x)} \le Const.\|\partial_t v^\varepsilon + H(\nabla_x v^\varepsilon)\|_{L^1(x,t)} \sim \mathcal{O}(\varepsilon). \tag{4.3.28}$$

This corresponds to the Lip'-error estimate of (1.3.20) with $(s,p)=(-1,1)$. One can then interpolate from (4.3.28) an L^p-error estimates of order $\mathcal{O}(\varepsilon^{\frac{1+p}{2p}})$. For a general L^∞-convergence theory for approximate solutions to HJ equations we refer to [1] and the references therein.

4.4 Examples

4.4.1 Regularized Chapman-Enskog expansion

Of course, the usual viscous approximation

$$\frac{\partial}{\partial t}[v^\varepsilon(x,t)]+\frac{\partial}{\partial x}[f(v^\varepsilon(x,t))]=\varepsilon\frac{\partial^2}{\partial x^2}[Q(v^\varepsilon(x,t))],\quad \varepsilon Q'\downarrow 0, \tag{4.4.1}$$

is the canonical example for a family of approximate solutions whose convergence rate could be analyzed in terms of our Lip' theory outlined above. Here, we concentrate on yet another, more intricate regularization of the inviscid equations of the form

$$v_t^\varepsilon + f(v^\varepsilon)_x = \left[\frac{-\varepsilon k^2}{1+m^2\varepsilon^2k^2}\hat{v^\varepsilon}(k)\right]^\vee,$$

or equivalently,

$$v_t^\varepsilon + f(v^\varepsilon)_x = -\frac{1}{m^2\varepsilon}\left(u - Q_{m\varepsilon}*u\right),\quad Q_\mu := \frac{1}{2\mu}e^{-|x|/\mu}. \tag{4.4.2}$$

Rosenau [28] has proposed this type of equation as a model for his regularized version of the Chapman-Enskog expansion for hydrodynamics. The operator on the right side looks like the usual viscosity term $\varepsilon v_{xx}^\varepsilon$ at low wave-numbers k, while for higher wave numbers it is intended to model a bounded approximation of a linearized collision operator, thereby avoiding the artificial instabilities that occur when the Chapman-Enskog expansion for such an operator is truncated after a finite number of terms [28].

We shall study the convergence rate of v^ε to the inviscid solution, along the lines of [33]. It should be pointed out that the solution of (4.4.2) does

not admit all the entropy inequalities, except for the quadratic one; thus, the question of convergence in this case, is not easily answered in terms of the usual L^1-Kuznetsov theory. Instead, we use the Lip' theory outlined in §4.3.1. To this end, we first turn to show that the nonlinear Regularized Chapman-Enskog (RCE) equation (4.4.2) satisfies Oleinik's E-entropy condition.

Theorem 4.4.1 *Assume $f'' \geq \alpha > 0$. Then the following a priori estimate holds*

$$||v^\varepsilon(t)||_{Lip^+} \leq \frac{1}{||v^\varepsilon(0)||^{-1}_{Lip^+} + \alpha t} \quad , \quad t \geq 0. \tag{4.4.3}$$

Remark. The inequality (4.4.3) implies that the positive-variation and hence the total-variation of $v^\varepsilon(t)$ decays in time. Furthermore, this proves the zero mean-free-path convergence to the entropy solution of (4.2.1) for any L^∞_{loc}-initial data u_0

Proof. We add the artificial viscosity term δu_{xx} to regularize (4.4.2), obtaining

$$\partial_t v^\varepsilon_\delta + \partial_x f(v^\varepsilon_\delta) = -\frac{1}{m^2\varepsilon}\{v^\varepsilon_\delta - Q_{m\varepsilon} * v^\varepsilon_\delta\} + \delta\partial^2_x v^\varepsilon_\delta. \tag{4.4.4}$$

Differentiation of (4.4.4) yields for $w \equiv \partial_x v^\varepsilon_\delta$,

$$\partial_t w + f'(u^\delta_\varepsilon)\partial_x w + f''(u^\delta_\varepsilon)w^2 == -\frac{1}{m^2\varepsilon}\{w - Q_{m\varepsilon} * w\} + \delta\partial^2_x w.$$

Hence, since $f'' > \alpha > 0$, it follows that $W(t) \equiv max_x w(t)$ is governed by the differential inequality

$$\dot{W}(t) + \alpha W^2(t) \leq \frac{1}{m^2\varepsilon}\{W(t) - Q_{m\varepsilon} * W\} \leq 0$$

and (4.4.3) follows by letting $\delta \downarrow 0$. ■

Theorem 4.4.1 shows that solutions of the RCE equation (4.4.2) are Lip^+-stable. Moreover, (4.4.2) implies that the Lip'-size of their truncation if of order $\mathcal{O}(\varepsilon)$, for

$$||\partial_t v^\varepsilon + \partial_x f(v^\varepsilon)||_{Lip'} = \varepsilon||Q_{m\varepsilon} * \partial_x v^\varepsilon||_{L^1} \leq \varepsilon||Q_{m\varepsilon}||_{L^1}||v^\varepsilon(t)||_{BV} \leq \varepsilon||u_\varepsilon(0)||_{BV}.$$

Using our main result we conclude that the Lip'- convergence *rate* of the RCE solutions to the corresponding entropy solution is also of order $\mathcal{O}(\varepsilon)$.

Corollary 4.4.1 *Assume that $f'' \geq \alpha > 0$, and let v^ε be the unique RCE solution of (4.4.2) subject to C^1* initial conditions $v^\varepsilon(0) \equiv u(0)$. *then v^ε converges to the unique entropy solution of (4.2.1) and the following error estimates hold*

$$||v^\varepsilon(t) - u(t)||_{W^{s,p}} \leq Const \cdot \varepsilon^{\frac{1-sp}{2p}}, \quad -1 \leq s \leq \frac{1}{p}. \tag{4.4.5}$$

4.4.2 Finite-Difference approximations

We want to solve the conservation law (4.2.1)-(4.2.2) by difference approximations. To this end we use a grid ($x_\nu := \nu\Delta x, t^n := n\Delta t$) with a fixed mesh-ratio $\lambda \equiv \frac{\Delta t}{\Delta x} = \text{Const}$. The approximate solution at these grid points, $v_\nu^n \equiv v(x_\nu, t^n)$, is determined by a conservative difference approximation which takes the following viscosity form, e.g., [35][2]

$$v_\nu^{n+1} = v_\nu^n - \frac{\lambda}{2}[f(v_{\nu+1}^n) - f(v_{\nu-1}^n)] + \frac{1}{2}[Q_{\nu+\frac{1}{2}}^n \Delta v_{\nu+\frac{1}{2}}^n - Q_{\nu-\frac{1}{2}}^n \Delta v_{\nu-\frac{1}{2}}^n], \quad (4.4.6)$$

and is subject to Lip^+-bounded initial conditions,

$$v_\nu^0 = \frac{1}{\Delta x}\int_{x_{\nu-\frac{1}{2}}}^{x_{\nu+\frac{1}{2}}} u_0(\xi)d\xi, \quad L_0^+ = \|u_0\|_{Lip^+} < \infty. \quad (4.4.7)$$

Let $v^\varepsilon(x,t)$ be the piecewise linear interpolant of our grid solution, $v^\varepsilon(x_\nu, t^n) = v_\nu^n$, depending on the small discretization parameter $\varepsilon \equiv \Delta x \downarrow 0$. It is given by

$$v^{\Delta x}(x,t) = \sum_{j,m} v_j^m \Lambda_j^m(x,t), \quad \Lambda_j^m(x,t) := \Lambda_j(x)\Lambda^m(t),$$

where $\Lambda_j(x)$ and $\Lambda^m(t)$ denote the usual 'hat' functions,

$$\Lambda_j(x) = \frac{1}{\Delta x}\min(x - x_{j-1}, x_{j+1} - x)_+, \quad \Lambda^m(t) = \frac{1}{\Delta t}\min(t - t^{m-1}, t^{m+1} - t)_+.$$

In [24] we show that these schemes are Lip'-consistent of order $\mathcal{O}(\Delta x)$, thus arriving at

Theorem 4.4.2 *Assume that the difference approximation (4.4.6)-(4.4.7) is Lip^+-stable in the sense that the following one-sided Lipschitz condition is fulfilled:*

$$\max_\nu \frac{(\Delta v_{\nu+\frac{1}{2}}^n)_+}{\Delta x} \le \frac{1}{[L_0^+]^{-1} + \beta t^n}, \quad 0 \le t^n \le T. \quad (4.4.8)$$

Then the following error estimates hold:

$$\|v^{\Delta x}(\cdot,T) - u(\cdot,T)\|_{W^{s,p}} \le C_T \cdot (\Delta x)^{\frac{1-sp}{2p}}, \quad -1 \le s \le \frac{1}{p}, \quad (4.4.9)$$

$$|v^{\Delta x}(x,T) - u(x,T)| \le C_x \cdot \max_{|\xi - x| \le \sqrt[3]{\Delta x}} |u_x(\xi,T)| \cdot \sqrt[3]{\Delta x}. \quad (4.4.10)$$

[2] We use the usual notations for forward and backward differences, $\Delta_\pm v_{\nu+\frac{1}{2}} := \pm(v_{\nu\pm1} - v_\nu)$.

The following first order accurate schemes (identified in a decreasing order according to their numerical viscosity coefficient, $Q_{\nu+\frac{1}{2}} \equiv Q^n_{\nu+\frac{1}{2}}$), are frequently referred to in the literature.

$$\text{Lax} - \text{Friedrichs scheme} \qquad Q^{LxF}_{\nu+\frac{1}{2}} \equiv 1, \tag{4.4.11}$$

$$\text{Engquist} - \text{Osher scheme} \qquad Q^{EO}_{\nu+\frac{1}{2}} = \frac{\lambda}{v^n_{\nu+1} - v^n_\nu} \int_{v_\nu}^{v_{\nu+1}} |f'(v)| dv, \tag{4.4.12}$$

$$\text{Godunov scheme} \qquad Q^{G}_{\nu+\frac{1}{2}} = \lambda \max_v \left[\frac{f(v^n_{\nu+1}) + f(v^n_\nu) - 2f(v)}{v^n_{\nu+1} - v^n_\nu} \right] \tag{4.4.13}$$

$$\text{Roe scheme} \qquad Q^{R}_{\nu+\frac{1}{2}} = \lambda \left| \frac{\Delta f^n_{\nu+\frac{1}{2}}}{\Delta v^n_{\nu+\frac{1}{2}}} \right|. \tag{4.4.14}$$

In [24] we prove the Lip^+ stability of these schemes, and together with their Lip' consistency (of order $\mathcal{O}(\Delta x)$) we arrive at

Corollary 4.4.2 *Consider the conservation law (4.2.1), (4.2.2) with Lip^+-bounded initial data (4.2.10). Then the Roe, Godunov, Engquist-Osher, and Lax-Friedrichs difference approximations (4.4.11)-(4.4.14) with discrete initial data (4.4.7) converge, and their piecewise-linear interpolants $v^{\Delta x}(x,t)$, satisfy the convergence rate estimates (4.4.9), (4.4.10).*

Remark. The Lip^+-stability (4.4.8) of Roe scheme with $\beta = 0$ (no decay), was proved in [3]. Note that the assumption of Lip^+-bounded initial conditions is essential for convergence to the entropy solution in this case, in view of the discrete steady-state solution, $v^0_\nu = \text{sgn}(\nu + \frac{1}{2})$, which shows that convergence of Roe scheme to the correct entropy rarefaction fails due to the fact that the initial data are *not* Lip^+-bounded.

4.4.3 Godunov type schemes

Godunov type schemes form a special class of transport projection methods for the approximate solution of nonlinear hyperbolic conservation laws. This class of schemes takes the following form:

$$v^{\Delta x}(\cdot,t) = \begin{cases} T_{\{t-t^{n-1}\}} v^{\Delta x}(\cdot, t^{n-1}), & t^{n-1} < t < t^n \\ P(\{I^n_j\}) v^{\Delta x}(\cdot, t^n - 0), & t = t^n = n\Delta t \end{cases} \tag{4.4.15}$$

where the initialization step is:

$$v^{\Delta x}(\cdot, t^0 = 0) = P(\{I^0_j\}) u_0(\cdot) \quad . \tag{4.4.16}$$

These schemes are composed of the following four ingredients:

(i) The possibly variable size grid cells, $I^n_j \equiv [x^n_{j-\frac{1}{2}}, x^n_{j+\frac{1}{2}})$, where the grid is regular in the sense that:

$$\Delta x \equiv \Delta x_{min} \le |I^n_j| \le \Delta x_{max} \quad ; \quad \frac{\Delta x_{max}}{\Delta x_{min}} \le Const. \; ; \tag{4.4.17}$$

(ii) A conservative piecewise polynomial grid projection, $P = P(\{I_j^n\})$,

$$\int_x Pw(x)dx = \int_x w(x)dx \quad ; \tag{4.4.18}$$

(iii) The exact entropy solution operator associated with (4.1.1), $T = T_t$;
(iv) The time step Δt, which is restricted by the CFL condition:

$$\lambda \max_{x,t} |f'(v^{\Delta x}(x,t))| \leq 1 \quad , \quad \lambda = \frac{\Delta t}{\Delta x} \quad . \tag{4.4.19}$$

As an example we recall here the subclass of Godunov-type schemes based on piecewise-polynomial projections, which was discussed already in the 'short guide' introduced in Lecture II.

To study the convergence rate of this class of schemes, we are required to verify the Lip'-consistency and Lip^+-stability of the scheme in question. We begin by reducing the question of Lip'-consistency to the level of a mere approximation problem, namely, measuring in Lip'-semi-norm the distance between the exact solution and its grid projection. Thus, our first theorem below enables us to avoid the delicate bookkeeping of error accumulation due to the dynamic transport part of the scheme.

Theorem 4.4.3 *(Lip'-consistency.) The Godunov type approximation (4.4.15)-(4.4.16) satisfies the following truncation error estimate:*

$$\|v_t^{\Delta x} + f(v^{\Delta x})_x\|_{Lip'(x,[0,T])} \leq \frac{T}{\Delta t} \max_{0<t^n\leq T} \|(P-I)v^{\Delta x}(\cdot, t^n - 0)\|_{Lip'} \tag{4.4.20}$$

Remark. We emphasize that this theorem applies to both fixed and variable grid schemes.

Proof. Let N denote the number of time steps in $[0,T]$, i.e.

$$T = t^N = N\Delta t \quad . \tag{4.4.21}$$

Then for every $\phi \in C_0^1(\Re \times [0,T])$

$$(v_t^{\Delta x} + f(v^{\Delta x})_x, \phi)_{x,t} = \sum_{n=1}^{N} \left[\int_{t^{n-1}}^{t^n} \int_x v_t^{\Delta x} \phi dx dt + \int_{t^{n-1}}^{t^n} \int_x f(v^{\Delta x})_x \phi dx dt \right] \quad .$$

Integration by parts gives that

$$(v_t^{\Delta x} + f(v^{\Delta x})_x, \phi)_{x,t} = \sum_{n=1}^{N} \left[(v^{\Delta x}, \phi)\Big|_{t^{n-1}}^{t^n} - \int_{t^{n-1}}^{t^n} \left((v^{\Delta x}, \phi_t) + (f(v^{\Delta x}), \phi_x) \right) dt \right] \quad . \tag{4.4.22}$$

But since $v^{\Delta x}$ is a weak solution in the strip $\Re \times (t^{n-1}, t^n)$, as definition (4.4.15) implies, then

$$\int_{t^{n-1}}^{t^n} \left((v^{\Delta x}, \phi_t) + (f(v^{\Delta x}), \phi_x) \right) dt = (v^{\Delta x}, \phi) \Big|_{t^{n-1}+0}^{t^n-0} \quad . \tag{4.4.23}$$

Therefore, by (4.4.22) and (4.4.23),

$$(v_t^{\Delta x} + f(v^{\Delta x})_x, \phi)_{x,t} = \sum_{n=1}^{N} \left[(v^{\Delta x}, \phi) \Big|_{t^{n-1}}^{t^n} - (v^{\Delta x}, \phi) \Big|_{t^{n-1}+0}^{t^n-0} \right] \quad ,$$

and since, by (4.4.15), $v^{\Delta x}(\cdot, t^{n-1}+0) = v^{\Delta x}(\cdot, t^{n-1})$, we have that

$$(v_t^{\Delta x} + f(v^{\Delta x})_x, \phi)_{x,t} = \sum_{n=1}^{N} (v^{\Delta x}, \phi) \Big|_{t^n-0}^{t^n} = \sum_{n=1}^{N} ((P-I)v^{\Delta x}(\cdot, t^n - 0), \phi(\cdot, t^n)) \quad .$$

Recall the conservation of P asserted in (4.4.18), $\int (P-I)v^{\Delta x} dx = 0$. Therefore, using the definition of the Lip'-seminorm, together with (4.4.21), we get

$$|(v_t^{\Delta x} + f(v^{\Delta x})_x, \phi)_{x,t}| \leq \frac{T}{\Delta t} \max_{1 \leq n \leq N} \|(P-I)v^{\Delta x}(\cdot, t^n - 0)\|_{Lip'} \|\phi(\cdot, t^n)\|_{Lip} \quad .$$

Dividing by $\|\phi(x,t)\|_{Lip}$ and taking the supremum over ϕ, we arrive at (4.4.20). ■

Next, we turn to the question of Lip^+-stability. The standard Lip^+-seminorm, $\|\cdot\|_{Lip^+}$, is inappropriate measure for the size of *discontinuous* piecewise polynomial functions, since increasing jumps – even on the acceptable scale of the gridsize, are Lip^+-unbounded. Instead, we replace it by its discrete analogue – $\|\cdot\|_{\ell ip^+}$, requiring

$$\|v^{\Delta x}(\cdot, t^n)\|_{\ell ip^+} := \max_x \left(\frac{v^{\Delta x}(x + \Delta x, t^n) - v^{\Delta x}(x, t^n)}{\Delta x} \right)^+ \leq Const. \tag{4.4.24}$$

The discrete ℓip^+ stability is weaker than Lip^+ stability, yet, as we shall show below, it will suffice for our convergence rate estimates to hold. To see this, we introduce a compactly supported non-negative unit mass mollifier,

$$\psi_\delta(x) = \frac{1}{\delta} \psi(\frac{x}{\delta}) \quad , \quad \int_x \psi_\delta(x) dx = \int_x \psi(x) dx = 1 \quad . \tag{4.4.25}$$

The discrete ℓip^+ stability is related to the stronger Lip^+ bound on the *mollified* solution. The following lemma shows that Lip'-consistency of order $\mathcal{O}(\Delta x)$ remains invariant under a mollification with ψ_δ, $\delta = \mathcal{O}(\Delta x)$. Thus, $\mathcal{O}(\Delta x)$-mollification does not sacrifice accuracy yet we have the advantage of using the weaker discrete ℓip^+ stability.

Lemma 4.4.1 *Assume $v^{\Delta x}(x,t)$ has a bounded variation and is Lip'-consistent with (4.1.1) of order $\mathcal{O}(\Delta x)$,*

$$\|F^{\Delta x}(x,t)\|_{Lip'} = O(\Delta x) \quad , \quad F^{\Delta x}(x,t) \equiv v_t^{\Delta x} + f(v^{\Delta x})_x \quad . \tag{4.4.26}$$

Then $v^{\Delta x,\delta} \equiv \psi_\delta * v^{\Delta x}$ is Lip'-consistent with (4.1.1) of order $\mathcal{O}(\Delta x) + \mathcal{O}(\delta)$.

We omit the straightforward proof (which could be found in [26]). Finally, we combine Theorem 4.4.3 and Lemma 4.4.1 to achieve our main convergence rate estimate for Godunov type schemes.

Theorem 4.4.4 *(Convergence rate estimates.) Assume that the Godunov type approximation (4.4.15)-(4.4.16) is ℓip^+-stable, (4.4.24), and Lip'-consistent in the sense that*

$$\|(P-I)w\|_{Lip'} \le O(\Delta x^2)\|w\|_{BV} \quad . \tag{4.4.27}$$

Then the following error estimates hold:

$$\|v^{\Delta x}(\cdot,t) - u(\cdot,t)\|_{W^{s,p}} = \mathcal{O}(\Delta x^{\frac{1-sp}{2p}}), -1 \le s \le \frac{1}{p}. \tag{4.4.28}$$

Proof. Let us denote $\tilde{v}^{\Delta x}(\cdot,t) \equiv \psi_{\Delta x} * v^{\Delta x}(\cdot,t)$, where $\psi_{\Delta x}$ is the dilated mollifier of

$$\psi(x) = \begin{cases} 1, & |x| \le \frac{1}{2} \\ 0, & |x| > \frac{1}{2} \end{cases} \quad . \tag{4.4.29}$$

This choice of mollifier satisfies the *Lip'*-error estimate

$$\|\psi_{\Delta x} * w - w\|_{Lip'} \le \mathcal{O}(\Delta x^2)\|w\|_{BV} \quad . \tag{4.4.30}$$

We show that $\tilde{v}^{\Delta x}$ satisfies the Lip^+-stability condition (4.2.7), and it is *Lip'*-consistent of order $\mathcal{O}(\Delta x)$.

We start with the Lip^+-stability question. The definition of the discrete ℓip^+-seminorm, (4.4.24), implies that $\|\tilde{v}^{\Delta x}(\cdot,t^n)\|_{Lip^+} = \|v^{\Delta x}(\cdot,t^n)\|_{\ell ip^+}$. Since $v^{\Delta x}$ is assumed to be discrete ℓip^+-stable, we conclude that at each time level t^n we have

$$\|\tilde{v}^{\Delta x}(\cdot,t^n)\|_{Lip^+} = D_n \le C \quad . \tag{4.4.31}$$

This, together with the fact that the intermediate exact solution operator decreases the Lip^+-seminorm, (4.2.6) imply Lip^+-boundedness for all $t \ge 0$:

$$\|\tilde{v}^{\Delta x}(\cdot,t)\|_{Lip^+} \le Const. \qquad \forall t \ge 0 \quad . \tag{4.4.32}$$

Namely, the mollified approximation $\tilde{v}^{\Delta x}$ is Lip^+-stable.

We note in passing that $v^{\Delta x}(\cdot,t)$, being compactly supported and Lip^+-bounded, has bounded variation. Turning to the question of *Lip'*-consistency we therefore conclude from assumption (4.4.27) together with the truncation error estimate (4.4.20), that $v^{\Delta x}$ is *Lip'*-consistent with (4.2.1) of order $\mathcal{O}(\Delta x)$, and hence by lemma 4.4.1, so does $\tilde{v}^{\Delta x}$,

$$\|\tilde{v}_t^{\Delta x} + f(\tilde{v}^{\Delta x})_x\| = O(\Delta x) \quad .$$

Furthermore, $\tilde{v}^{\Delta x}$ is also Lip'-consistent with the initial condition (4.2.2), since by (4.4.30), (4.4.16) and (4.4.27):

$$\|\tilde{v}^{\Delta x}(\cdot,0)-u(\cdot,0)\|_{Lip'} \le \|\tilde{v}^{\Delta x}(\cdot,0)-v^{\Delta x}(\cdot,0)\|_{Lip'}+\|v^{\Delta x}(\cdot,0)-u_0(\cdot)\|_{Lip'} \le O(\Delta x^2) \ .$$

Therefore, Theorem 4.3.1 holds; in particular (4.3.1) tells us that

$$\|\tilde{v}^{\Delta x}(\cdot,T)-u(\cdot,T)\|_{Lip'} = \mathcal{O}(\Delta x) \ . \tag{4.4.33}$$

In addition, we have by (4.4.30),

$$\|\tilde{v}^{\Delta x}(\cdot,T)-v^{\Delta x}(\cdot,T)\|_{Lip'} = O(\Delta x^2) \ . \tag{4.4.34}$$

Combining (4.4.33) and (4.4.34) we end up with

$$\|v^{\Delta x}(\cdot,T)-u(\cdot,T)\|_{Lip'} = O(\Delta x) \ . \tag{4.4.35}$$

The Lip'-error estimate (4.4.35) may now be interpolated into the $W^{s,p}$-error estimates (4.4.28). ■

Examples of the first-order Godunov and Engquist-Osher schemes as well as the second-order (upwind) MUSCL and (central) Nessyahu-Tadmor schemes are discussed in [26].

4.4.4 Glimm scheme

We recall the construction of Glimm approximate solution for the conservation law (4.2.1), see [10, 32]. We let $v(x,t)$ be the entropy solution of (4.2.1) in the slab $t^n \le t < t^{n+1}, n \ge 0$, subject to piecewise constant data $v(x,t^n) = \sum_\nu v_\nu^n \chi_\nu(x)$. To proceed in time, the solution is extended (in a staggered fashion) with a jump discontinuity across the lines $t^{n+1}, n \ge 0$, where $v(x,t^{n+1})$ takes the piecewise constant values

$$v(x,t^{n+1}) = \sum_\nu v_{\nu+\frac{1}{2}}^{n+1}\chi_{\nu+\frac{1}{2}}(x), \quad v_{\nu+\frac{1}{2}}^{n+1} = v(x_{\nu+\frac{1}{2}}+r^n\Delta x, t^{n+1}-0). \tag{4.4.36}$$

Notice that in each slab, $v(x,t)$ consists of successive noninteracting Riemann solutions provided the CFL condition, $\lambda \cdot \max|a(u)| \le \frac{1}{2}$ is met. This defines the Glimm approximate solution, $v(x,t) \equiv v^\varepsilon(x,t)$, depending on the mesh parameters $\varepsilon = \Delta x \equiv \lambda \Delta t$, and the set of random variables $\{r^n\}$, uniformly distributed in $[-\frac{1}{2},\frac{1}{2}]$. In the deterministic version of the Glimm scheme, Liu [21] employs equidistributed rather than random sequence of numbers $\{r^n\}$. We note that in both versions, we make use of exactly *one* random or equidistributed choice per time step (independently of the spatial cells), as was first advocated by Chorin [5].

It follows that both versions of Glimm scheme share the Lip^+-stability estimate (4.2.7). Indeed, since the solution of a scalar Riemann problem remains in the convex hull of its initial data, we may express $v_{\nu+\frac{1}{2}}^{n+1}$ as $(1-\theta_{\nu+\frac{1}{2}}^n)v_\nu^n + \theta_{\nu+\frac{1}{2}}^n v_{\nu+1}^n$ for some $\theta_{\nu+\frac{1}{2}}^n \in [0,1]$, and hence

$$v_{\nu+\frac{1}{2}}^{n+1} - v_{\nu-\frac{1}{2}}^{n+1} = \theta_{\nu+\frac{1}{2}}^n \Delta v_{\nu+\frac{1}{2}}^n + (1-\theta_{\nu-\frac{1}{2}}^n)\Delta v_{\nu-\frac{1}{2}}^n .$$

We now distinguish between two cases. If either $\Delta v^n_{\nu-\frac{1}{2}}$ or $\Delta v^n_{\nu+\frac{1}{2}}$ is negative, then

$$v^{n+1}_{\nu+\frac{1}{2}} - v^{n+1}_{\nu-\frac{1}{2}} \le \max(\Delta v^n_{\nu+\frac{1}{2}}, \Delta v^n_{\nu-\frac{1}{2}}). \tag{4.4.37}$$

Otherwise — when both $\Delta v^n_{\nu+\frac{1}{2}}$ and $\Delta v^n_{\nu-\frac{1}{2}}$ are positive, the two values of $v^{n+1}_{\nu+\frac{1}{2}}$ and $v^{n+1}_{\nu-\frac{1}{2}}$ are obtained as sampled values of two consecutive rarefaction waves, and a straightforward computation shows that their difference satisfies (4.4.37). Thus in either case, the Lip^+-stability (4.2.7) holds with $\beta = 0$.

Although Glimm approximate solutions are conservative "on the average," they do not satisfy the conservation requirement (4.2.3). We therefore need to slightly modify our previous convergence arguments in this case.

We first recall the truncation error estimate for the deterministic version of Glimm scheme [14, Theorem 3.2],

$$\begin{aligned} &\left(v_t^{\Delta x} + f(v^{\Delta x})_x, \phi(x,t)\right)_{L^2(x,[0,T])} \le \\ &\le \mathrm{Const}_T \left[\sqrt{\Delta x}|\ln \Delta x| \cdot \|\phi\|_{L^\infty} + \Delta x \cdot \|\phi(x,t)\|_{Lip(x,[0,T])}\right]. \end{aligned} \tag{4.4.38}$$

Let $\phi(x,t) = \phi^{\Delta x}(x,t)$ denote the solution of the adjoint error equation (4.3.4). Applying (4.4.38) instead of (4.3.10) and arguing along the lines of Theorem (4.3.1), we conclude that Glimm scheme is Lip'-consistent (and hence has a Lip'-convergence rate) of order $\sqrt{\Delta x}|\ln \Delta x|$,

$$|(e^{\Delta x}(\cdot,T), \phi(\cdot))| \le \mathrm{Const}_T \left[\sqrt{\Delta x}|\ln \Delta x| \cdot \|\phi\|_{L^\infty} + \Delta x \cdot \|\phi(x)\|_{Lip}\right]. \tag{4.4.39}$$

To obtain an L^1-convergence rate estimate we employ (4.4.39) with $\phi_\delta \equiv \phi * \frac{1}{\delta}\zeta\left(\frac{\cdot}{\delta}\right)$ yielding

$$|(e^{\Delta x}(\cdot,T), \phi_\delta)| \le \mathrm{Const}_T \left[\sqrt{\Delta x}|\ln \Delta x| + \frac{\Delta x}{\delta}\right] \|\phi(x)\|_{L^\infty}. \tag{4.4.40}$$

Using this estimate together with

$$(e^\varepsilon(\cdot,T), [\phi(\cdot) - \phi_\delta(\cdot)]) \equiv (e^\varepsilon(\cdot,T) - e^\varepsilon_\delta(\cdot,T), \phi) \le \mathrm{Const} \cdot \|e^\varepsilon(\cdot,T)\|_{BV} \cdot \delta \|\phi\|_{L^\infty},$$

imply (for $\delta \sim \sqrt{\Delta x}$), the usual L^1-convergence rate of order $O(\sqrt{\Delta x|\ln \Delta x|})$. As noted in the closing remark of §4.3.1, the Lip^+-stability of Glimm's approximate solutions enables us to convert the L^1-type into pointwise convergence rate estimate.

We close this section by stating the following.

Theorem 4.4.5 *Consider the conservation law (4.2.1), (4.2.2) with sufficiently small Lip^+-bounded initial data (4.2.10). Then the (deterministic version of) Glimm approximate solution $v^{\Delta x}(x,t)$ in (4.4.36) converges to the entropy solution $u(x,t)$, and the following convergence rate estimates hold:*

$$\|v^{\Delta x}(\cdot,T) - u(\cdot,T)\|_{L^1} \le \mathrm{Const}_T \cdot \sqrt{\Delta x|\ln \Delta x|}, \tag{4.4.41}$$

$$|v^{\Delta x}(x,T) - u(x,T)| \le \mathrm{Const}_{x,T} \cdot [1 + \max_{|\xi - x| \le \sqrt[4]{\Delta x}} |u_x(\xi,T)|] \cdot \sqrt[4]{\Delta x|\ln \Delta x|}. \tag{4.4.42}$$

Remarks.

1. A sharp L^1-error estimate of order $O(\sqrt{\Delta x})$ can be found in [22], improving the previous error estimates of [14].

2. Theorem 4.4.5 hinges on the truncation error estimate (4.4.38) which assumes initial data which sufficiently small variation [14]. Extensions to strong initial discontinuities for Glimm scheme and the front tracking method can be found in [6, Theorems 4.6 and 5.2].

4.4.5 The Spectral Viscosity method

We want to solve the 2π-periodic initial-value problem (4.1.1)-(4.1.2) by spectral methods. To this end we use an N-trigonometric polynomial, $v_N(x,t) = \sum_{k=-N}^{N} \hat{v}_k(t)e^{ikx}$, to approximate the spectral (or pseudospectral) projection of the exact entropy solution, $P_N u$. Starting with $v_N(x,0) = P_N u_0(x)$, the standard Fourier method reads,

$$\frac{\partial}{\partial t}v_N + \frac{\partial}{\partial x}P_N f(v_N) = 0. \tag{4.4.43}$$

Together with one's favorite ODE solver, (4.4.43) gives a fully discrete spectral method for the approximate solution of (4.1.1).

Although the spectral method (4.4.43) is a spectrally accurate approximation of the conservation law (4.1.1) in the sense that its local error does not exceed

$$\|(I - P_N)f(v_N(\cdot,t))\|_{H^{-s}} \leq \text{Const} \cdot N^{-s}\|v_N\|_{L^2}, \quad \forall s \geq 0, \tag{4.4.44}$$

the spectral solution, $v_N(x,t)$, need not approximate the corresponding entropy solution, $u(x,t)$. Indeed, the counterexamples in §4.1 show that the spectral approximation (4.4.43) lacks *entropy dissipation*, which is inconsistent with the entropy condition (4.1.2). Consequently, the spectral approximation (4.4.43) supports spurious Gibbs oscillations which prevent strong convergence to the exact solution of (1.1). To suppress these oscillations, without sacrificing the overall spectral accuracy, we consider instead the Spectral Viscosity (SV) approximation

$$\frac{\partial}{\partial t}v_N(x,t) + \frac{\partial}{\partial x}P_N f(v_N(x,t)) = \varepsilon_N \frac{\partial}{\partial x}Q_N * \frac{\partial}{\partial x}v_N(x,t). \tag{4.4.45}$$

The left-hand side of (4.4.45) is the standard spectral approximation of (4.1.1). On the right hand-side, it is augmented by *spectral viscosity* which consists of the following three ingredients: a vanishing viscosity amplitude of size $\varepsilon_N \downarrow 0$, a viscosity-free spectrum of size $m_N >> 1$, and a viscosity kernel, $Q_N(x,t) = \sum_{|k|=m_N}^{N} \hat{Q}_k(t)e^{ikx}$ activated only on high wavenumbers $|k| \geq m_N$, which can be conveniently implemented in the Fourier space as

$$\varepsilon_N \frac{\partial}{\partial x}Q_N * \frac{\partial}{\partial x}v_N(x,t) \equiv -\varepsilon_N \sum_{|k|=m_N}^{N} k^2 \hat{Q}_k(t)\hat{v}_k(t)e^{ikx}.$$

We deal with real viscosity kernels $Q_N(x,t)$ with increasing Fourier coefficients, $\hat{Q}_k \equiv \hat{Q}_{|k|}$, which satisfy

$$1-\left(\frac{m_N}{|k|}\right)^{2q} \le \hat{Q}_k(t) \le 1, \quad |k| \ge m_N, \quad \text{for some fixed } q \ge 1, \qquad (4.4.46_q)$$

and we let the spectral viscosity parameters, (ε_N, m_N), lie in the range

$$\varepsilon_N \sim \frac{1}{N^\theta \log N}, \quad m_N \sim N^{\frac{\theta}{2q}}, \quad \theta < 1. \qquad (4.4.47_q)$$

We remark that this choice of spectral viscosity parameters is small enough to retain the formal spectral accuracy of the overall approximation, since

$$\|\varepsilon_N \frac{\partial}{\partial x} Q_N * \frac{\partial}{\partial x} v_N(\cdot,t)\|_{H^{-s}} \le \text{Const} \cdot N^{-\frac{\theta s}{2q}} \|v_N(\cdot,t)\|_{L^2}, \quad \forall s \ge 2. \quad (4.4.48)$$

At the same time, it is sufficiently large to enforce the correct amount of entropy dissipation that is missing otherwise, when either $\varepsilon_N = 0$ or $m_N = N$. Indeed, it was shown in [38],[40],[23] that the SV approximation (4.4.45), $(4.4.46_q)$-$(4.4.47_q)$ has a bounded entropy production in the sense that

$$\varepsilon_N \|\frac{\partial}{\partial x} v_N(x,t)\|^2_{L^2_{loc}(x,t)} \le \text{Const}, \qquad (4.4.49)$$

and this together with an L^∞-bound imply – by compensated compactness arguments, that the SV approximation v_N converges to the unique entropy solution of (4.1.1). A detailed account on the SV method is outlined in Leture III of this volume.

Observe that in the limit case $q = \infty$, the SV method (4.4.45), $(4.4.46_q)$-$(4.4.47_q)$, coincides with the usual viscosity approximation,

$$\frac{\partial}{\partial t} v^\varepsilon(x,t) + \frac{\partial}{\partial x} P_N f(v^\varepsilon(x,t)) = \varepsilon_N \frac{\partial^2}{\partial x^2} v^\varepsilon(x,t).$$

But of course, the spectral accuracy (4.4.48) is lost in this limit case.

The Lip^+-stability and Lip'-consistency (of order $\mathcal{O}(N^{-\theta})$) of the SV approximation were studies in [40]. We thus arrive at

Theorem 4.4.6 *(Convergence rate estimates.) Consider the 2π-periodic nonlinear conservation law (4.2.1) with Lip^+-initial-data. Then the SV approximation (4.4.45),$(4.4.46_q)$-$(4.4.47_q)$ with $q \ge \frac{3}{2}$ converges to the entropy solution of (4.2.1) and the following error estimates hold for $0 < t_0 \le \forall t \le T$:*

$$\|v_N(\cdot,t) - u(\cdot,t)\|_{W^{s,p}} \le \text{Const}_T \cdot N^{-\frac{1-sp}{2p}\theta}, -1 \le s \le \frac{1}{p}; \qquad (4.4.50)$$

$$|v_N(x,t) - u(x,t)| \le \text{Const}_T \cdot N^{-\frac{\theta}{3}}, \qquad 0 < t_0 \le t \le T; \qquad (4.4.51)$$

Finally, any r-th order mollifier, (4.3.13), recovers the pointvalues of v_N to the order of

$$|v_N(x,t) * \psi_r - v_N(x,t)| \le C_r \cdot N^{-\frac{r}{r+2}\theta}. \qquad (4.4.52)$$

Remarks.

1. Theorem 4.4.6 requires the initial data of the SV method, $v_N(x,0)$, to be Lip^+-bounded independently of N. Consequently, one might need to pre-process the prescribed initial data u_0 unless they are smooth enough to begin with. The de la Vallee Poussin pre-processing, for example, will guarantee this requirement for arbitrary Lip^+-bounded initial data u_0.

2. The error estimates (4.4.50),(4.4.51) are not uniform in time as $t_0 \downarrow 0$, unless the initial data are sufficiently smooth to guarantee the uniformity (in time) of the Lip^+ bound. For arbitrary Lip^+-initial data, u_0, an initial layer may be formed, after which the spectral viscosity becomes effective and guarantees the spectral decay of the discretization error.

3. According to (4.4.51) and (4.4.52), the pointwise convergence rate of the SV solution in smooth regions of the entropy solution is of order $\sim N^{-\frac{1}{3}}$, and by *post-processing* the SV solution this convergence rate can be made arbitrarily close to N^{-1}. In fact, numerical experiments reported in [38] show that by post-processing the SV solution using the spectrally accurate mollifier of [12], $\psi_r(x) = \psi_0(x)D_n(x), n \sim \left[\varepsilon_N^{-\frac{1}{r+2}}\right]$, we recover the pointwise values in smooth regions of the entropy solution within spectral accuracy.

4. According to (4.4.50) with $(s,p) = (0,1)$, the SV approximation has an L^1-convergence rate of order $\sim N^{-\frac{1}{2}}$ in agreement with [30]. This correspond s to the usual L^1-convergence rate of order $\frac{1}{2}$ for monotone difference approximations, [15],[31].

Bibliography

[1] G. Barles & P.E. Souganidis, *Convergence of approximation schemes for fully nonlinear second order equations*, Asympt. Anal. 4 (1991), 271–283.

[2] F. Bouchut & B. Perthame, *Kruzkov's estimates for scalar conservation laws revisited*, Universite D'Orleans, preprint, 1996.

[3] Y. Brenier, *Roe's scheme and entropy solution for convex scalar conservation laws*, INRIA Report 423, France 1985.

[4] Y. Brenier & S. Osher, *The discrete one-sided Lipschitz condition for convex scalar conservation laws*. 1988, SIAM J. of Num. Anal. Vol. 25, 1, pp. 8-23.

[5] A. J. Chorin, *Random choice solution of hyperbolic systems*, J. Comp. Phys., 22 (1976, pp. 517-533.

[6] I. L. Chern, *Stability theorem and truncation error analysis for the Glimm scheme and for a front tracking method for flows with strong discontinuities*, Comm. Pure Appl. Math., XLII (1989), pp. 815-844.

[7] B. Cockburn, F. Coquel & P. LeFloch, *Convergence of finite volume methods for multidimensional conservation laws*, SIAM J. Numer. Anal. 32 (1995), 687–705.

[8] M. G. Crandall & P. L. Lions, *Viscosity solutions of Hamilton-Jacobi equations*, Trans. Amer. Math. Soc. 277 (1983), 1–42.

[9] M.G. Crandall & A. Majda, *Monotone difference approximations for scalar conservation laws*, Math.Comp.,34 (1980), 1-21.

[10] J. Glimm, *Solutions in the large for nonlinear hyperbolic systems of equations*, Comm. Pure Appl. Math., 18 (1965), pp. 697-715.

[11] J.B. Goodman & R.J. LeVeque, *A geometric approach to high resolution TVD schemes*, SIAM J. Numer. Anal., 25 (1988), pp. 268-284.

[12] D. Gottlieb & E. Tadmor, *Recovering Pointwise Values of Discontinuous Data within Spectral Accuracy*, in "Progress and Supercomputing in Computational Fluid Dynamics", Progress in Scientific Computing, Vol. 6 (E. M. Murman and S. S. Abarbanel, eds.), Birkhauser, Boston, 1985, 357–375.

[13] J. Goodman & P.D. Lax, *On dispersive difference schemes. I*, Comm. Pure Appl. Math. 41 (1988), 591–613.

[14] D. Hoff & J. Smoller, *Error bounds for the Glimm scheme for a scalar conservation law*, Trans. Amer. Math. Soc., 289 (1988), pp. 611-642.

[15] N.N. Kuznetsov, *On stable methods for solving nonlinear first order partial differntial equations in the class of discontinuous solutions*, Topics in Num. Anal. III, Proc. Royal Irish Acad. Conf. Trinity College, Dublin (1976), pp. 183-192.

[16] S.N. Kružkov, *The method of finite difference for a first order non-linear equation with many independent variables*, USSR comput Math. and Math. Phys. 6 (1966), 136–151. (English Trans.)

[17] S. N. KRUSHKOV, *First-order quasilinear equations in several independent variables*, Math. USSR Sb. 10 (1970), 217-243.

[18] A. KURGANOV & E. TADMOR, *Stiff systems of hyperbolic conservation laws. convergence and error estimates*, SIMA, in press.

[19] C.-T. LIN & E. TADMOR L^1*-Stability and error estimates for approximate Hamilton-Jacobi solutions*, preprint.

[20] P. L. LIONS, Generalized Solutions of Hamilton-Jacobi Equations, Pittman, London 1982.

[21] T. P. LIU, *The deterministic version of the Glimm scheme*, Comm. Math. Phys., 57 (1977), pp. 135-148.

[22] B. LUCIER, *Error bounds for the methods of Glimm, Godunov, and LeVeque*, SIAM J. of Numer. Anal., 22 (1985), pp. 1074-1081.

[23] Y. MADAY & E. TADMOR, *Analysis of the spectral viscosity method for periodic conservation laws*, SINUM 26, 1989, pp. 854-870.

[24] H. NESSYAHU & E. TADMOR , *The convergence rate of approximate solutions for nonlinear scalar conservation laws*, SIAM J. Numer. Anal. 29 (1992), 1–15.

[25] H. NESSYAHU & T. TASSA, *Convergence rates of approximate solutions to conmservation laws with initial rarefactions*, SIAM J. Numer. Anal. 31 (1994), 628–654.

[26] H. NESSYAHU, E. TADMOR & T. TASSA, *The convergence rate of Godunov type schemes*, SIAM J. Numer. Anal. 31 (1994), 1–16.

[27] H. NESSYAHU, *Convergence rate of approximate solutions to weakly coupled nonlinear systems*, Math. Comp. 65 (1996) pp. 575-586.

[28] P. ROSENAU, *Extending hydrodynamics via the regularization of the Chapman-Enskog expansion*, Phys. Rev. A, 40(1989), 7193-6.

[29] R. RICHTMYER & K.W. MORTON, Difference methods for initial-value problems, 2nd ed., Interscience, New York, 1967.

[30] S. SCHOCHET, *The rate of convergence of spectral viscosity methods for periodic scalar conservation laws*, SINUM 27, 1990, pp. 1142-1159.

[31] R. SANDERS, *On convergence of monotone finite difference schemes with variable spatial differencing*, Math. of Comp., 40 (1983), pp. 91-106.

[32] J. SMOLLER, Shock Waves and Reaction-Diffusion Equations, Springer-Verlag, New York, 1983.

[33] S. SCHOCHET & E. TADMOR, *The regularized Chapman-Enskog expansion for scalar conservation laws*, Arch. Rational Mech. Anal., 119 (1992), pp. 95-107.

[34] E. TADMOR, *The large time behavior of the scalar, genuinely nonlinear Lax-Friedrichs scheme*, Math. of Comp., 43, 168 (1984), pp. 353-368.

[35] E. TADMOR, *Numerical viscosity and the entropy condition for conservative difference schemes*, Math. Comp., 43 (1984), pp. 369-381.

[36] E. TADMOR, *The numerical viscosity of entropy stable schemes for systems of conservation laws. I*, Math.of Comp., 49 (1987), pp. 91-103.

[37] E. TADMOR, *Semi-discrete approximations to nonlinear systems of conservation laws; consistency and* L^∞*-stability imply convergence*,ICASE ICASE Report No. 88-41.

[38] E. TADMOR, *Convergence of spectral methods for nonlinear conservation laws*, SIAM J. Numer. Anal., 26 (1989), pp. 30-44.

[39] E. TADMOR, *Local error estimates for discontinuous solutions of nonlinear hyperbolic equations*, SIAM J. Numer. Anal., 28 (1991), pp. 811-906.

[40] E. TADMOR, *Total variation and error estimates fo spectral viscosity approximations*, Math. Comp., 60 (1993), pp. 245-256.

[41] E. TADMOR & T. TANG, *The pointwise convergence rate for piecewise smooth solutions for scalar conservatin laws*, in preparation.

[42] T. TANG & Z. H. TENG, *Viscosity methods for piecewise smooth solutions to scalar conservation laws*, Math. Comp., 66 (1997), pp. 495–526.

[43] T. TANG & P. -W. ZHANG, *Optimal L^1-rate of convergence for viscosity method and monotone schemes to piecewise constant solutions with shocks*, SIAM J. Numer. Anala. 34 (1997), pp 959–978.

Chapter 5

Kinetic Formulations and Regularity

Abstract. We discuss the kinetic formulation of nonlinear conservation laws (– and related equations), a kinetic formulation which describes both the equation and the entropy criterion. This formulation is a kinetic one, involving an additional variable called velocity by analogy. We apply this formulation to derive, based upon the velocity averaging lemmas, new compactness and regularity results. In particular, we highlight the regularizing effect of nonlinear entropy solution operators, and we quantify the gained regularity in terms of the nonlinearity. Finally, we show that this kinetic formulation is in fact valid and meaningful for more general classes of equations, including equations involving nonlinear second-order terms, and the 2×2 hyperbolic system of isentropic gas dynamics, in both Eulerian or Lagrangian variables (– the so called 'p-system').

5.1 Regularizing effect in one-space dimension

We consider the convex conservation law

$$\frac{\partial}{\partial t}u(x,t) + \frac{\partial}{\partial x}A(u(x,t)) = 0, \quad A'' \geq \alpha > 0. \tag{5.1.1}$$

Starting with two values at the different positions, $u_\ell = u(x_\ell, t)$ and $u_r = u(x_r, t)$, we trace these values by backward characteristics. They impinge on the initial line at $x_\ell^0 = x_\ell - ta(u_\ell)$ and $x_r^0 = x_r - ta(u_r)$, respectively. Since the characteristics of entropy solutions of convex conservation laws cannot intersect, one finds that the ratio $(x_r^0 - x_\ell^0)/(x_r - x_\ell)$ remains positive for all time. After rearrangement this yields

$$\frac{a(u(x_r,t)) - a(u(x_\ell,t))}{x_r - x_\ell} \leq \frac{1}{t}.$$

Thus we conclude that the velocity of $a(u)$ satisfies the Oleĭnik's one-sided Lip condition, $a(u(\cdot,t))_x \leq 1/t$. Thanks to the convexity of A, we obtain the Lip^+

bound on u itself,

$$u_x(x,t) \leq \frac{1}{\alpha t}. \tag{5.1.2}$$

We recall that Lip^+ bound (5.1.2) served as the cornerstone for the *Lip' convergence* theory outlined in Lecture IV. Here we focus on the issue of it regularity. Granted (5.1.2), it follows that the solution operator associated with convex conservation laws, T_t, has a nonlinear regularizing effect, mapping

$$T_t : L_0^\infty \longrightarrow BV, \quad t > 0. \tag{5.1.3}$$

Indeed, for uniformly bounded initial data, $u_0 \in L_0^\infty$, with compact support of size $L = |supp u_0|$, one obtains $|supp u(\cdot,t)| \lesssim L + Const.t$. The Lip^+ bound (5.1.2) then yields an upper bound on the positive variation, $\int u_x^+(x,t)dx \leq Const.$; since the sum of the positive and negative variations is bounded,

$$\int u_x^+(x,t) + u_x^-(x,t)dx = \int u_x(x,t) \leq Const.\|u_0\|_{L^\infty},$$

it follows that their difference is also bounded,

$$\|u(x,t)\|_{BV} = \int \left[u_x^+(x,t) - u_x^-(x,t)\right] dx \leq Const. \tag{5.1.4}$$

Observe that no regularity is 'gained' in the linear case, where $A''(u) \equiv 0$. Indeed, the compactness asserted in (5.1.3) is a purely nonlinear regularizing phenomenon which reflects the irreversibility of nonlinear conservation laws, due to loss of entropy (information) across shock discontinuities. Here, nonlinearity is quantified in terms of convexity; in the prototype example of the inviscid Burgers' equation,

$$\frac{\partial}{\partial t}u + \frac{\partial}{\partial x}(\frac{u^2}{2}) = 0, \tag{5.1.5}$$

one finds a time decay, $u_x(x,t) \leq 1/t$. Tartar [31] proved this regularizing effect for general nonlinear fluxes — *nonlinear* in the sense of $A''(\cdot) \neq 0, a.e.$.

The situation with *multidimensional* equations, however, is less clear. Consider the 'two-dimensional Burgers' equation', analogous to (5.1.5)

$$\frac{\partial}{\partial t}u + \frac{\partial}{\partial x_1}(\frac{u^2}{2}) + \frac{\partial}{\partial x_2}(\frac{u^2}{2}) = 0. \tag{5.1.6}$$

Since $u(x_1,x_2,t) \equiv u_0(x_1 - x_2)$ is a steady solution of (5.1.6) for *any* u_0, it follows that initial oscillations persist (along $x_1 - x_2 = Const$), and hence there is no regularizing effect which guarantee the compactness of the solution operator in this case. More on oscillations and discontinuities can be found in Tartar's review [32].

5.2 Velocity averaging lemmas ($m \geq 1, d \geq 1$)

We deal with solutions to transport equations

$$a(v) \cdot \nabla_x f(x,v) = \partial_v^s g(x,v). \tag{5.2.1}$$

The averaging lemmas, [13], [12], [11], state that in the generic non-degenerate case, averaging over the velocity space, $\bar{f}(x) := \int_v f(x,v)dv$, yields a gain of *spatial* regularity. The prototype statement reads

Lemma 5.2.1 ([13],[11],[22]) *Let $f \in L^p(x,v)$ be a solution of the transport equation (5.2.1) with $g \in L^q(x,v), 1 \le q \le p \le 2$. Assume the following non-degeneracy condition holds*

$$meas_v\{v|\ |a(v)\cdot\xi/|\xi|| < \delta\} \le Const\cdot\delta^\alpha, \quad \alpha\in(0,1). \tag{5.2.2}$$

Then $\bar{f}(x) := \int_v f(x,v)dv$ belongs to Sobolev space $W^\theta(L^r(x))$,

$$\bar{f}(x)\in W^\theta(L^r(x)), \qquad \theta < \frac{\alpha}{\alpha(1-\frac{p'}{q'})+(s+1)p'}, \quad \frac{1}{r}=\frac{\theta}{q}+\frac{1-\theta}{p}. \tag{5.2.3}$$

Variants of the averaging lemmas were used by DiPerna and Lions to construct global weak (renormalized) solutions of Boltzmann, Vlasov-Maxwell and related kinetic systems, [9], [10]; in Bardos et. al., [1], averaging lemmas were used to construct solutions of the incompressible Navier-Stokes equations. We turn our attention to their use in the context of nonlinear conservation laws and related equations.

Proof. (Sketch). We shall sketch the proof in the particular case, $p = q$ which will suffice to demonstrate the general $p \neq q$ case.

Let $\Omega_\delta(\xi,v)$ denote the set where the symbol $a(v)\cdot\xi'$ is 'small',

$$\Omega_\delta(\xi,v) := \{(v,\xi)|\quad |a(v)\cdot\xi'| \le \delta\}, \quad \xi' := \frac{\xi}{|\xi|}, \tag{5.2.4}$$

and decompose the average, $\bar{f}(x)$ accordingly:

$$\begin{aligned}
\overline{f}(x) &= \int_v f(x,v)dv = \\
&= \int_v \mathcal{F}^{-1}|\xi|^{-1}\left[\frac{\partial_v^s \hat{g}(\xi,v)}{a(v)\cdot\xi'}\chi_{\Omega_\delta^c}(\xi,v)\right]dv + \quad \longleftarrow \overline{f}^\delta(x) \qquad (5.2.5)\\
&+ \int_v \mathcal{F}^{-1}\left[\hat{f}(\xi,v)\chi_{\Omega_\delta}(\xi,v)\right]dv \qquad \longleftarrow \overline{f}(x)-\overline{f}^\delta(x).
\end{aligned}$$

Here, χ_Ω represents the usual *smooth* partitioning relative to Ω_δ and its complement, Ω_δ^c. On Ω^c, the symbol is 'bounded away' from zero, so we gain one derivative:

$$\|\overline{f}^\delta\|_{W^1(L^p))} \le Const.\|g\|_{L^p(x,v)}\delta^{\frac{\alpha}{p'}-(m+1)}; \tag{5.2.6}$$

On Ω – along the 'non uniformly elliptic' rays, we have no gain of regularity, but instead, our non-degeneracy assumption implies that $|\Omega|$ is a 'small' set and therefore

$$\|\overline{f}-\overline{f}^\delta\|_{L^p} \le Const.\|f\|_{L^p(x,v)}\delta^{\frac{\alpha}{p'}} \tag{5.2.7}$$

Both (5.2.6) and (5.2.7) are straightforward for $p = 2$ and by estimating the corresponding $\mathcal{H}^1$ multipliers, the case $1 < p \le 2$ follows by interpolation. Finally, we consider the K-functional

$$K(\overline{f},t) := \inf_{\overline{g}} \left[\|\overline{f}-\overline{g}\|_{L^p} + t\|\overline{g}\|_{W^1(L^p)} \right];$$

The behavior of this functional, $K(\overline{f},t) \sim t^\theta$, characterize the smoothness of $\overline{f}$ in the intermediate space between L^p and $W^1(L^p)$: more precisely, $\overline{f}$ belongs to Besov space B^θ_∞ with 'intermediate' smoothness of order θ.
Now set $g = \overline{f}^\delta$, then with appropriately scaled δ we find that $K(\overline{f},t) \sim t^\theta$ with $\theta = \frac{\alpha}{(s+1)p'}$. This means that $\overline{f}(x)$ belongs to Besov space, $\overline{f}(x) \epsilon B^\theta_\infty(L^p(x))$ and (5.2.3) (with $p=q=r$) follows. ■

Remark. In the limiting case of $\alpha = 0$ in (5.2.2), one finds that if

$$meas_v\{v|\ |a(v)\cdot\xi'| = 0\} = 0, \tag{5.2.8}$$

then averaging is a compact mapping, $\{f(x,v)\} \in L^{x,v} \hookrightarrow \{\overline{f}\} \in L^p$. The case $p=2$ follows from Gèrard's results [12].

5.3 Regularizing effect revisited ($m = 1, d \geq 1$)

In this section we resume our discussion on the regularization effect of nonlinear conservation laws. The averaging lemma enables us to identify the proper notion of 'nonlinearity' in the multivariate case, which guarantee compactness.
The following result, adapted from [22], is in the heart of matter.

Theorem 5.3.1 *Consider the scalar conservation law*

$$\partial_t u + \nabla_x \cdot A(u) = 0, \quad (t,x) \in \mathbb{R}^+_t \times \mathbb{R}^d_x. \tag{5.3.1}$$

and assume that the following non-degeneracy condition holds (consult (5.2.2))

$$\exists \alpha \in (0,1):\ meas_v\{v|\ |\tau + A'(v)\cdot\xi| < \delta\} \leq Const\cdot\delta^\alpha, \quad \forall \tau^2 + |\xi|^2 = 1. \tag{5.3.2}$$

Let $\{u^\epsilon\}$ be a family of approximate solutions with bounded measures of entropy production,

$$\partial_t \eta(u^\epsilon) + \nabla_x \cdot F(u^\epsilon) \in \mathcal{M}((0,T)\times\mathbb{R}^d_x), \qquad \forall \eta'' > 0. \tag{5.3.3}$$

Then $u^\epsilon(t,x) \in W^{\frac{\alpha}{\alpha+4}}_{loc}(L^r(t,x))$, $r = \frac{\alpha+4}{\alpha+2}$.

Remark. Note that the bounded measure of entropy production in (5.3.3) need not be negative; general bounded measures will do.

Proof. To simplify notations, we use the customary 0^{th} index for time direction,

$$x = (t \leftrightarrow x_0, x_1, \ldots, x_d), \qquad A(u) = (A_0(u) \equiv 1, A_1(u), \ldots, A_d(u)).$$

The entropy condition (5.3.3) with Kružkov entropy pairs (1.2.1), reads

$$\nabla_x \cdot [sgn(u^\epsilon - v)(A(u^\epsilon) - A(v))] \leq 0.$$

This defines a family of non-negative measures, $m^\varepsilon(x,v)$,

$$\nabla_x \cdot [sgn(v)A(v) - sgn(u^\varepsilon - v)(A(u^\varepsilon) - A(v))] =: m^\varepsilon(x,v). \tag{5.3.4}$$

Differentiate (5.3.4) w.r.t. v: one finds that the indicator function, $f(x,v) = \chi_{u^\varepsilon}(v)$, where

$$\chi_{u^\varepsilon}(v) := \begin{cases} +1 & 0 < v < u^\varepsilon \\ -1 & u^\varepsilon < v < 0 \\ 0 & |v| > u^\varepsilon \end{cases}, \tag{5.3.5}$$

satisfies the transport equation,

$$\partial_t f^\varepsilon + a(v) \cdot \nabla_x f^\varepsilon = \frac{\partial}{\partial v} m^\varepsilon(t,x,v), \tag{5.3.6}$$

which corresponds to (5.2.1) with $s = 1, g(x,v) = m^\varepsilon(x,v) \in \mathcal{M}_{x,v}$ [1]. We now apply the averaging lemma with $(s = q = 1, p = 2)$, which tells us that $u^\varepsilon(t,x) = \int \chi_{u^\varepsilon}(v)dv \in W^{\frac{\alpha}{\alpha+4}}_{loc}(L^r(t,x))$ as asserted. ■

It follows that if the non-degeneracy condition (5.3.2) holds, then the family of approximate solutions $\{u^\varepsilon\}$ is compact and strong convergence follows. In this context we refer to the convergence statement for measure-valued solutions for general multidimensional scalar conservation laws – approximate solutions measured by their nonpositive entropy production outlined in Lecture I, §1.5.

Here, Theorem 5.3.1 yields even more, by *quantifying* the regularity of approximate solutions with bounded entropy productions in terms of the non-degeneracy condition (5.3.2). In fact, more can be said if the solution operator associated with $\{u^\varepsilon\}$ is translation invariant: a bootstrap argument yields an improved regularity, [22],

$$u^\varepsilon(t > 0, \cdot) \in W^{\frac{\alpha}{\alpha+2}}(L^1(x)). \tag{5.3.7}$$

In particular, if the problem is nonlinear in the sense that the non-degeneracy condition (5.2.8) holds,

$$meas_v\{v|\ \tau + A'(v) \cdot \xi = 0\} = 0, \tag{5.3.8}$$

then the corresponding solution operator, $T_t, t > 0$, has a *regularization* effect mapping $T_{\{t>0\}} : L^\infty_0 \hookrightarrow L^1$. This could be viewed as a multidimensional generalization for Tartar's regularization result for a.e. nonlinear one-dimensional fluxes, $A''(\cdot) \neq 0$, *a.e.*.

We continue with few multidimensional examples which illustrate the relation between the non-degeneracy condition, (5.3.2) and regularity.

Example #1. The 'two-dimensional Burgers' equation' (5.1.6),

$$\frac{\partial}{\partial t}u + \frac{\partial}{\partial x_1}(\frac{u^2}{2}) + \frac{\partial}{\partial x_2}(\frac{u^2}{2}) = 0,$$

[1] Once more, it is the symmetry property (1.2.6) which has a key role in the derivation of the transport kinetic formulation (5.2.1).

has a linearized symbol $\tau'+v\xi_1'+v\xi_2'$ which fails to satisfy the non-degeneracy/non-linearity condition (5.3.2), since it vanishes $\forall v$'s along $\tau' = \xi_1' + \xi_2' = 0$. This corresponds to its persistence of oscillations along $x_1 - x_2 = const$, which excludes compactness.

Example #2. We consider

$$\frac{\partial}{\partial t}u + \frac{\partial}{\partial x_1}(\frac{u^2}{2}) + \frac{\partial}{\partial x_2}(e^u) = 0. \tag{5.3.9}$$

In this case the linearized symbol is given by $\tau' + v\xi_1' + e^v\xi_2'$; Here we have

$$meas\{v \mid \ |\tau' + v\xi_1' + e^v\xi_2'| \le \delta\} \le Const.\delta^{\frac{1}{2}}$$

(just consider the second-order touch-point at $v = 1$). Hence, the solution operator associated with (5.3.9) is compact (– in fact, mapping $L_0^\infty \longrightarrow W^{\frac{1}{3}}(L^1)$.)

Example #3. Consider

$$\frac{\partial}{\partial t}u + \frac{\partial}{\partial x_1}(|u^m|u) + \frac{\partial}{\partial x_2}(|u|^n u) = 0. \tag{5.3.10}$$

For $n \neq m$ we obtain an index of non-degeneracy/non-linearity of order $\alpha = 1/\max\{1+m, 1+n\}$.

5.3.1 Kinetic and other approximations

Theorem 5.3.1 provides an alternative route to analyze the convergence of *general* entropy stable multi-dimensional schemes, schemes whose convergence proof was previously accomplished by measure-valued arguments; here we refer to finite-difference, finite-volume, streamline-diffusion and spectral approximations ..., which were studied in [4, 18, 19, 15, 16, 3]. Indeed, the feature in the convergence proof of all these methods is the $W_{loc}^{-1}(L^2)$-compact entropy production, (5.4.3). Hence, if the underlying conservation law satisfies the non-linear degeneracy condition (5.3.8), then the corresponding family of approximate solutions, $\{u^\varepsilon(t > 0, \cdot)\}$ becomes compact. Moreover, if the entropy production is bounded measure, then there is actually a *gain* of regularity indicated in Theorem 5.3.1 and respectively, in (5.3.7) for the translation invariant case.

Remark. Note that unlike the requirement for a *nonpositive* entropy production from measure-valued solutions (consult (1.5.1) in Lecture I), here we allow for an arbitrary bounded measure.

So far we have not addressed explicitly a kinetic formulation of the multidimensional conservation law (5.3.1). The study of regularizing effect for multidimensional conservation laws was originally carried out in [22] for the approximate solution constructed by the following BGK-like model, [136] (see also [2],[14]),

$$\begin{aligned} \frac{\partial f^\varepsilon}{\partial t} + a(v)\cdot\nabla_x f^\varepsilon &= \frac{1}{\varepsilon}\big(\chi_{u^\varepsilon}(v) - f^\varepsilon\big), \quad (t,x,v) \in \mathbb{R}_t^+ \times \mathbb{R}_x^d \times \mathbb{R}_v & (5.3.11)\\ f^\varepsilon|_{t=0} &= \chi_{u_0(x)}(v), \quad (x,v) \in \mathbb{R}_x^d \times \mathbb{R}_v. & (5.3.12) \end{aligned}$$

Here, $\chi_{u^\varepsilon(t,x)}(v)$ denotes the 'pseudo-Maxwellian',

$$\chi_{u^\varepsilon}(v) := \begin{cases} +1 & 0 < v < u^\varepsilon \\ -1 & u^\varepsilon < v < 0 \\ 0 & |v| > u^\varepsilon \end{cases}, \tag{5.3.13}$$

which is associated with the average of f^ε,

$$u^\varepsilon(t,x) = \bar{f}^\varepsilon := \int_{\mathbb{R}} f^\varepsilon(t,x,v)dv, \quad (t,x) \in R_t^+ \times R_x^d. \tag{5.3.14}$$

The key property of this kinetic approximation is the existence of a nonnegative measure, m^ε such that $\frac{1}{\varepsilon}(\chi_{u^\varepsilon}(v) - f^\varepsilon) = \frac{\partial m^\varepsilon}{\partial v}$ (The existence of such measures proved in [22] and is related to H-functions studied in [28] and Brenier's lemma [2].) Thus, we may rewrite (5.3.11) in the form

$$\frac{\partial f^\varepsilon}{\partial t} + a(v) \cdot \nabla_x f^\varepsilon = \frac{\partial m^\varepsilon}{\partial v}, \quad m^\varepsilon \in \mathcal{M}((0,T) \times \mathbb{R}_x^d \times \mathbb{R}_v^+). \tag{5.3.15}$$

Let (η, F) be an entropy pair associated with (5.3.1). Integration of (5.3.15) against $\eta'(v)$ implies that the corresponding macroscopic averages, $u^\varepsilon(t,x)$, satisfy

$$\partial_t \eta(u^\varepsilon) + \nabla_x \cdot F(u^\varepsilon) \leq 0, \qquad \forall \eta'' > 0. \tag{5.3.16}$$

Thus, the entropy production in this case is nonpositive and hence a bounded measure, so that Theorem 5.3.1 applies. Viewed as a measure-valued solution, convergence follows along DiPerna's theory [8]. If, moreover, the nondegeneracy condition (5.3.2) holds, then we can further quantify the W^s-regularity (of order $s = \frac{\alpha}{\alpha+2}$.)

Theorem 5.3.1 offers a further generalization beyond the original, 'kineticly' motivated discussion in [22]. Indeed, consideration of Theorem 5.3.1 reveals the intimate connection between the macroscopic assumption of bounded entropy production in (5.3.3), and an underlying kinetic formulation (5.3.6), analogous to (5.3.15). For a recent application of the regularizing effect for a convergence study of finite-volume schemes along these lines we refer to [24].

5.4 Degenerate parabolic equations

As an example one can treat convective equations together with (possibly degenerate) diffusive terms

$$\partial_t u^\varepsilon + \nabla_x \cdot A(u^\varepsilon) = \nabla_x \cdot (Q \nabla_x u^\varepsilon), \quad Q \geq 0. \tag{5.4.1}$$

Assume the problem is not linearly degenerate, in the sense that

$$meas_v\{v|\ \tau + A'(v) \cdot \xi = 0,\ \langle Q(v)\xi, \xi \rangle = 0\} = 0. \tag{5.4.2}$$

Let $\{u^\varepsilon\}$ be a family of approximate solutions of (5.2.1) with $W_{loc}^{-1}(L^2)$-compact entropy production,

$$\partial_t \eta(u^\varepsilon) + \nabla_x \cdot F(u^\varepsilon) \hookrightarrow W_{loc}^{-1}(L^2(t,x)), \quad \forall \eta'' > 0. \tag{5.4.3}$$

Then $\{u^\varepsilon\}$ is compact in $L^2_{loc}(t,x)$, [22].
The case $Q = 0$ corresponds to our multidimensional discussion in §5.3.1; the case $A = 0$ correspond possibly degenerate parabolic equations (consult [17] and the references therein, for example). According to (5.4.2), satisfying the ellipticity condition, $\langle Q(v)\xi, \xi\rangle > 0$ on a set of non-zero measure, guarantees regularization, compactness ...

Again, a second-order version of the averaging lemma 1.6.1 enables us to quantify the gained regularity which we state as

Lemma 5.4.1 *Let $f \in L^1(x,v)$ be a solution of the diffusive equation*

$$-\sum q_{ij}(v)\partial^2_{x_i x_j} f = \frac{\partial m}{\partial v}, \quad Q := (q_{ij}) \geq 0,\ m(t,x,v) \in \mathcal{M}_+.$$

Assume the following non-degeneracy condition holds

$$meas_v\{v|\ |0 \leq \langle \xi', Q(v)\xi'\rangle < \delta\} \leq Const \cdot \delta^\alpha, \quad \alpha \in (0,1). \tag{5.4.4}$$

Then $\bar{f}(x) := \int_v f(x,v)dv$ belongs to Sobolev space $W^\theta(L^1(x))$,

$$\bar{f}(x) \in W^\theta(L^1(x)), \qquad \theta < \frac{8\alpha}{3\alpha+2} \tag{5.4.5}$$

Example. Consider the isotropic equation

$$u_t + \Delta\psi(u) = 0, \quad \psi \uparrow .$$

Here $Q_{ij}(v) = \delta_{ij}\psi'(v)$ and the lemma 5.4.1 applies. The kinetic formulation of such equations was studied in [17]. In the particular case of porous media equation, $\psi(u) = u^m, m \geq 2$, (5.4.4) holds with $\alpha = \frac{1}{m-1} \leq 2$ and one conclude a regularizing effect of order $s < \frac{8}{2m+1}$, i.e., $u(t>0,\cdot) : L^\infty_0 \longrightarrow W^s(L^1)$.
A particular attractive advantage of the kinetic formulation in this case, is that it applies to *non-isotropic* problems as well.

5.5 The 2×2 isentropic equations

We consider the 2×2 system of isentropic equations, governing the density ρ and momentum $m = \rho u$,

$$\frac{\partial}{\partial t}\begin{pmatrix} \rho \\ \rho u \end{pmatrix} + \frac{\partial}{\partial x}\begin{pmatrix} m \\ \frac{m^2}{\rho} + p(\rho) \end{pmatrix} = 0. \tag{5.5.1}$$

Here $p(\rho)$ is the pressure which is assumed to satisfy the (scaled) γ law, $p(\rho) = \kappa\rho^\gamma$, $\kappa = \frac{(\gamma-1)^2}{4\gamma}$.

The question of existence for this model, depending on the γ-law, $1 < \gamma < 3$, was already studied [7],[6] by compensated compactness arguments. Here we revisit this problem with the kinetic formulation presented below which leads to existence result for $3 < \gamma < \infty$, consult [23], and is complemented with a new existence proof for $1 < \gamma < 3$, consult [21].

For the derivation of our kinetic formulation of (5.5.1), we start by seeking *all* weak entropy inequalities associated with the isentropic 2×2 system (5.5.1),

$$\partial_t w + \partial_x A(w) = 0, \qquad w := \begin{bmatrix} \rho \\ m \end{bmatrix}, \quad A(w) := \begin{bmatrix} m \\ \frac{m^2}{\rho} + \kappa\rho^\gamma \end{bmatrix} \tag{5.5.2}$$

The family of entropy functions associated with (5.5.2) consists of those $\eta(w)$'s whose Hessians symmetrize the Jacobian, $A'(w)$; the requirement of a symmetric $\eta''(w)A'(w)$ yields the Euler-Poisson–Darboux equation, e.g, [6]

$$\eta_{\rho\rho} = \frac{(\gamma-1)^2}{4}\rho^{\gamma-3}\eta_{uu}.$$

Seeking *weak* entropy functions such that $\eta(\rho,u)_{|\rho=0} = 0$, leads to the family of weak (entropy, entropy flux) pairs, $(\eta(\rho,u), F(\rho,u))$, depending on an arbitrary φ,

$$\begin{aligned} \eta(\rho,u) &= \rho \int \omega(\xi)\varphi(u+\xi\rho^\theta)d\xi, \\ q(\rho,u) &= \rho \int \omega(\xi)\varphi(u+\xi\rho^\theta)(u+\theta\xi\rho^\theta)d\xi. \end{aligned} \tag{5.5.3}$$

Here, $\omega(\xi)$ is given by

$$\omega(\xi) := (1-\xi^2)_+^\lambda \qquad \lambda := \frac{3-\gamma}{2(\gamma-1)} > 0, \ \theta := \frac{\gamma-1}{2}.$$

We note that η is convex iff φ is. Thus by the formal change of variables, $v \longleftrightarrow u + \xi\rho^\theta$, the weight function $\omega(\xi)$ becomes the 'pseudo-Maxwellian', $\chi_{\rho,u}(v) \longleftrightarrow \rho\omega((v-u)\rho^{-\theta})$,

$$\chi_{\rho,u}(v) := (\rho^{\gamma-1} - (v-u)^2)_+^\lambda. \tag{5.5.4}$$

We arrive at the kinetic formulation of (5.5.1) which reads

$$\partial_t \chi_{\rho,u}(v) + \partial_x \left[a(v,\rho,u)\chi_{\rho,u}(v)\right] = \partial_{vv}^2 m, \qquad m \epsilon \mathcal{M}_-. \tag{5.5.5}$$

Observe that integration of (5.5.5) against any convex φ recovers all the weak entropy inequalities. Again, as in the scalar case, the nonpositive measure m on the right of (5.5.5), measures the loss of entropy which concentrates along shock discontinuities.

The transport equation (5.5.5) is not purely kinetic due to the dependence on the macroscopic velocity u (unless $\gamma = 3$ corresponding to $\theta = 1$),

$$a(v,\rho,u) = \theta v + (1-\theta)u \longleftrightarrow u + \xi\theta\rho^\theta.$$

Compensated compactness arguments presented in [23] yield the following compactness result.

Theorem 5.5.1 *[23] Consider the isentropic equations (5.5.1) with $\gamma \geq 3$ and let $(\rho_n = \rho_n(t,x), u_n = u_n(t,x))$ be a family of approximate solution with bounded entropy production and finite energy, $E_n := \rho_n u_n^2 + \rho_n^\gamma \in L^\infty(\mathbb{R}_t^+, L^1(\mathbb{R}_x))$. Then a subsequence of ρ_n (still denoted by ρ_n) converges pointwise to ρ, and (a subsequence of) u_n converges pointwise to u on the set $\{\rho(x,t) > 0\}$. In particular, $\rho_n u_n$ converges pointwise to ρu.*

Finally, we consider the 2×2 system

$$\begin{cases} \partial_t v - \partial_x w = 0, \\ \partial_t w + \partial_x p(v) = 0, \quad t \geq 0, x \in \mathbb{R}, \end{cases} \tag{5.5.6}$$

endowed with the pressure law

$$p(v) = \kappa v^{-\gamma}, \quad \gamma > 0, \quad \kappa = \frac{(\gamma-1)^2}{4\gamma}. \tag{5.5.7}$$

The system (5.5.6)-(5.5.7) governs the isentropic gas dynamics written in Lagrangian coordinates. In general the equations (5.5.6)-(5.5.7) will be referred to as the p-system (see [20],[30]).

For a kinetic formulation, we first seek the (entropy,entropy flux) pairs, (η, F), associated with (5.5.6)-(5.5.7). They are determined by the relations

$$\eta_{vv} + p'(v)\,\eta_{ww} = 0, \tag{5.5.8}$$

where F is computed by the compatibility relations

$$F_v = \eta_w\, p'(v), \quad F_w = -\eta_v. \tag{5.5.9}$$

The solutions of (5.5.8) can be expressed in terms of the fundamental solution

$$\eta(v,w) = \int_{\mathbb{R}} \varphi(\xi)\chi_{v,w}(\xi)d\xi,$$

where the fundamental solutions, $\chi_{v,w}(\xi)$, are given by

$$\chi_{v,w}(\xi) = v\left(v^{1-\gamma} - (w-\xi)^2\right)_+^{\lambda}, \quad \lambda = \frac{3-\gamma}{2(\gamma-1)}. \tag{5.5.10}$$

Here and below, ξ (rather than v occupied for the specific volume) denotes the kinetic variable. The corresponding kinetic fluxes are then given by

$$h_{v,w}(\xi) = \theta\frac{\xi - w}{v}\chi_{v,w}(\xi).$$

We arrive at the kinetic formulation of (5.5.6)-(5.5.7) which reads, [23]

$$\partial_t \chi_{v,w} + \partial_x[a(\xi,v,w)\chi_{v,w}(\xi)] = \partial_{\xi\xi} m, \quad m(t,x,\xi) \in \mathcal{M}_-, \tag{5.5.11}$$

with macroscopic velocity, $a(\xi,v,w) := \theta(\xi - w)/v$.

Bibliography

[1] C. BARDOS, F. GOLSE & D. LEVERMORE, *Fluid dynamic limits of kinetic equations II: convergence proofs of the Boltzmann equations*, Comm. Pure Appl. Math. XLVI (1993), 667–754.

[2] Y. BRENIER, *Résolution d'équations d'évolution quasilinéaires en dimension N d'espace à l'aide d'équations linéaires en dimension N + 1*, J. Diff. Eq. 50 (1983), 375–390.

[3] G.-Q. CHEN, Q. DU & E. TADMOR, *Spectral viscosity approximation to multidimensional scalar conservation laws*, Math. of Comp. 57 (1993).

[4] B. COCKBURN, F. COQUEL & P. LEFLOCH, *Convergence of finite volume methods for multidimensional conservation laws*, SIAM J. Numer. Anal. 32 (1995), 687–705.

[5] C. CERCIGNANI, The Boltzmann Equation and its Applications, Appl. Mathematical Sci. 67, Springer, New-York, 1988.

[6] G.-Q. CHEN, *The theory of compensated compactness and the system of isentropic gas dynamics*, Preprint MCS-P154-0590, Univ. of Chicago, 1990.

[7] R. DIPERNA, *Convergence of the viscosity method for isentropic gas dynamics*, Comm. Math. Phys. 91 (1983), 1–30.

[8] R. DIPERNA, *Measure-valued solutions to conservation laws*, Arch. Rat. Mech. Anal. 88 (1985), 223-270.

[9] R. DIPERNA & P. L. LIONS, *On the Cauchy problem for Boltzmann equations: Global existence and weak stability*, Ann. Math. 130 (1989), 321–366.

[10] R. DIPERNA & P.L. LIONS, *Global weak solutions of Vlasov-Maxwell systems*, Comm. Pure Appl. Math. 42 (1989), 729–757.

[11] R. DIPERNA, P.L. LIONS & Y. MEYER, *L^p regularity of velocity averages*, Ann. I.H.P. Anal. Non Lin. 8(3-4) (1991), 271–287.

[12] P. GÉRARD, *Microlocal defect measures*, Comm. PDE 16 (1991), 1761–1794.

[13] F. GOLSE, P. L. LIONS, B. PERTHAME & R. SENTIS, *Regularity of the moments of the solution of a transport equation*, J. of Funct. Anal. 76 (1988), 110–125.

[14] Y. GIGA & T. MIYAKAWA, *A kinetic construction of global solutions of first-order quasilinear equations*, Duke Math. J. 50 (1983), 505–515.

[15] C. JOHNSON & A. SZEPESSY, *Convergence of a finite element methods for a nonlinear hyperbolic conservation law*, Math. of Comp. 49 (1988), 427–444.

[16] C. JOHNSON, A. SZEPESSY & P. HANSBO, *On the convergence of shock-capturing streamline diffusion finite element methods for hyperbolic conservation laws*, Math. of Comp. 54 (1990), 107–129.

[17] Y. KOBAYASHI, *An operator theoretic method for solving $u_t = \Delta\psi(u)$*, Hiroshima Math. J. 17 (1987) 79–89.

[18] D. KRÖNER, S. NOELLE & M. ROKYTA, *Convergence of higher order upwind finite volume schemes on unstructured grids for scalar conservation laws in several space dimensions*, Numer. Math. 71 (1995) 527–560.

[19] D. KRÖNER & M. ROKYTA, *Convergence of Upwind Finite Volume Schemes for Scalar Conservation Laws in two space dimensions*, SINUM 31 (1994) 324–343.

[20] P.D. LAX, Hyperbolic Systems of Conservation Laws and the Mathematical Theory of Shock Waves (SIAM, Philadelphia, 1973).

[21] P. L. LIONS, B. PERTHAME & P. SOUGANIDIS, *Existence and stability of entropy solutions for the hyperbolic systems of isentropic gas dynamics in Eulerian and Lagrangian coordinates*, Comm. Pure and Appl. Math. 49 (1996), 599-638.

[22] P. L. LIONS, B. PERTHAME & E. TADMOR, *Kinetic formulation of scalar conservation laws and related equations*, J. Amer. Math. Soc. 7(1) (1994), 169–191

[23] P. L. LIONS, B. PERTHAME & E. TADMOR, *Kinetic formulation of the isentropic gas-dynamics equations and p-systems*, Comm. Math. Phys. 163(2) (1994), 415–431.

[24] S. NOELLE & M. WESTDICKENBERG *Convergence of finite volume schemes. A new convergence proof for finite volume schemes using the kinetic formulation of conservation laws*, Preprint.

[25] O. A. OLĔINIK *Discontinuous solutions of nonlinear differential equations*, Amer. Math. Soc. Transl. (2), 26 (1963), 95–172.

[26] B. PERTHAME, *Global existence of solutions to the BGK model of Boltzmann equations*, J. Diff. Eq. 81 (1989), 191-205.

[27] B. PERTHAME, *Second-order Boltzmann schemes for compressible Euler equations*, SIAM J. Num. Anal. 29, (1992), 1–29.

[28] B. PERTHAME & E. TADMOR, *A kinetic equation with kinetic entropy functions for scalar conservation laws*, Comm. Math. Phys.136 (1991), 501–517.

[29] K. H. PRENDERGAST & K. XU, *Numerical hydrodynamics from gas-kinetic theory*, J. Comput. Phys. 109(1) (1993), 53–66.

[30] J. SMOLLER, Shock Waves and Reaction-Diffusion Equations, Springer-Verlag, New York, 1983.

[31] L. TARTAR, *Compensated compactness and applications to partial differential equations*, in *Research Notes in Mathematics 39*, Nonlinear Analysis and Mechanics, Heriott-Watt Symposium, Vol. 4 (R.J. Knopps, ed.) Pittman Press, (1975), 136–211.

[32] L. TARTAR, *Discontinuities and oscillations*, in Directions in PDEs, Math Res. Ctr Symposium (M.G. Crandall, P.H. Rabinowitz and R.E. Turner eds.) Academic Press (1987), 211-233.